Rolf Klein

WILEY-VCH

Laser Welding of Plastics

Rolf Klein

Laser Welding of Plastics

Related Titles

Elias, H.-G.

Macromolecules

Volume 4: Applications of Polymers

727 pages with 295 figures and 193 tables

2008
Hardcover
ISBN: 978-3-527-31175-0

Kannatey-Asibu, E.

Principles of Laser Materials Processing

approx. 820 pages

Hardcover
ISBN: 978-0-470-17798-3

Harper, C. A.

Handbook of Plastic Processes

approx. 744 pages

2006
Hardcover
ISBN: 978-0-471-66255-6

Rolf Klein

Laser Welding of Plastics

WILEY-
VCH

WILEY-VCH Verlag GmbH & Co. KGaA

The Author

Dr.-Ing. Rolf Klein
Am Turnplatz 2
64823 Gross-Umstadt
Germany

All books published by **Wiley-VCH** are carefully produced. Nevertheless, authors, editors, and publisher do not warrant the information contained in these books, including this book, to be free of errors. Readers are advised to keep in mind that statements, data, illustrations, procedural details or other items may inadvertently be inaccurate.

Library of Congress Card No.: applied for

British Library Cataloguing-in-Publication Data
A catalogue record for this book is available from the British Library.

Bibliographic information published by the Deutsche Nationalbibliothek
The Deutsche Nationalbibliothek lists this publication in the Deutsche Nationalbibliografie; detailed bibliographic data are available on the Internet at http://dnb.d-nb.de.

© 2012 Wiley-VCH Verlag & Co. KGaA,
Boschstr. 12, 69469 Weinheim, Germany

All rights reserved (including those of translation into other languages). No part of this book may be reproduced in any form – by photoprinting, microfilm, or any other means – nor transmitted or translated into a machine language without written permission from the publishers. Registered names, trademarks, etc. used in this book, even when not specifically marked as such, are not to be considered unprotected by law.

Cover Design Adam-Design, Weinheim
Typesetting Thomson Digital, Noida, India
Printing and Binding

Printed in the Singapore
Printed on acid-free paper

Print ISBN: 978-3-527-40972-3
ePDF ISBN: 978-3-527-63698-3
oBook ISBN: 978-3-527-63696-9
ePub ISBN: 978-3-527-63697-6

Contents

Introduction *1*

1 Material Properties of Plastics *3*
1.1 Formation and Structure *3*
1.2 Types of Plastics *7*
1.2.1 Thermoplastic Resins *9*
1.2.1.1 Amorphous Thermoplastics *10*
1.2.1.2 Semicrystalline Thermoplastics *10*
1.2.2 Elastomers *13*
1.2.3 Thermosets *13*
1.2.4 Polymer Compounds *14*
1.2.4.1 Polymer Blends *14*
1.2.4.2 Copolymers *15*
1.2.4.3 Thermoplastic Elastomers *15*
1.2.5 Polymer Composites *18*
1.3 Thermal Properties *19*
1.3.1 Phase Transitions *20*
1.3.1.1 Glass Transition (T_g) *20*
1.3.1.2 Flow Temperature (T_f) *20*
1.3.1.3 Crystallite Melting Temperature (T_m) *20*
1.3.1.4 Thermal Decomposition (T_d) *21*
1.3.2 Specific Volume *22*
1.3.3 Heat Capacity *24*
1.3.4 Heat Conduction *27*
1.3.5 Temperature Conduction *30*
1.3.5.1 Amorphous Thermoplastics *32*
1.3.5.2 Semicrystalline Thermoplastics *33*
1.4 Optical Properties *35*
1.4.1 Optical Constants *36*
1.4.2 Reflection, Transmission and Absorption Behavior *42*
1.4.3 Scattering of NIR- and IR-Radiation in Plastics *46*
1.4.4 Absorption of NIR-Laser Radiation ($\lambda = 800$ nm to 1200 nm) *49*

1.4.4.1 Electronic Excitation *50*
1.4.4.2 Vibronic Excitation *51*
1.4.4.3 Summarizing Comment *52*
1.4.5 Absorption of NIR-Laser Radiation ($\lambda = 1200$ nm to 2500 nm) *54*
1.4.6 Absorption of MIR-Laser Radiation ($\lambda = 2.5$ μm to 25 μm) *55*
1.4.7 Adaptation of NIR-Radiation Absorption by Additives *59*
1.4.7.1 Carbon Black *59*
1.4.7.2 Inorganic Pigments *61*
1.4.7.3 Organic Dyes *66*
1.4.7.4 Summarizing Comment *66*
References *66*

2 Laser Sources for Plastic Welding *71*
2.1 Properties of Laser Radiation *71*
2.1.1 Laser Wavelength *73*
2.1.2 Intensity Distribution *74*
2.1.3 Beam Propagation *74*
2.1.4 Focusing Properties *76*
2.2 Types of Lasers *78*
2.2.1 Diode Lasers (800 to 2000 nm) *78*
2.2.2 Nd:YAG-Lasers (1064 nm) *80*
2.2.3 Fiber Lasers *83*
2.2.4 CO_2-Lasers (10.6 μm) *85*
2.2.5 Summary *87*
2.3 Beam Guiding and Focusing *88*
2.3.1 Beam-Guiding Systems *88*
2.3.1.1 Glass-Fiber Systems *88*
2.3.1.2 Mirror Systems *93*
2.3.2 Focusing Systems *95*
2.3.2.1 Static Focusing Systems *95*
2.3.2.2 Dynamic Focusing Systems *99*
2.3.3 Beam-Shaping Optics *100*
2.4 Principle Setup of Laser Welding Systems *101*
References *107*

3 Basics of Laser Plastic Welding *109*
3.1 Heat Generation and Dissipation *109*
3.1.1 Absorption of Laser Radiation *109*
3.1.1.1 Direct Absorption *109*
3.1.1.2 Indirect Absorption *110*
3.1.1.3 Hindered Absorption by Internal Scattering *111*
3.1.2 Transfer of Laser Energy into Process Heat *114*
3.1.3 Dissipation of Process Heat *118*
3.1.4 Process Simulation by Complex Computation *121*
3.2 Theory of Fusion Process *126*

3.2.1 Interdiffusion Process (Reptation Model) *127*
3.2.2 Interchange of Macromolecules by Squeeze Flow Process *132*
3.2.3 Mixing of Crystalline Phases *133*
3.3 Material Compatibility *135*
References *138*

4 **Process of Laser Plastic Welding** *141*
4.1 Basic Process Principles *141*
4.1.1 Butt-Joint Welding *141*
4.1.2 Through-Transmission Welding *143*
4.2 Process Types *145*
4.2.1 Contour Welding *145*
4.2.2 Quasisimultaneous Welding *148*
4.2.3 Simultaneous Welding *150*
4.2.4 Special Processes *154*
4.2.4.1 Mask Laser Welding *154*
4.2.4.2 TWIST Laser Welding *155*
4.2.4.3 Globo Laser Welding *156*
4.2.4.4 IR-Hybrid Laser Welding *158*
4.2.4.5 Ultrasonic Hybrid Laser Welding *159*
4.2.4.6 Laser-Assisted Tape Laying and Winding *160*
4.3 Adaption of Absorption *163*
4.3.1 Use of Surface Coatings *163*
4.3.2 Use of Absorbing Additives *172*
4.3.3 Use of Special Lasers *178*
4.4 Design of Joint Geometry *181*
4.4.1 Joint Geometries *182*
4.4.2 Tolerances and Clamping *186*
4.4.3 Obstacles to Avoid *191*
4.4.4 Gap Bridging *193*
4.5 Methods of Quality Monitoring and Control *195*
4.5.1 Quality Control before Processing *196*
4.5.2 Quality Control During Processing *199*
4.5.2.1 Pyrometric Monitoring *199*
4.5.2.2 Thermography Monitoring *203*
4.5.2.3 Digital Imaging Monitoring *205*
4.5.2.4 Optical Reflection Monitoring *207*
4.5.2.5 Mechanical Set-Path Monitoring *208*
4.5.2.6 Summary of Monitoring Techniques *209*
References *212*

5 **Case Studies** *217*
5.1 Automotive Components *218*
5.2 Consumer Goods *223*

5.3 Electronic Devices *227*
5.4 Medical Devices *232*
5.5 Others *238*

Index *243*

Introduction

Laser is a short form for "*l*ight *a*mplification by *s*timulated *e*mission of *r*adiation." The first theoretical description of stimulated emission of radiation was given by Einstein in 1917. It took many years for a first technical realization of a laser source based on Einstein's theory by Mainman in 1960, developing a solid-state ruby laser emitting red laser radiation. In 1972 lasers entered industrial application for metal sheet processing. From this time laser processing of metals, especially laser cutting and welding steel sheets or stainless steel, changed from an exotic processing tool to well-established industrial applications from small-size serial to large-scale production.

Up to the early 1990s, laser welding of thermoplastics was a potential but exotic way for joining plastic components. Available laser sources for plastic welding at this time were CO_2 or Nd:YAG lasers having high investment costs not capable of economical industrial application. Also, the technique of through transmission laser welding (TTLW) was not developed yet.

Then, two fundamental developments were made almost simultaneously, giving a basis for introduction of laser plastic welding into industrial application: development of TTLW as a new processing technique for laser welding plastics and development of high-power diode lasers previously known as low-power laser sources produced in mass production for example, for communication technology, computer data storage or consumer goods like CD players.

The opportunity for mass production of high-power diode laser sources generating decreasing investment cost for such laser sources as well as high plug efficiency compared to other laser sources like Nd:YAG lasers enabled development of laser welding plastics in conjunction with the new TTLW process ready for introduction into the market. As a result, laser welding thermoplastic components entered the market rapidly. One of the first industrial applications for laser welding plastic components entering mass production was an electronic car key, starting production in 1997 for the new Mercedes Benz type 190.

Since that time laser welding plastics has grown rapidly as an alternative joining technology in competition with conventional joining technologies like heat contact, ultrasonic, vibration and other welding methods.

Advantages of laser welding plastic components compared to conventional joining technologies are localized heat input to the joint interface without damaging of

Laser Welding of Plastics, First Edition. Rolf Klein.
© 2011 Wiley-VCH Verlag GmbH & Co. KGaA. Published 2011 by Wiley-VCH Verlag GmbH & Co. KGaA.

sensitive inner components like electronics or mechanics by heat or internal mechanical forces, extremely reduced welding flash while maintaining part geometry and visual appearance as well as generating weld seams of high mechanical strength and outstanding quality.

Laser welding of thermoplastic components enables flexible production with economical benefits from small-scale production with varying geometries of the work pieces up to industrial mass production with high output rates.

Even laser welding of thermoplastics seems to be an investment-intensive production technology, considering the entire production chain using laser welding in comparison with conventional joining technologies may result in reduced efforts for component preparation and logistics as well as high joint quality and increased production output. Highly developed quality monitoring and online control during laser welding enables industrial production of thermoplastic parts by laser welding with reduced scrap rate compared to conventional joining processes. However, laser welding in industrial applications has to meet the economic conditions compared to competitive joining technologies.

This book gives a basic introduction to the principles, processes and applications of lasers for welding thermoplastic materials. The first part of the book gives an introduction into the structure and physical properties of plastics, especially to thermoplastics and thermoplastic elastomers, considering the interaction of material and radiation in the NIR and IR spectral ranges. Secondly, a brief introduction into the basics of laser radiation and laser sources used for plastic welding is given. The third part describes the main processes of laser welding thermoplastics as well as the possibilities of process control, design of joint geometry, material compatibilities and adaption of absorption of plastics to NIR radiation. The fourth part of the book will explain applications of laser welding plastics by several industrial case studies.

The book is targeted at students in physics, material science, mechanical engineering, chemistry and other technical subject areas in universities and universities of applied sciences as well as engineers in product and/or process development and production engineers in the field of automotive, consumer goods, electronics, medical devices, textiles and others who will use or already use laser welding of plastics.

I want to give special thanks to all who supported me by realization of the book. Special thanks go to Mr. Brunnecker from LPKF, Mr. Hinz from Leister and Mr. Rau from bielomatik for their support by case studies from industrial applications of laser welding plastics, pointing out the outstanding technical and economical opportunities of this process today.

Dr.-Ing. Rolf Klein, Groß-Umstadt, Germany, May 2011

1
Material Properties of Plastics

1.1
Formation and Structure

The basic structure of plastics (or polymers) is given by macromolecule chains, formulated from monomer units by chemical reactions. Typical reactions for chain assembling are polyaddition (continuous or step wise) and condensation polymerization (polycondensation) [1] (Figure 1.1).

- **Polyaddition as chain reaction**: Process by chemical combination of a large number of monomer molecules, in which the monomers will be combined to a chain either by orientation of the double bond or by ring splitting. No byproducts will be separated and no hydrogen atoms will be moved within the chain during the reaction. The process will be started by energy consumption (by light, heat or radiation) or by use of catalysts.
- **Polyaddition as step reaction**: Process by combination of monomer units without a reaction of double bonds or separation of low molecular compounds. Hydrogen atoms can change position during the process.
- **Polycondensation**: Generation of plastics by build up of polyfunctional compounds. Typical small molecules like water or ammonia can be set free during the reaction. The reaction can occur as a step reaction.

The monomer units are organic carbon-based molecules. Beside carbon and hydrogen atoms as main components elements like oxygen, nitrogen, sulfur, fluorine or chlorine can be contained in the monomer unit. The type of elements, their proportion and placing in the monomer molecule gives the basis for generating different plastics, as shown in Table 1.1.

The coupling between the atoms of a macromolecular chain happens by primary valence bonding [2]. The backbone of the chain is built by carbon atoms linked together by single or double bonding. Given by the electron configuration of carbon atoms, the link between the carbon atoms occurs at a certain angle, for example, for single bonding at an angle of 109.5°. Atoms like hydrogen, which are linked to the carbon atoms, hinder the free rotation of the carbon atoms around the linking axis.

Laser Welding of Plastics, First Edition. Rolf Klein.
© 2011 Wiley-VCH Verlag GmbH & Co. KGaA. Published 2011 by Wiley-VCH Verlag GmbH & Co. KGaA.

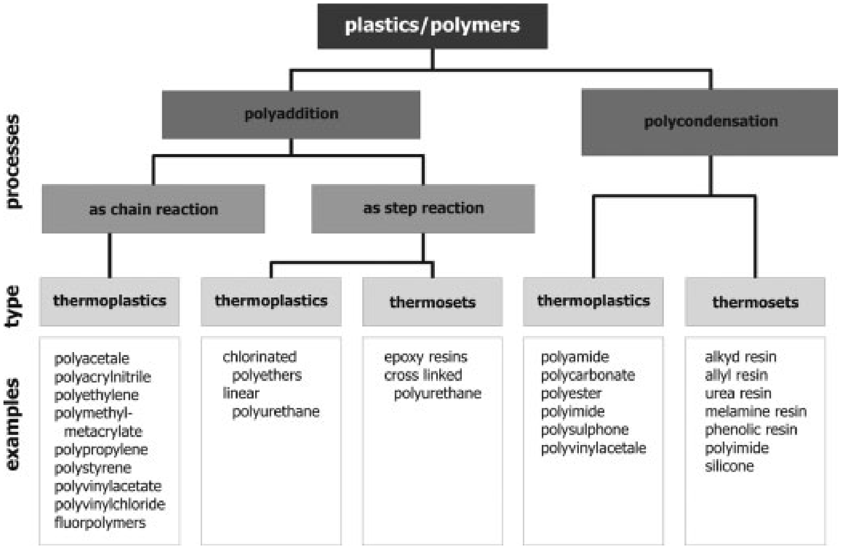

Figure 1.1 Processes for generating plastics and examples [1].

The “cis”-link of carbon atoms has the highest bonding energy while the "trans"-link has the lowest (Figure 1.2) [3].

Depending on the type of bonding partners several chain conformations are possible. Examples of such conformations are zig-zag conformation (e.g., PE or PVC) or helix conformation (e.g., PP, POM or PTFE) (Figure 1.3) [2].

Table 1.1 Examples of some common plastics and their monomers.

Monomer		Polymer	
Ethylene	$CH_2=CH_2$	Polyethylene (PE)	$-[CH_2-CH_2]_n-$
Propylene	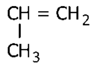 $\underset{CH_3}{\underset{\vert}{CH}}=CH_2$	Polypropylene (PP)	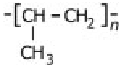 $-[\underset{CH_3}{\underset{\vert}{CH}}-CH_2]_n-$
Vinylchloride	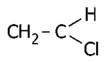 $CH_2-C\begin{smallmatrix}H\\Cl\end{smallmatrix}$	Polyvinylchloride (PVC)	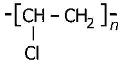 $-[\underset{Cl}{\underset{\vert}{CH}}-CH_2]_n-$
Caprolactame	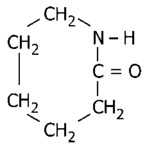	Poly(E-Caprolactame) (PA6)	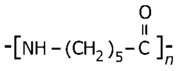 $-[NH-(CH_2)_5-\overset{O}{\overset{\Vert}{C}}]_n-$
Tetraflourethylene $CF_2=CF_2$	Polytetraflourethylene (PTFE)	$-[CF_2-CF_2]-$	$-[CF_2-CF_2]_n-$

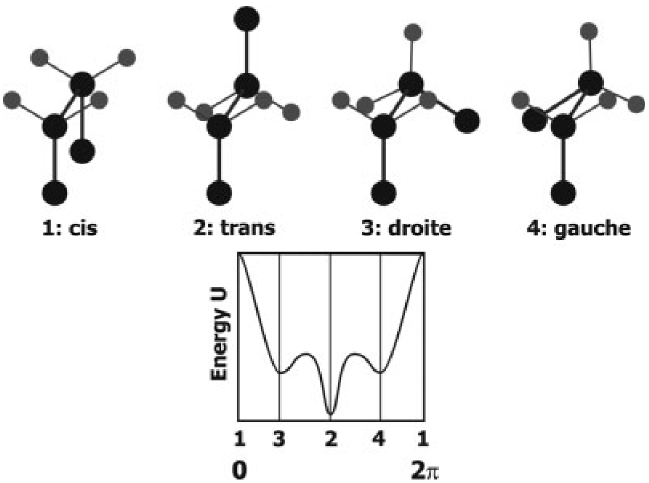

Figure 1.2 Potential energy for rotation of ethylene molecules around the carbon-linking axis [3].

The chain length and by this also the molecular weight of macromolecules have a statistical distribution [4] (Figure 1.4). By influencing the conditions of the polymerization process, the average molecular weight and the width of the distribution function can be controlled within certain limits.

During the polymerization process, depending on the type of polymer, side chains can be built to the main chain in a statistical way [5]. As for the length of the main chain, frequency and length of the side chains depend on the macromolecular structure and the physical/chemical conditions of the polymerization process [6].

An example for the order of size of macromolecules is the length and width of polystyrene molecules with an average molecular weight of 10^5. Corresponding to the molecular weight the macromolecular chain consists of a number of approximately

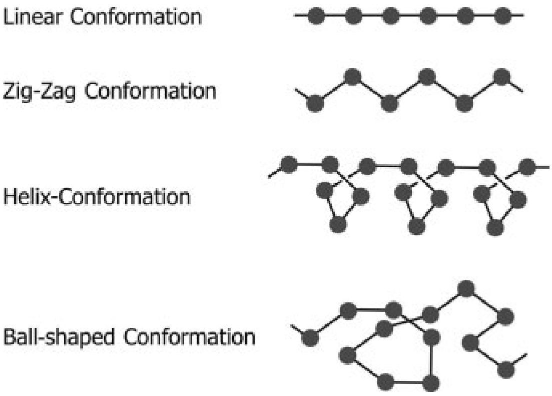

Figure 1.3 Conformation types of macromolecules.

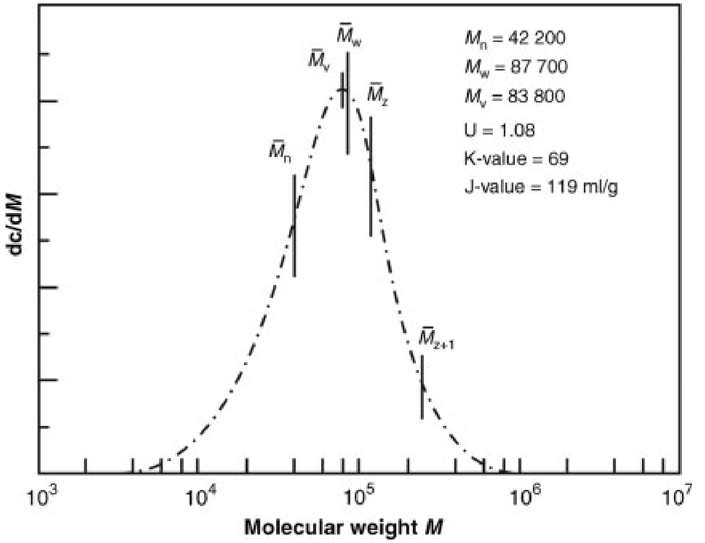

Figure 1.4 Statistical distribution of macromolecule chain length using polyvinylchloride (PVC) as an example [4].

2×10^5 carbon atoms. The average distance between each carbon atom is 1.26×10^{-10} m. Using this distance and the number of atoms in the chain takes to a length of 25×10^{-6} m and $4\text{–}6 \times 10^{-10}$ m width for a stretched chain.

The statistical forming of the macromolecular structure of plastics results in the fact that physical properties of plastics, like temperatures of phase changes, can only be given as average values. Unlike materials like metals, phase changes of plastics occur in certain temperature ranges. The width of such temperature ranges is dependent on the homogeneity of the materials structure [6].

The physical and chemical structure of the macromolecule is given by the primary valence bonding forces between the atoms (Figure 1.5) [1]. The secondary valence bonding forces, like dispersion bonding, dipole bonding or hydrogen bridge bonds, have a direct influence to the macroscopic properties of the plastic like mechanical, thermal, optical, electrical or chemical properties.

The secondary valence forces are responsible for the orientation of the macromolecules among themselves [6–8]. During processing of plastics the orientation of molecule segments can result in an orientation of segments of the macromolecular chain. Under suitable conditions, like specific placements of atoms in the monomer structure and by this within the macromolecular chain, a partial crystallization of the plastic is possible. The strength of the secondary valences is directly correlated with the formation of the macromolecular chains. The strength increases with increasing crystallization, with higher polarity between the monomer units, decreased mobility of molecule segments and increased strapping of chains with others. Because of the small range and low energy of secondary valences in comparison with the main valences, effects caused by them are strongly temperature dependent.

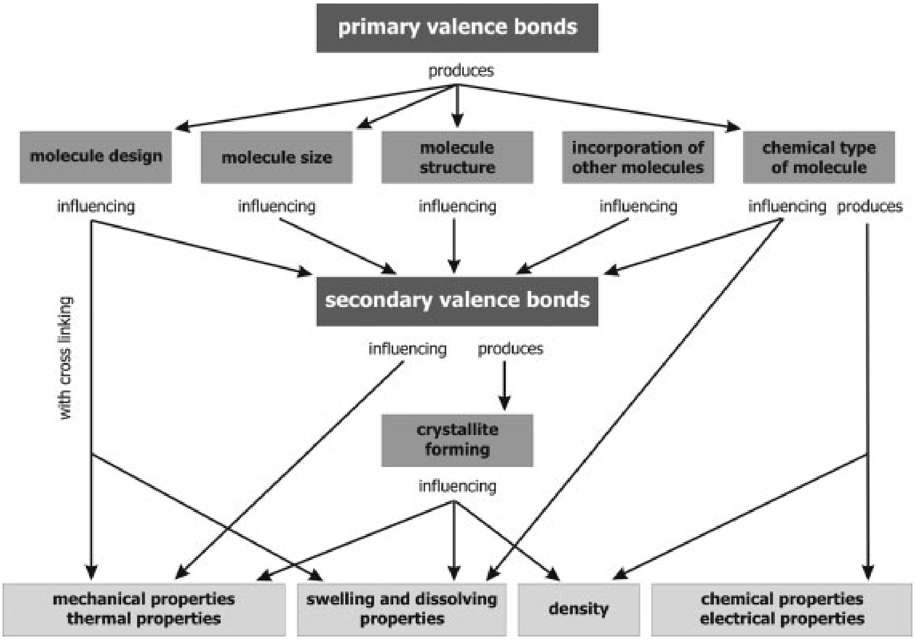

Figure 1.5 Context of molecular and macroscopic material properties [1].

In the case of possible atom bonds between macromolecular chains, a crosslinking of the molecule structure can happen. While secondary valences can be dissolved with increasing temperatures and rebuilt during cooling, atom bonds cannot dissolve reversibly. By dissolving these bonds the plastic will be chemically destroyed.

Taking the chemical structure and the degree of crosslinking between the macromolecules, plastics can be classified as thermoplastics, elastomers and thermosets (Figure 1.6) [1]. Compounds like polymer blends, copolymers and composite materials are composed of several base materials. This composition can be done on a physical basis (e.g., polymer blends or composite materials) or on a chemical basis (copolymers).

1.2
Types of Plastics

Caused by the macromolecular structure and the temperature-dependent physical properties plastic materials are distinguished into different classes. Figure 1.7 gives an overview of the classification of plastics with some typical examples.

Thermoplastics are in the application range of hard or tough elasticity and can be melted by energy input (mechanical, thermal or radiation energy). Elastomers are of soft elasticity and usually cannot be melted. Thermosets are in the application range of hard elasticity and also cannot be melted.

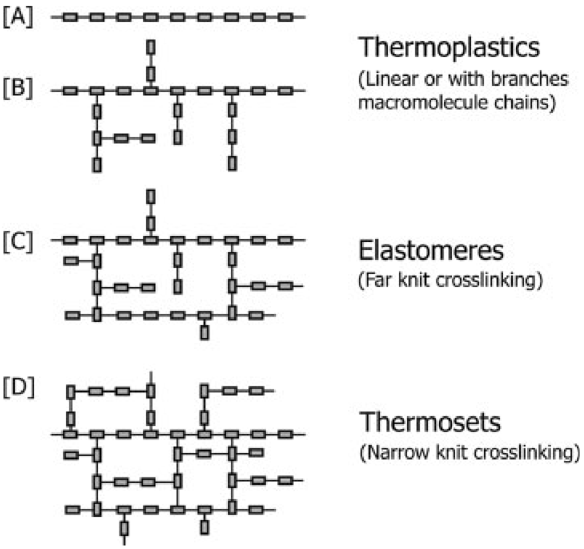
[A]
[B]
Thermoplastics
(Linear or with branches macromolecule chains)
[C]
Elastomeres
(Far knit crosslinking)
[D]
Thermosets
(Narrow knit crosslinking)

Figure 1.6 Principle structure of linear (A), with side chains (B) and crosslinked macromolecules (C + D). Chain structure (A) and (B) are thermoplastic types, structures with low crosslinking (C) elastomers and with strong crosslinking thermosets (D).

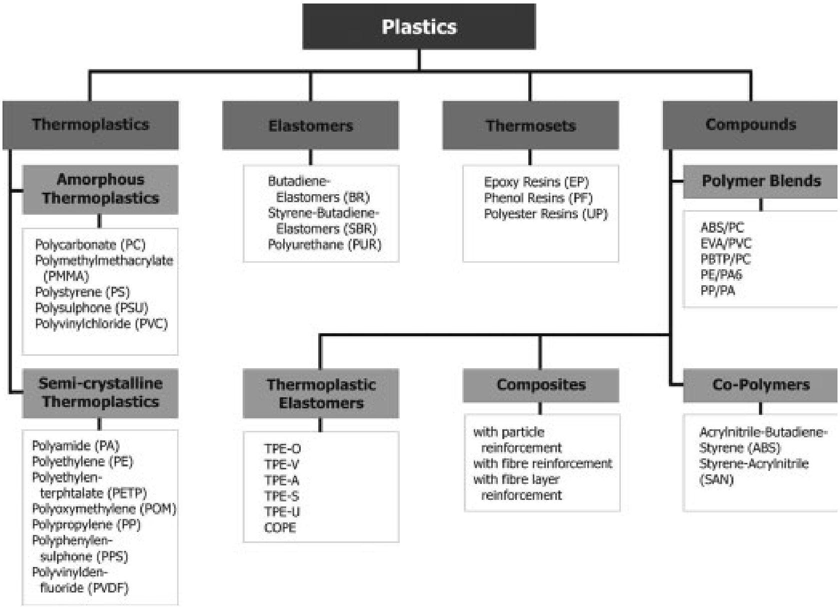

Figure 1.7 Classification of plastics.

Plastics as polymer mixtures are composed of two or more polymers with homogeneous or heterogeneous structure. Homogeneous structures are for example copolymers or thermoplastic elastomers, built by chemical composition of two or more different monomer units in macromolecules. When using thermoplastic monomers such plastic material can be melted by thermal processes. Heterogeneous structures are for example polymer blends or thermoplastic elastomers, built by physical composition of separate phases from different polymers. Polymer blends with thermoplastic components also can be melted by thermal processes.

Plastic composites consist of a polymeric matrix with integrated particles or fibers. When using thermoplastics as matrix, such composites can be melted. If thermosets are used as matrix the composite cannot be melted.

Characteristic of the different classes of plastics are the phase transitions that occur in contrast to metallic materials in temperature intervals. Data given in tables (e.g., [9]), are usually mean values of such temperature intervals.

Phase-transition temperatures are dependent on the molecular structure of the plastic. Limited mobility of the molecule chains, for example, by loop forming, long side chains or high molecular weight cause an increased phase-transition temperature [6]. A large variance of the molecule chain length or number and length of side chains also have an effect on the spreading of the phase-transition ranges.

1.2.1
Thermoplastic Resins

Thermoplastic resins consist of macromolecular chains with no crosslinks between the chains. The macromolecular chains themselves can have statistical oriented side chains or can build statistical distributed crystalline phases. The chemistry and structure of thermoplastic resins have an influence on the chemical resistance and resistance against environmental effects like UV radiation. Naturally, thermoplastic resins can vary from optical transparency to opaque, depending on the type and structure of the material. In opaque material, the light is internally scattered by the molecular structure and direct transmission of light is very poor with increasing material thickness.

Thermoplastic resins can be reversibly melted by heating and resolidified by cooling without significant changing of mechanical and optical properties. Thus, typical industrial processes for part manufacturing are extrusion of films, sheets and profiles or molding of components.

The viscosity of the melt is dependent on the inner structure, like average molecular weight and spreading of the molecular weight around the average value. According to DIN EN ISO 1133:2005–2009 [10], the melt-flow index (MFI) is a measure for the melt viscosity. The MFI gives the amount of material that will be extruded in 10 min through a standardized nozzle diameter by using a determined force.

Low MFI values signify high viscosity with glutinous flow behavior of the melt (materials for extrusion). Increasing MFI values result in decreasing viscosity and lighter melt flow behavior (materials for molding). It has to be noted that MFI values

Table 1.2 Examples for amorphous thermoplastic resins with typical material properties according to [1].

Resin	Temperature of use [°C]	Specific weight [g/cm^3]	Tensile strength [N/mm^2]
PC	−40–120	1.2	65–70
PMMA	−40–90	1.18	70–76
PS	−20–70	1.05	40–65
PSU	−100–160	1.25	70–80
PVC	−15–60	1.38–1.24	40–60

are only a rough estimation for the melt flow behavior because the structure viscosity of thermoplastics strongly depend on the loading [11].

The macromolecular structure of thermoplastics is given by the chemical structure of the monomer units, the order of the monomer units in the molecule chain and the existing side chains. A pure statistical distribution of the macromolecules results in an amorphous material structure, but also semicrystalline structures can occur depending on the material. Therefore, thermoplastic resins are differentiated into amorphous and semicrystalline types [1, 6].

1.2.1.1 **Amorphous Thermoplastics**

Amorphous thermoplastic resins consist of statistical oriented macromolecules without any near order. Such resins are in general optically transparent and mostly brittle. Typical amorphous thermoplastic resins are polycarbonate (PC), polymethylmethacrylate (PMMA), polystyrene (PS) or polyvinylchloride (PVC).

Table 1.2 shows examples of amorphous thermoplastic resins with typical material properties.

Temperature state for application of amorphous thermoplastic resins is the so called glass condition below the glass temperature T_g. The molecular structure is frozen in a definite shape and the mechanical properties are barely flexible and brittle (Figure 1.8).

On exceeding the glass temperature, the mechanical strength will decrease by increased molecular mobility and the resin will become soft elastic. On reaching the flow temperature T_f the resin will come into the molten phase. Within the molten phase the decomposition of the molecular structure begins by reaching the decomposition temperature T_d.

1.2.1.2 **Semicrystalline Thermoplastics**

Semicrystalline thermoplastic resins consist of statistical oriented macromolecule chains as amorphous phase with embedded crystalline phases, built by near-order forces. Such resins are usually opaque and tough elastic. Typical semicrystalline thermoplastic resins are polyamide (PA), polypropylene (PP) or B (POM) (Table 1.3).

The crystallization grade of semicrystalline thermoplastic depends on the regularity of the chain structure, the molecular weight and the mobility of the molecule chains, which can be hindered by loop formation [6]. Due to the statistical chain

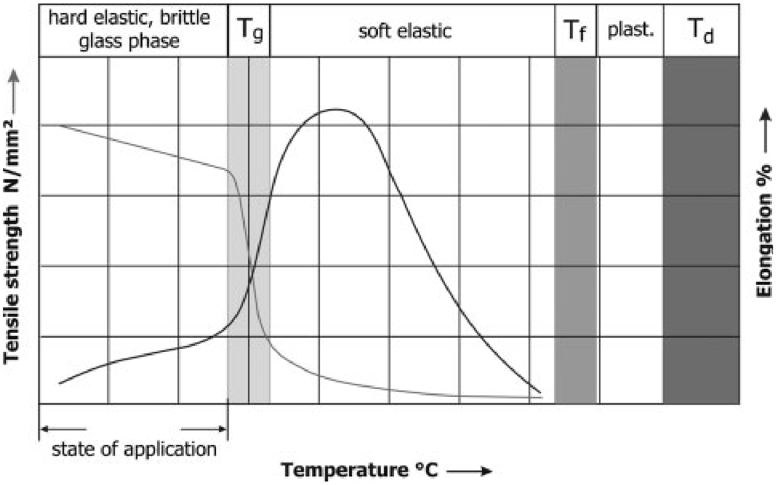

Figure 1.8 Temperature behavior of amorphous thermoplastic resins (schematically) [1].

structure of plastics complete crystallization is not feasible on a technical scale. Maximum technical crystallization grades are of the order of approximately 80% (see Table 1.3).

The process of crystallization can be controlled by the processing conditions. Quick cooling of the melt hinders crystallization. Slowly cooling or tempering at the crystallization temperature will generate an increased crystallization grade. Semicrystalline thermoplastics with low crystallization grade and small crystallite phases will be more optically transparent than materials of high crystallization grade and large crystallite phases.

Below the glass temperature T_g the amorphous phase of semicrystalline thermoplastics is frozen and the material is brittle (Figure 1.9). Above the glass temperature, usually the state of application [1], the amorphous phase thaws and the macromolecules of the amorphous phase gain more mobility. The crystalline phase still exists and the mechanical behavior of the material is tough elastic to hard. Above the

Table 1.3 Examples for semicrystalline thermoplastic resins with typical material properties according to [1].

Resin	Temperature of use [°C]	Crystallization grade [%]	Specific weight [g/cm^3]	Tensile strength [N/mm^2]
PA 6	−40–100	20–45	1.12–1.15	38–70
HDPE	−50–90	65–80	0.95–0.97	19–39
PETP	−40–110	0–40	1.33–1.38	37–80
PP	−5–100	55–70	0.90–0.91	21–37
PPS	<230	30–60	1.35	65–85
PVDF	−30–150	−52	1.77	30–50

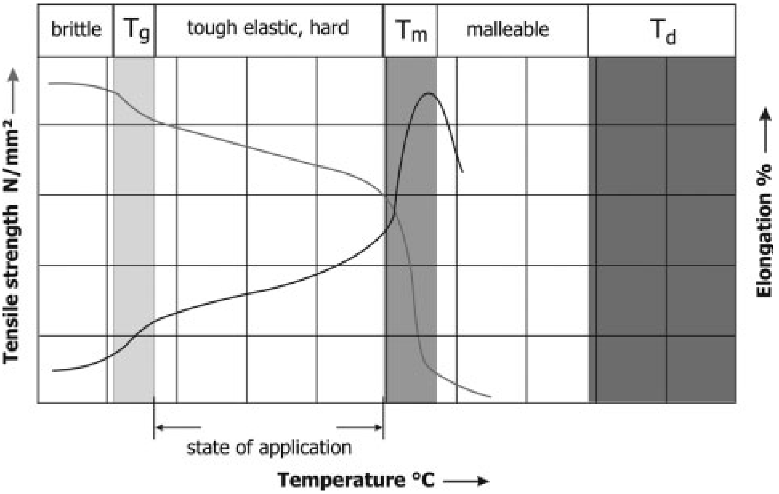

Figure 1.9 Temperature behavior of semicrystalline thermoplastic resins (schematically) [1].

crystal melt temperature T_m the crystalline phase also starts to melt and the material becomes malleable. As for amorphous thermoplastics, the flow ability of semicrystalline thermoplastics in the molten phase is characterized by the melt-flow index MFI.

The melt temperature of semicrystalline thermoplastics depends among other things on the size of the crystallites and the ratio between the amorphous and crystalline phases. Larger size and a higher proportion of crystallites will increase the melt temperature (Figure 1.10) [12]. As with amorphous thermoplastics, degradation of semicrystalline thermoplastics will start in the molten phase by exceeding the decomposition temperature T_d.

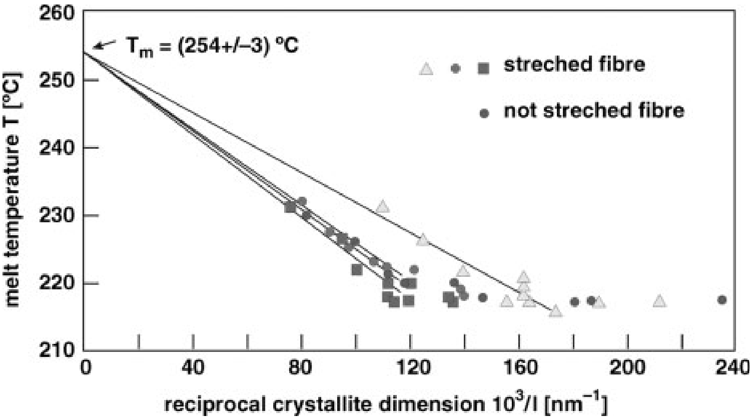

Figure 1.10 Influence of the crystallite size to the melt temperature for PA6 fiber material [12].

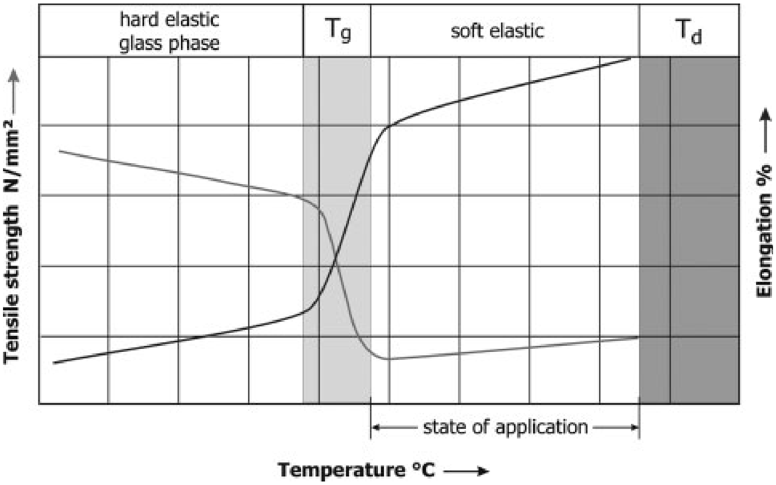

Figure 1.11 Temperature behavior of mechanical properties of elastomers (schematically) [1].

1.2.2
Elastomers

Elastomers are plastics with wide netlike crosslinking between the molecules. Usually, they cannot be melted without degradation of the molecule structure. Above the glass temperature T_g, as the state of application (Figure 1.11), elastomers are soft elastic. Below T_g they are hard elastic to brittle. The value of the glass temperature increases with increasing number of crosslinks. Examples of elastomers are butadiene resin (BR), styrene butadiene resin (SBR) or polyurethane resin (PUR) [13].

Raising temperature affects an increase of elasticity, caused by reducing the stiffening effects of the crosslinks and increasing the mobility of the molecule chains. On exceeding the decomposition temperature T_d, the atom bonding within and between the molecule chains will be broken and the material will be chemical decomposed.

1.2.3
Thermosets

Thermosets are plastic resins with narrow crosslinked molecule chains [1]. Examples of thermosets are epoxy resin (EP), phenolic resin (PF) or polyester resin (UP).

In the state of application (Figure 1.12) thermosets are hard and brittle. Because of the strong resistance of molecular movement caused by the crosslinking, mechanical strength and elasticity are not temperature dependent, as with thermoplastics or elastomers.

Thermosets cannot be melted and joining by thermal processes like ultrasonic welding or laser welding is not possible. On exceeding the decomposition temperature T_d, the material will be chemical decomposed.

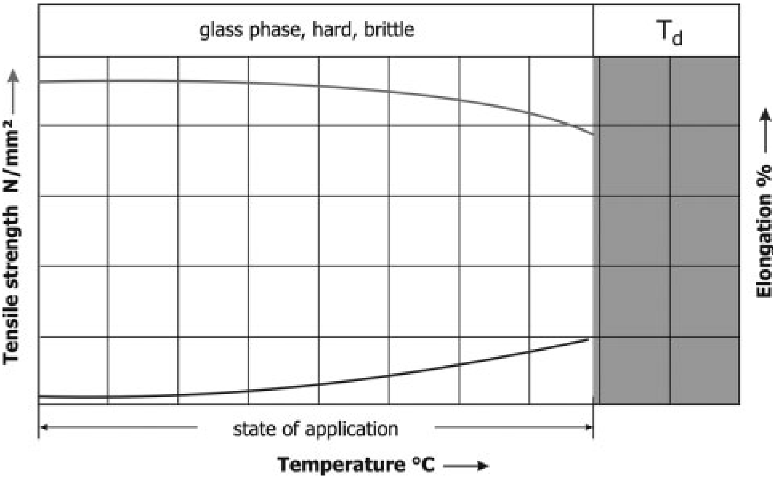

Figure 1.12 Temperature behavior of mechanical properties of thermosets (schematically) [1].

1.2.4
Polymer Compounds

The term polymer compound summarizes materials like polymer blends, copolymers and thermoplastic elastomers (TPEs). Polymer compounds are physical or chemical composed from different polymers to achieve special material properties like elasticity or fatigue strength.

1.2.4.1 Polymer Blends

Polymer blends are combinations of different polymers [14], usually mixed in the molten state. After solidification the different polymeric proportions are combined by physical but not chemical reaction (Figure 1.13).

The extent to which a mixture can be achieved depends on the miscibility of the polymers among each other. Chemical, thermal or mechanical properties of polymer

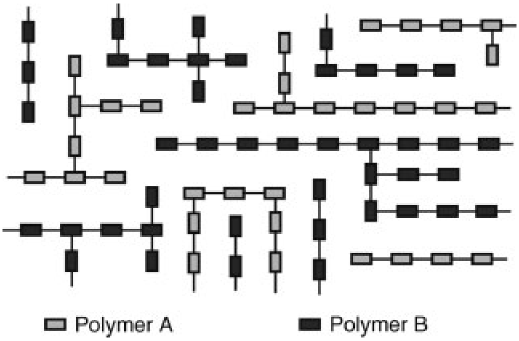

Figure 1.13 Schematic molecule structure of polymer blends.

Table 1.4 Examples of thermoplastic polymer blends. Condition of application, specific weight and typical mechanical strength [15].

Resin	Temperature of use [°C]	Specific weight [g/cm^3]	Tensile strength [N/mm^2]
PC/ABS	<90	1.10–1.16	45–55
PC/ASA	<105	1.15	53–63
PPE/SB	<100	1.06	52–64

blends are defined by the type of different polymers used and their proportions within the polymer blend.

Polymer blends, designed from thermoplastic materials, can be joined together by thermal processes like ultrasonic or laser welding. Examples of thermoplastic polymer blends are PC/ABS, PC/ASA or PPE/SB (see Table 1.4).

1.2.4.2 **Copolymers**

Copolymers are built by chemical composition at least from two different monomer units. Processes to built up copolymers are block polymerization, group transfer polymerization or graft copolymerization [1, 6, 16]. Examples of copolymers are ABS or SAN (see Table 1.5).

Beside grade of polymerization, chain-length distribution, type of end groups and chain side branches, composition and distribution of monomer units inside the molecule chain have to be known to achieve specific chemical, thermal, optical or mechanical properties of the copolymer. Especially influential on the properties is the regularity of the chain composition, which means a statistical or more regular distribution of the different monomers within the molecule chain (Figure 1.14) [11].

1.2.4.3 **Thermoplastic Elastomers**

Thermoplastic elastomers (TPEs) are elastic, flexible polymers with similar qualities as elastomers or rubber but of a thermoplastic nature [17, 18]. TPEs close the gap between stiff thermoplastics and vulcanized elastomers. Due to the thermoplastic nature, TPEs can be processed to parts by extrusion and molding and can also be joined together or to other thermoplastic material by adhesive bonding, solvent bonding and welding processes or by coextrusion and multicomponent injection molding.

Table 1.5 Examples of thermoplastic copolymers. Conditions of application, specific weight and typical mechanical strength [1].

Resin	Temperature of use [°C]	Specific weight [g/cm^3]	Tensile strength [N/mm^2]
ABS	−30–95	1.04	38–58
COC	−50–130	1.02	46–63
SAN	−20–80	1.08	70–79

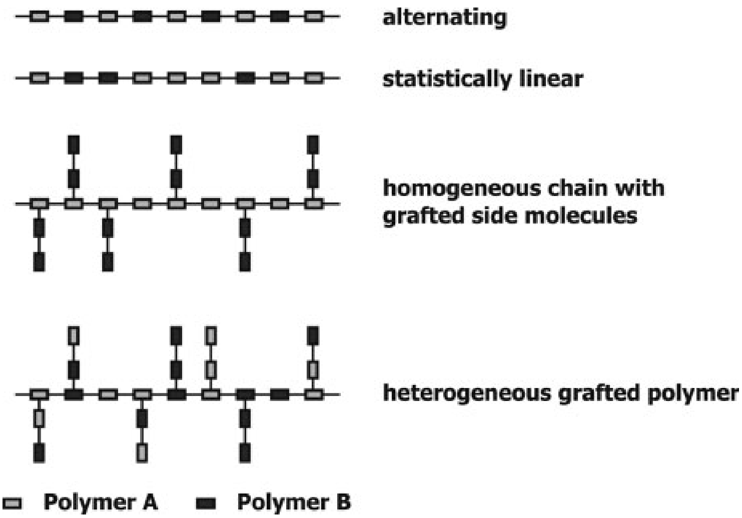
alternating
statistically linear
homogeneous chain with grafted side molecules
heterogeneous grafted polymer
Polymer A
Polymer B

Figure 1.14 Schematic build up of copolymers.

In principal, the material group of TPEs consists of two different base structures as a physical or chemical mixture, polymeric blends and block copolymers. Depending on the molecular structure given by the thermoplastic component, both of them could be amorphous or semicrystalline.

TPE blends consist of a thermoplastic matrix, for example, PP or PE, and softer particles, for example, EPDM, which are well dispersed in the matrix (see Figure 1.15). Two types of TPE blends are available:

- Thermoplastic vulcanization elastomers (TPE-V): are TPE blends with a chemically crosslinked elastomer proportion produced by dynamic vulcanization that is a process of intimate melt mixing of a thermoplastic polymer like PP and a suitable reactive elastomer like EPDM.
- Thermoplastic polyolefin elastomers (TPE-O): two-component elastomer systems consisting of elastomers like EPR and EPDM finely dispersed in a thermoplastic polyolefin (e.g., PP).

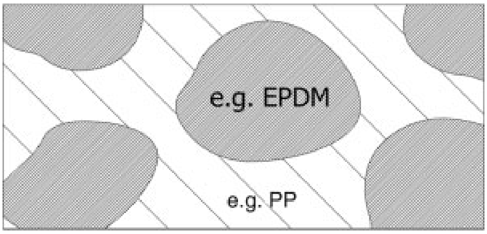

Figure 1.15 Schematic structure of TPE blends [18].

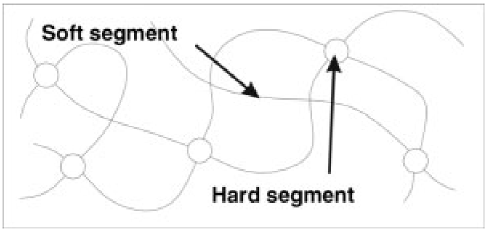

Figure 1.16 Schematic structure of TPE block copolymers [18].

In *block copolymers*, the hard and soft segments are linked within the macromolecules (Figure 1.16). Materials used as hard segments are for example, styrene and for soft segments butylenes. Common block copolymers are:

- Styrene block copolymers (SBC, TPE-S): consist of block segments of styrene monomer units and elastomer monomer units. Their most common structure are linear A–B–A block type: styrene-butadiene-styrene (SBS), styrene-isoprene-styrene (SIS), styrene-ethylene/butylenes-styrene (SEBS) or styrene-ethylene/propylene-styrene (SEPS) type.
- Thermoplastic polyurethane elastomers (TPE-U): were first commercialized in the 1950s and are one of the oldest TPE types in existence.
- Copolyester elastomers (COPE): are a family of engineering thermoplastic elastomers based on copolyester chemistry. They have both hard and soft parts. The hard segment is a semicrystalline polybutylene terephthalate (PBT), while the soft segment is made of amorphous glycol.
- Copolyamides (COPA, TPE-A): also called polyether block amides (PEBA), are extremely versatile, high-performance engineering thermoplastic elastomers that combine the properties of nylon and elastomers. The polymer structure consists of a regular linear chain of rigid polyamide segments, usually based on polyamide PA 6 or high-performance PA12 infiltrated with flexible polyether segments.

Depending on the type of TPE, a wide variation from very soft to more rigid materials is given. The hardness values can vary in a wide range of shore A values. Table 1.6 gives an overview about typical thermal and mechanical properties of TPEs.

Table 1.6 Examples of thermoplastic elastomers. Condition of application, specific weight and typical hardness values [18].

Resin	Temperature of use [°C]	Specific weight [g/cm^3]	Shore A hardness
TPE-A	−40–170	1.01	70–90
TPE-E	−65–150	>1	70–80
TPE-U	−50–135	>1	70–90
TPE-0	−60–110	089–1.00	40–90
TPE-V	−60–110	089–1.00	40–90
TPE-S	−50–100	0.89–1.30	10–90

Table 1.7 Examples for thermoplastic composites with glass fibers. Condition of application, proportion of glass fibers, specific weight and typical mechanical strength [15].

Resin	Temperature of use [°C]	Proportion of glass fibers [%]	Specific weight [g/cm^3]	Tensile strength [N/mm^2]
PA6/GF30	<200	30	1.36	65–170
PC/GF30	<140	30	1.44	70–110
PP/GF30	<110	30	1.11–1.14	60–100
PPS/GF60	<240	60	1.90	170
PC/ABS/GF20	<95	20	1.25	75

Because of low melting temperatures TPEs can easily be processed by molding or extrusion within a temperature range of 190–240 °C (depending on the TPE type). But to achieve a good homogenization during the processing high shear forces have to be used.

Uncolored TPEs can vary from optical transparency to opaque, depending on type and structure of the material. In opaque material, the light is internally scattered by the molecular structure and direct transmission of light is very poor with increasing material thickness.

Most of the TPEs show good weather and chemical resistance. Natural TPEs are usually colorless transparent or opaque and can be easily colorized.

1.2.5
Polymer Composites

Polymer composites are composed of a polymer matrix material (thermoplastic or thermosets) with organic or inorganic fillers (Figure 1.17) [1] like mineral pigments, short fibers, long fibers, continuous fibers, paper or fabrics to enhance the mechanical properties for special applications.

Particles like mineral powder, wood flour or carbon black are used to increase the stiffness of the matrix material. The fatigue strength of the matrix material usually will be not increased, but is sometimes decreased. Short fibers, long fibers and continuous fibers from glass, carbon or aramid cause an increase of the fatigue strength (Figure 1.18), although the effect depends on the orientation of the fibers [19].

Continuous fibers from glass, carbon or aramid will influence the mechanical properties of the polymer compound by the adjustable orientation of the fibers. Besides increasing fatigue strength and stiffness the temperature-dependent expansion of the compound can also be decreased [20].

Polymer compounds with thermoplastic matrix usually can be melted by thermal processes like welding, but not polymer compounds with thermoset matrix.

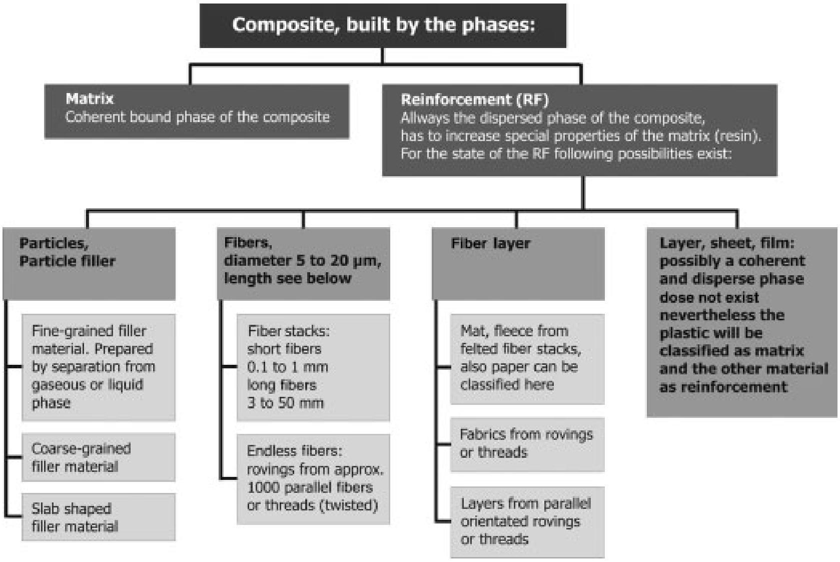
Composite, built by the phases:
Matrix
Coherent bound phase of the composite
Reinforcement (RF)
Allways the dispersed phase of the composite,
has to increase special properties of the matrix (resin).
For the state of the RF following possibilities exist:
Particles,
Particle filler
Fine-grained filler material. Prepared by separation from gaseous or liquid phase
Coarse-grained filler material
Slab shaped filler material
Fibers,
diameter 5 to 20 µm,
length see below
Fiber stacks:
short fibers
0.1 to 1 mm
long fibers
3 to 50 mm
Endless fibers:
rovings from approx. 1000 parallel fibers or threads (twisted)
Fiber layer
Mat, fleece from felted fiber stacks, also paper can be classified here
Fabrics from rovings or threads
Layers from parallel orientated rovings or threads
Layer, sheet, film:
possibly a coherent and disperse phase dose not exist nevertheless the plastic will be classified as matrix and the other material as reinforcement

Figure 1.17 Classification of polymer composites [1].

1.3
Thermal Properties

Successful processing of thermoplastic resins by laser radiation needs a basic knowledge of the temperature dependence of the thermal material properties. The temperature ranges of the different phase transitions (e.g., glass transition and softening temperatures of amorphous thermoplastics, melt temperatures of crystalline phases of semicrystalline thermoplastics) but also material properties linked

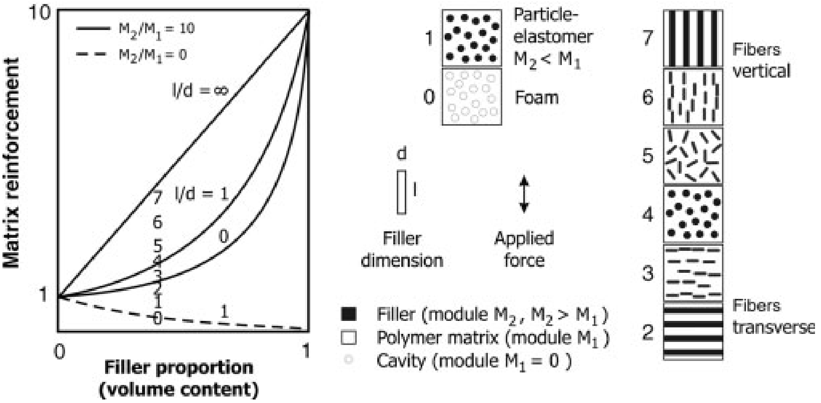

Figure 1.18 Dependence of the reinforcement on the type and structure of the filler material [11].

with heat conduction (e.g., heat capacity, heat conduction or specific volume) influence of laser power and processing speed of a laser application.

Thermal properties of thermoplastics strongly depend on the molecular structure. Orientation and length of macromolecular chains, number and distribution of side chains, crystalline structure or level of molecular links influence such thermal properties.

Typical phase transitions of thermoplastic resins are glass transition, melting of crystallites and thermal degradation of macromolecular chains. Physical properties like specific volume, heat capacity, heat conduction or thermal conduction, which characterize the material behavior regarding thermal energy absorption and transport, partly show a distinctive dependence of the material temperature and vary particularly in the ranges of phase transitions.

1.3.1
Phase Transitions

Depending on the physical and chemical structure of thermoplastic resins, the following phase transitions will occur on increasing material temperature [1, 6]:

1.3.1.1 Glass Transition (T_g)

Below the glass temperature (T_g) the mobility of the molecules (Brown's macromobility) is strongly curbed by intermolecular interaction. There are no position-change processes and only restricted thermal induced movements of chain segments or side chains. At the glass temperature Brown's micromobility of chain segments and side chains starts to occur and the plastic becomes softer but is still mechanical stable. Before reaching the glass temperature second-order relaxation processes are possible, single-molecule segments obtain a restricted mobility.

1.3.1.2 Flow Temperature (T_f)

On increasing temperature the hindering influence of intermolecular interaction decreases. On reaching the flow temperature (T_f) complete macromolecular chains can slip against each other (Brown's macromobility). The amorphous structures of the plastic become softer and start to melt. No chemical degradation of the macromolecules of the plastic will occur in this state.

1.3.1.3 Crystallite Melting Temperature (T_m)

By reaching the crystallite melting temperature (T_m) of semicrystallite thermoplastics the near forces, responsible for crystallite forming, will vanish and the crystallites start to melt. Because the temperature range of crystallite melting exceeds the flow temperature of the amorphous state, the entire thermoplastic will be plasticized. As long as no thermal degradation will occur in the molten phase, the resin can reversibly get back into the solidified state by cooling. Depending on the cooling conditions (speed and duration of cooling) crystallite phases will again be generated. The size and distribution of these crystallites can be differing from the original status.

Table 1.8 Examples for phase-transition temperatures for thermoplastic resins [1, 6].

Resin	Glass temp. T_g (°C)	Flow temp. T_f (°C)	Crystallite melt temp. T_m (°C)	Decomposition T_d (°C)
Amorphous Thermoplastics				
PC	145	240		about 327
PMMA	104	180		226–256
PS	97	160		318–348
PVC	80	175		about 250
Semicrystalline Thermoplastics				
HDPE	−95		130–146	360–390
PA 6	40		220	about 327
PEEK	120		340	
PP	−18		160–208	336–366
PTFE	−20		327	424–513

1.3.1.4 Thermal Decomposition (T_d)

Exceeding the decomposition temperature (T_d) in the molten phase of thermoplastics and thermoplastic elastomers, the macromolecules start to decompose caused by intensive thermal oscillations. Separation of monomer units (e.g., PMMA) [6], oxidation or chemical conversion into reaction products like HCl during decomposition of PVC are possible reactions [4]. The resin will be irreversibly chemically modified.

The decomposition products will be separated as gaseous phase or will remain as components in the residual material. The start of decomposition, which means the value of the decomposition temperature, is greatly dependent on the intensity and duration of the thermal input. The decomposition temperature is lower by long duration and low intensity than by short duration and high intensity of the thermal input.

For laser welding of thermoplastic resins and thermoplastic elastomers phase transitions in the thermal range from room temperature up to the start of degradation are of interest. Table 1.8 summarizes phase-transition temperatures of typical thermoplastic resins. The indicated temperatures refer to average values or temperature ranges of phase transitions.

Plasticization of amorphous thermoplastics starts with exceeding the flow temperature (T_f) and for semicrystalline thermoplastics with exceeding the crystallite melting temperature (T_m). Figure 1.19 shows for a number of thermoplastics a compilation of the temperature ranges of the molten phase and the start of decomposition (from [1]). The decomposition temperatures in Table 1.8 or Figure 1.19 are dependent on the reference values of thermal degradation under vacuum [21] or estimated values (from [1]) and can possibly differ somewhat under atmospheric influence.

Increasing the temperature of a solid material will be done by energy input for example, using friction energy, ultrasonic energy or absorption of radiation. In the

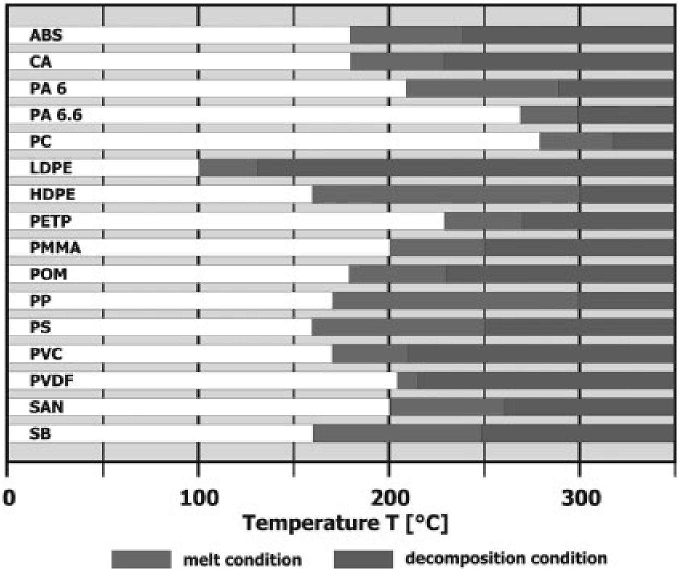

Figure 1.19 Melt-temperature ranges and decomposition in the molten state of some thermoplastic resins [1].

range of phase transitions an additional energy input is necessary to start the phase transition. For amorphous thermoplastics phase transition will occur at the flow temperature and for semicrystalline thermoplastics at the crystallite melting temperature. To start a phase transition an additional energy input as melting energy (or melting enthalpy) is necessary. The height of the melting energy for semicrystalline thermoplastics is dependent on the grade of crystallinity of the material.

Table 1.9 gives examples of the melting energy relative to the mass proportion of the crystalline phase of semicrystalline thermoplastics.

1.3.2
Specific Volume

The volume of thermoplastics expands with increasing temperature. Caused by more intense thermal oscillation of atoms and molecule elements the balance positions of

Table 1.9 Melt energy for some typical semicrystalline thermoplastics [1].

Resin	Melting Energy Δ [J/g]
HDPE	310
PA 6	213
PETP	145
POM	333
PP	238

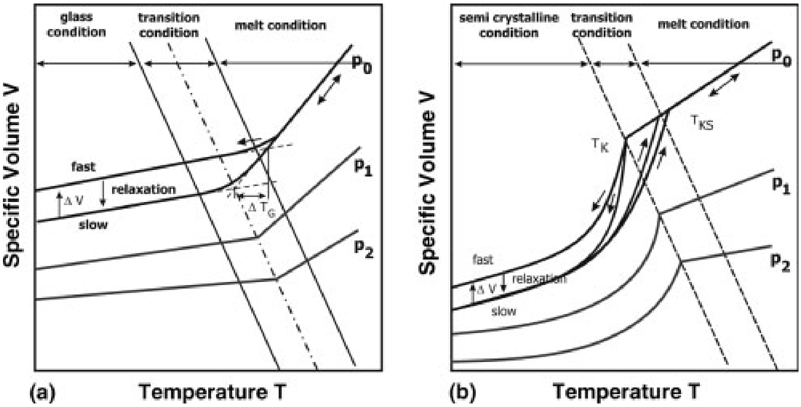

Figure 1.20 Schematic behavior of specific volume in dependence from the temperature for amorphous (a) and semicrystalline thermoplastics (b) [23].

the oscillation segments are moving apart [22]. As for example, heat capacity or heat conductivity, the type of bonding and caused by this the material structure is an important influence on the quantity of the volume change. For the temperature dependence of the specific volume a distinction is given between amorphous and semicrystalline plastics (Figures 1.20a and b) [23].

Within the glass state of amorphous thermoplastics the specific volume shows a linear increase with increasing temperature (see Figure 1.20a) [23], described by Equation 1.1:

$$V(T) = V_0(1 + \beta \cdot \Delta T) \tag{1.1}$$

V_0: volume at start of heating
β: cubic expansion coefficient
ΔT: increase of temperature.

On exceeding the glass-transition temperature the linear increase rapidly rises, depending on the distribution of the molecular weight. This means with increasing temperature the increase of the specific volume will be intensified, caused by decreasing strength of molecular bonds in the molten state. In Figure 1.21a a graphic portrayal of the temperature-dependent course of the specific volume for some amorphous thermoplastics is given.

Below the glass temperature the volume change of semicrystalline thermoplastics rises almost linearly with increasing temperature. On exceeding the crystallite melting temperature a difference to the linear behavior occurs. The volume change on increasing temperature will be almost linear again if the plastic is completely plasticized. Figure 1.21b shows the temperature-dependent course of the specific volume from some semicrystalline thermoplastics.

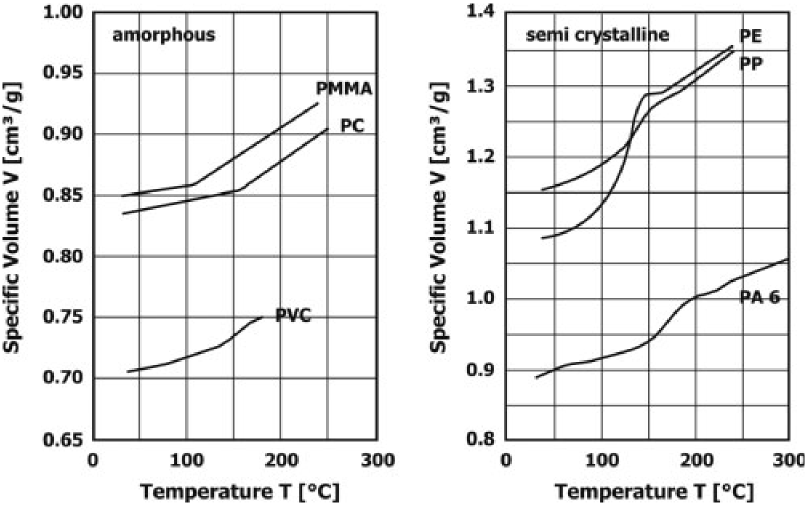

Figure 1.21 Specific volume of amorphous (left) and semicrystalline thermoplastics (right) in correlation with the temperature [23].

Depending on the cooling rate out of the molten state a different crystallization of the thermoplastic material can occur [24]. The faster the cooling the smaller will be the crystalline phases in dimension and they will be less numerous. The specific volume of a fast-cooled semicrystalline thermoplastic with low crystallization will be higher than of a slowly cooled material with high crystallization.

1.3.3
Heat Capacity

The heat capacity of a solid material is fixed by the ability of individual components (atoms, molecule segments or molecule chains) to carry out oscillations around their center positions [25]. Among other influences the strength of such oscillations is dependent on the bonding forces and the weight of atoms or molecule segments (molar weight). The oscillations are an addition of individual grid oscillations of atoms bound in a macromolecule, of group oscillations of molecular segments (elongation or tilt oscillations) and rotation oscillations of molecular segments.

Due to the covalent bonding of segments within the molecule chain and the coupling of molecule chains among themselves (e.g., second-order valence bonding, hydrogen bridge bonding or dipole bonding) the individual oscillations are not independent of each other. The individual oscillations will be composed of collective oscillations that will be spread as waves in all directions of the material. The frequency spectrum of the grid oscillations reaches from translation of the whole grid (frequency zero) up to maximum frequencies of 10^{13} to 10^{14} Hz caused by intermolecular bonding forces and the weight of the molecules.

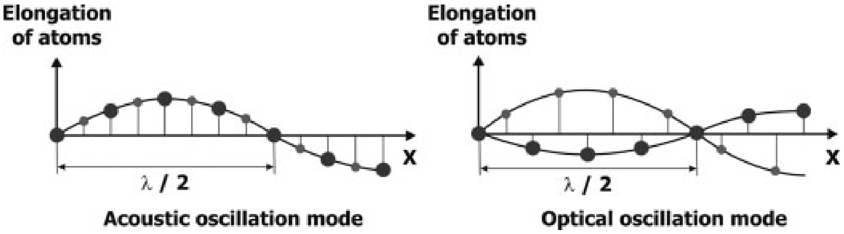

Figure 1.22 Principle portrayal of acoustic (left) and optical (right) oscillation modes of the grid segments. from [22].

Between adjoining grid segments in the molecule chain strong covalent bonding forces are prevalent while between different molecular chains considerably weaker bonding forces like van der Waals or dipole bonding exists [6]. The frequency spectrum of oscillations corresponds up to approximately 10^{12} Hz to a three-dimensional solid body. For higher frequencies the spectrum will change to the oscillation spectrum of isolated chain molecules [25].

The oscillation spectrum can be divided up into an acoustic and an optical mode. In the acoustic mode the grid segments are elongated in the same direction. In the optical mode the adjoining grid segments oscillate in contrary elongations (Figure 1.22) [22].

The optical mode of grid oscillations can be stimulated by absorption of electromagnetic radiation. By oscillation coupling between optical and acoustic modes an energy transfer occurs from optical to acoustical modes. A schematic drawing of the frequency spectrum for a linear molecule chain with two segments of alternating weights M_A and M_B are shown in Figure 1.23 for different mass proportions.

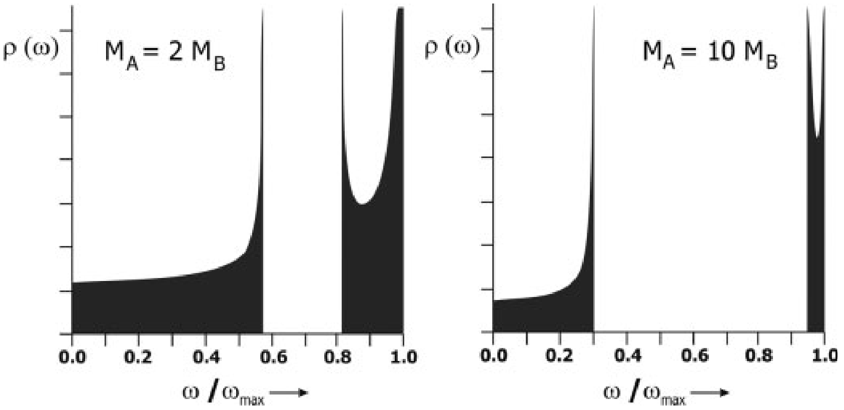

Figure 1.23 Frequency spectrum of an oscillating linear molecule chain with alternating segments of weights M_A and M_B [21].

The heat capacity at constant volume c_v is given by integration (Equation 1.2) over the entire oscillation spectrum [21]:

$$c_v = k \cdot \int \left(\frac{\hbar\omega}{kT}\right)^2 \cdot \frac{\exp(\hbar\omega/kT)}{(\exp(\hbar\omega/kT)-1)^2} \varrho(\omega)\mathrm{d}\omega \tag{1.2}$$

$\hbar$: Planck constant
ω: oscillation frequency
k: Boltzmann constant
T: temperature
$\varrho(\omega)$: density distribution of oscillation spectrum.

The density distribution $\varrho(\omega)$ of the oscillation spectrum is standardized by following equation:

$$\int \varrho(\omega)\mathrm{d}\omega = 3N \tag{1.3}$$

N: numbers of oscillation centers.

In general, an exact evaluation of Equation 1.2 is not possible because of an unknown density distribution of the oscillation spectrum [21]. The starting point for an approach is given by the models from Einstein and Debye [25]. The acoustic mode of the oscillation will be described by Debye's approach and the optical mode by Einstein's approach [26, 27].

Consideration of the heat capacity at constant volume c_v enables a theoretical determination of molecule chain oscillations induced by acoustic or optical waves, related with the heat capacity. In contrast to the heat capacity at constant pressure c_p, the heat capacity c_v cannot be measured, however. Therefore, for computation of temperature distributions in the material by numerical or analytical computer simulation the heat capacity c_p is of practical importance.

Caused by interaction processes within and between molecule chains and the temperature dependence of such processes, the heat capacity c_p of thermoplastics is also dependent on the temperature. In the state of melting the heat capacity increases caused by the melt heat (also called melt enthalpy) as an additional energy need for generating the phase shift.

Especially for semicrystalline thermoplastics the heat capacity c_p has a significant discontinuousness in the state of melting. After all crystalline phases are melted the value of the heat capacity will decrease back to the value before reaching the molten state. By melting of the crystallites a lot of oscillation modes will be activated that were hindered before by the first-order forces of the crystalline phases. With further increase of the temperature, interactions between the molecule chains will decrease and energy transfer between the molecule chains will be lower. Hence, the value of the heat capacity of semicrystalline thermoplastics will decrease again.

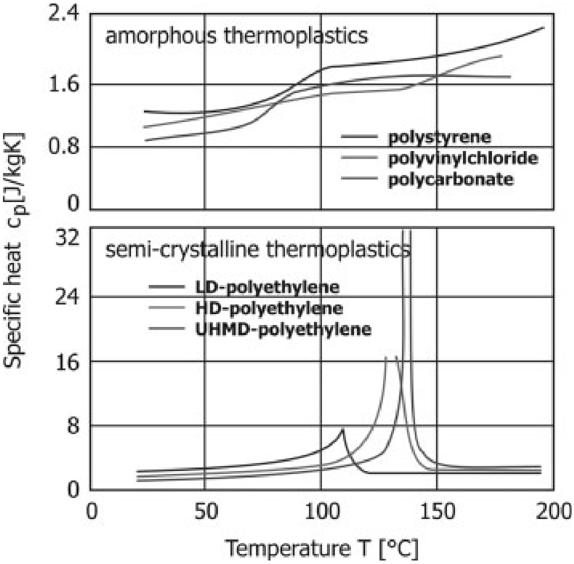

Figure 1.24 Examples for specific heat capacity c_p of amorphous and semicrystalline thermoplastics [11].

In Figure 1.24 examples of the behavior of the heat capacity in dependence on the temperature is shown for some amorphous and semicrystalline thermoplastics [11].

1.3.4
Heat Conduction

Thermoplastics are usually electrical insulators. They have no free electrons enabling high heat conduction like for metals. Heat conduction in thermoplastics will only be done by spreading through elastic oscillations of chain segments. According to Debye [28] a relationship between heat conduction and spreading of elastic oscillations can be described by Equation 1.4.

$$\lambda = K \cdot \varrho \cdot c \cdot u \cdot l \tag{1.4}$$

K: dimensionless constant $\sim 1/3$
ϱ: density
c: heat capacity
u: transmission speed for elastic oscillations
l: free length of elastic oscillations.

The free length l of elastic oscillations is, for amorphous thermoplastics, of the order of the atomic distance. The transmission speed u for elastic oscillations corresponds to the speed of sound within the material. The type of bonding between

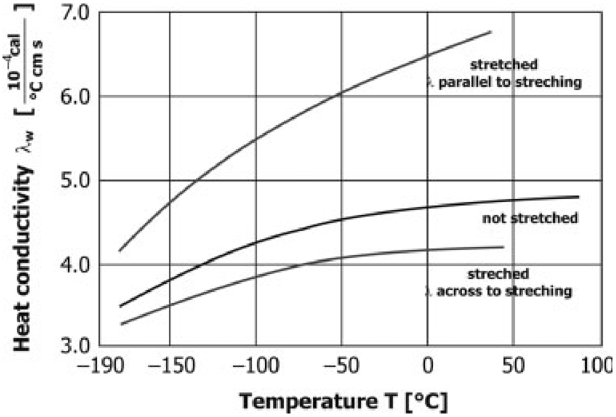

Figure 1.25 Heat conductivity as function of the temperature for nonstretched and stretched by 375% PMMA. For the stretched material the heat conductivity is given parallel to and across the stretching direction [30].

atoms or molecule segments is of importance for the quantity of the heat conductivity. Due to covalent bonding within a macromolecule the heat conduction is 10 times higher than by essentially van der Waals bonding between the macromolecules [29].

By measuring the heat conductivity on stretched thermoplastics the influence of the bonding type can be demonstrated [23]. Stretching the material in one direction causes a stretching and an orientation of the macromolecules to one another. In the direction of stretching covalent bonding is predominant, while vertical to the stretching van der Waals bonding will be the dominant bonding type. Hence, the heat conduction will be anisotropy for stretched thermoplastics.

Figure 1.25 shows the heat conductivity on stretched and unstretched PMMA as examples. For stretched PMMA the heat conductivity is given separately parallel to and across the direction of stretching [30]. Parallel to the stretching direction the heat conductivity is higher than for not stretched material. Across the stretching direction the heat conductivity is less than for unstretched material.

The dependence on temperature of the heat conductivity is different for amorphous and semicrystalline thermoplastics. For amorphous thermoplastics in the glass state at moderate to low temperatures the temperature dependence of the heat conductivity is not really significant (see Figure 1.26). The observed increase of the heat conductivity on increasing temperature is here essential given by an increasing specific heat [31]. The material history and the measurement technique for recording the heat conductivity depending on the temperature will give nonuniform results for the course of the heat conductivity at higher temperatures for amorphous thermoplastics. In comparison to semicrystalline thermoplastics amorphous thermoplastics show, however, a clearly lower temperature dependence. Figure 1.26 demonstrates the temperature behavior of the heat conductivity for some amorphous and semicrystalline thermoplastics [6].

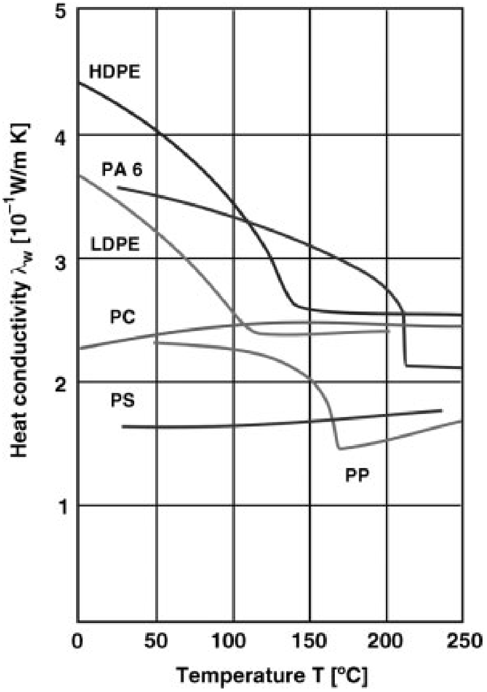

Figure 1.26 Heat conductivity for amorphous (PC, PS) and semicrystalline thermoplastics (HDPE, LDPE, PA6 and PP) [11].

The heat conductivity of semicrystalline thermoplastics depends on the crystallization level of the material. Increasing crystallization level causes increasing density of the material, which results in a more intense heat conductivity (Figure 1.27).

A semicrystalline thermoplastic can be considered as a biphasic system, composed from amorphous and crystalline phases. The total heat conductivity λ of the amorphous and crystalline partition can be calculated in accordance with the composition formula (1.5) [6]:

$$\lambda = \frac{2\lambda_a + \lambda_c + 2\gamma_c(\lambda_c - \lambda_a)}{2\lambda_a + \lambda_c - \gamma_c(\lambda_c - \lambda_a)}\lambda_a \tag{1.5}$$

λ_a: heat conductivity of amorphous phase
λ_c: heat conductivity of crystalline phase
γ_c: volume partition of crystalline phase.

Figure 1.28 shows schematically the contribution of amorphous and crystalline phases to the heat conductivity as a function of the temperature. For the given course of the heat conductivity λ_c of the crystalline phase different temperature proportionalities are valid, caused by the average free path length for elastic oscillations (see Equation 1.4) depending on the temperature [31].

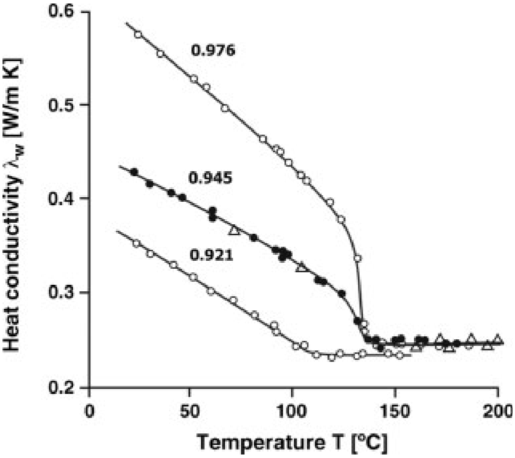

Figure 1.27 Influence of the crystallization level to the heat conductivity of PE. Parameter of the graph is the materials density, caused by the crystallization level [6].

Up to the glass temperature T_g of the material the dependence of the heat conductivity from the temperature has a proportionality of $1/T$. On reaching the crystallite melting temperature T_m the near order of the crystalline phases will be broken up and the heat conductivity λ_c of the crystalline phases will decrease to the value of the heat conductivity λ_a of the amorphous phase.

1.3.5
Temperature Conduction

An important factor for a thermal processing of thermoplastics is the spreading speed of a temperature change within the material. A temperature difference ΔT in a solid material causes a heat flux j from a warm to a cold segment (see Figure 1.29) [6]:

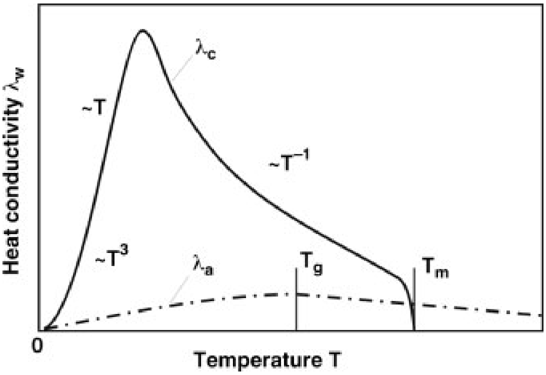

Figure 1.28 Schematic diagram of the heat conductivity in amorphous and crystalline phases of a semicrystalline thermoplastic [31].

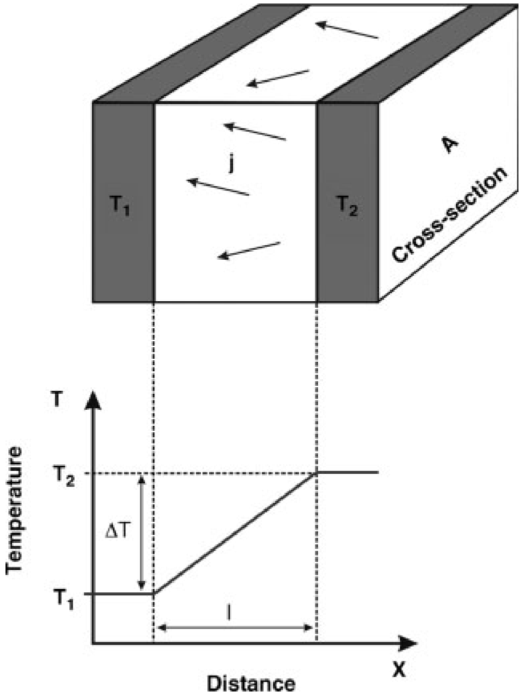

Figure 1.29 Heat transfer through a material cross section under stationary heat flux [6].

$$j = -\lambda \cdot \mathrm{grad}(T) \tag{1.6}$$

j: heat flux
λ: specific heat conductivity.

Under stationary conditions the heat flux j is given by the quantity of heat ΔQ, which will pass a material segment of cross section A and length l in a time interval Δt from the warm segment (T_2) to the cold one (T_1):

$$\frac{1}{A} \cdot \frac{\Delta Q}{\Delta t} = -\lambda \cdot \frac{T_2 - T_1}{l} \tag{1.7}$$

A: cross section of a material segment
ΔQ: quantity of heat
Δt: time interval
λ: specific heat conductivity
T_1, T_2: temperature.

The difference of inflow and outflow heat flux (div (j)) in connection with a change of the inner energy u per segment volume and time t corresponds to zero, because no heat energy can disappear:

$$\varrho \cdot \frac{\partial u}{\partial t} + \operatorname{div}(j) = 0 \tag{1.8}$$

ϱ: specific density
u: inner energy
t: time
j: heat flux.

The inner energy u changes with temperature T according:

$$\partial u = c \cdot \mathrm{d}T \tag{1.9}$$

c: specific heat capacity.

Combination of Equations and 1.9 results in the heat conduction Equation 1.10:

$$\operatorname{div}(\lambda \cdot \operatorname{grad}(T)) = \varrho \cdot c \cdot \frac{\partial T}{\partial t} \tag{1.10}$$

By the assumption of a place-independent specific heat conductivity λ, Equation 1.11 results from Equation (1.10):

$$\frac{\lambda}{c \cdot \varrho} \cdot \operatorname{div}(\operatorname{grad}(T)) = \frac{\partial T}{\partial t} \tag{1.11}$$

and hence the temperature conductivity a, built by the quotient of the heat conductivity λ with the heat capacity c and the specific density ϱ of the material:

$$a = \frac{\lambda}{c \cdot \varrho} \tag{1.12}$$

The temperature conductivity has the dimension cross section A per time interval t and describes the speed of a temperature change for heat conduction processes. A change of temperature occurs faster the higher the heat conductivity and the lower the specific heat and specific density of the material are.

Because heat conductivity, specific heat and specific density depend on the temperature, the temperature conductivity has a complex temperature dependence for amorphous and semicrystalline thermoplastics:

1.3.5.1 Amorphous Thermoplastics

- Heat conductivity shows a gentle rise with increasing temperature.
- Heat capacity increases on rising temperature. At the glass-transition temperature the increase is more distinctive.
- Specific density decreases slowly below the glass-transition temperature. Exceeding the glass-transition temperature the decrease is more intensive with increasing temperature.

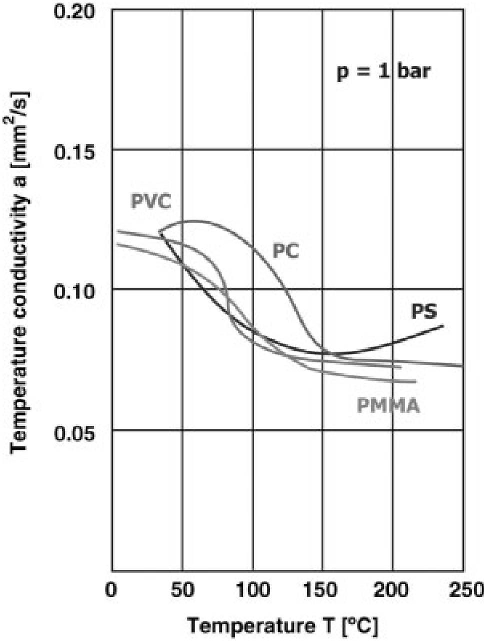

Figure 1.30 Temperature conductivity as a function of the temperature for some amorphous thermoplastics [11].

The superposition of these effects results in a slow decrease of the temperature conductivity in the state of application by increasing temperature. At the glass-transition temperature the decrease is stronger. On increasing plasticization of the material the temperature conductivity again decreases slowly. Figure 1.30 shows the temperature dependence of the temperature conductivity for some amorphous thermoplastics [11].

1.3.5.2 **Semicrystalline Thermoplastics**

- Heat conductivity decreases noticeably up to the crystallite melt temperature. On exceeding the crystallite melt temperature the heat conductivity shows a slow increase.
- Heat capacity increases on rising temperature. At the crystallite melt temperature the heat capacity has a strong increase and then drops down above the crystallite melt temperature to lower values.
- Specific density has a quasilinear decrease below the glass-transition temperature of the amorphous phases. On exceeding the crystallite melt temperature a nonlinear decrease follows. If the material completely plasticizes the decrease of the specific density is again quasilinear.

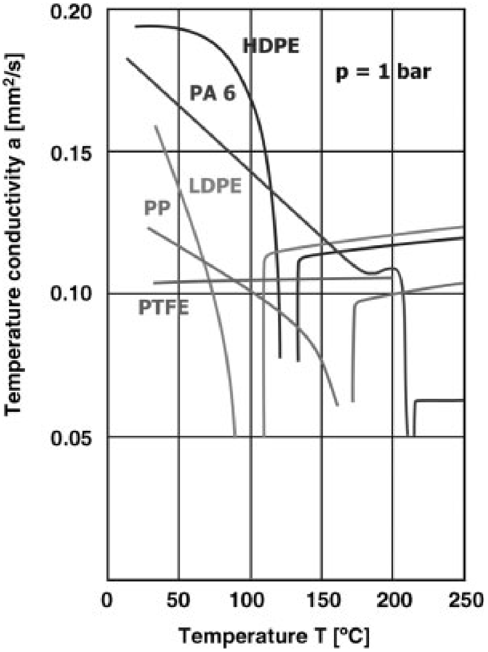

Figure 1.31 Temperature conductivity as function of the temperature for some semicrystalline thermoplastics [11].

The temperature conductivity of semicrystalline thermoplastics is strongly dependent on the temperature of the material (Figure 1.31) caused by the superposition of the given effects. The temperature conductivity decreases on increasing temperature during the state of application and has a discontinuity at the crystallite melt temperature. Exceeding the crystallite melt temperature the temperature conductivity increases quasilinearly by increasing temperature.

Average values of the temperature conductivity for several thermoplastics are summarized in Table 1.10. As a comparison, the temperature conductivity of steel is 100 times higher than the values of thermoplastics.

Table 1.10 Average values of temperature conductivity for some thermoplastics [32].

Resin	Temperature conductivity *a* [mm^2/s]
ABS	0.19
PA 6	0.05
PE	0.08
PMMA	0.17
POM	0.11
PP	0.10
PPO	0.20
SAN	0.23

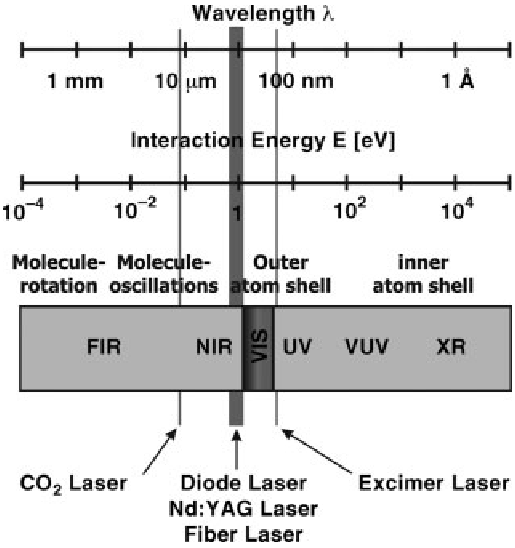

Figure 1.32 Interaction between electromagnetic radiation and material. NIR lasers like diode, Nd:YAG or fiber lasers are in the range of electronic and starting of molecule excitation [33].

1.4
Optical Properties

Beside thermal properties the optical properties of thermoplastics are of importance for laser processing. The optical properties of thermoplastics without any additives like coloration dyes or reinforcement particles are influenced by the macromolecule chain structure and the type of bonding within the macromolecule chain and between the chains. The interaction of electromagnetic radiation with the material depends on the wavelength of the radiation and can be done by bonded electrons (molecule orbital) or molecule segments (Figure 1.32).

Radiation of NIR lasers like various diode lasers (e.g., $\lambda = 808$ nm, 940 nm or 980 nm), Nd:YAG-laser ($\lambda = 1064$ nm) or fiber lasers (e.g., $\lambda = 1070$ nm or 1090 nm) interacts with the material by stimulating electron oscillations. Some diode and fiber lasers with wavelength between 1.5 μm and 2 μm interact with the material in the transition state from stimulation of electron oscillations to vibration oscillations of molecular segments. CO_2-laser radiation ($\lambda = 10.6$ μm) in the MIR spectrum induces molecular oscillations.

Because the material structure of thermoplastics is influenced by the temperature the optical properties are in principle also dependent on the temperature. Due to the complicated molecule structure of thermoplastics a theoretical analysis of the optical properties is only approximately possible.

Appropriate determination of the optical properties can be done by measurement of the reflection and transmission behavior. From the measured reflection and transmission data the absorption property of the material can be calculated.

In this chapter the principle properties of optical constants will first be discussed. Next follows a consideration of reflection, transmission and scattering of optical radiation by thermoplastics. The absorption of radiation in pure resins in the different wavelength areas and in particular the possibilities of influencing the absorption by additives will be discussed in detail.

1.4.1
Optical Constants

The distribution of electromagnetic waves in a solid body is described by the wave equation:

$$-\Delta E + \frac{1}{c^2}\ddot{E} = -\mu \cdot \mu_0 \cdot \ddot{P} \tag{1.13}$$

E: electric field strength
c: speed of light
μ: relative permeability (= 1 for insulators)
μ_0: magnetic field constant
P: macroscopic polarization.

The macroscopic polarization P of the material is linked with the electric field strength of a light wave by [34]:

$$P(t) = (\hat{\varepsilon} - 1) \cdot \varepsilon_0 \cdot E(t) \tag{1.14}$$

$\hat{\varepsilon}$: complex dielectric constant
ε_0: electric field constant
$E(t) = E_0 \exp(-i(kz - \omega t))$: electric field strength of light wave.

The macroscopic polarization P is the sum of all oscillating dipole moments $p = q\, x(t)$ in the solid body:

$$P(t) = N \cdot q \cdot x(t) \tag{1.15}$$

N: number of possible oscillating dipoles
q: charge
$x(t)$: oscillation amplitude.

Effecting as dipoles depending on the light wave frequency are in the NIR spectral range ($\lambda < 2\,\mu\text{m}$) e.g., bonded electrons or in the MIR spectral range ($2\,\mu\text{m} < \lambda < 30\,\mu\text{m}$) charge distributions of macromolecule chain segments. Oscillations of such dipoles can be stimulated by the electric field of the light wave. The oscillation amplitude $x(t)$ of the oscillating components is given by the solution of the wave equation:

$$\ddot{x} + \gamma\dot{x} + \xi x = \frac{q}{m} \cdot E(t) \tag{1.16}$$

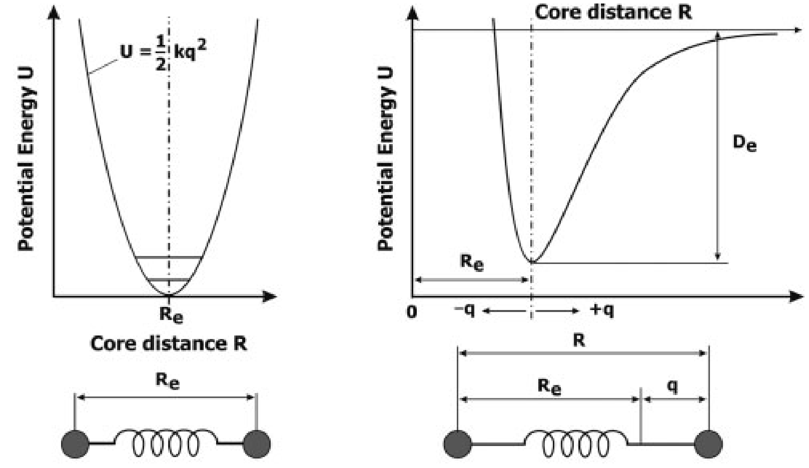

(a) Model and potential energy of harmonic oscillator

(b) Model and potential energy of inharmonic oscillator

Figure 1.33 Potential-energy course of harmonic (a) and inharmonic (b) oscillator [35]. The term q is used for the mass elongation out of the balance position.

γ: damping constant
ξ: spring constant.

The second term of Equation 1.16 describes the speed-dependent damping of the oscillation. The third term gives the bonding force for the oscillating system.

In the case of low oscillation amplitudes the bonding force is proportional to the elongation (harmonic oscillator). For high oscillation amplitudes the bonding force tends to zero and the oscillating system will break up. In this case, the theoretical model of the oscillating system has to be replaced by the model of an inharmonic oscillator (Figure 1.33) [35]. As an approximation, the following considerations will be restricted to the case of low oscillation amplitudes.

Attempting the harmonic oscillator model the general solution of the oscillation Equation 1.16 results in the amplitude $x(t)$:

$$x(t) = \frac{q \cdot E(t)}{m\left(\omega_o^2 - \omega^2\right) + i\gamma\omega} \tag{1.17}$$

Using Equation 1.15 the macroscopic polarization Equation 1.14 results in:

$$P(t) = N \cdot \frac{q^2}{m} \cdot \frac{E(t)}{\left(\omega_0^2 - \omega^2\right) + i\gamma\omega} \tag{1.18}$$

Equation 1.18 is valid for a single resonance oscillation of a dipole system. For an expansion to all possible resonance oscillations of the system the sum over all oscillation numbers has to be made, regarding the connection strength. For atomistic systems this will be summarized by the optical polarization $\hat{a}$ [36]:

Table 1.11 Molecule groups of polymer materials and their mol refraction [37].

Molecule group	**Mol refraction P_m ($\times 10^{-16}$ [$C^2\ m^2/J$])**
$-CH_3$	6.20
$-CH_2-$	5.01
$>CH-$	3.98
$>CH<$	2.84
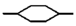	27.5
$-O-$	5.72
$>C{=}O$	11.0
$-CO_2-$	16.5
$-CONH-$	33.0
$-O-CO_2-$	24.2
$-S-$	8.80
$-F$	1.98
$-Cl$	10.45
$-C\equiv N$	12.1
$-CF_2-$	6.88
$-CCl_2-$	19.47
$-CHCl-$	13.7

$$P(t) = \hat{a} \cdot N \cdot E(t) \tag{1.19}$$

For molecular systems like polymeric materials the optical polarization â will be replaced by the mol refraction $\hat{P}_m$. The mol refraction indicates the ability of molecules to become polarized. The polarization of the monomer unit of a macromolecule is also valid in sum for the entire macromolecule [37]. The optical polarization â is linked with the mol refraction $\hat{P}_m$ by the molecular weight M of the monomer unit and the specific volume V of the polymeric material [36]:

$$\hat{a} = \frac{1}{N} \cdot \frac{\hat{P}_m}{M \cdot V} \tag{1.20}$$

$\hat{a}$: complex optical polarization
$\hat{P}_m$: mol refraction of one monomer unit
M: molecular weight of monomer unit
V: specific volume of polymer.

Table 1.11 gives some examples of molecule groups and values of their mol refraction (from [37]).

The wave Equation 1.13 results in Equation 1.21, inserting Equations 1.18 and 1.19 by using $\mu_0\varepsilon_0 = c^{-2}$:

$$-\Delta E + \frac{1}{c^2} \cdot \left(1 + \frac{1}{\varepsilon_0} \cdot \frac{\hat{P}_m}{M \cdot V}\right) \cdot \ddot{E} = 0 \tag{1.21}$$

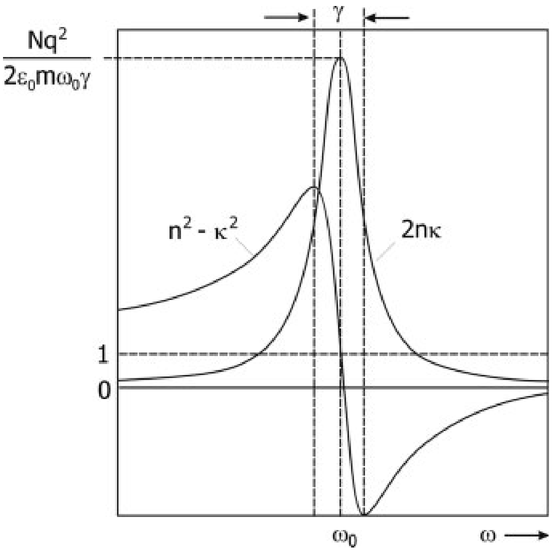

Figure 1.34 Schematic course of Equations 2.23a, b around a resonance frequency ω_0 [38].

Using the solution attempt of plane waves for the electrical field of a light wave, the complex refractive index of the material results in:

$$\hat{n}^2 = 1 + \frac{1}{\varepsilon_0} \cdot \frac{\hat{P}_\mathrm{m}}{M \cdot V} \tag{1.22}$$

$\hat{n}^2 = k^2c^2/\omega^2$: complex refractive index ($\hat{n} = n - \mathrm{i}\kappa$)

Dividing into real and imaginary parts of the complex refractive index around a resonance point will give by using Equation 1.17:

$$n^2 - \kappa^2 = 1 + \frac{N \cdot q^2}{\varepsilon_0 \cdot m} \cdot \frac{\omega_0^2 - \omega^2}{\left(\omega_0^2 - \omega^2\right)^2 + \gamma^2 \cdot \omega^2} \tag{1.23a}$$

$$2n \cdot \kappa = \frac{N \cdot q^2}{\varepsilon_0 \cdot m} \cdot \frac{\gamma \cdot \omega}{\left(\omega_0^2 - \omega^2\right)^2 + \gamma^2 \cdot \omega^2} \tag{1.23b}$$

Figure 1.34 shows the schematic course of Equations 1.23a and 1.23b around a resonance point.

The imaginary part Equation 1.23b tends to zero outside the resonance and from Equation 1.23a follows for the real refractive index by using the mol refraction according to the Lorentz–Lorenz law [36]:

$$n = \sqrt{1 + \frac{3 \cdot P_\mathrm{m}}{M \cdot V \cdot P_\mathrm{m}}} \tag{1.24}$$

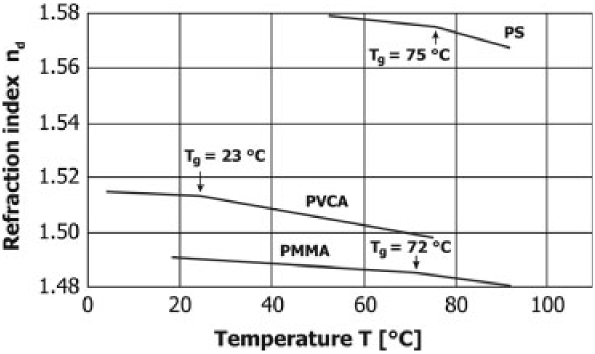

Figure 1.35 Temperature dependency of the refractive index for PMMA, PS and PVCA [40].

By the assumption of temperature independence for mol refraction and molecular weight, the temperature dependence of the specific volume of the polymeric material will influence the temperature dependence of the refractive index. Usually, the specific volume will increase on increasing temperature [39], which results in a decrease of the refractive index on increasing temperature.

Figure 1.35 shows for some polymers the course of the refractive index as a function of the temperature, calculated by Equation 1.24 with regard to the temperature-dependent specific volume. On reaching the glass temperature of the polymer the course of the refractive index shows a bend. This is given by a rapid increase of the specific volume, caused by increased mobility of the molecule chains [6].

At the maximum of the resonance the frequency of the wave is $\omega = \omega_0$. Using Equation 1.23b the absorption constant κ is given by:

$$\kappa = \sqrt{\frac{N \cdot q^2}{2 \cdot \varepsilon_0 \cdot m \cdot \omega_0 \cdot \gamma}} \tag{1.25}$$

N: number of oscillators
q: electric charge
ε_0: dielectricity constant
m: mass
γ: damping constant.

The line width of a resonance in a solid body is dependent on the density distribution of the absorption spots, the damping strength for the forced oscillation and the influence on the oscillation by connection with further oscillation-capable components of the material. In polymeric materials the absorption line course is determined by the inhomogeneous line spreading. The course of the line can be described by the Gauß line spreading (Figure 1.36) [41].

$$\kappa_\nu = \kappa_0 \cdot \frac{2\sqrt{\ln 2}}{\pi(\Delta\nu_0)} \cdot \exp\left(-4 \cdot \ln 2 \frac{(\nu - \nu_0)^2}{(\Delta\nu_0)^2}\right) \tag{1.26}$$

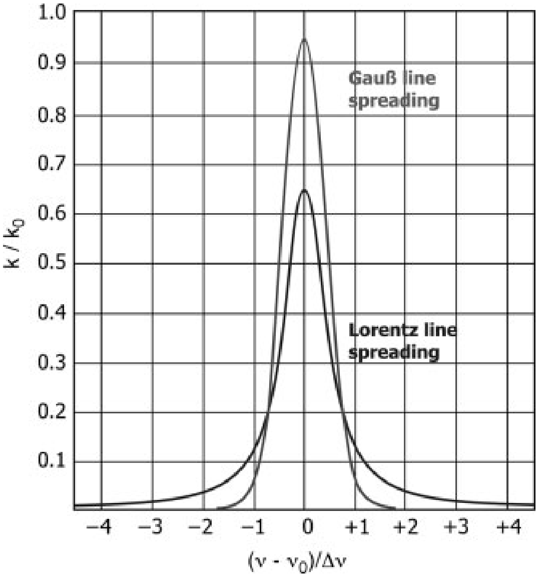

Figure 1.36 Schematic sketch of Gauß and Lorentz line spreading [41], shown is the normalized wave number k/k_0 as function of the frequency difference $\nu - \nu_0$ in regard to the line width.

ν: frequency
ν_0: resonance frequency.

The line spreading results from the statistical surrounding of the molecule chains, which causes a resonance frequency shift of the oscillation modes of individual recurring molecule components. The shifted resonance frequencies themselves have a homogeneous line spreading, described by the Lorentz line spreading (Figure 1.36) [41]:

$$\kappa_\nu = \frac{\kappa_0 \cdot \gamma}{(\nu - \nu_0)^2 + \gamma^2/4} \tag{1.27}$$

The envelope of all resonance lines results in the inhomogeneous line spreading of the absorption spot.

As a model assumption, in areas with strong near order and regular molecular structure – as for crystalline structures – a band structure of energy levels is given for the bonding electrons within the molecule orbital that enables primarily electronic stimulation. In contrast to this in amorphous areas it is more probable that absorption of NIR-laser radiation will occur as vibration excitation caused by the statistical molecule chain order with unhindered chain components. In polymeric materials usually no resonant stimulated base oscillations are given within the NIR wavelength spectrum so absorption of such radiation can only occur by stimulation of higher-order oscillations.

Due to the complex and irregular molecule structure the energy levels of electronic and vibration oscillations of the molecule chains will be influenced by adjoining molecule chains [42] like for crystalline phases by highly orientated chains or for streched amorphous molecule chains in streched polymer fibers. Influencing of oscillation levels will result in a shift of the resonance frequency for the oscillation stimulation. Because the state of the molecule structure is dependent on the temperature also the influencing of the oscillation levels are dependent on the temperature. Increasing temperature affects a shift of the resonance frequencies, resulting in increasing or decreasing absorption as a function of the temperature.

Complicating the theoretical consideration is the availability of additives like filler materials, coloration dyes or reinforcement fibers that can reflect or absorb the radiation themselves.

The preceded discussion is important for the theoretical understanding of the processes during interaction of electromagnetic radiation and solid material. The following considerations will deal in more detail with the special features of the interaction with plastic material.

Starting with the macroscopic behavior, like reflection and transmission, the absorption mechanism for the wavelength areas used for laser welding plastics and internal scattering by additives in the resin will be considered.

1.4.2

Reflection, Transmission and Absorption Behavior

When electromagnetic radiation hits the surface of a solid material, usually a part of the radiation will be reflected at the surface. The nonreflected part of the radiation will enter the material and can be weakened by scattering on internal elements like pigments or crystalline phases and by absorption [43]. Depending on material thickness and internal radiation loss the rest of the radiation will be transmitted (Figure 1.37).

Reflection and transmission of radiation are quantities that can be measured by spectral photometers [44]. Figure 1.38 shows as an example the reflection and transmission measurement results on PC at visible and NIR wavelengths between 400 and 2500 nm and the corresponding calculated absorption.

Absorption of electromagnetic radiation in an electric insulating material is done by stimulation of dipole oscillations [45]. Depending on the frequency, induced or permanent dipoles are given by for example, bonded electrons for NIR radiation ($\lambda < 2000$ nm) or charge distributions of molecule segments from macromolecules for IR radiation ($2\,\mu m < \lambda < 30\,\mu m$).

From measured reflection and transmission data the radiation loss by absorption in the material can be calculated (see Figure 1.38). If necessary, the influence of internal scattering has to be taken into consideration.

The energy balance of the radiation in principle will have no losses during pure scattering, whereas by absorption the radiation energy will be transformed into

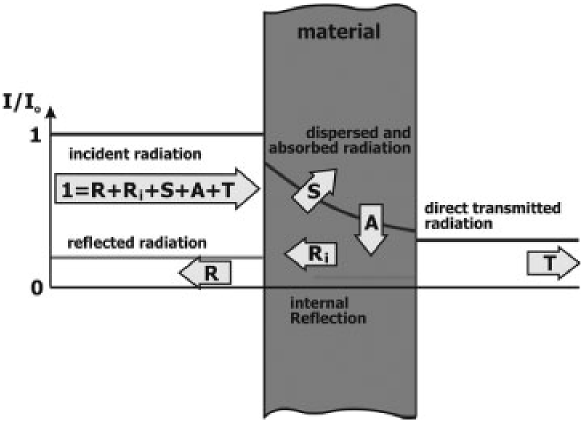

Figure 1.37 Radiation intensity weakening by reflection as well as internal scattering and absorption during passing material.

another energy state like heat energy as induced molecule motion. Under the assumption of linear absorption mechanism the reduction of the radiation intensity can be described by the Lambert absorption rule [36]:

$$I_{\mathrm{T}}(z) = I_0 \cdot \exp\left(-\frac{4 \cdot \pi \cdot \kappa}{\lambda} \cdot z\right) \tag{1.28}$$

z: material thickness
$\alpha = 4\pi\kappa/\lambda$: absorption constant.

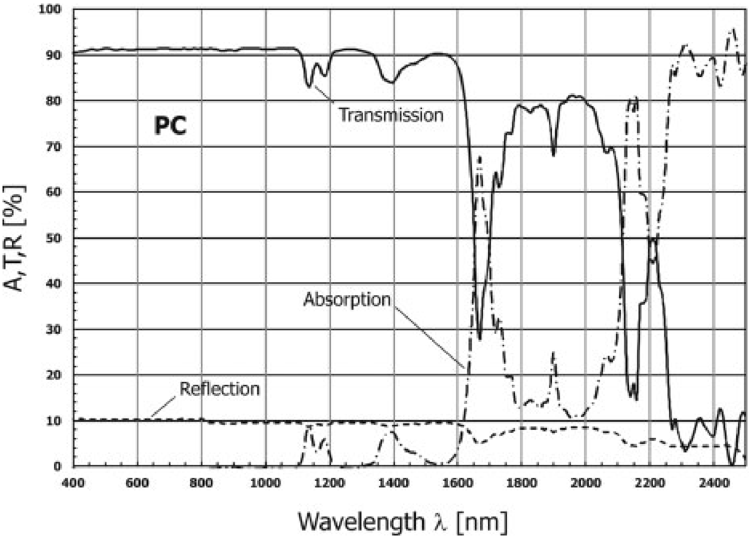

Figure 1.38 Reflection, transmission and absorption of PC at wavelengths between 400 and 2500 nm.

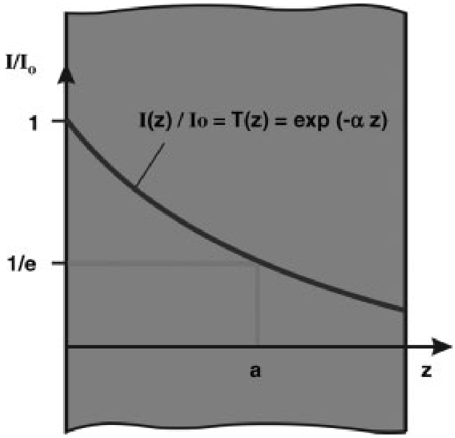

Figure 1.39 Exponential decrease of radiation intensity in a material, described by the Lambert absorption rule.

The Lambert absorption rule indicates that by increasing material thickness z the transmitted radiation will decrease exponential (Figure 1.39). Within every differential layer δz of the material the same fraction of the radiation will be absorbed [36].

The absorption constant $\alpha = 4\pi\kappa/\lambda$ in Equation 1.28 is generally correlated with the radiation wavelength λ and the material properties, which are summarized in the absorption coefficient κ. The absorption constant has the dimension of a reciprocal length (e.g., 1/mm).

In ratio to the incident radiation intensity I_o the radiation intensity I_T at the optical penetration depth ($z = a$) within the material is decreased by the value 1/e (Figure 1.39):

$$\frac{1}{e} = \frac{I_T(a)}{I_0} = \exp(-\alpha \cdot a) \tag{1.29}$$

By reciprocal and logarithm calculation it results from Equation 1.29:

$$\ln e = 1 = \alpha \cdot a \tag{1.30}$$

and therefore

$$\alpha = \frac{1}{a} \tag{1.31}$$

The quantity a in Equation 1.31 has the dimension of a length (e.g., mm) and defines the optical penetration depth of the material as a measure for the absorption property of the material for a specific wavelength.

Inserting Equation 1.31 into Equation 1.28 results in:

$$I_T(z) = I_0 \cdot \exp\left(-\frac{z}{a}\right) \tag{1.32a}$$

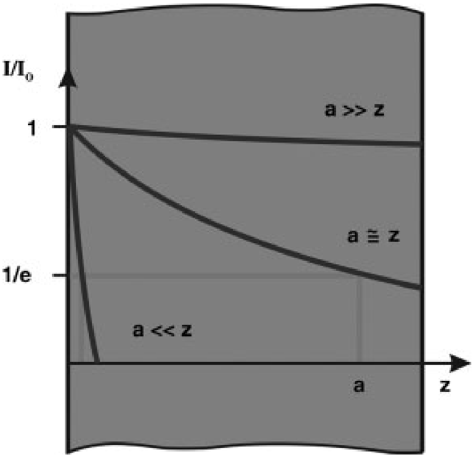

Figure 1.40 State distinction for the ratio of optical penetration depth *a* to the material thickness *z*.

Dividing Equation 1.32a by the incident radiation intensity I_o will give the transmitted radiation $T(z)$, which is a measurable quantity:

$$\frac{I_T(z)}{I_0} = T(z) = \exp\left(-\frac{z}{a}\right) \tag{1.32b}$$

Further transformation by logarithm and reciprocal computation and clearing up the optical penetration depth will give a term that can be used for calculation of the optical penetration depth by the well-known thickness of the work piece and the measured transmission value:

$$a = -\frac{z}{\ln T(z)} \tag{1.32c}$$

Using the optical penetration depth a in correlation with the work piece thickness z the absorption behavior of a material can be classified for the given wavelength of the radiation (Figure 1.40):

- $a \gg z$: the material is transparent to the radiation,
- $a \cong z$: the radiation will be absorbed in the volume,
- $a \ll z$: the radiation will be absorbed at the material surface.

An example of surface and volume absorption of laser radiation with a natural plastic is given in Figure 1.41 for a CO_2 (left) and Nd:YAG laser (right) on PA6 with a sample thickness of 2 mm [46]. In both cases the same laser power (50 W) and processing speed (100 mm/s) was used for processing.

At PA6 the CO_2-laser radiation at $\lambda = 10.6\,\mu m$ has an optical penetration depth of approximately 60 μm, much smaller than the material thickness. The radiation was absorbed at the surface of the PA6 sample and essentially sublimated the resin material; a molten layer of a thickness of the optical penetration depth can be seen.

In the same resin Nd:YAG-laser radiation at $\lambda = 1.06\,\mu m$ has an optical penetration depth of around 3 mm, which is of the order of the sample thickness. The Nd:YAG-

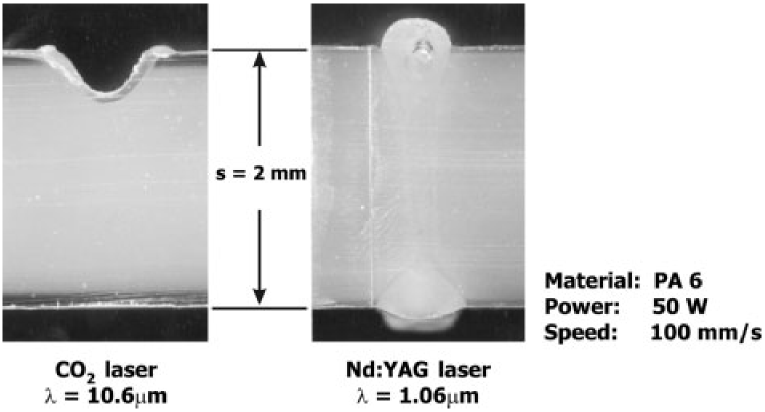

Figure 1.41 Influence of the optical penetration depth to the processing result on PA6 using CO_2- and Nd:YAG-laser radiation with the same processing parameters [46].

laser radiation was absorbed in the volume and the sample is melted through, supported by the transmitted radiation backscattered from the aluminum plate.

Table 1.12 gives the optical penetration depth for CO_2-laser radiation and diode laser radiation ($\lambda = 940$ nm) for some typical natural plastics. The given values show very clearly that CO_2-laser radiation is usually absorbed at the resin surface while diode-laser radiation will transmit the material with no effective absorption.

1.4.3
Scattering of NIR- and IR-Radiation in Plastics

Beside absorption an intensity loss (not an energy loss) of the incident radiation within the plastic can occur by scattering caused by inhomogeneous structures in the material.

In polymeric material, scattering of radiation can be caused by the structure of the macromolecules by themselves, on crystalline phases incorporated in the amorphous

Table 1.12 Optical penetration depth of some typical thermoplastic resins for CO_2- and diode-laser radiation.

Resin	*a* [mm] $\lambda = 940$ nm	*a* [mm] $\lambda = 1064$ nm	*a* [mm] $\lambda = 1550$ nm	*a* [mm] $\lambda = 10.6\,\mu$m
Amorphous Thermoplastics				
PC	22.82	23.04	18.94	0.070
PMRA	37.93	36.56	22.10	—
PVC	—	—	—	0.020
Semicrystalline Thermoplastics				
LDPE	8.49	10.34	9.71	0.280
PA 6	5.06	5.06	3.01	0.040
PP	11.63	12.87	12.96	0.190

phase [47] as well as by filler materials, fibers or coloration pigments incorporated in the polymeric matrix [48]. The kind of scattering is correlated with the wavelength of the radiation and the size of the dispersing structure [49]. Additionally, the scattering structures can themselves absorb the radiation.

Generally, for scattering in correlation with the structure size l and the wavelength λ following case distinctions can be made [43]:

I: $l \gg \lambda$: diffraction on microscopic structures,
II: $l > \lambda$: Mie scattering on statistic distributed scattering structures,
III: $l \ll \lambda$: Rayleigh scattering, Raman scattering.

Under the assumption of intensity independence, weakening of the radiation intensity by scattering can by described by the exponential rule of Lambert [50]:

$$I_s = I_0 \cdot \exp(-K^+ \cdot z) \tag{1.33}$$

I_s: decreased scattering intensity
K^+: scattering constant
z: material thickness.

For spherical scattering structures with dimension smaller than the wavelength (Rayleigh scattering) the scattering constant is depending on the number N and the volume V of the particles as well as from the wavelength of the radiation [50]:

$$K^+ = -\frac{N \cdot V^2}{\lambda^4} \tag{1.34}$$

N: number of scattering structures
V: volume
λ: wavelength.

For large dimension of the spherical scattering structures versus the wavelength (diffraction on microscopic structures), the scattering constant is proportional to the sum of the cross-sectional areas of the particles:

$$K^+ = -\pi \sum_{1}^{N} \varrho_i^2 \tag{1.35}$$

ϱ_i: Scattering cross section of particle i.

Thus, it is assumed that the scattering structures have no interaction between themselves.

Figure 1.42 shows a graphical portrayal, taken from [50], of the spherical structure scattering constant at low particle concentration as a function of the radiation wavelength.

The relationship of the scattering constants given in Equations 1.34 and 1.35 as well as the graphical portrayal in Figure 1.42 are only valid for spherical scattering structures. They are a simple assumption with regard to realistic geometries of particles in the resin. The mathematical link between scattering constants and geometrical structure of structures like molecule chains, crystalline phases or filler

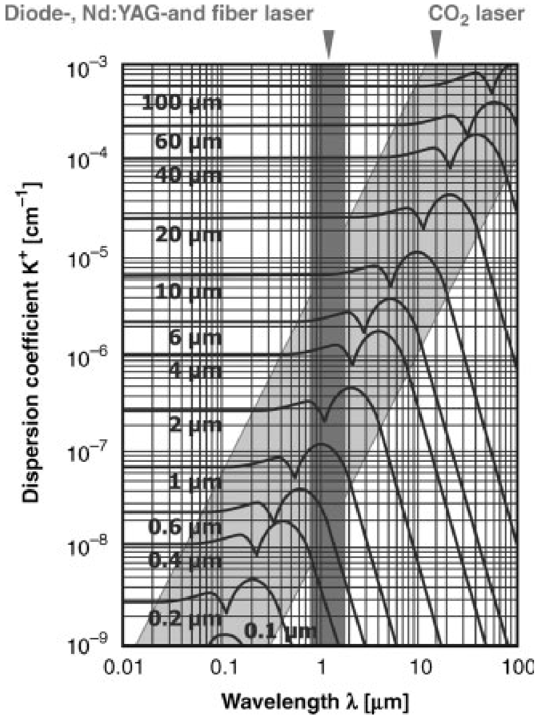

Figure 1.42 Calculated scattering coefficient of spherical particles as function of the wavelength. The parameter of the individual graphs is the radius of the particles [50].

materials is considerably more complex [49]. For a simple assessment of the scattering influence the consideration of spherical scattering structures is sufficient. To carry out a quantitative analysis of the scattering constants the real geometric structures have to be taken into consideration.

Table 1.13 gives a summary of possible scattering structures in polymers and their dimensions. The comparison of the dimension with the wavelength of NIR radiation (e.g., diode, Nd:YAG and fiber lasers) as well as MIR radiation (e.g., CO$_2$ laser) results in a selection of the effective scattering processes.

Scattering caused by the polymer matrix corresponds to Rayleigh scattering and is proportional to λ^{-4}. Thus, scattering of CO$_2$-laser radiation is by a factor 10^{-4} lower than for Nd:YAG-laser radiation. In principle, scattering by the polymer matrix can be neglected for application of CO$_2$-laser radiation.

For filler materials and pigments the scattering is dependent on the particle size. In this case, diffraction on microscopic structures and Rayleigh-scattering is predominant (see Table 1.13). For diffraction on microscopic structures the dependence is given by the particle size and not by the wavelength. The influence of the scattering caused by filler materials or pigments on the decrease of the radiation intensity in the polymer material always has to be considered in correlation with the absorption by the base material.

Table 1.13 Dimension of scattering structures in polymers and their effect to NIR and MIR radiation [51, 52].

Structure	**Dimension**	**Dispersion process**	
		NIR radiation for example, $\lambda = 1.06$ pm	**MIR radiation for example, $\lambda = 10.6$ pm**
Polymer matrix:			
Crystallites	about 10 nm	III	III
Spherolithes	30–40 nm	III	III
Filler materials:			
Asbestos flour	20–80 nm	III	III
Calcium carbonate	4–25 μm	II	II
Glimmer	20–80 nm	III	III
Wood flour	<200 μm	I	I–II
Microglass spheres	5–50 μm	I-II	II
Color pigments	0.01–1 μm	II–III	III
Quartz flour	16–300 μm	I	I–II
Carbon particles	10–120 μm	I	I–II
Slate flour	<100 μm	I	I–II
Fiber materials:			
Aramid fibers	ϕ about 10 μm	I	II
Cellulose fibers	l about 220–650 μm	I	I
	ϕ about 20–25 μm	I	I–II
Carbon fibers	ϕ about 10 μm	I	II
Short glass fibers	l about 140–300 μm	I	I
	ϕ about 10–20 μm	I	II
Long glass fibers	$1 < 6$ mm	I	I
	ϕ about 10–20 μm	I	II

I: $l \gg \lambda$: Diffraction on microscopic structures ($K^+ \propto N \cdot \varrho^2$).
II: $l > \lambda$: Mie scattering on statistic distributed scattering structures.
III: $l \ll \lambda$: Rayleigh scattering, Raman scattering ($K^+ \propto N \cdot \lambda^{-4}$).

Scattering by fiber materials will be done by diffraction and is not dependent on the wavelength. The influence of the scattering on the decrease of radiation intensity passing a material is correlated with the absorption properties of the material. For low optical penetration depths the scattering can be in principle neglected. When the optical penetration depth is in the range of mm, the scattering has to be taken into consideration.

1.4.4
Absorption of NIR-Laser Radiation ($\lambda = 800$ nm to 1200 nm)

In the NIR wavelength range with diode lasers (e.g., $\lambda = 808$ nm, 940 nm or 980 nm), Nd:YAG-lasers ($\lambda = 1064$ nm) or fiber lasers (e.g., $\lambda = 1070$ nm or 1090 nm), interaction of the radiation with the material occurs by electronic excitation of electrons in

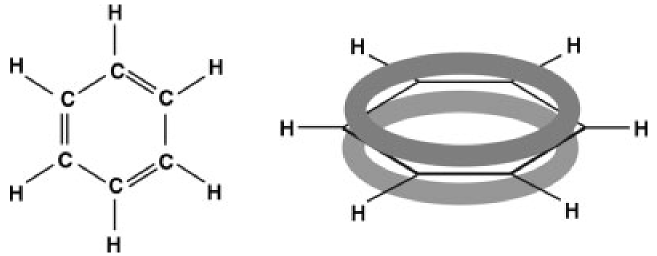

Figure 1.43 Molecule structure (left) and molecule orbital order of the carbon valence electrons (right) for benzene.

the outer shell of atoms and by higher-order vibrational excitation of molecule segments [37] (see Figure 1.32).

In correlation with the statistical molecule structure of polymers an exact assignment of the corresponding processes for absorption of the laser radiation is not unambiguously possible [37]. For absorption of NIR laser radiation both processes have to be considered.

1.4.4.1 Electronic Excitation

In polymers, the valence electrons of the individual atoms are bound in molecule orbitals of the macromolecules [53]. For covalent bonds the outer electron shells are overlapping, while the inner electrons are not significantly influenced.

An example of the placement of the carbon atom valence electrons is the benzene molecule [53] (Figure 1.43), which for example, is present in polymers like polyethylenterephtalate (PET), polycarbonate (PC) or polyphenylensulfide (PPS). The structure of a benzene molecule is given by 6 carbon atoms in a hexagonal ring with one hydrogen atom on each corner. The valence electrons of the carbon atoms form two rings as electron clouds above and below the molecule level.

At room temperature generally the valence electrons are in the basic level. Under resonant influence of electromagnetic radiation the electron energy will increase by absorption and the electrons will gain a higher energy level (Figure 1.44). According to the Born–Oppenheimer theorem [42] the level change will occur so fast that the atom nucleus can be assumed as static. The time constant for the level change is in the order of 10^{-16} s [42], while atom nucleus oscillations have a time constant of 10^{-13} s.

Each electron state has an own characteristic potential course for the bonding energy between electron and atom nucleus. Hence, the inharmonious of the potential curve has to be noted. Only oscillation bands occur in an absorption spectra of which the distances are specific to the oscillation states of the excited electrons. The intensities of the occurring spectral lines are correlated according to the Franck–Condon principle [42]. The level-change probability for a change from the basic level to a higher-order level is greatest for electron oscillations where the oscillation eigenfunctions at the near-nucleus and far-nucleus branches have amplitude minima for the potential curves (Figure 1.44).

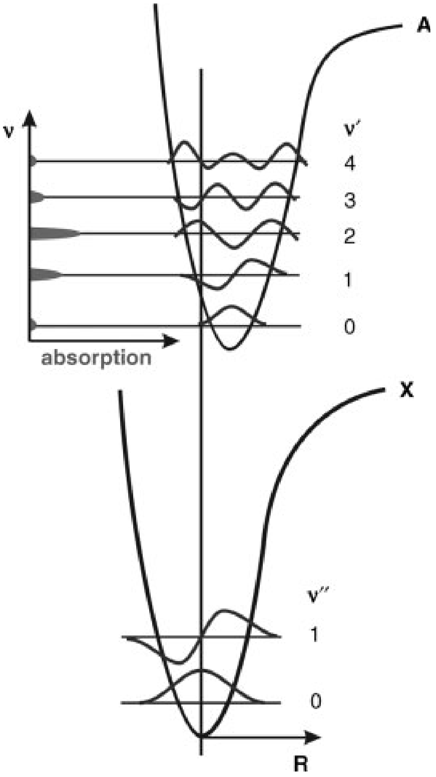

Figure 1.44 Excitation of electronic-level change from basic level X to higher level A. According to the Franck–Condon principle the absorbed intensity is at its highest if the maxima or minima of oscillation eigenfunctions are overlapping [42].

The electron state change causes a disruption of the coulomb forces equilibrium state between the electrons and thereby a disruption of the force equilibrium state within the molecule [54]. This results in an increase of the distances of all equilibrium states and thereby in a change of the oscillation levels. The molecules will experience oscillations that will be transmitted to the rest of the molecule chain. This process will generate a transformation of electromagnetic radiation into thermal oscillation energy of the molecule chains.

1.4.4.2 **Vibronic Excitation**

In polymers, components of the macromolecular chains can oscillate in different ways like elongation, bending or rotating oscillation. Such oscillations can be induced by absorption of electromagnetic radiation when resonant wavelengths are available. For NIR radiation usually no resonant base oscillations can be stimulated. But influence by electromagnetic radiation can stimulate higher-order oscillations with lower oscillation frequencies than the base oscillation [55]. The intensity of higher-order oscillations is noticeably reduced compared with the base oscillation [56]

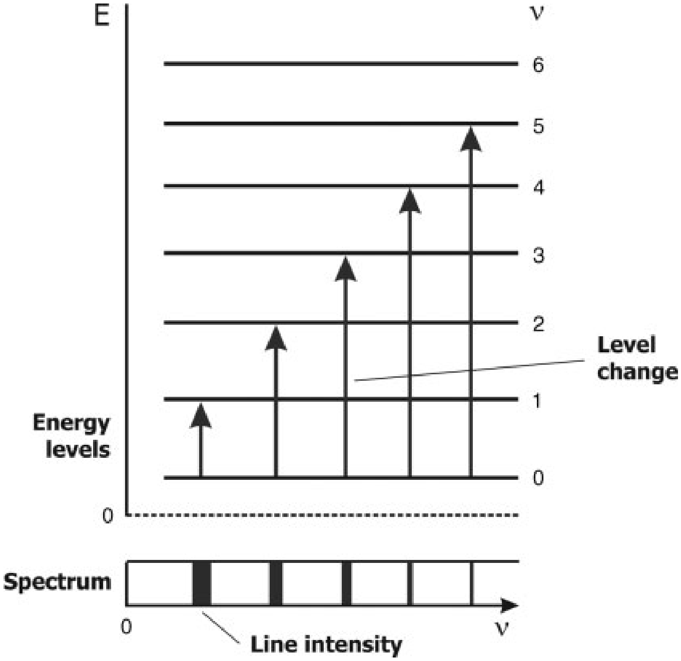

Figure 1.45 Schematic portrayal of absorbed radiation intensity for base and higher-order oscillations caused by vibronic excitation [56].

(Figure 1.45), which caused an increased optical penetration depth for absorption of electromagnetic radiation by vibronic excitation in natural polymers.

An example of absorption of NIR radiation is the stimulation of third-order vibronic oscillation of the CH valence oscillation with a base oscillation frequency of $\nu = 3100\,\mathrm{cm}^{-1}$ [55] corresponding to a wavelength of $\lambda = 3.23\,\mu\mathrm{m}$.

1.4.4.3 **Summarizing Comment**

In a regular structured material like metals or semiconductors, caused by the crystalline structure, a distinctive electronic band structure exists that is responsible for an effective absorption of NIR radiation. In contrast to this, in a natural polymeric material only statistically distributed molecule segments exist that can have an electronic band structure. Electronic as well as vibronic oscillation excitation, also higher-order vibronic excitation, occurs only with minor quantum effectiveness. Hence, an effective absorption of NIR radiation between 800 and 1200 nm on natural polymers is of little value. Figure 1.46 shows as an example the directed transmission for PC, PMMA and PP in the wavelength range from 800 to 1200 nm.

While the incident radiation is nearly completely transmitted by the amorphous plastics PC and PMMA, the semicrystalline PA6 and PP show a decrease of the radiation by scattering on crystalline structures. This indicates not an effective absorption of the radiation but a decrease of the radiation intensity by scattering.

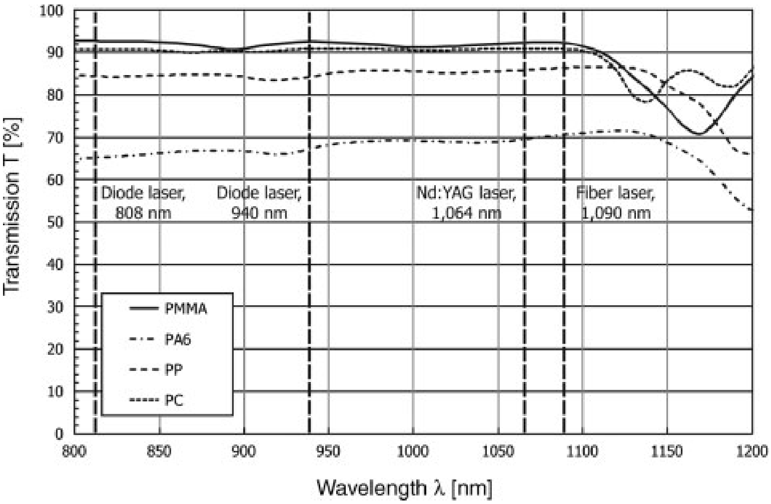

Figure 1.46 Transmission of PA6, PC, PMMA und PP in the wavelength range from 800 to 1200 nm (sample thickness 2 mm).

An example of this shows the transmission measurement on semicrystalline PA6, carried out with low-power Nd:YAG-laser radiation (Figure 1.47). The radiation is noticeably dispersed by the semicrystalline structure of the 4-mm thick PA6 sample but not absorbed. Using for comparison a mostly amorphous and optically clear PA6 film the transmission measurement results in an optical penetration depth of

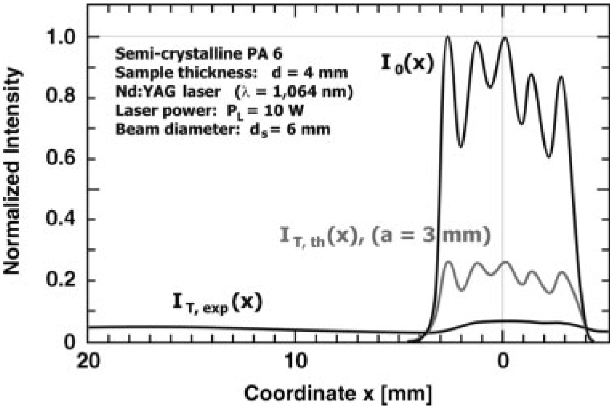

Figure 1.47 Transmission measurement on a 4-mm thick semicrystalline PA6 sample using a Nd:YAG laser. Given is the measured intensity distribution without $I_0(x)$ and with the sample $I_{T,exp}(x)$. For comparison the calculated transmitted intensity distribution $I_{T,th}(x)$ of a 4-mm thick amorphous PA6 sample is given (marked green) [57].

Table 1.14 Characteristic C—H group oscillations in the wavelength range between 1200 and 2500 nm [59].

Oscillation type of C—H group	Wave number range [cm^{-1}]	Wavelength range [nm]
Combination oscillation	4500–4200	2220–2380
First high-order oscillation, stretching oscillation	5600–6200	1790–1610
Combination oscillation	6400–7700	1560–1300
Second high-order oscillation, stretching oscillation	7800–8900	1280–1120

around 3 mm. Transferring this to an amorphous PA6 sample of 4 mm thickness a transmission of around 26% should be measured.

1.4.5

Absorption of NIR-Laser Radiation ($\lambda = 1200$ nm to 2500 nm)

Within the wavelength range of 1200–2500 nm a transition from electronic to molecule oscillation excitation occurs for electromagnetic radiation absorption in polymeric materials. While absorption of electromagnetic radiation at natural plastics can be neglected in the spectral range below 1200 nm, the absorption increased from 1200 to 2500 nm, depending on the molecule structure (see Figure 1.38). For wavelengths more than 2500 nm electromagnetic radiation will be effectively absorbed by excitation of molecule oscillations.

Lightweighted bonding partners in a macromolecule like hydrogen atoms can show extended oscillation amplitudes. Asymmetric oscillation types, where light atoms can oscillate around a strong bond, cause a relative intensive change of the dipole momentum and can be excited by absorption of electromagnetic radiation. In particular, C—H, O—H, S—H and N—H groups in the macromolecule chain can be activated [58]. Base oscillation frequencies of these groups are in the MIR spectral range. But first, higher-order oscillations are in the spectral range between 1550 and 2000 nm and additional higher-order oscillations and combination oscillations are in the spectral range between 800 and 1600 nm.

As an example Table 1.14 summarizes several oscillation types of the C–H group with oscillation frequencies in the spectral range between 1200 and 2500 nm [59].

Excitation of higher-order oscillations in the transition range is considerably weaker than excitation of base oscillations within the MIR spectral range. This causes a deeper penetration of the NIR radiation in polymeric material than MIR radiation.

Figure 1.48 shows as an example the absorption spectra of several thermoplastic resins indicating oscillation types of the C—H group.

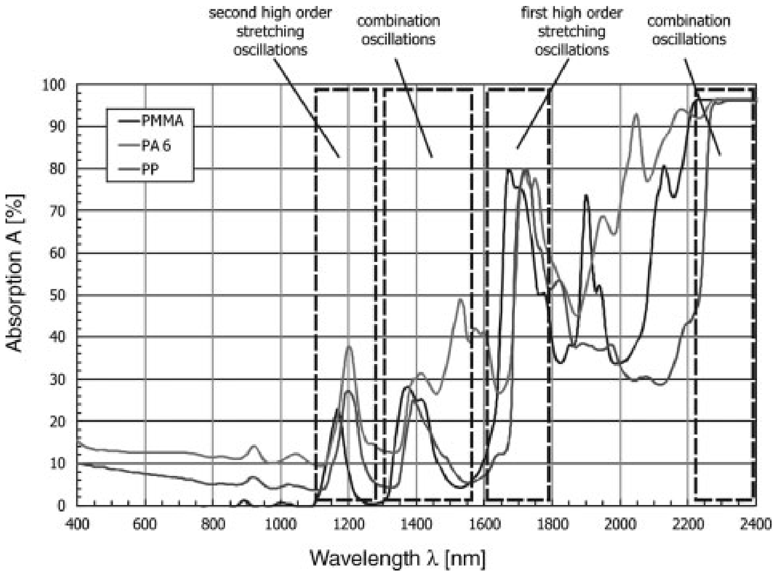

Figure 1.48 Absorption spectra of natural PMMA, PA6 and PP with indication of C—H group oscillations.

1.4.6
Absorption of MIR-Laser Radiation ($\lambda = 2.5\,\mu m$ to $25\,\mu m$)

In the spectral range of mid-infrared electromagnetic radiation (MIR spectral range), in which for example is the wavelength of CO_2 lasers ($\lambda = 10.6\,\mu m$), interaction between electromagnetic radiation and solid polymeric material occurs by excitation of elongation or bending oscillations of individual segments of the macromolecule chains [60]. Table 1.15 summarizes examples of possible chain-segment oscillation types in correlation with their spectroscopic terms.

Generally, oscillation frequencies of oscillators can only be indicated for a frequency range, because the oscillations are influenced by the statistical surrounding of the oscillators within the macromolecular chain. Influencing effects are for example [61]:

- mass of bonding partners neighbor atoms,
- bonding force,
- permanent dipoles in the near surrounding,
- conformation of the molecule chain.

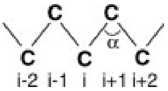

Figure 1.49 Conformation angle of frame atoms in zigzag conformation.

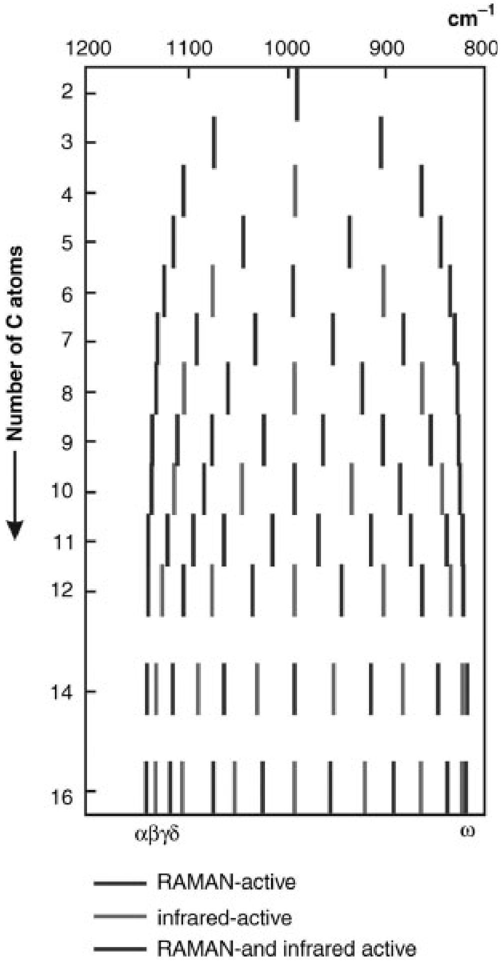

Figure 1.50 Frequencies of frame oscillations by stretched N-paraffin molecules disregarding the valence angle forces [61].

Out of the entire number of base oscillations only such oscillations can be excited by absorption of IR radiation for which the dipole momentum *m* will be changed during an oscillation period [36]. The following considerations will deal only with such IR-active oscillation types, for which the excitation frequency is in the range of the CO_2 laser frequency ($\nu = 943\,\mathrm{cm}^{-1}$, $\lambda = 10.6\,\mu\mathrm{m}$).

For absorption of CO_2-laser radiation, frame oscillations of the molecule chains, group oscillations of side-chain molecules or end-chain molecule oscillations should be considered [61].

The frequency of frame oscillations, for example, for C−C single bonds, is dependent on the number of C atoms within the molecule chain and from the conformation of the molecule chain (see. Figures 1.3 and 1.49 for zigzag conformation):

Table 1.15 Oscillation types of atoms and atom groups within a molecule chain and their spectroscopic terms [61].

Oscillation type	Term	Geometry
Valence or elongation oscillation	ν	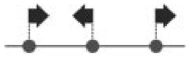
Deformation or bending oscillation in the bonding plane	δ	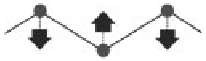
Deformation or bending oscillation vertical to the bonding plane	γ	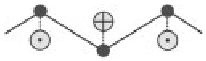
Rocking, tilting or swinging oscillation of a side group	ϱ	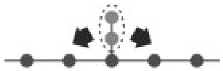
Torsion oscillation	τ	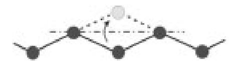

$$\nu = \nu_0 \cdot \sqrt{1 \pm \cos(\alpha) \cdot \cos\left(\frac{\pi \cdot i}{N}\right)} \tag{1.36}$$

ν_0: base oscillation frequency
α: conformation angle of frame atoms
i: 1,2, . . ., N–1
N: number of C atoms within the chain.

For a molecule chain with N atoms, which are fixed to their base positions by elastic bonding forces, there result $3N$ from each other independent base oscillations given by three spatial free oscillation degrees per atom. Translation and rotation oscillations of the entire molecule chain have to be subtracted because these oscillations cause no change of atom distances within the chain and thereby no change of the dipole momentum, generating no contribution to the absorption of electromagnetic radiation. Caused by the symmetrical quality of linear molecule chains the number of possible oscillation frequencies results in $3N$–5, while for molecule conformations like zigzag type, helix type or statistical knotted macromolecules (see Figure 1.3) the possible oscillation frequencies results in $3N$–6 [61].

The oscillation frequency of two C atoms in a molecule chain is at $\nu = 980\,\mathrm{cm}^{-1}$ ($\lambda = 10.20\,\mu\mathrm{m}$). With increasing number N of C atoms the oscillation frequency will be expanded according to Equation 1.36. For a zigzag conformation of the molecule chain with $N \mapsto \infty$, the frequency range will become $890\,\mathrm{cm}^{-1} < \nu < 1180\,\mathrm{cm}^{-1}$ ($\lambda = 11.24$–$8.47\,\mu\mathrm{m}$) [61] and CO_2-laser radiation can be absorbed.

An often occurring end group of molecule chains or their side chains is for example, the methylene group CH_3 [6]. The oscillation frequency of the methylene group is

Table 1.16 Frame and group oscillations of polymer chains in the range of the CO_2-laser wavelength (from [61]). Oscillation frequencies are given as wave numbers (cm^{-1}).

Oscillator	Oscillation type	Wave number range cm^{-1}
C–C-frame oscillation	Valence oscillation (ν)	890–1150
Methylene group -CH_2	Deformation oscillation, rocking (ϱ)	700–1000
Olefine group $X{-}CH{=}CH_2$	Deformation oscillation, wagging (g)	905–910
$X{-}CH{-}CH{-}X$		985–995 965–980
Methyl groups $-CH_3$	Deformation oscillation, rocking (ϱ)	800–1200
Carbonyl group $-C{-}O{-}H$	Deformation oscillation, bonding (δ) wagging (γ)	900–1500
		600–1000

mainly dominated by the angular force constant of the X–C–H bonding angle. The angular force constant itself depends on the influence of the atom X; properties influenced by this are for example, the electron negativity or the atom mass.

Frame oscillations of C atoms within the molecule chain as well as group oscillations of side-chain molecules like methyl or methylene groups have to be considered for absorption of CO_2-laser radiation [61]. Table 1.16 summarizes possible oscillation types and their frequency range in wave number units.

Additionally Table 1.17 shows for the thermoplastics PC, PA6 and PPS examples of molecule chain components, which can be stimulated to oscillation by absorption of CO_2-laser radiation.

Oscillation excitation by absorption of electromagnetic radiation is generally depending on the state of the material [61]. For a solid state, like crystalline areas, the macromolecules are mostly present in a zigzag or helical conformation.

Table 1.17 Thermoplastic polymers and potential structure components that can stimulated to oscillation by absorption of CO_2-laser radiation.

Polymer	Structure formula	Oscillation type
PA 6	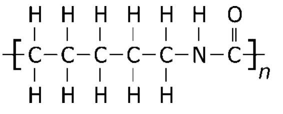 $\left[\overset{H}{\underset{H}{C}} - \overset{H}{\underset{H}{C}} - \overset{H}{\underset{H}{C}} - \overset{H}{\underset{H}{C}} - \overset{H}{\underset{H}{C}} - \overset{H}{N} - \overset{O}{\overset{\parallel}{C}} \right]_n$	–C–C– Frame oscillation
PC	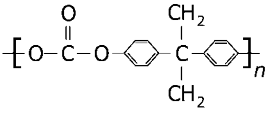	$-CH_2$ Deformation oscillation 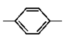 Circle deformation oscillation
PPS	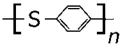	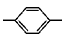 Circle deformation oscillation

Between the molecule chains, forces like hydrogen bridges or dipole bonds exist that can be increased within crystalline areas caused by near-order effects between the molecule chains. By such intermolecular forces, oscillations of atoms or atom groups will be influenced; they can be hindered or the oscillation frequency can be shifted in a way that monochromatic radiation cannot stimulate oscillations [62].

Changing from the solid state into the molten state of thermoplastics the intermolecular forces will be decreased or completely broken up. Molecule oscillations will no longer be hindered and previously inactive oscillations will be activated. Abolition of the geometrical translation symmetry of the molecule chains can additionally activate previously inactive oscillations. The entire absorption of the electromagnetic radiation can be increased by this.

1.4.7
Adaptation of NIR-Radiation Absorption by Additives

The previous considerations result in the fact that natural thermoplastic polymers have only low absorption within the NIR spectral range from 800 to 1200 nm (see Figure 1.46). Additives for coloration of plastic resins in the visible as well as filler materials and additives for reinforcement of plastics usually don't noticeably increase the absorption in the NIR. In particular, filler materials like glass spheres or fiber reinforcements increase the scattering of NIR radiation in the material but not the absorption.

To enable thermoplastic polymers for laser welding with diode, Nd:YAG or fiber lasers specially suited additives have to be mixed with the resin to increase the absorption of NIR radiation. A couple of suitable additive types like carbon black, inorganic pigments, organic dyes or nanoparticles will be discussed in the following with regard to adapting NIR absorption and influencing the visible appearance of the thermoplastic resin.

1.4.7.1 Carbon Black

Carbon black pigments are produced by incomplete combustion and/or thermal decomposition of hydrocarbons [63]. Carbon black pigments consist of carbon and are almost spherical in shape [64].

According to DIN 53206 [65] the structural occurrence of carbon black pigments is distinguished between "primarily particles," "aggregates" and "agglomerates:"

- Primarily particles are the smallest individual particles mostly occurring as spheres with diameter between 10 and 60 nm [66].
- Aggregates are built by cohesion bonding of primarily particles.
- Agglomerates are loose-packed primarily particles or aggregates with dimension of 0.3 μm up to several μm. Agglomerates can be cut up into smaller particle sizes by scattering for example, during extrusion and molding processes.

Usually, carbon black is used in plastic resins as fine dispersed pigments with typical additive weight proportions in the range between 0.01 and 3%.

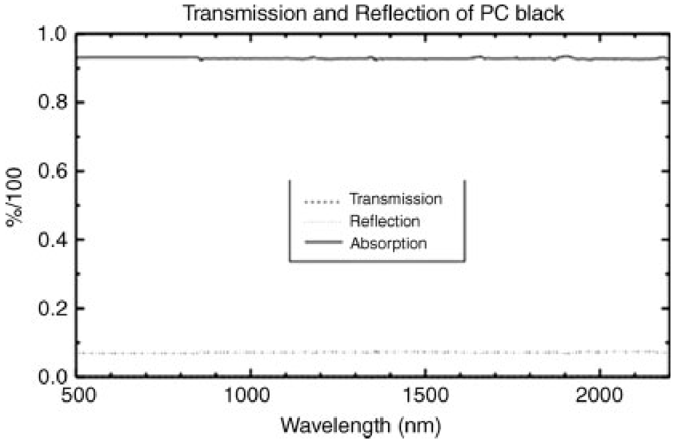

Figure 1.51 Transmission of carbon black in PC [67].

Carbon black shows a distinctive absorption for electromagnetic radiation over the entire spectral range from UV over VIS up to NIR (Figure 1.51). Caused by the high absorption property of carbon black as additive in plastic materials the optical penetration depth for NIR-laser radiation is typical limited to a range of 10 to some 100 μm, depending on the carbon black concentration. Figure 1.52 shows as an example the optical penetration depth on PP for various carbon black concentrations at the wavelength 940 nm [68].

Because of its economical cost, carbon black is a common used additive to adapt plastic resins for laser welding in various applications like automotive components.

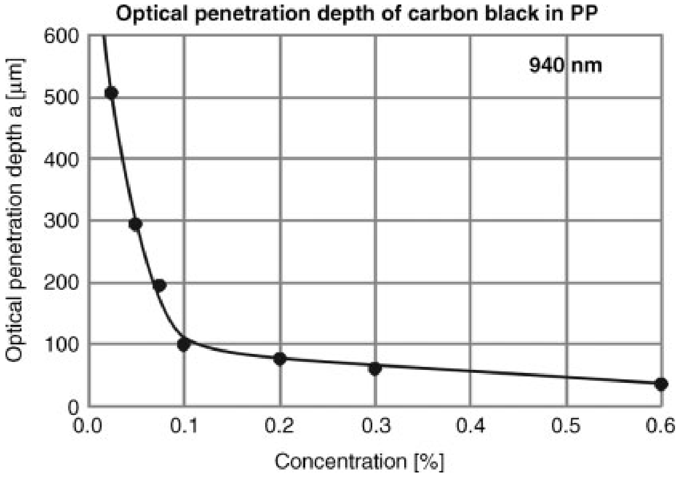

Figure 1.52 Optical penetration depth on PP with varying carbon black concentration at 940 nm from [68].

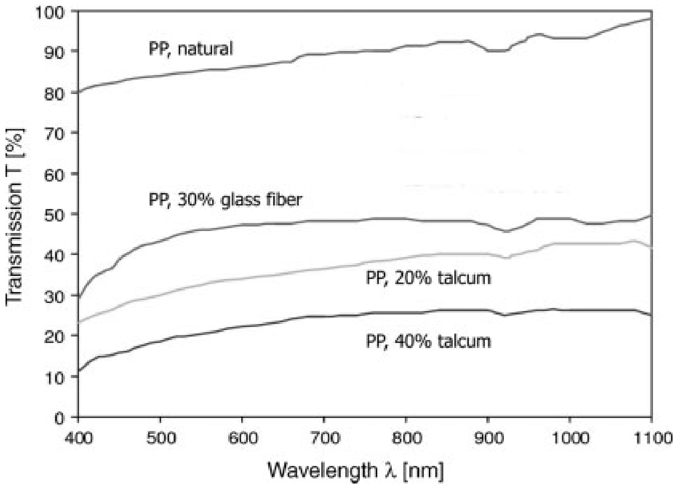

Figure 1.53 Transmission on PP with varying talcum and titanium dioxide concentration [70].

The disadvantage of carbon black is the black coloration of plastics in the visible for applications like medical devices or other goods were transparency or light coloration are required. Additionally, carbon black influences the electric conductivity of plastics, which can be a disadvantage for use at electric or electronic components.

1.4.7.2 **Inorganic Pigments**

Inorganic pigments are used as filler materials (e.g., chalk or talcum), functional additives like flame retardants or for visible coloration of plastics. Typical inorganic pigments for coloration are for example, titanium dioxide, iron oxide or other metal oxides [69]. In principle, inorganic pigments are thermally and chemically stable and can be used as additive for a wide range of thermoplastics. Due to their particle size in the range from several μm to nm inorganic pigments are dispersed in the polymer matrix as individual particles. Inorganic pigments are fixed in position by the polymer matrix and usually migration of the pigments can be neglected.

Typical inorganic pigments don’t have a noticeable influence on the absorption of NIR radiation but do increase NIR radiation scattering in the material. Figure 1.53 shows the transmission of PP with various concentrations of talcum in comparison with natural PP and with 30% reinforcement by glass fibers [70]. Increasing pigment concentration results in decreasing transmission caused by internal scattering of the radiation.

Some special inorganic pigments like Lazerflair® pigments, copper phosphates or indium tin oxide (ITO) have noticeable absorption of NIR radiation and can be used for enhancing laser weldability of plastics.

Lazerflair® pigments are structured as multilayer platelets with a core of glimmer, double-sided coated by metal oxides like TiO_2 or SnO_2 (Figure 1.54), having a platelet diameter of around 15 μm and smaller [71].

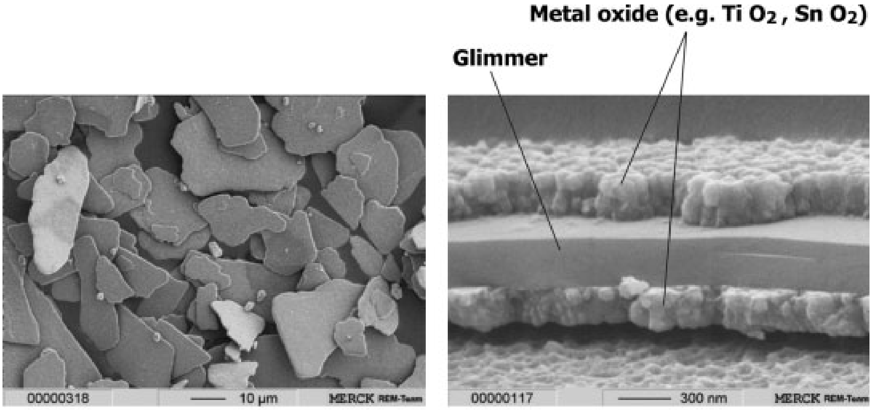

Lazerflair platelets

Platelet structure

Figure 1.54 Particle structure of Lazerflair® pigments [72].

Typically used Lazerflair® concentrations as additive in thermoplastic resins for laser welding are in the range of 0.5–2%, concentrations used for laser marking are below 0.5%. Using low concentration, transmission in the visible is relative high with some influence of internal scattering caused by the pigment size. Increasing concentrations will increase internal scattering, resulting in a noticeable haze on transparent thermoplastic resins.

Lazerflair® pigments are broad-band NIR absorbers. For example, Lazerflair® 825 has absorption from approximately 900 nm up to 2200 nm. Figure 1.55 shows as an example Lazerflair® 825 with concentration of 0.3% in a PP resin with a sample thickness of 1.5 mm.

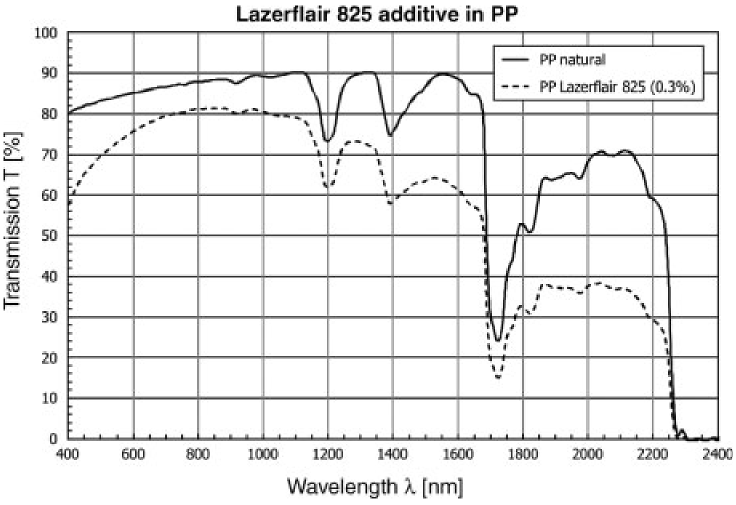

Figure 1.55 Transmission of Lazerflair® 825 in PP, sample thickness 1.5 mm.

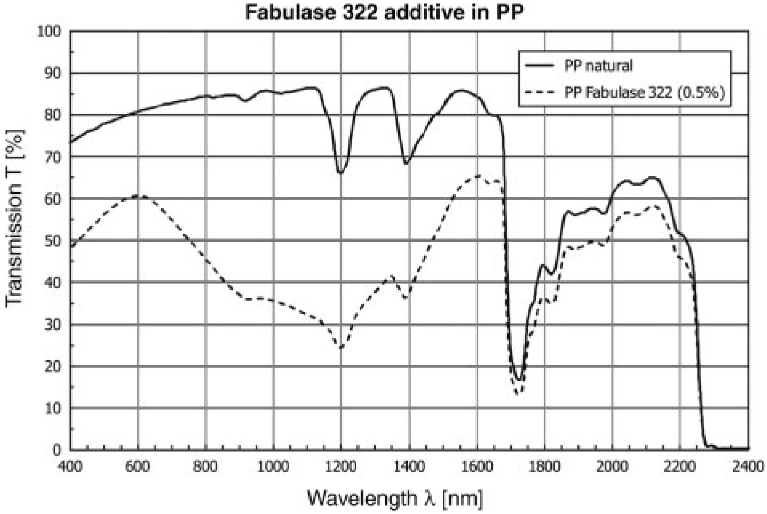

Figure 1.56 Transmission of FABULASE® 322 in PP, sample thickness 2 mm [73].

Additives based on copper phosphates like FABULASE® 322 have noticeable broad-band absorption for NIR radiation between 900 nm and 1500 nm (Figure 1.56). In the visible they add a slightly green coloration to the resin, depending on the used concentration that is commonly like Lazerflair® in the range of 0.5–2%.

FABULASE® 322 additives are available as powder with pigment sizes smaller than 3 μm and as special micronized powder with particle size smaller than 0.8 μm. Like Lazerflair®, FABULASE® 322 creates a haze in transparent thermoplastics

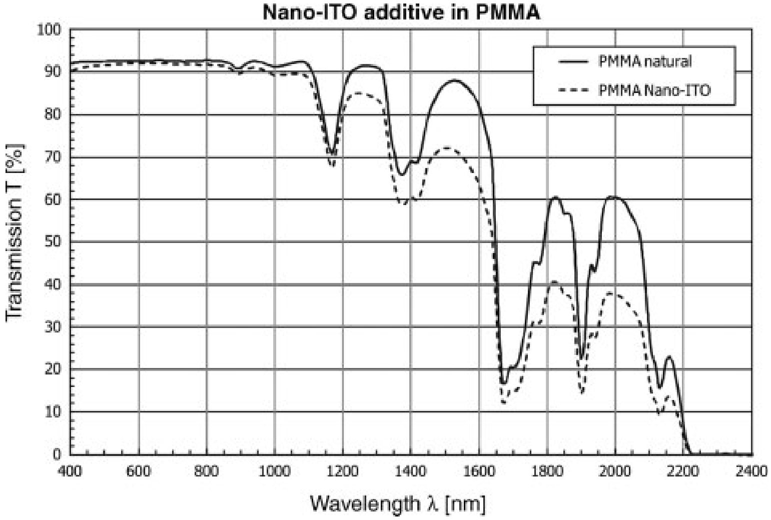

Figure 1.57 Transmission of nano-ITO particles in PMMA, sample thickness 2 mm.

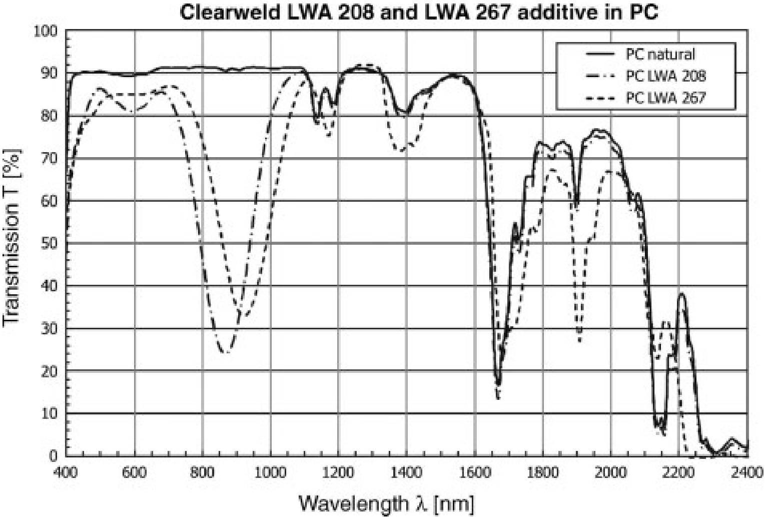

Figure 1.58 Transmission of Clearweld® A208 and A267 dye in PC, sample thickness 2 mm.

caused by internal scattering of visible radiation. The absorption properties of FABULASE® 322 in the given wavelength area are higher than for Lazerflair® 825.

Indium tin oxide (ITO) is used as nanoscale particles for example, in PMMA and transparent PA resins with low concentrations [74]. As fine dispersed particles with low concentration used for laser marking they add no coloration or haze by internal scattering to the resin because the particle size is much smaller than the wavelength of visible radiation. On increasing concentration for use for laser welding transparent

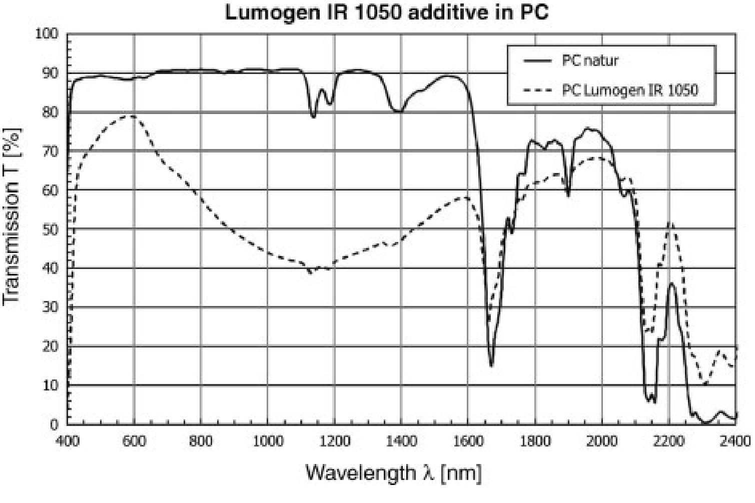

Figure 1.59 Transmission of Lumogen® IR 1050n nano-pigment in PC, sample thickness 2 mm.

Table 1.18 Absorbing additives and their properties regarding laser welding application.

Additive	Particle size [µm]	Absorption range [nm]	Thermal stability	Chemical stability	Visible influence	Can be used in (e.g.,)
Inorganic pigments						
Carbon Black	<0.3	entire spectrum	500	+ + +	Black coloration	All thermoplastics and thermoplastic elastomers
Fabulase 322	<5	900–1600	500	+ + +	Slightly green coloration with influence to hue	PE, PP, PA
Fabulase 322S	<5	900–1600	500	+ + +	Slightly green coloration with some influence to hue	PE, PP, PA
Lazerflair 825	<5	>1000	500	+ + +	Slightly gray coloration with influence to hue	PE, PP, PA
Lazerflair xxx	<S	900–1600	500	+ + +	Slightly green coloration with influence to hue	PE, PP, PA
ITO	<5	>1000	500	+ + +	Transparent colorless	PMMA, PA
Lumogen IR 1050*		900–1500	<800	+ + +	Slightly transparent green coloration	PE, PP, PA
Organic dyes						
Clearweld A267		850–1000	<300	+	Slightly transparent green coloration	PE, PP, PA
Clearweld A225		900–1100	<300	+	Slightly transparent green coloration	PE, PP, PA
Lumogen IR 788		700–810	<350	+ +	Slightly transparent green coloration	PE, PP, PA

thermoplastic resins will get a slightly bluish color with some haze. Nano-ITO additive has a broad-band absorption in the NIR spectral rang from approximately 1000–2000 nm (Figure 1.57).

1.4.7.3 **Organic Dyes**

Organic dyes like azo, perionon or perylene dyes are used for visible coloration of plastics [69]. Most of organic dyes are restricted in thermally and chemical stability and cannot be used for example, in high-temperature thermoplastics. Organic dyes, built by organic monomers, are dissolved in the polymeric matrix. Due to the state as dye solution in the matrix, internal location changes are possible and migration of organic dyes can occur especially on polyolefin resins and thermoplastic elastomers.

Usually, organic dyes for visible coloration of plastics have no significant absorption in the NIR-radiation region. But there are some special organic dyes (Clearweld® [75–78] and Lumogen® dyes [79–82]) with narrow-band absorption maxima at certain wavelengths in the NIR and less absorption in the visible. Using these dyes as additives with weight percentages between 0.02 and 0.001% will enable thermoplastics for laser welding having neglectable influence of the dye to the visible coloration also for optical transparent thermoplastics like PC or PMMA.

The narrow-band absorption of such organic dyes enables matching the absorption properties of thermoplastic resins to dedicated laser wavelengths like Lumogen® IR 788 and Clearweld® LWA 208 for 808 nm diode lasers or Clearweld® LWA 267 for 940 nm diode lasers. Figure 1.58 shows as an example the transmission spectra of Clearweld® LWA 208 and LWA 267 dyes in PC resin with a sample thickness of 2 mm.

Within the Lumogen IR product family the Lumogen IR 1050 additive is a different type, not built by an organic dye but by a special designed nano-pigment. Figure 1.59 shows the transmission spectra of Lumogen® IR 1050 in PC for a sample thickness of 2 mm.

1.4.7.4 **Summarizing Comment**

For laser welding of thermoplastics with typically used lasers like diode, Nd:YAG or fiber lasers, the material has to be adapted by suitable additives for absorbing the laser radiation. The several NIR-radiation absorbing additives previously described have different optical, chemical and geometrical properties, which are summarized in Table 1.18.

Depending on the conditions of the prevailing application like laser wavelength used, thermoplastic material, demands on color and transparency and economic aspects, the suitable absorbing additive has to be chosen to adapt the thermoplastic resin to the laser-welding process.

References

1 Frank, A. and Biederbick, K. (1984) *Kunststoffkompendium*, Vogel-Buchverlag, Würzburg.

2 Kaufmann, H. (1988) *Grundlagen Der Organischen Chemie*, 8. Auflage, Birkhäuser Verlag, Basel.

3 Jarecki, L. (1979) Thermodynamics of deformation of an isolated polymer chain. *Colloid Polym. Sci.*, **257**, 711–719.

4 Becker, W. and Braun, D. (1985) *Kunststoff-Handbuch, Bd. 2 Teil 1: Polyvinylchlorid*, 2. Auflage, C. Hanser-Verlag, München.

5 Arndt, K.F., Schröder, E., and Körner, A. (1981) Studien zur Verzweigung von Kettenmolekülen. *Acta Polymerica*, **32** (10), pp. 620–625.

6 Batzer, C. (1985) *Polymere Werkstoffe Bd.1, Chemie Und Physik*, G. Thieme Verlag, Stuttgart.

7 Henrici-Olivè, G. and Olivè, S. (1979) Molecular interactions and macroscopic properties of polyacrylonitrile and model substances, in *Advances in Polymer Science*, Springer Verlag, Berlin.

8 Skovranek, D.J., Painter, P.C., and Coleman, M.M. (1986) hydrogen bonding in polymers, 2. Infrared temperature studies of nylon 11. *Macromolecules*, **19**, 699–705.

9 Carlowitz, B. (1995) *Kunststoff-Tabellen*, 4. Auflage, C. Hanser Verlag, München.

10 DIN EN ISO 1133:2005-09 (D); Kunststoffe - Bestimmung der Schmelze-MasseflieSSrate (MFR) und der Schmelze-Volumenfliessrate (MVR) von Thermoplasten (ISO 1133:2005); Deutsche Fassung EN ISO 1133:2005; Beuth Verlag GmbH, Berlin.

11 Menges, G., Haberstroh, E., Michaeli, W., and Schmachtenberg, E. (2002) *Werkstoffkunde Kunststoffe*, 5. Auflage, C. Hanser-Verlag, München.

12 Avramova, N. and Fakirov, S. (1981) Melting behaviour of drawn and undrawn annealed nylon 6. *Acta Polymerica*, **32** (6), pp. 318–322.

13 Bhowmick, A.K. and Stephens, H.L. (2000) *Handbook of Elastomers*, 2nd edn, CRC-Press, Boca Raton, US.

14 Robeson, L.M. (2007) *Polymer Blends: A Comprehensive Review*, Hanser Verlag.

15 Albis Guide Chart, Application and Processing of Selected Thermoplastics, company brochure, Albis Plastic GmbH, Hamburg.

16 Hagiopol, C. (2000) *Copolymerizetion*, Springer Press.

17 Holden, G., Kricheldorf, H.R., and Quirk, R.P. (2004) *Thermoplastic Elastomers*, 3rd edn, Hanser Verlag.

18 ALLOD (2009) Werkstoff GmbH & Co. KG; GRUNDLAGEN TPE; www.allod.com.

19 Batzer, H. (1985) *Polymere Werkstoffe, Bd. 3: Technologie II*, Georg Thieme Verlag, Stuttgart.

20 Niederstadt, G. (1988) Konstruieren mit Faserverstärkten Polymeren – Das Heterogene Wärmeausdehnungsverhalten als neues Dimensionierungskriterium für Faserverbund-Werkstoffe. Proceedings Verbundwerk ’88, Wiesbaden.

21 Wunderlich, B. and Baur, H. (1970) Heat capacities of linear high polymers. *Adv. Polym. Sci.*, **7**, 159–368.

22 Bergmann, L. and Schäfer, C. (1981) *Lehrbuch Der Experimentellen Physik, Bd. 3v Teil 1 Aufbau Der Materie*, 2. Auflage, De Gruyter Verlag, Berlin.

23 VDMA (1979) *Kenndaten Für Die Verarbeitung Thermoplastischer Kunststoffe, Teil 1: Thermodynamik*, C. Hanser Verlag, München.

24 Rein, D.M. *et al.* (1981) The model of polymer crystallisation under non-isothermal conditions. *Acta. Polymerica.*, **32** (1), pp. 1–5.

25 Becker, R. (1985) *Theorie Der Wärme*, 3. Auflage, Springer Verlag, Berlin.

26 Debye, P. (1912) Zur Theorie der spezifischen Wärme. *Ann. Physik*, **39**, 789.

27 Einstein, A. (1907) Die Plancksche Theorie der Strahlung und die Theorie der spezifischen Wärme. *Ann. Physik*, **22**, 180.

28 Debye, P. (1914) *Vorträge Über Die Kinetische Theorie Der Materie und Der Elektrizität*, Wolfskehlvorträge, Teubner Verlag, Berlin, pp. 19–60.

29 Eiermann, K. (1964) Modellmässige Deutung der Wärmeleitfähigkeit von Hochpolymeren, teil 1: amorphe hochpolymere. *Kolloid-Zeitschrift & Zeitschrift für Polymere*, **198** (1–2), pp. 5–16.

30 Eiermann, K. (1964) Modellmässige deutung der wärmeleitfähigkeit von hochpolymeren, teil 2: verstreckte amorphe hochpolymere. *Kolloid-Zeitschrift Zeitschrift für Polymere*, **199** (2), pp. 125–128.

31 Knappe, W. (1971) Wärmeleitung in Polymeren. *Adv. Polym. Sci.*, **7**, 477–535.

32 Potente, H. (2004) *Fügen von Kunststoffen*, C. Hanser Verlag, München.

33 Herziger, G. and Loosen, P. (1993) *Werkstoffbearbeitung mit Laserstrahlung*, C. Hanser Verlag, München.

34 Bergmann, L. and Schäfer, C. (1978) *Lehrbuch Der Experimentalphysik, Bd. III Optik*, 7. Auflage, De Gruyter Verlag, Berlin.

35 Engelke, F. (1985) *Aufbau der Moleküle*, B. G. Teubner, Stuttgart.

36 Born, M. (1981) *Optik*, 3. Auflage, Springer-Verlag, Berlin, Nachdruck der.

37 Bunget, I. and Popescu, M. (1984) *Physics of Solid Dielectrics*, Elsevier, Amsterdam.

38 Wooten, F. (1972) *Optical Properties of Solids*, Academic Press, New York.

39 VDMA (1979) *Kenndaten für die Verarbeitung Thermoplastischer Kunststoffe, Teil 1: Thermodynamik*, C. Hanser Verlag, München.

40 Schreyer, G. (1972) *Konstruieren mit Kunststoffen*, C. Hanser Verlag, München.

41 Steinfeld, J.I. (1985) *Molecules and Radiation*, 2. Auflage, MIT Press, Cambridge.

42 Ben Shaud, A., Haas, Y., Kompa, K.L., and Levine, R.D. (1981) *Lasers and Chemical Change*, Springer Verlag, Berlin.

43 Bergmann, L. and Schäfer, C. (1978) *Lehrbuch der Experimentalphysik, Bd. 333 Optik*, 7. Auflage, De Gruyter Verlag, Berlin.

44 Günzler, H. and Böck, H. (1983) *IR-Spektroskopie*, 2. Auflage, Verlag Chemie, Weinheim.

45 Wooten, F. (1972) *Optical Properties of Solids*, Academic Press, New York.

46 Klein, R. (1988) Kunststoffbearbeitung Mit Laser, Technika No. 7.

47 Lenz, R.W. and Stein, R.S. (1973) *Structure and Properties of Polymer Films*, Plenum Press, New York.

48 Adrio, J. (1969) Strahlungseigenschaften Pigmentierter Kunststoffe Im Bereich Der Temperaturstrahlung, Dissertation, RWTH Aachen.

49 Kreker, M. (1969) *The Scattering of Light*, Academic Press, New York.

50 Brügel, W. (1961) *Physik und Technik der Ultrarotstrahlung*, C. R. Vincentz Verlag, Hannover.

51 Becker, G.W. and Braun, D. (1988) *Kunststoff-Handbuch, Band 10 Duroplaste*, C. Hanser Verlag, München.

52 Batzer, H. (1985) *Polymere Werkstoffe, Bd. 3, Technologie II*, Georg Thieme Verlag, Stuttgart.

53 Kaufmann, H. (1988) *Gundlagen der Organischen Chemie*, 8.Auflage, Birkhäuser Verlag.

54 Engelke, F. (1985) *Aufbau der Moleküle*, B.G. Teubner, Stuttgart.

55 Günzler, H. and Böck, H. (1983) *IR-Spektroskopie*, 2. Auflage, Verlag Chemie, Weinheim.

56 Herzberg, G. (1950) *Molekular Spectra and Molecular Structure Bd. 1: Spectra of Diatomic Molecules*, Van Nostrand Reinhold Co., New York/USA.

57 Klein, R. (1990) Bearbeitung von Polymerwerkstoffen mit Infraroter Laserstrahlung, Dissertation RWTH Aachen.

58 Hesse, M., Meier, H., and Zeeh, B. (2005) *Sperktroskopische Methoden in Der Organischen Chemie*, Georg Thieme Verlag, Stuttgart.

59 Marquardt, J. (2003) Nah-Infrarot-Spektroskopie für die schnelle Polymeranalytik und die zerstörungsfreie Evaluierung von Materialeigenschaften, Dissertation Albert-Ludwigs-Universität Freiburg I. Br.

60 Hummel, D. (1974) *Polymerspectroscopie*, Verlag Chemie, Weinheim.

61 Stuart, H.A. (1967) *Molekülstruktur*, Springer-Verlag, Berlin.

62 Steinfeld, J.I. (1985) *Molecules and Radiation*, 2nd edn, MIT Press, Cambridge.

63 Ferch, H. (1995) *Pigmentrusse*, Vincentz Verlag, Hannover.

64 Klein, H.M. (2001) Laser Beam Welding of Plastics in Micro Technology, Thesis, RWTH Aachen.

65 N.N. (1996) *DIN 53206*, Beuth Verlag, Berlin.

66 Schulz, J.E. (2002) Material, Process and Component Investigations at Laser Beam Welding of Polymers, Thesis, RWTH Aachen.

67 Staub, H. (2001) Experimenteller Vergleich des Kontur- und Simultanfügens von Thermoplasten mittels Hochleistungsdiodenlaserstrahlung hinsichtlich Fügbarkeit und

Spaltüberbrückbarkeit, Diplomarbeit, Fachhochschule Würzburg-Schweinfurt.

68 Russek, U.A. (2006) *Prozesstechnische Aspekten des Laserdurchstrahlschweißens von Thermoplasten*, Shaker Verlag, Aachen.

69 Etzrodt, G. (2003) *Die Farbenwelt der Kunststoffe*, Verlag Moderne Industrie, Landsberg/Lech.

70 Russek, U.A., et al. (2007) Anwenderhandbuch zum Laserschweißen von Kunststoffen, BMBF-Förderprojekt “Verfahrensoptimierte Werkstoffpaarungen zum Kunststoffschweißen mit Laserstrahlung” FKZ 03N3116.

71 Merck KGaA (2009) When Light Welds - laser Welding of Plastics, company product brochure June 2009.

72 Rosenberger, S. and Hopfner, M. (2005) Kunststoffe und Pigmentierungen für das Beschriften und Schweißen MIT Laser. Proceedings Wolf Technologieseminar, Freudenstadt.

73 Klein, R. and Wissemborski, R. (2010) Welding and marking of plastics with lasers. *Laser Technik Journal*, Sept. 2010 No. 5, Wiley-VCH Verlag, Weinheim.

74 Wolff, W. (2005) *Hochtransparente Kunststoffe Dauerhaft Beschriften; Kunststoffe, 9/2005*, Carl Hanser Verlag, München.

75 Hoult, A.P. and Burrell, M. (2002) The effect of diode laser wavelength on the clearweld welding process. Proceedings ICALEO.

76 Woosman, N.M. and Burrell, M. (2003) A study of the effect of weld parameters on strengths of clearwelded thermoplastics. Proceedings ICALEO.

77 Woosman, N.M. and Sallavanti, R.A. (2003) Achievable weld strengths for various thermoplastics using the clearweld process. Proceedings Antec.

78 Klein, R. (2007) Laserstrahlschweißen transparenter und farbiger Kunststoffe. *Laser Tech. Journal*, Sept. 2007 No. 4, Wiley-VCH Verlag, Weinheim.

79 Boehm, A.J. and Edison, M. (2005) Laser Transmission Welding Of Plastics In Medical Device Manufacturing – How To Choose The Right Laser Additive, SPE-TopCon.

80 Boehm, A.J. and Edison, M. (2005) The Quaterrylimides – Highly Efficient Nir Absorbers for Laser Transmission Welding of Plastics, SPE-TopCon.

81 Boehm, A.J. and Glaser, A. (2004) The quaterrylimides – highly efficient NIR absorbers for plastics. Proceedings Antec.

82 Boehm, A.J. (2006) NIR radiation management part III – rational design of novel NIR absorbers for plastics. Proceedings Antec.

2
Laser Sources for Plastic Welding

2.1
Properties of Laser Radiation

Natural electromagnetic radiation like sunlight as well as conventional technical radiation generated by electrical, thermal or chemical processes for example, electric light bulbs, heated bodies or oxidation processes usually contains a large number of wavelengths. The radiance spread is spherically isotropic and the photons of such radiation have no correlation between themselves. Focusing properties of conventional electromagnetic radiation are limited to spot sizes much larger than the wavelengths of the radiation (Figure 2.1) [1].

In contrast to this, laser radiation has a narrow selective frequency spectrum with a major wavelength, is in principle linearly directed and can be theoretically focused to spot sizes around half the wavelength of the radiation (Figure 2.1).

In the following, a brief description of generating a laser beam and the properties of laser radiation will be given. For more details the reader is referred to specialized literature dealing with the principles of lasers (e.g., [2–4]).

Laser is short for "*l*ight *a*mplification by *s*timulated *e*mission of *r*adiation." The basic principle of the process is given by an oscillation system like a bonded electron or a molecule that can be excited by electrical, optical or chemical energy input to a higher energy level with an energy difference of $\Delta h\nu$ to the ground energy level (Figure 2.2). The excited state has a certain lifetime before statistical relaxation back to the ground state occurs by spontaneous emission of a photon with energy $\Delta h\nu$. As long as the system is excited an external photon of energy $\Delta h\nu$ can stimulate the relaxation process to the ground level (or a lower energy level) by emitting a second photon of energy $\Delta h\nu$. In case of a high number of excited oscillation systems a cascade process of stimulated emission will occur generating the light amplification.

The medium carrying optical active oscillation systems can be solid material, a fluid or a gas. Typical laser media for plastic welding are for example, crystal materials

Laser Welding of Plastics, First Edition. Rolf Klein.
© 2011 Wiley-VCH Verlag GmbH & Co. KGaA. Published 2011 by Wiley-VCH Verlag GmbH & Co. KGaA.

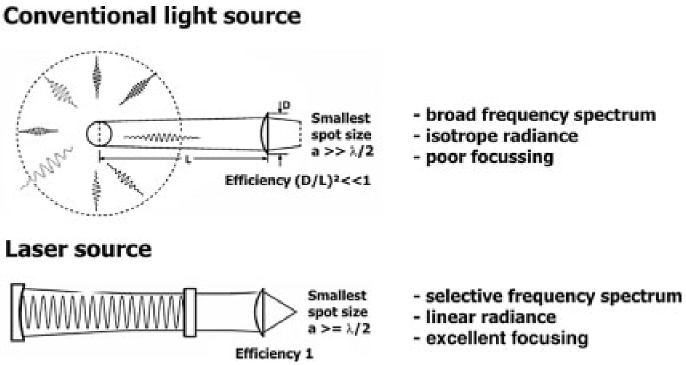

Figure 2.1 Characteristics of laser light compared to conventional light source [1].

like Nd:YAG, semiconductor materials (diode lasers), special doped glass fibers or in some cases CO_2-gas mixtures.

To generate laser radiation the optically active medium is placed in-between an optical resonator built by one reflective and one semitransparent mirror (Figure 2.3). A pumping source like a flash lamp, an arc lamp, an electric current or an electrical discharge activates the oscillating systems of the optically active medium to a higher energy level. A spontaneously emitted photon starts a cascade of stimulated emission of photons of the same frequency. The generated light is reflected inside the optical resonator, increases the stimulated emission of radiation and generates a static wave oscillation with longitudinal and transversal intensity distributions (longitudinal and

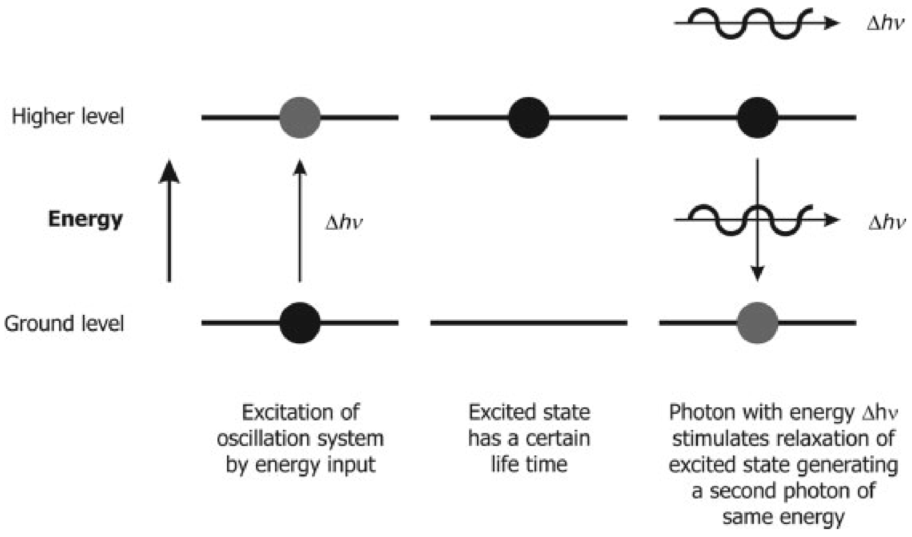
Δhν
Higher level
Energy
Δhν
Δhν
Ground level
Excitation of oscillation system by energy input
Excited state has a certain life time
Photon with energy Δhν stimulates relaxation of excited state generating a second photon of same energy

Figure 2.2 Basic process for stimulated emission of radiation.

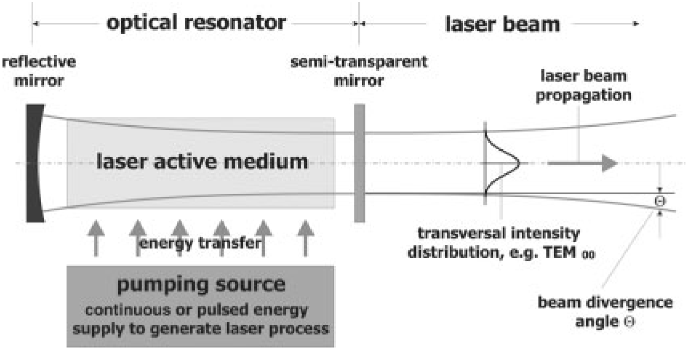

Figure 2.3 Basic laser setup.

transversal modes). The number of longitudinal modes results in the line width of the laser, while the transversal mode number influences the quality of the laser radiation, like beam propagation and focusing properties.

A fraction of the radiation inside the optical resonator passes the semitransparent mirror and generates the laser beam with high optical quality compared to conventional light, given by coherency, major wavelength, divergence and intensity distribution of the radiation.

For laser welding plastics, wavelength, intensity distribution and beam propagation are of major interest because these properties influence the focusing properties and the interaction of laser radiation with plastic materials.

2.1.1
Laser Wavelength

The typical wavelength of a laser depends on the type of laser active media (Table 2.1). For laser welding plastics, mostly NIR-laser radiation generated by diode, Nd:YAG or fiber lasers in the spectral range from 800 to 2500 nm is of interest because the laser radiation can penetrate the plastic materials to some extent.

Only for special applications like welding thin plastic films can CO_2-laser radiation with a wavelength of 10.6 μm be used, because of its limited penetration depth in plastic materials.

Table 2.1 Wavelength of laser sources typical used for plastic welding.

Laser source	Active medium	Pumping process	Wavelength
Diode laser	Semiconductor	Electric current	800 nm to 2000 nm typical: 940 nm, 980 nm
Nd:YAG laser	Doped crystal	Optical radiation	1064 nm
Fiber laser	Doped glass fiber	Optical radiation	1030 nm to 1620 nm, typical: 1070 nm, 1090 nm
CO_2 laser	Gas mixture	Electric gas discharge	10,6 μm

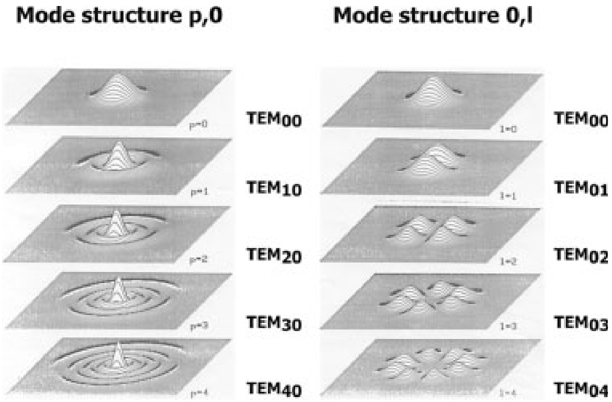

Figure 2.4 Typical intensity distributions of lasers [5].

2.1.2
Intensity Distribution

Due to the generation process of laser radiation within an optical resonator the intensity distribution of a laser beam has a discrete state that can be described by Hermite or Laguerre mathematic functions [5].

The basic intensity distribution (Figure 2.4) of a laser beam is a Gaussian shape called TEM_{00} (basic transversal excited mode) and has the lowest divergence and in principle the best focusing properties. Higher-order modes like TEM_{01} or TEM_{03} show higher divergence and lower focusing properties compared to TEM_{00}.

Laser sources used for plastic welding are diode, Nd:YAG or fiber lasers. Fiber lasers suitable for this application commonly generates high-quality laser beams with Gaussian beam shape. Nd:YAG lasers work with lower mode quality, sometimes with an intensity distribution called a top-hat mode, which is a superposition of a number of modes resulting in a more or less homogeneous intensity distribution over the beam diameter. Diode lasers are a special type of laser built by a high number of single laser emitters [6]. The laser beam shape is a superposition of the single laser beams resulting in a nearly Gaussian distribution in one direction and a top-hat distribution perpendicular to the Gaussian distribution.

2.1.3
Beam Propagation

Compared to conventional light laser beams have in principle very low divergence and allow propagation over long distances without noticeable spreading of the beam. Depending on the configuration of the laser resonator the smallest radius r_0 (beam waist) of the laser beam can be for example, at the semitransparent mirror or at a location z in the propagation direction [2].

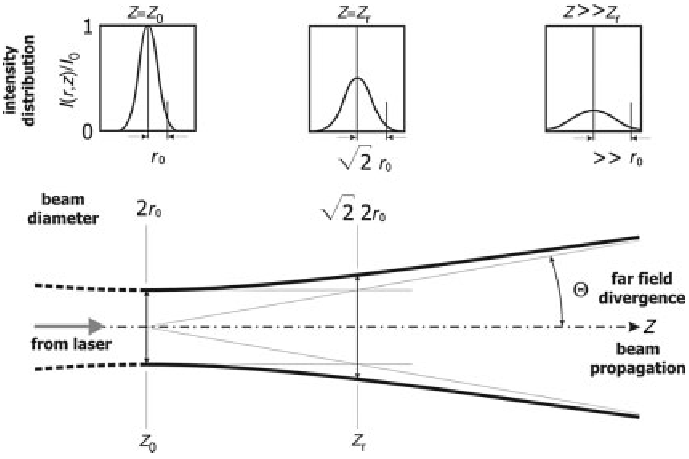

Figure 2.5 Beam propagation of TEM_{00} mode [5].

Propagation of a free-running laser beam, for example in basic mode TEM_{00} with a Gaussian beam shape, can be distinguished between two characteristic areas and separated by the Rayleigh length z_r (see Figure 2.5) [1, 5]:

$z_0 < z < z_r$: beam propagation is nearly parallel (near field),
$z = z_r$: beam radius is twice the radius of the beam waist,
$z > z_r$: beam radius increases proportional to the distance z (far field).

For TEM_{00} radiation the Rayleigh length z_r is defined by the beam waist and the laser wavelength:

$$z_r = \frac{\pi r_0^2}{\lambda} \tag{2.1}$$

z_r: Rayleigh length
r_0: beam waist radius
λ: wavelength.

For laser beams with higher mode structure Equation 2.1 is in principle also valid, but lower beam quality have to be taken into consideration by adding a beam quality factor K. The beam quality K is 1 for TEM_{00} radiation and <1 for higher beam modes.

The proportionality of increasing the beam radius in dependence to the distance in the far field is given by the far field divergence θ as function of the wavelength λ and the beam waist radius r_0 as:

$$\theta = \frac{\lambda}{\pi r_0} \tag{2.2}$$

λ: wavelength
r_0: beam waist radius.

Table 2.2 BPP of typical laser sources for plastic welding.

Laser source	Wavelength	Mode structure	BPP [mm mrad]
Diode laser	808 nm, 940 nm, 980 nm	TEM_{00} in fast axis, high order in slow axis	Fast axis: < 1 Slow axis: < 300
Nd:YAG laser	1064 nm	commonly high order	25
Fiber laser	1050 nm, 1090 nm	TEM_{00}	0.34 to 1.8
CO_2 laser	10,6 μm	TEM_{00} or low order	6

The unit of the divergence is usually given in mrad. Equation 2.2 is valid for TEM_{00} radiation, for higher mode structures the factor K has to be taken into consideration. The better the beam quality the lower the divergence of the laser beam.

A constant quantity for laser-beam propagation in an optical train is the beam parameter product BPP, given by multiplication of far field divergence θ_0 and beam waist radius r_0:

$$\mathrm{BPP} = \theta_0 r_0 \tag{2.3}$$

The unit of the BPP is given as mm × mrad. Table 2.2 gives some BPP examples for several laser sources used for laser plastic welding.

The BPP is an unchanging quantity for the beam propagation also for changing the beam shape by optical elements like mirrors or lenses. For example, a focusing element will decrease the beam waist radius at the focal spot but will increase the divergence angle of the beam according to the constant BPP.

2.1.4
Focusing Properties

For laser material processing the laser beam coming from the laser source has to be focused by optical elements like lenses or mirrors. Given by the physical properties of laser radiation, like single wavelength, mode structure and low divergence, laser radiation can be focused to spot sizes much smaller than for conventional light. Theoretical spot sizes of diffraction-limited laser radiation are of the order of half of the laser wavelength and the minimum spot size of a CO_2 laser ($\lambda = 10.6\,\mu m$) is in principle ten times larger than the minimum spot size of a Nd:YAG laser ($\lambda = 1.064\,\mu m$) of the same beam quality. Practical spot sizes are larger than the theoretical size because of the optical qualities of focusing elements like geometrical aberration [2].

For a fully illuminated focusing element the achievable spot size of focused laser radiation depends on the focal length of the focusing element and the wavelength of the laser radiation. The focal length determines the aperture angle Θ_f of the focused radiation. For a Gaussian beam in TEM_{00} mode the focal beam radius is given by:

$$r_f = \frac{\lambda}{\pi\theta_f} \tag{2.4}$$

λ: wavelength
θ_f: aperture angle of focusing element.

In correlation with the beam propagation parameter BPP of the free-running laser beam it is:

$$\text{BPP} = \theta_0 r_0 = \theta_f r_f \tag{2.5}$$

The quality of the laser beam as well as the focusing length influences the focal spot diameter and the field of depth (Rayleigh length) of the focused laser beam. Figure 2.6 shows the principal behavior of a focused laser beam in correlation with good and poor BPP as well as in dependence on the focal length of the focusing element [7].

The left part of Figure 2.6 illustrates the achievable spot size (beam waist) for a good and poor BPP at the same focal length and indecent beam size on the focusing element. Poor BPP results in a larger spot size than for a good BPP.

The middle part of Figure 2.6 shows that for the same achieved beam waist radius by constant focal length the Rayleigh length for good BPP is larger than for poor BPP even the laser beam with good BPP illuminates the focal element not as completely as the beam with poor BPP.

The right part of Figure 2.6 gives the portrayal for different focal lengths and the same illumination of the focusing element to achieve the same beam waist for

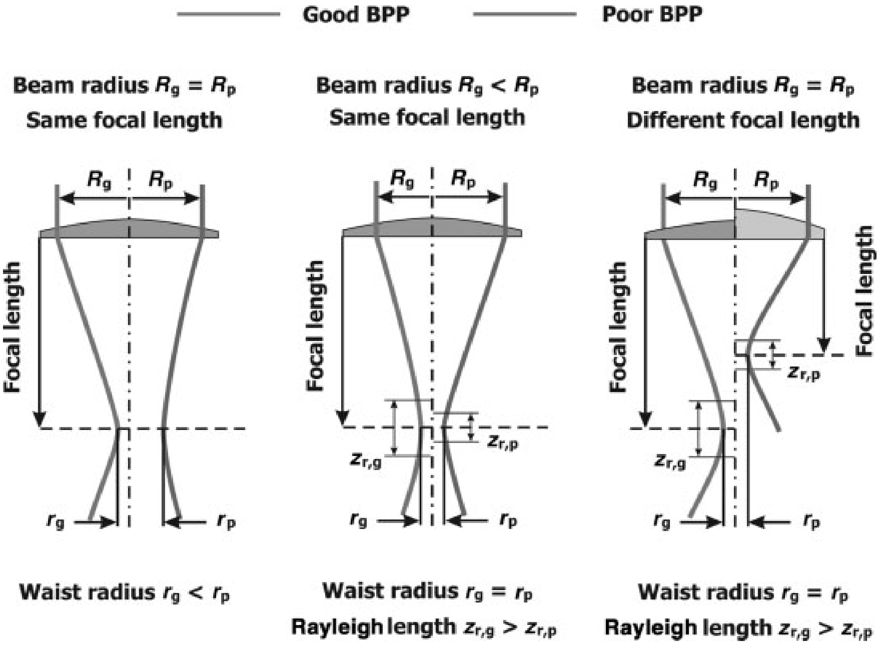

Figure 2.6 Spot sizes and Rayleigh length in correlation with BPP and focal length [7].

good and poor BPP. For good BPP the focal length and Rayleigh length is larger than for poor BPP.

2.2
Types of Lasers

For laser welding plastics various laser sources in the spectral range from 800 to 2000 nm are available. The first industrial laser welding applications were made using diode lasers with 808 nm wavelength and Nd:YAG lasers with 1064 nm wavelength. But application of these lasers is decreasing because of process reliability, laser working life and especially for Nd:YAG lasers maintenance costs and low plug efficiency. Current production mainly used are diode lasers with 940 nm or 980 nm wavelength with excellent plug efficiency and reliability. For most applications the beam quality of such lasers is good enough, generating weld line widths in the mm range.

New developments of lasers like fiber lasers with excellent beam quality, reliability and plug efficiency and also diode lasers with wavelength of more than 1000 nm opens up new possibilities for plastic laser welding applications. Due to the good beam quality of fiber lasers small geometrical dimensions like microfluidics can be welded as well as large-sized components. Higher diode laser wavelengths enables laser-welding processes on plastic materials without the need for absorbing additives in the plastic like carbon black, inorganic pigments of organic dyes, needed for laser welding applications in the spectral range between 800 and 1100 nm.

In some special cases like welding of thin plastic films also CO_2 lasers can be used. In the following, a brief description of these lasers will be given in order of typical wavelengths of the lasers used for plastic welding.

2.2.1
Diode Lasers (800 to 2000 nm)

Today, diode lasers are one of the most important laser sources for industrial applications, available in a broad wavelength range from UV to IR radiation with laser power from mW to several kW. The application spectrum is widespread from information technology, like signal transmission over large distances via glass fiber cable, light sources for CD, DVD and Blue Ray players, up to optical pumping sources for lasers used in material processing and direct use as lasers sources for material processing [8].

Especially for laser welding plastics, the wavelength range from 800 to 2000 nm is of special interest. Commonly used diode laser wavelengths for laser welding plastics are 808 nm, 940 nm or 980 nm with laser power up to 300 W. However, longer wavelengths for plastic laser welding are also under development or starting application because of their absorption properties on thermoplastic materials.

The laser-active medium of diode lasers are semiconductor materials like GaAlAs or InGaAsP, which have a direct influence on the wavelength of the laser radiation

Table 2.3 Semiconductor materials and wavelengths of diode lasers [6].

Laser active semiconductor material	Laser wavelength λ [nm]
GaAsP	780, **810**
AlInGaAs	810
InGaAs	880, **940**, **980**, 1060

bold typed: main wavelength for material processing.

(see Table 2.3). Activating the process for generating laser emission will be done directly by applying an electrical current to the laser diodes. Given by this and the quantum efficiency of the laser process, diode lasers have a high degree of plug effectiveness in the range up to 40%. But caused by the general set up of diode lasers the laser beam quality is much lower than for other laser sources.

For more detailed information about the basic physical principles of the laser generating process for diode lasers the reader is referred to special literature like [6, 9].

The general set up of a typical diode laser used for material processing is given by a couple of single emitters placed on a diode bar (Figure 2.7). The diode laser will be built up by stacking several diode bars into a diode stack.

Each single emitter of the diode bar carries his own laser resonator on the front and back end to generate laser radiation. The laser radiation of the single emitters will be transformed by microlenses to a laser beam. The laser radiation from a single emitter has an elliptical cross section caused by the rectangular facet of the single emitter; the divergence of the beam is different in the x-direction ("slow axis") than in the y-direction ("fast axis").

As a result, the sampling of the single laser beams of a diode bar by the microlens array to a combined laser beam will generate a laser beam with different beam shape and divergence for both directions. The fast axis will have a Gaussian shape with high divergence, while the slow axis is a superposition of the single beams with nearly rectangular shape and low divergence.

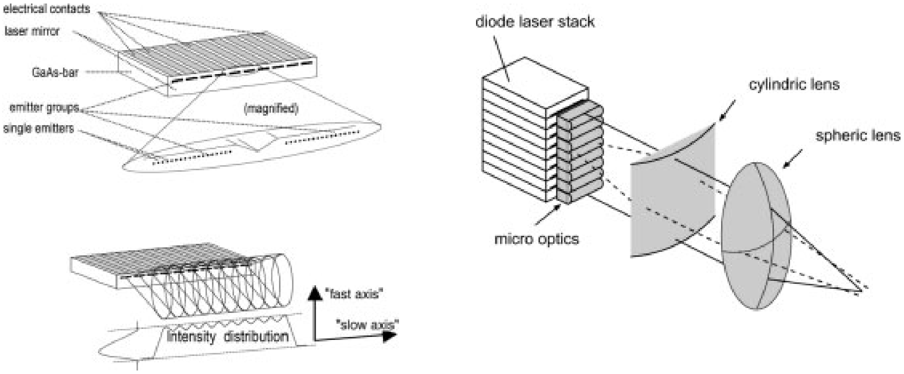

Figure 2.7 Schematic setup of a diode laser [1].

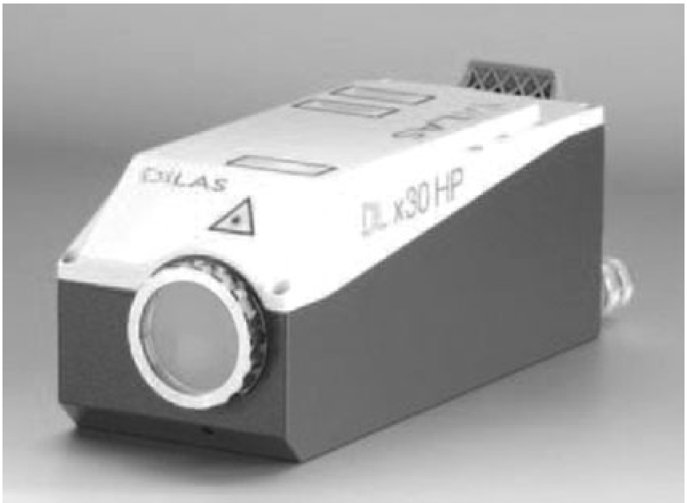

Figure 2.8 Diode laser with direct beam emission [10].

The combination of the laser diode bars to diode stack results in a rectangular beam shape of the diode laser beam. Diode lasers can be used as direct coupled or fiber-coupled lasers.

Direct coupled diode lasers (Figure 2.8) emit laser radiation of square or rectangular beam shape that can be transformed to square or rectangular spot sizes by focusing lenses. The beam shape of the free-running beam is correlated with the stacking of the diode bars. The quality of the laser beam is in principle low and the divergence of the beam is different for the fast and slow axis. This can cause astigmatism of the focused laser beam resulting in a different focal position for fast and slow axis, which can be corrected by using special designed lens systems using for example, different cylindrical lenses for fast and slow axes.

Fiber-coupled diode lasers (Figure 2.9) uses a glass fiber to transport the laser beam from the diode laser to the focusing unit. The laser radiation of the diode laser will be coupled into the glass fiber by a specially designed lens system having a certain loss of laser power. The beam shape after the glass fiber will have a circular top-hat intensity distribution with better beam quality than direct coupled diode lasers.

For example, the diode laser shown in Figure 2.9 has an output power after the glass fiber up to 500 W at 980 nm wavelength with a plug efficiency of around 40%. The beam quality after the glass fiber is 30 mm mrad [11] having a circular beam shape.

2.2.2
Nd:YAG-Lasers (1064 nm)

Nd:YAG lasers as solid-state lasers with wavelength of 1064 nm have been used in industrial applications for a long time up to laser powers of several kW. Before development of diode lasers, Nd:YAG lasers were available as pulsed (pw) or

Figure 2.9 Fiber-coupled diode laser with laser power up to 500 W [11].

continuous wave (cw) lasers, optical pumped by flash lamps for pw or arc lamps for cw modes [12, 13].

Figure 2.10 shows a typical setup of a lamp-pumped Nd:YAG laser. The Nd:YAG crystal rod as the laser medium is placed together with the pump lamp(s) within a mirror like polished elliptical (using one lamp) or double elliptical cavity (using two

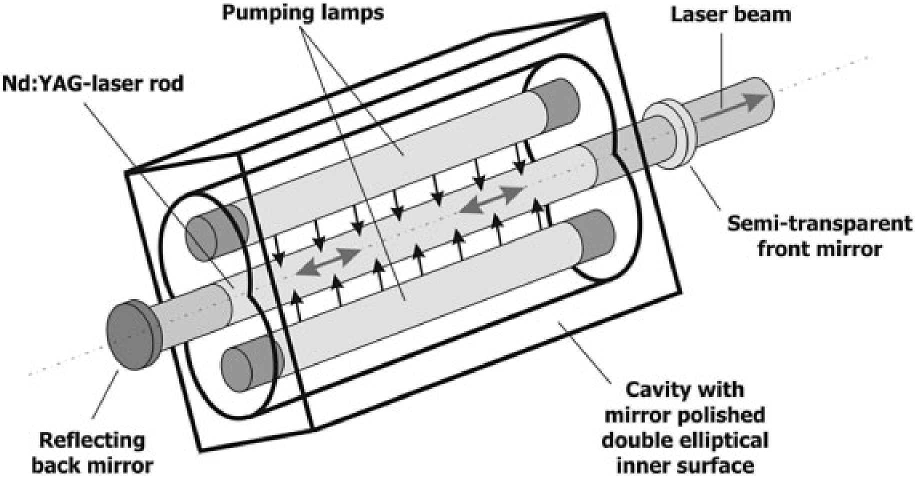
Pumping lamps
Laser beam
Nd:YAG-laser rod
Semi-transparent front mirror
Cavity with mirror polished double elliptical inner surface
Reflecting back mirror

Figure 2.10 Principle setup of a lamp-pumped Nd:YAG laser [1].

lamps). Lamp(s) and crystal rod are each located in the center of the elliptical cavity. Hence, the optical radiation from the lamp(s) is focused to the crystal rod for effective stimulation of the laser process. The laser radiation is built up by two resonator mirrors; one mirror as a total reflector and the other as a semitransparent mirror for outcoupling the laser beam.

Plug effectiveness of such lasers is very low with a ratio of laser power to electrical input of around 3%. Most of the lamp emission generates heat that has to be dissipated by a steady flow of cooling water around the laser medium. The laser medium itself heats up during operation and influences the quality of the generated laser beam by the thermal lens effects of the laser medium.

With the development of high-power diode lasers, working on a wavelength appropriate to the absorption properties of the Nd:YAG-laser medium, the quality of Nd:YAG lasers increased noticeably. Diode lasers bars replace the pumping lamps and the laser light from the diode lasers is directly directed to the crystal rod for high-efficiency laser process stimulation (Figure 2.11). The laser wavelength of the diode lasers is matched to the absorption band for optical pumping of the Nd:YAG crystal rod and thermal input to the crystal rod like using pumping lamps is noticeably decreased. The plug effectiveness increases to values around 10%, the thermal influence of the laser medium decreases and the beam quality becomes much better than lamp-pumped Nd:YAG lasers.

Further developments of Nd:YAG lasers resulted by optimization of the geometry of the laser medium and pumping by diode lasers in so-called Nd:YAG-disk lasers. The laser-active medium is a thin Nd:YAG-crystal disk, mounted on a heat sink for effective cooling. The slab is optically pumped by diode lasers and a complex resonator structure generates the laser radiation (Figure 2.12) with an outcoupled laser beam of high quality.

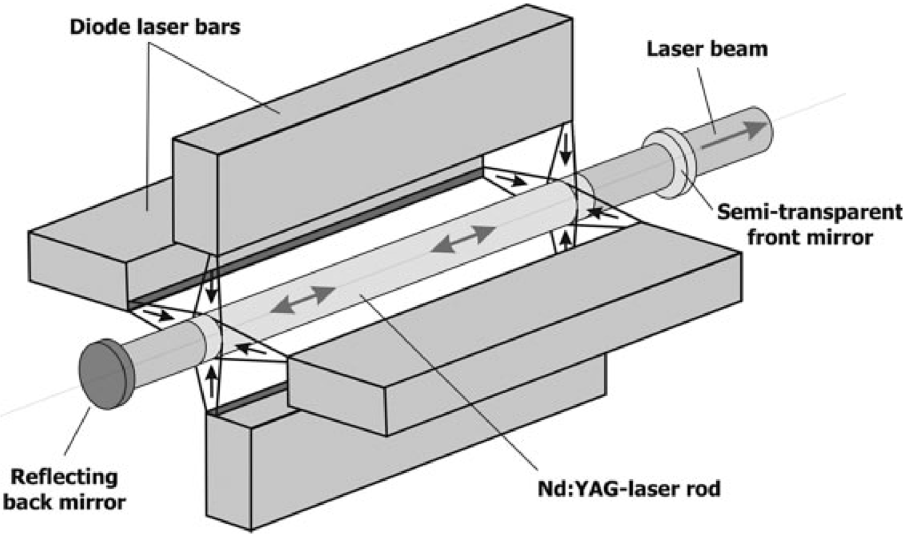

Figure 2.11 Principle setup of a diode-pumped Nd:YAG laser [1].

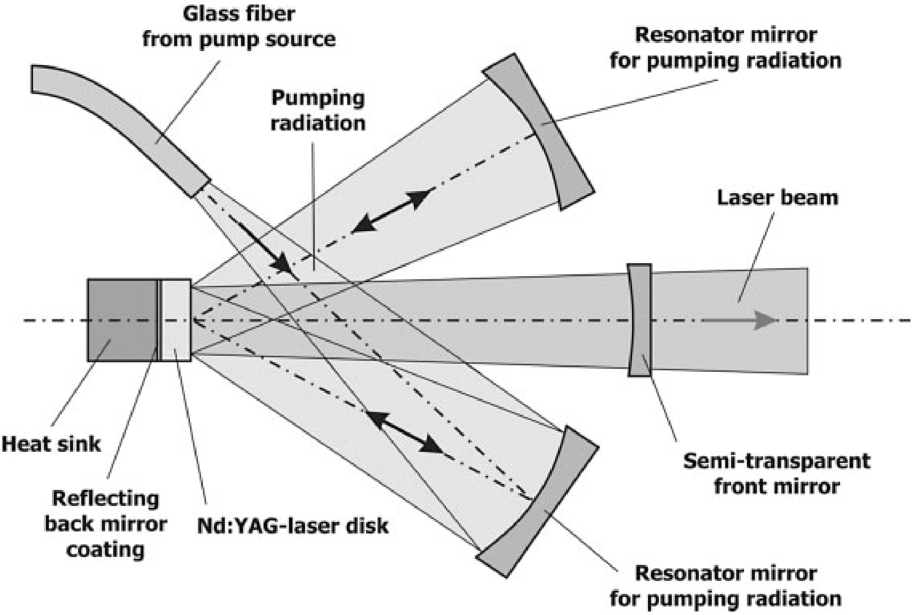
Glass fiber from pump source
Pumping radiation
Resonator mirror for pumping radiation
Laser beam
Heat sink
Reflecting back mirror coating
Nd:YAG-laser disk
Semi-transparent front mirror
Resonator mirror for pumping radiation

Figure 2.12 Principle setup of a diode-pumped Nd:YAG-disk laser [1].

As for diode lasers, Nd:YAG lasers are used with direct working beam or as fiber-coupled lasers. Usually, the laser beam coming direct from the laser source will be guided through a beam expander to increase the beam radius for better focusing properties and focused to the work piece by a two-axis scanner head. Fiber-coupled lasers use a glass fiber for flexible guiding of the beam to a focusing unit like a scanner head of a lens system.

2.2.3
Fiber Lasers

Within the family of NIR lasers fiber lasers are the latest development of laser sources for material processing applications [14–16]. Fiber lasers are available with optical output power up to some kW, working at different wavelengths depending on the type of the active medium (see Table 2.4). In the field of welding thermoplastics, fiber lasers are an interesting alternative to diode and Nd:YAG lasers because of their high beam quality (TEM_{00} mode) and plug efficiency up to approximately 30%.

The base unit of a fiber laser (Figure 2.13) is a small diameter single-mode glass fiber with special doped silica core (Θ some 10 μm) as the laser-active medium, a first silica cladding ($\Theta = 125$–$600\,\mu$m) around as waveguide for the pumping radiation and a second thin cladding for total reflection of the pumping radiation. The type of doping of the silica core will set the wavelength of the generated laser radiation like $\lambda = 1070\,\text{nm}$ for an ytterbium-doped silica core.

Table 2.4 Laser active fiber materials and wavelengths of fiber lasers in the NIR spectral range [17].

Laser active doping in glass fiber	Laser wavelengths λ, [nm]
Er	1500 to 1620
Ho	1900 to 2010
Nd	1060 to 1120
Pr	1300 to 1330
Tm	1820 to 2090 and 2190 to 2210
Yb	990 to 1200

The laser resonator of a fiber laser is built by special coatings on both ends of the glass fiber. The coating is reflective for the generated laser radiation while transparent for the pumping radiation, generating the laser process within the silica core.

Pumping is done by optical radiation with a certain wavelength, for example, coming from a diode-laser source. The pumping radiation will be coupled into the silica cladding of the glass fiber and will be transmitted along the length of the glass fiber into the doped silica core to generate the laser radiation of the fiber laser.

Two different pumping setups are used for generating the laser radiation (Figure 2.13). The end pump configuration uses a diode laser beam directly coupled into the cladding from one end surface of the glass fiber, while the fiber pump configuration uses a number of fiber-coupled diode lasers, connecting the fibers to the cladding of the glass fiber for incoupling the pumping radiation into the cladding.

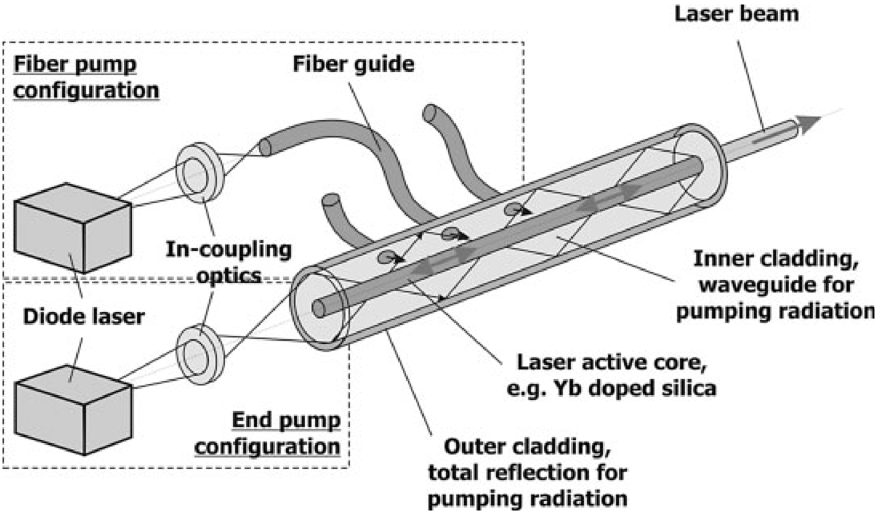
Laser beam
Fiber pump configuration
Fiber guide
In-coupling optics
Inner cladding, waveguide for pumping radiation
Diode laser
Laser active core, e.g. Yb doped silica
End pump configuration
Outer cladding, total reflection for pumping radiation

Figure 2.13 Principle setup of a diode-pumped fiber laser.

Due to the length and diameter of the glass fiber the laser beam of a fiber laser is of high beam quality like TEM_{00} mode and will be coupled into a fiber beam-delivery system with low diameter for guiding the beam to a focusing device.

Single-fiber lasers are available with laser power up to some 100 W. For higher laser power up to several kW several single-fiber lasers are combined to generate the laser beam with high-order mode also coupled to a fiber beam delivery, but with larger diameter of the glass fiber.

2.2.4
CO_2-Lasers (10.6 μm)

CO_2 lasers are gas lasers working with a gas mixture of nitrogen (N_2), helium (He) and carbon dioxide (CO_2) at a low gas pressure. Several types of CO_2 lasers like waveguide, slow-flow, fast-flow or slab lasers are available for material processing up to several 10 kW of laser power [1]. Preferably used for plastic processing are slow-flow or waveguide CO_2 lasers with high beam quality (commonly TEM_{00} mode) and laser power up to 500 W. Because of their low penetration depth of 10 μm to some 100 μm in thermoplastic materials, CO_2 lasers are not common laser sources for laser plastic welding, but used for some special application like welding of thin thermoplastic films.

The pumping process for CO_2 lasers is different from optical pumping of Nd:YAG and fiber lasers as well as direct electrical currency pumping of diode lasers. The pumping process is an electrical gas discharge under low gas pressure like a DC discharge or high-frequency discharge [5].

Figure 2.14 shows the principle setup of a slow-flow CO_2 laser. The base unit of the laser is a cylindrical glass tube with a gas in and gas outlet containing also the

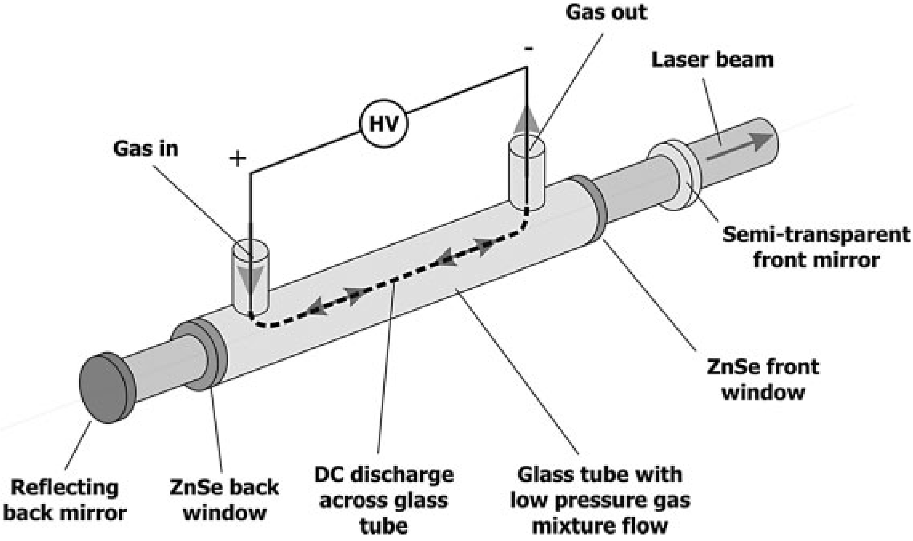
Gas out
-
Laser beam
HV
Gas in
+
Semi-transparent front mirror
ZnSe front window
Reflecting back mirror
ZnSe back window
DC discharge across glass tube
Glass tube with low pressure gas mixture flow

Figure 2.14 Principle setup of a slow-flow CO_2 laser [1].

cathode and anode for the electrical DC discharge. The glass tube is sealed at both ends against atmospheric pressure by two ZnSe windows, transparent to CO_2 radiation. The laser gas mixture (N_2, CO_2, He) streams as a laminar flow through the glass tube while the discharge is burning between the cathode and anode.

The electrical discharge increases the energy of the nitrogen molecules by activating linear molecule oscillations. The activated nitrogen molecules collide with the carbon dioxide molecules and transfer the activation energy to the carbon dioxide molecules. The exited state of the carbon dioxide molecules relaxes to a lower energy state by emitting photons of 10.6 μm wavelength, generating the laser process between the resonator mirrors. By collision of the carbon dioxide molecules with helium atoms the lower energy state of the carbon dioxide molecules will be transferred into the ground state ready for new excitation by collision with activated nitrogen molecules. A fraction of the generated laser radiation passes the semi-transparent mirror to build the CO_2-laser beam.

The principle setup of a CO_2-waveguide laser (Figure 2.15) is different from a slow-flow CO_2 laser. The base unit is a ceramic cavity with a small bore containing the laser gas mixture. The bore in the ceramic is sealed at both ends against atmospheric pressure by two ZnSe windows or directly by the laser resonator mirrors, as given in Figure 2.15.

The gas mixture is static in the bore without any gas flow. Stimulating the laser process in the gas mixture is done by high-frequency electrical discharge coupled into the gas mixture by two electrodes on the top and bottom of the ceramic cavity.

Waveguide lasers with one ceramic cavity are available up to approximately 100 W laser power. For higher power up to 500 W, several cavities are combined into one laser beam, still having high beam quality.

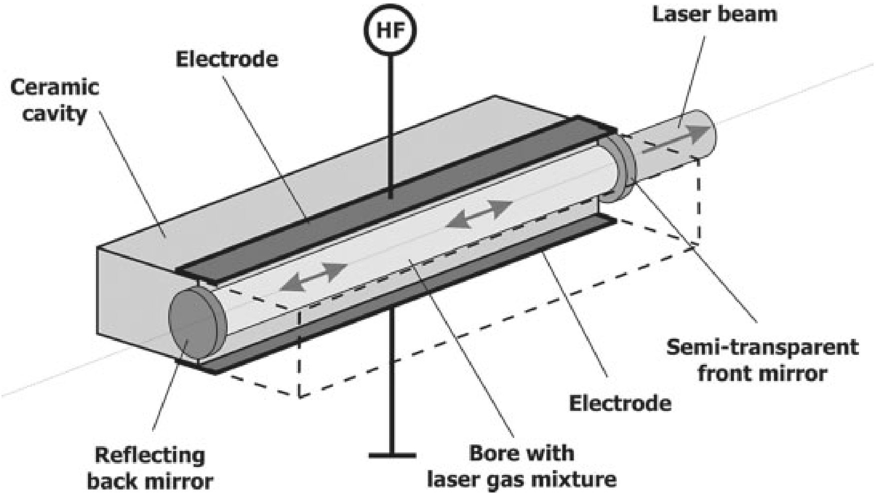

Figure 2.15 Principle setup of a waveguide CO_2 laser.

2.2.5
Summary

The previously described laser sources can be used for plastic laser welding. Which laser source is suitable for a special application depends on factors like absorption behavior of the plastic resin or demands of the preferred joint geometry. Also, the plug efficiency of the laser source can be of interest for an economic application.

The absorption of thermoplastic resins can be adapted to the process by using laser-absorbing agents and in most cases the laser beam quality is not a critical factor because of some mm weld width. Standard laser sources for plastic welding are diode lasers with wavelength of 940 nm or 980 nm. Nd:YAG lasers with 1064 nm today plays a minor role.

New application developments for laser welding transparent thermoplastic components without the need for an additional absorber are enabled by diode lasers with wavelengths of 1500 nm or 2000 nm. But such laser sources can be more expensive than conventional lasers so it is an economical decision to use these lasers instead of additional absorbing agents.

For small-sized welding geometries fiber lasers with high beam quality can be used. Again, standard fiber lasers with wavelengths of ~1000 nm need absorbing agents for plastic welding. However, higher wavelengths of fiber lasers are available for laser welding without additional absorbers. Again it is an economical decision as for diode-laser sources.

Table 2.5 summarizes for the different laser types typical available wavelengths, beam quality and plug efficiency with regard to the absorption behavior of natural thermoplastic resins and the required additional absorbing agents to enable a sufficient laser-welding process.

Table 2.5 Typical laser sources for laser plastic welding.

Laser	Wavelength	Beam quality	Efficiency	Absorption to natural plastic	Need for additional absorber
Diode laser	808 nm	low	>35%	transparent	yes
	940 nm	low	>40%	transparent	yes
	980 nm	low	>40%	transparent	yes
	1550 nm	low	>10%	volume	no[a]
	1940 nm	low	>6%	volume	no[a]
Fiber laser	1050 nm	good	n.a.	transparent	yes
	1070 nm	good	>25%	transparent	yes
	1090 nm	good	n.a.	transparent	yes
	1550 nm	good	>10%	volume	no[a]
	2000 nm	good	>5%	volume	no[a]
Nd:YAG laser	1064 nm	medium	<5%	transparent	yes
CO_2 laser	10.6 μm	good	10%	surface	no

a) If laser intensity is sufficiently high.

2.3
Beam Guiding and Focusing

The basic elements of beam guiding and focusing systems are optical components like mirrors, lenses and glass fibers. The following chapter deals with systems for beam guiding from the laser source to the focusing unit as well as with different types of focusing and beam-shaping systems typically used for laser welding plastics.

Throughout the main emphasis will be given to techniques used in combination with NIR lasers but also methods for beam guiding and focusing of CO_2-laser radiation will be discussed briefly.

2.3.1
Beam-Guiding Systems

For transmission of high-power laser radiation from the laser source to the focusing optics two different alternatives are used in industrial applications: beam guiding by glass fibers and beam guiding through the air by mirror systems.

The first alternative is not really feasible for CO_2-laser radiation because of a lack of suitable materials with high transparency to transmit the laser radiation over a certain length without noticeable power loss. But in the case of NIR lasers like diode, fiber or Nd:YAG-lasers, glass fibers are a common way for transmission of laser radiation, sometimes used in combination with mirror systems.

The advantage of glass fibers versus mirror systems is easier adjustment and maintenance of laser processing systems. Changing components like the laser source, focusing units and the glass fiber itself needs less optical adjustment effort than for mirror systems, especially for use in multiaxis beam-delivery systems.

2.3.1.1 Glass-Fiber Systems

A glass-fiber beam-delivery system like that shown in Figure 2.16 is built by a focusing optics for incoupling a parallel laser beam into the glass fiber, the glass fiber itself and collimation optics to transform the divergent radiation from the end of the glass fiber again to a parallel laser beam for further transformation for example, to a focused spot by focusing optics.

A glass fiber for transmission of high-power laser radiation is in principle built up by a three-layer system with a core of typical diameter between 100 and 1000 μm, a cladding around the core with a thickness of around 100 μm and a special outer surface coating of the cladding to achieve flexibility of the glass fiber. Typical lengths of glass fibers in industrial applications are up to 10 m and in some special cases up to 50 m. Such a glass fiber will be encapsulated by a plastic and/or spiral metallic hose to protect the glass fiber against mechanical damage.

Glass fibers are available as gradient-index or step-index fibers [8, 19], defined by the radial distribution of the refractive index in the fiber core. For transmission of high-power laser radiation usually step-index glass fibers are used [1]. For step-index fibers the refractive index of the core is radially constant with a gradual change (step)

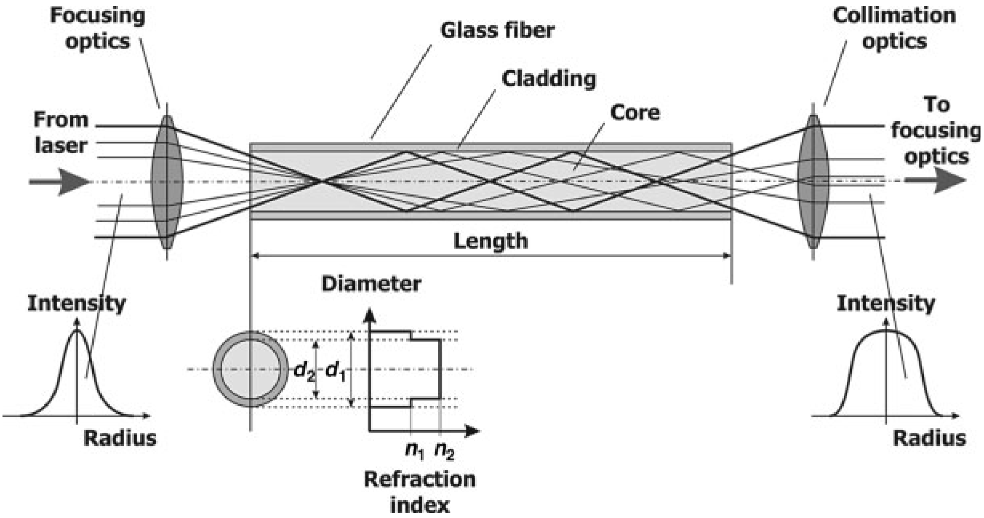

Figure 2.16 Glass-fiber beam-delivery system.

in the refractive index of the cladding (see detail in Figure 2.16), achieved by different doped glass materials for example, based on fused silica.

Beam guiding by glass fibers is done by total optical reflection on the interface of core and cladding caused by the difference of refractive indices of both materials (Figure 2.17), a lower index n_1 for the cladding and a higher index n_2 for the core. The limit angle θ_l for total reflection is depending on the difference of both refractive indices as given by Equation 2.6, using geometrical optics:

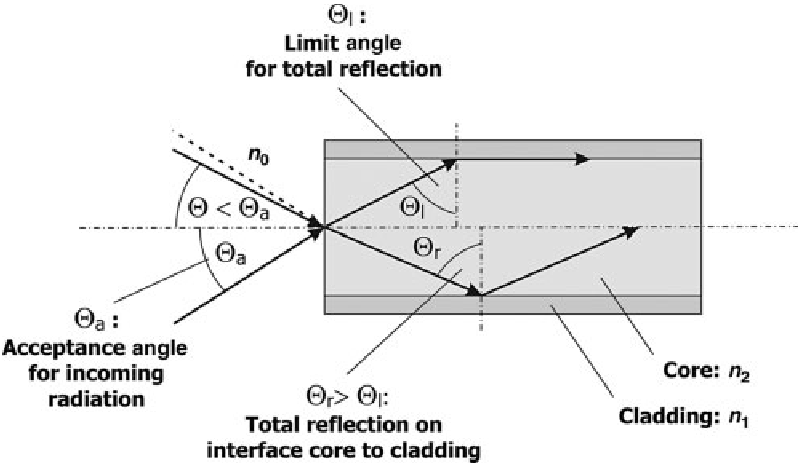

Figure 2.17 Geometrical optics from [18].

$$\theta_l = \sin^{-1}\left(\frac{n_1}{n_2}\right) \tag{2.6}$$

n_1: refractive index of cladding
n_2: refractive index of core.

θ_l also defines the limit angle θ_a on the surface of the fiber core for incoupling of radiation into the core:

$$n_0 \sin\theta_a = n_1\sqrt{1-\sin^2(\theta_l)} \tag{2.7}$$

n_0: refractive index of air
n_1: refractive index of cladding.

This limit angle is called the acceptance angle of the fiber system and defines the maximum possible angle for incoupling of radiation into the fiber core (Figure 2.17) [1,18].

In the first approach of the right side of Equation 2.7, the term numeric aperture NA as a measure for the fiber guide system is given by:

$$\mathrm{NA} \cong \sqrt{n_1^2-n_2^2} \tag{2.8}$$

n_1: refractive index of cladding
n_2: refractive index of core.

A typical NA value of fiber guide systems for transmission of laser radiation in industrial applications is 0.22.

Figure 2.17 shows the conditions for reflection in the core and incoupling of radiation into the core described by geometrical optics with an infinitesimal focal spot on the incoupling surface. Instead of geometrical optics usually Gaussian optics is valid to describe laser beam propagation in transparent media. Figure 2.18 shows the conditions for incoupling a laser beam into the glass fiber based on Gaussian optics.

Rules for reflection and transmission are still valid, but the focal spot of a Gaussian beam has a particular size, for example, defined by the beam parameter product BPP of the incident laser beam and the acceptance angle of the glass fiber [1]:

$$\mathrm{BPP} = \theta_a r_a \tag{2.9}$$

θ_a: acceptance angle of glass fiber
r_a: beam waist radius on fiber incoupling.

The acceptance angle itself has to be matched by the focusing lens system for incoupling the laser beam into the glass fiber core and will be given by the focal length f of the optics and the beam radius r_o on the lens:

$$\theta_a = \tan\left(\frac{r_0}{f}\right) \tag{2.10}$$

r_0: beam waist radius on lens
f: focal length of lens.

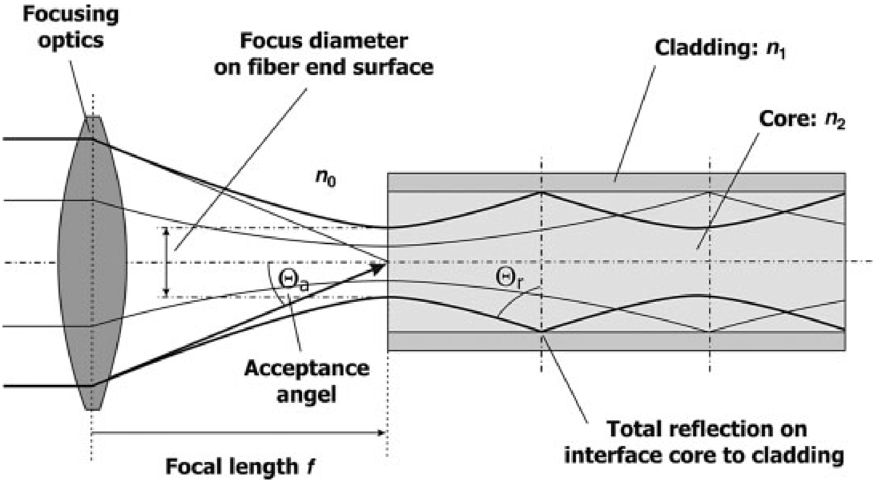

Figure 2.18 Gaussian beam optics.

Under the assumption of small acceptance angle Equation 2.11 can be simplified to:

$$\theta_a \cong \frac{r_0}{f} \tag{2.11}$$

Combination of Equations 2.9 and 2.11 and transformation to the waist radius results in:

$$r_a = \mathrm{BPP}\left(\frac{f}{r_0}\right) \tag{2.12}$$

A typical spot radius on the entrance of the fiber core is approximately one half of the core radius, which gives a certain safety for transversal and longitudinal positioning of the focused beam regarding the entrance surface. The better the BPP of the incident laser beam, the longer can be the focal length or the smaller can be the dimension of the focusing lens in principle.

Beside the spot size on the fiber core entrance the focusing of the laser beam has to be matched to the acceptance angle of the glass fiber, given by the numerical aperture NA of the glass fiber [1]:

$$\mathrm{NA} = n_0 \sin \theta_a \tag{2.13}$$

Combination of Equations 2.11 and 2.13 results in:

$$\mathrm{NA} = n_0 \sin\left(\frac{r_0}{f}\right) \tag{2.14}$$

and transformation to the focal length regarding $n_0 = 1$ as the refractive index for air yields in a formula for an estimation of the focal length needed for incoupling the laser beam into the glass fiber:

$$f = \frac{r_0}{\sin^{-1}(\mathrm{NA})} \tag{2.15}$$

After incoupling into the fiber core, the laser beam will be transmitted by total reflection on the interface of fiber core and cladding. Parts of the beam nearer to the optical axis will have a first reflection later than outer parts, which will be reproduced over the entire length of the glass fiber by multiple reflections. Hence, the beam shape of the incident laser beam will be changed during transmission through the glass fiber to a broader intensity distribution (see Figure 2.16) than for the incident laser beam. The laser beam leaving the end of the glass fiber will have a divergence corresponding to the acceptance angle of the glass fiber and has to be transformed by collimation optics to a parallel laser beam for further guiding to a focusing or beam-shaping optics for material processing.

Typical glass fibers for industrial application are encapsulated in a plastic and/or spiral metal hoses. On both ends of the glass fiber plug connectors are placed to fix the glass fiber ends in a defined position for reproducible in- and outcoupling of the laser beam after plugging into the socket of the collimation and focusing optic devices.

In principle, two different glass-fiber system types are in use for industrial application. The first is a basic system with plastic or metallic spiral hose and SMA connectors, as shown in Figure 2.19, typical used for diode lasers of power up to around 100 W. Such simple glass-fiber systems have no online monitoring for cable brake, plug temperature and positioning control.

The second type is a more technically advanced system with specially designed connectors as shown in Figure 2.20. Such glass-fiber types are used for high power lasers like diode, Nd:YAG or fiber lasers with high-quality laser radiation up to kW of laser power. The connectors are designed for high mechanical stability and repeatability of the connector position in the plug to assure a reliable in- and outcoupling of the laser radiation.

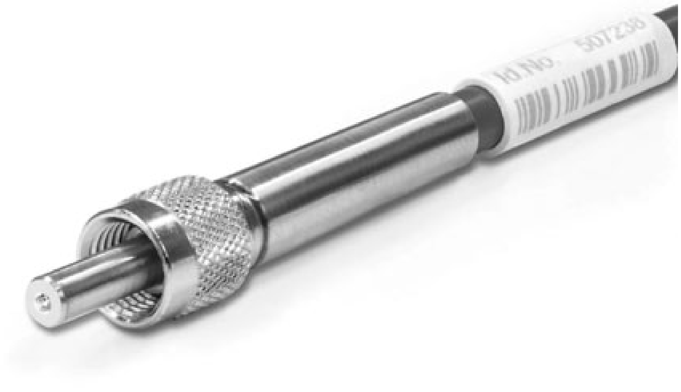

Figure 2.19 Glass fiber system with SMA connector for low laser power.

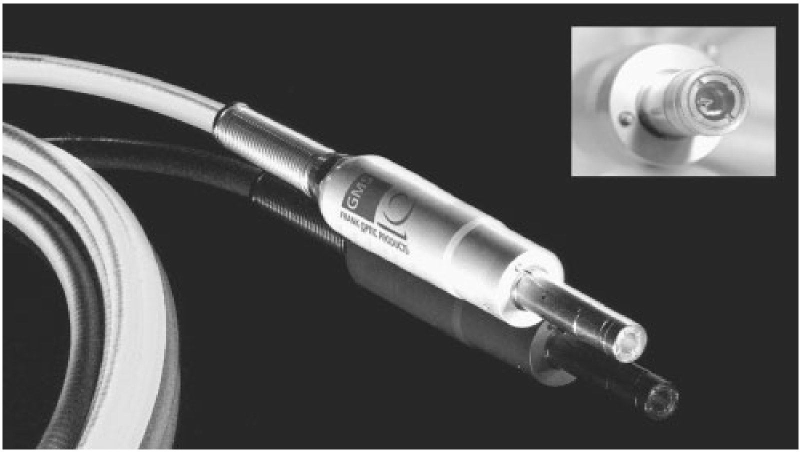

Figure 2.20 Advanced glass-fiber system for high laser power [20].

The connectors at both ends of the glass-fiber system have electrical contacts for an integrated safety circuit [20]. In combination with the laser source and the collimation optic device the safety circuit monitors the plug-in status and temperature of both connectors as well as the glass-fiber condition by an electrical resistance measurement. In the case of no or insufficient plug in or too high temperatures of the fiber connectors the laser source will be disabled for running the laser radiation. If mechanical damage of the glass fiber occurs, the electrical resistance measurement will give a signal to the controller for immediate shut down of the laser source to protect the surroundings against free-running laser radiation.

2.3.1.2 **Mirror Systems**

For CO_2-laser systems, but also in some cases for NIR lasers, mirror systems are used for beam guiding from the laser source to the focusing unit. Typical materials for mirrors to reflect the laser beam are fused silica with a highly reflecting surface coating (Figure 2.21) for NIR lasers and copper (Figure 2.22) or silicon for CO_2-laser radiation, as summarized in Table 2.6.

In a mirror system for laser-beam guiding it is crucial to the functionality of the system that the optical axis of the system and the beam path are well adjusted to each other, especially in a multiaxis beam-delivery system. Figure 2.23 shows as an example a well-adjusted simplified two mirror system with the second mirror on a linear moving axis.

The incident laser beam is reflected by mirror 1 to mirror 2. During movement of mirror 2 along the linear axis, the outgoing laser beam is stable relative to mirror 2 and the optical axis of the beam-guiding system.

Insufficient alignment of the beam-guiding system can be caused by poor adjustment of the mirrors (e.g., mirror 1 in Figure 2.24, upper part) or a not well-aligned incident laser beam (Figure 2.24, lower part). Both cases will effect a mismatch of the transmitting laser beam to the optical axis of the beam-guiding

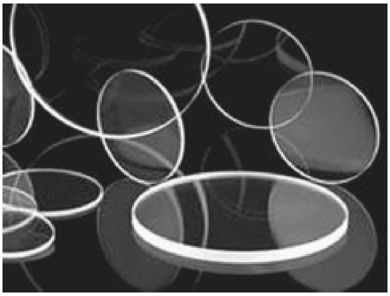

Figure 2.21 Beam-bending mirror for NIR-laser radiation.

Figure 2.22 Beam-bending mirror for CO_2-laser radiation.

Table 2.6 Materials used for reflecting the laser beam.

Material	**Surface coating**	**Reflection**	**Application**
Fused silica	High reflecting coating for dedicated wavelength	99.9%	NIR lasers
Silicon	High reflecting coating for CO_2 laser wavelength	99.9%	CO_2 laser
Copper (OFCU)	Uncoated or high reflecting coating for dedicated wavelength	95–99.9%	NIR or CO_2 lasers (preferred)

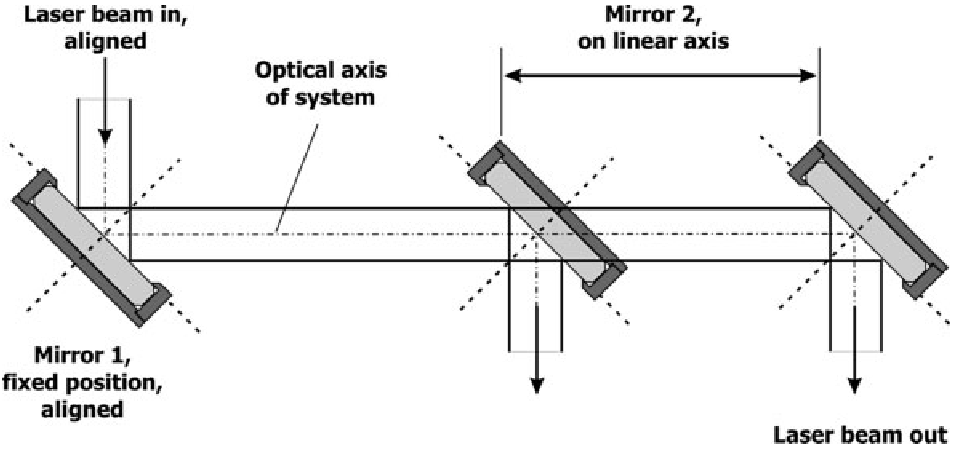

Figure 2.23 Aligned two-mirror beam-guiding system with second mirror on a linear axis.

system. During movement of mirror 2 by the linear axis, the laser beam will hit mirror 2 on different positions on the mirror surface. The outgoing laser beam has a different angle and shift in position corresponding to the optical axis of the beam-guiding system.

If a focusing device like a lens system is the next optical element after the beam-guiding system, for example, moved together with mirror 2 by the linear axis, the mismatch of the laser beam will tend to a shift of the focus position or astigmatism of the focused laser beam.

2.3.2
Focusing Systems

For laser welding plastics the laser beam has to be transformed to a certain spot geometry, generating sufficient radiation intensity to melt the plastic material at the interaction zone where the laser radiation has to be absorbed. This can be done by optical systems like static or dynamic lenses and mirrors as well as special beam-shaping optics to form lines, circular or more complex geometries.

2.3.2.1 **Static Focusing Systems**

Static focusing systems are built by optical elements like lenses or mirrors (Figure 2.25) to focus the laser beam to the work piece. To generate the laser weld on the work piece with a desired geometry, work piece and focusing unit have to carry out a relative motion using a robotic system. Hence, the focused laser beam has a stable position in the focusing device and is moved together with the optics.

Typical lens material (Table 2.7) for NIR lasers is fused silica with special nonreflective surface coatings to optimize the transmission for the laser radiation. In the case of CO_2-laser radiation lens material is ZnSe because fused silica is not transparent for CO_2-laser radiation.

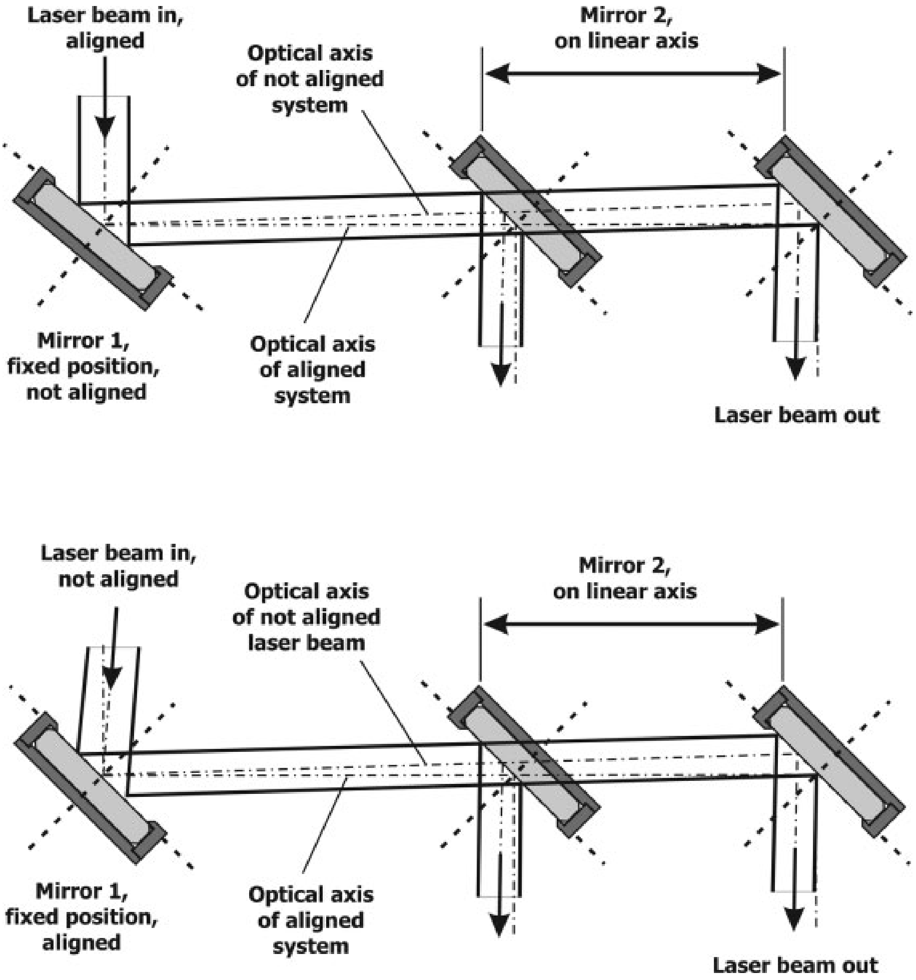
Laser beam in, aligned
Optical axis of not aligned system
Mirror 2, on linear axis
Mirror 1, fixed position, not aligned
Optical axis of aligned system
Laser beam out
Laser beam in, not aligned
Optical axis of not aligned laser beam
Mirror 2, on linear axis
Mirror 1, fixed position, aligned
Optical axis of aligned system
Laser beam out

Figure 2.24 Not well aligned two-mirror beam-guiding system with second mirror on a linear axis, upper drawing shows beam out mismatch by not aligned first mirror and lower drawing by not aligned incident laser beam.

Focusing optics for NIR lasers and CO_2 lasers can also be built up by mirrors. For NIR lasers mirror materials can be highly reflective coated glass materials or optical polished metallic substrates. Common material of focusing mirrors for CO_2-laser radiation is oxygen-free copper with an optical polished surface, mostly in combination with a highly reflecting coating.

Because focusing mirror systems and CO_2-laser radiation are not commonly used for industrial plastic laser welding application the further discussion will refer to static lens-based focusing systems for NIR lasers, mostly used in combination with a glass-fiber beam-delivery system.

A principal setup of such a focusing device is given in Figure 2.26. The laser radiation is delivered from the laser source to the focusing device by a glass-fiber

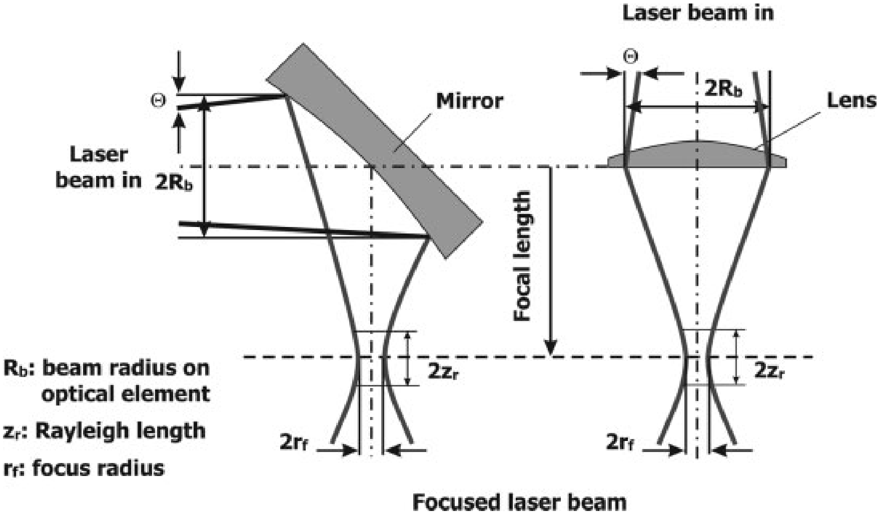

Figure 2.25 Lens (right) and mirror (left) as focusing elements, from [1].

cable. The laser beam, outcoupled from the glass-fiber end at the cable connector, is collimated by a lens. Next, the parallel laser beam is reflected by a bending mirror to the focusing lens to focus the laser beam to the work piece. The focusing lens itself is protected against soiling by a protective glass window. Typical focal lengths of such devices are between 80 and 200 mm.

To monitor the laser-welding process a system for measurement of the actual temperature at the interaction zone can be integrated into the focusing head, as shown for example in Figure 2.27.

The temperature radiation from the interaction zone is collected by the focusing optics and will be transmitted by the beam-bending mirror to a second mirror. The second mirror reflects the radiation to a focusing lens that focuses the thermal radiation onto a glass fiber. The glass fiber guides the radiation to an external pyrometer for detection and analysis.

The example given in Figure 2.27 is only one possibility for temperature measurement during laser welding. Alternatively, the pyrometer detector can also be integrated directly into the focusing device.

Table 2.7 Materials used for focusing lenses.

Material	Transmittance	Refractive index	Application
Boronsilicate glass (BK7)	400–1.400 nm	1.48–1.35	Low power NIR lasers
Fused silica	150–3.500 nm	1.4–1.5	NIR lasers (preferred)
Gallium arsenide (GaAs)	2.5–16 μm	2.1–3.3	CO_2 laser
Zinc selenide (ZnSe)	0.6–22 μm	2.3–2.5	CO_2 laser (preferred)

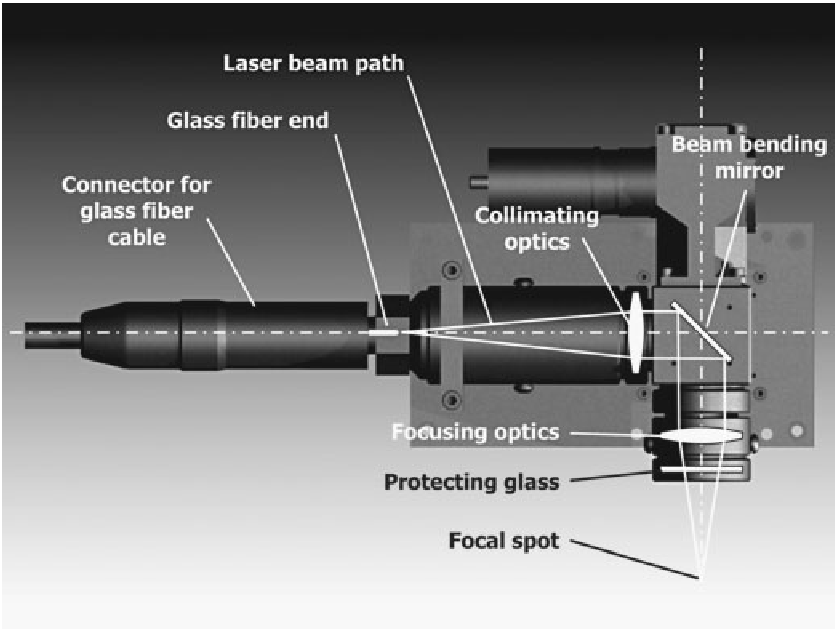

Figure 2.26 Principle setup of a static focusing device.

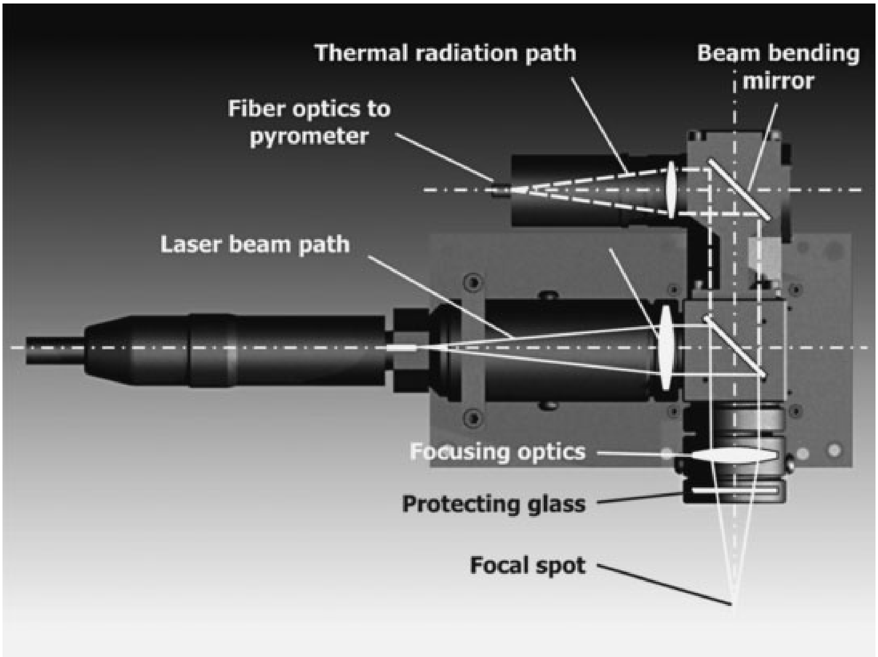

Figure 2.27 Integrated temperature radiation measurement during laser welding.

2.3.2.2 **Dynamic Focusing Systems**

Dynamic focusing systems are devices to move the focused laser beam along a work piece contour while the focusing device and the work piece are in principle fixed in position. For laser welding plastics a typical dynamic focusing system is a scanner head.

A scanner head (Figure 2.28) [21] is built by two galvanic-driven mirrors to move the laser beam in two axes, perpendicular to each other. After the mirror system the laser beam passes an optical corrected lens system (f-theta lens) to focus the laser beam onto the work piece. The focusing lens is specially designed to focus the laser beam on a plane square area, for example, of 100 mm × 100 mm or 200 mm × 200 mm dimensions.

The motion of the two galvanic driven mirrors is settled by an electronic controller (CNC controller), enabling processing of complex geometries in a wide range of processing speed. By the high dynamic oscillation capabilities of the galvanic drives it is also possible to superpose a zigzag or circular motion of the focused laser beam along the basic motion of the laser beam to adapt the focused laser spot to a desired weld width.

Scanner heads are used in combination with direct beam lasers like diode and Nd:YAG lasers or in some rare application with CO_2 lasers. The laser beam coming from the laser source is parallel or of low divergence, matched to the dimension of the beam-bending mirrors in the scanning head by optical systems like beam expanders.

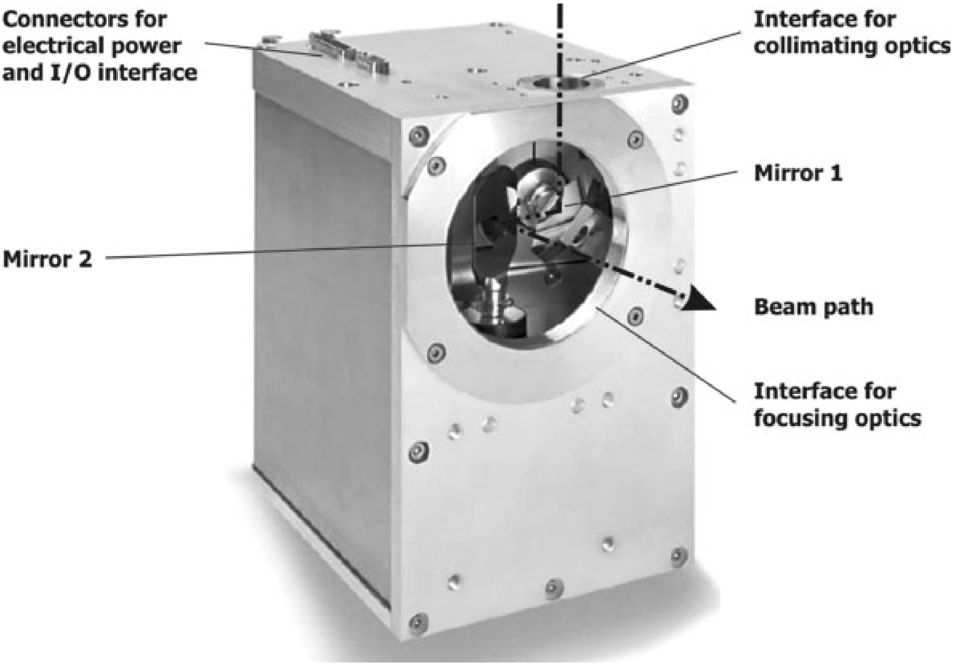
Connectors for electrical power and I/O interface
Interface for collimating optics
Mirror 1
Mirror 2
Beam path
Interface for focusing optics

Figure 2.28 Basic setup of a scanner head [21].

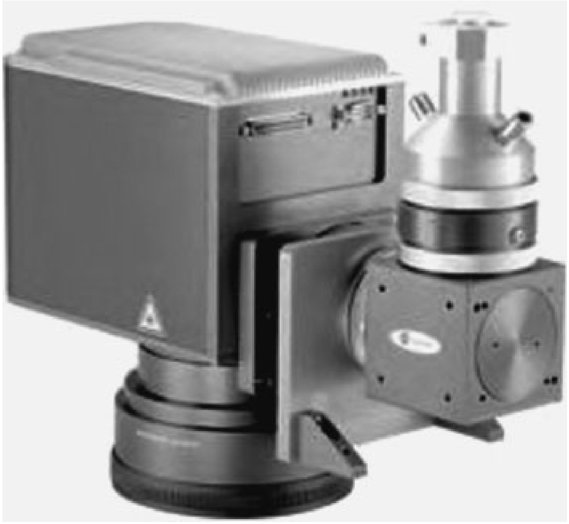

Figure 2.29 Scanner head in combination with a fiber-guide system for industrial application [22].

Today more common is the use of scanner heads in combination with fiber-guide systems (Figure 2.29) [22], especially for NIR lasers like diode, Nd:YAG or fiber lasers. The laser beam from the glass fiber will be transformed to a parallel beam by collimation optics before entering the scanner head.

2.3.3
Beam-Shaping Optics

In some cases it is desired to generate a special beam geometry like lines, circles or more complex geometries for laser plastic welding. Such beam shaping can be done by scanner heads but also by static beam-shaping optics like mirror systems, wedge plates, cylindrical lenses or diffractive optical elements. In the following, exemplarily beam-shaping optics to generate circular laser patterns will be described.

Producing a circular laser spot on a circumference of a cylindrical work piece like a plastic tube can be done by a specially designed cylindrical beam-bending mirror in combination with a two-axis scanner device, as shown in Figure 2.30. The scanner head will focus the laser beam and carry out circular motion of the focused laser beam. The focused laser beam itself will be reflected by the mirror unit to the circumference of the work piece.

Concentric circular plane ring spots on a work piece can be generated for example, by diffractive optical systems as shown in Figure 2.31. A homogeneous circular laser beam coming from a fiber-guide system will be transformed to a special circular beam pattern by internal transmitting diffractive optical elements.

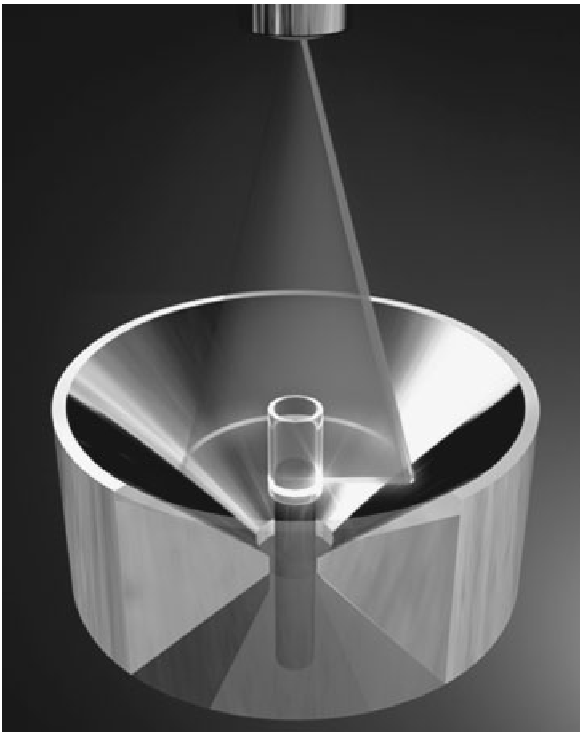

Figure 2.30 Beam-shaping optics for circular beam pattern at the circumference of a work piece [23].

2.4
Principle Setup of Laser Welding Systems

A typical basic setup of a laser system for plastic welding is schematically given in Figure 2.32, consisting of components like a laser source with power supply and cooling device, beam-delivery system and focusing unit, work-piece handling system

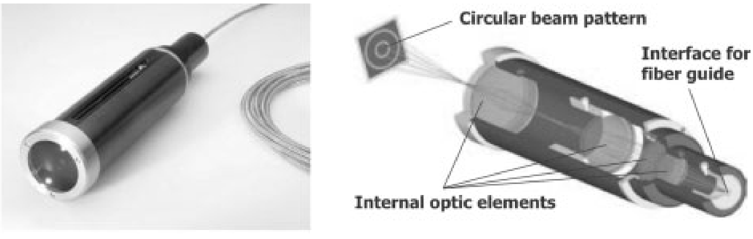

Circular beam shaping optics **Schematical optic setup**

Figure 2.31 Beam-shaping optics for circular beam pattern [24].

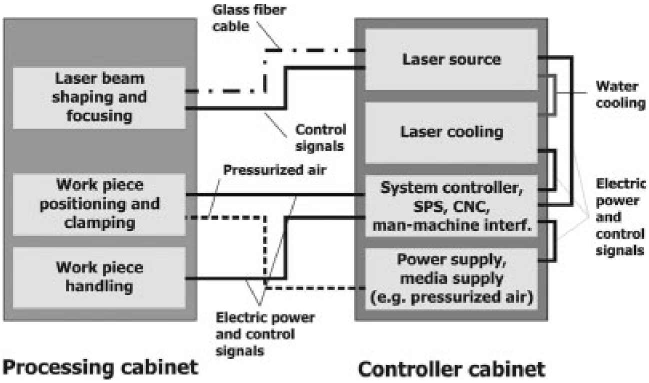
Glass fiber cable
Laser beam shaping and focusing
Control signals
Pressurized air
Work piece positioning and clamping
Work piece handling
Electric power and control signals
Processing cabinet
Laser source
Laser cooling
System controller, SPS, CNC, man-machine interf.
Power supply, media supply (e.g. pressurized air)
Water cooling
Electric power and control signals
Controller cabinet

Figure 2.32 Typical setup of a plastic laser welding system.

with clamping device as well as controller unit to drive and control all the components.

Possible devices for laser sources, beam-delivery systems and focusing units have been described previously. As further main components of a laser system the work piece handling system and the controller unit will be treated in the following.

Design of the work-piece handling system in combination with the focusing unit has to be done according to the application demands. The following configurations, as shown in Figure 2.33, are possible alternatives for work-piece handling systems:

- move work piece (e.g., by three-axis feeding system) – locally fixed focusing unit;
- horizontally move work piece (e.g., by two-axis feeding system) – vertically move focusing optic to align the focus to the moved working part;
- linear movement of work piece (e.g., by one-axis feeding system) – horizontally and vertically move focusing optic (e.g., by two-axis feeding system); and
- locally fix work piece – move focusing unit (e.g., by a three-axis gantry system).

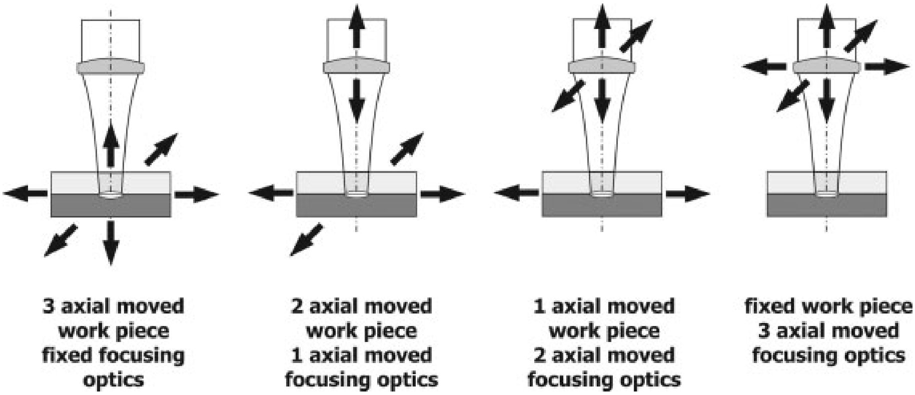
3 axial moved work piece fixed focusing optics
2 axial moved work piece 1 axial moved focusing optics
1 axial moved work piece 2 axial moved focusing optics
fixed work piece 3 axial moved focusing optics

Figure 2.33 Basic configurations of work-piece handling systems.

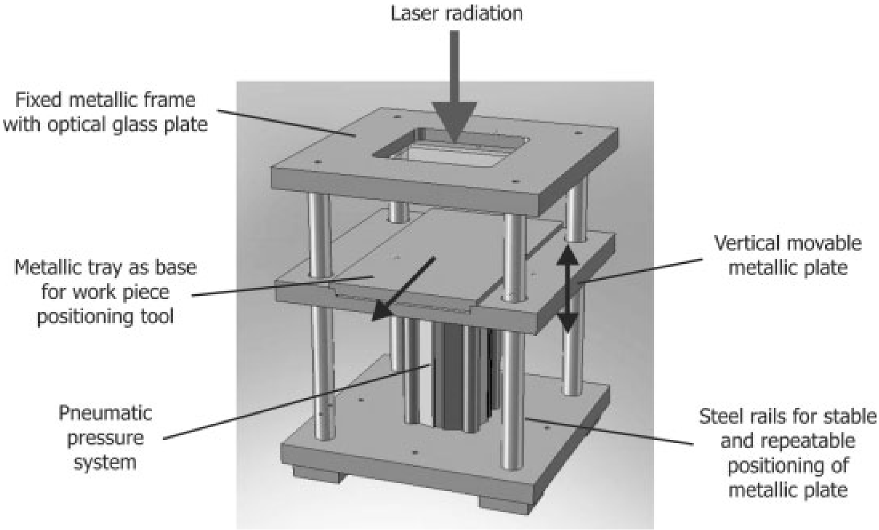
Laser radiation
Fixed metallic frame with optical glass plate
Vertical movable metallic plate
Metallic tray as base for work piece positioning tool
Pneumatic pressure system
Steel rails for stable and repeatable positioning of metallic plate

Figure 2.34 Principle setup for a pneumatic clamping device [25].

Positioning and fixing of the work piece to carry out the laser-welding process needs a clamping device, designed especially for the geometry of the work piece or designed as a general device with special positioning tools for different work-piece geometries. Clamping of the work pieces to apply the needed welding pressure to the work piece is commonly realized by pneumatic pressuring systems.

An often used setup of the clamping device is a vertically movable table carrying a positioning tool for the work piece, which will be pneumatically pressed against a locally fixed mechanical stable frame or glass plate, transmitting the focused laser radiation to the work piece (Figure 2.34). Supply and removal of the work piece to and from the clamping device can be done manually or by automatical work-piece manipulating systems.

The electronic heart (or brain) of the laser welding system is the controller device. In many cases the controller device is split into two basic units:

- a SPS controller to monitor and control the basic functions of the system; and
- a CNC controller to set the system parameters and sequence of movements for the processing of the work piece.

Depending on the components and their functionalities for the welding system the SPS controller has a specially designed program that will drive and monitor all peripheral systems like for example, general power supply, air-pressure supply, cooling-water supply, laser source working, feeding and clamping systems, safety circuits and others.

The CNC controller is the man/machine interface and consists typically on a PC with graphic display, keyboard with mouse or track ball and tableau with system status lamps, switches and push buttons (Figure 2.35) [26] to operate the welding system.

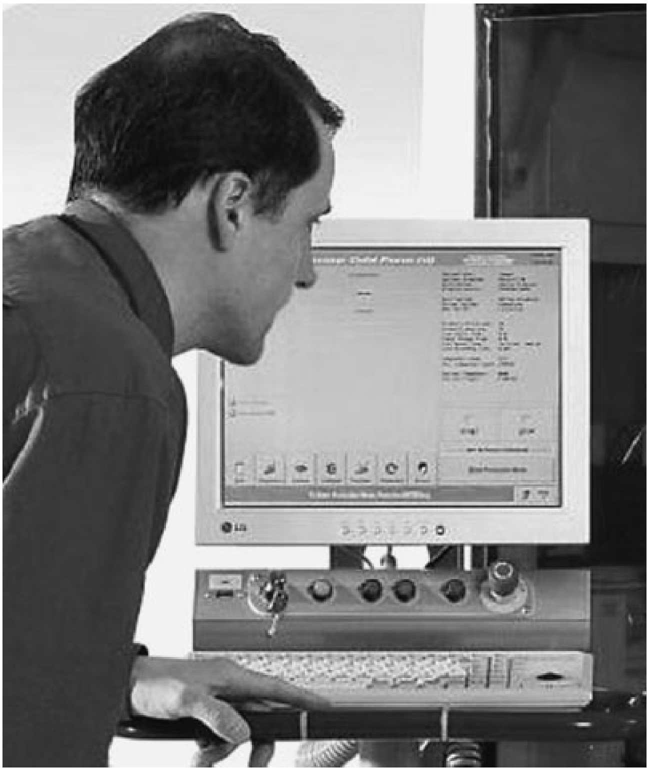

Figure 2.35 CNC controller as man/machine interface [26].

Also, the CNC controller has typically a specially designed software to drive the welding system, for example, for programming the sequence of movements (like weld-path geometry, welding speed, focus position) for the processing of the work piece and parameter settings for the laser source (laser power, laser start/stop sequence) as well as the clamping force (clamping pressure) needed to fix the working part.

Laser systems for plastic welding can be designed as a stand-alone or inline system integrated into a work flow for the component processing.

An example of a stand-alone system is shown in Figure 2.36 [27]. It is built as a compact unit integrating all system components in a single cabinet. For this system the work-piece handling is done manually.

The work piece will be supplied manually to the positioning and clamping device in the welding system. While the work piece is welded inside the laser system a new work piece can be supplied in a second positioning device outside the system. Manually started as the next processing step, the turntable will feed the welded work piece outside and the second work piece inside the machine. While the second work piece is processed the first will be removed manually from the positioning device and replaced by a new work piece to be welded.

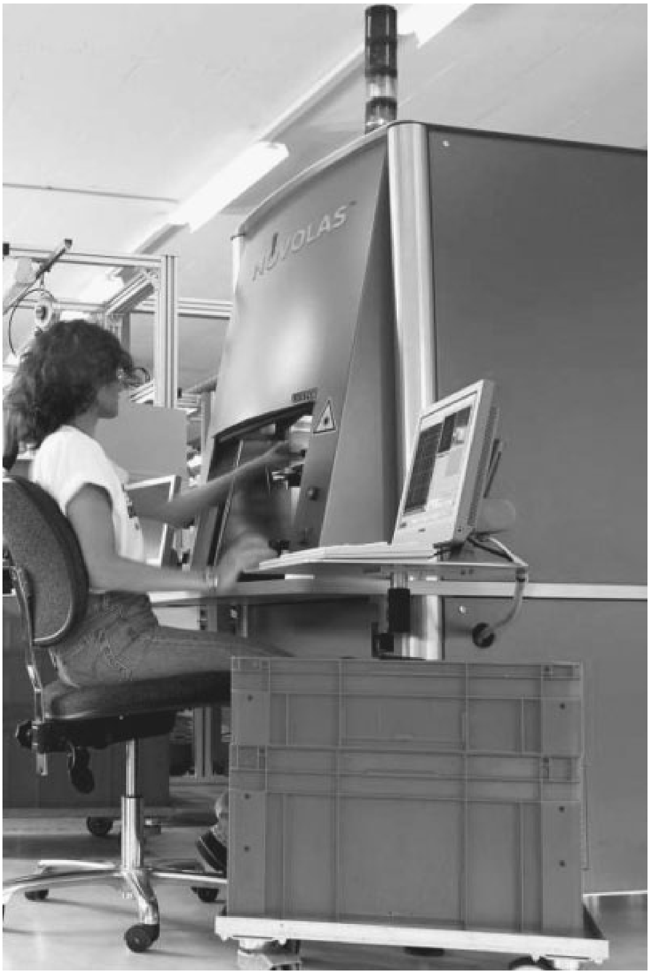

Figure 2.36 Stand-alone laser welding system [27].

Not only small size geometries of work pieces can be handled by stand-alone systems. Figure 2.37 [28] demonstrates a laser welding system for production of plastic chairs made from two PC components. Both components will be placed on the positioning device outside the system. A linear feeder will move the components into the welding system for clamping and laser welding after closing the system. The welded chair will be fed out of the system for manual removal and replaced by a new chair to start the next processing.

The described laser welding systems are suitable for a small and medium-sized number of units to be processed. For higher volume production rates inline laser welding systems are used.

In many industrial applications inline laser welding systems are used. Figure 2.38 [29] shows as an example a laser welding device consisting of

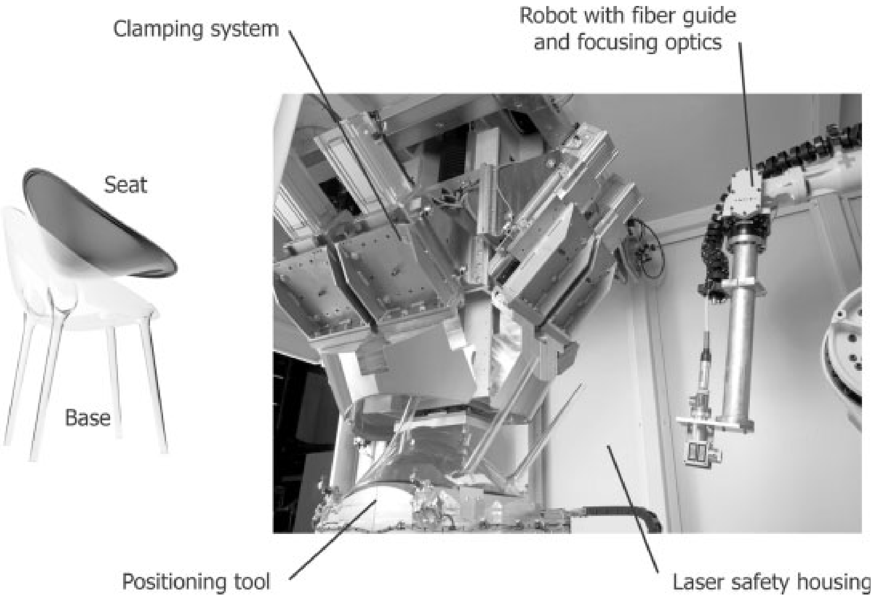

Figure 2.37 Stand-alone laser welding system for plastic chairs [28].

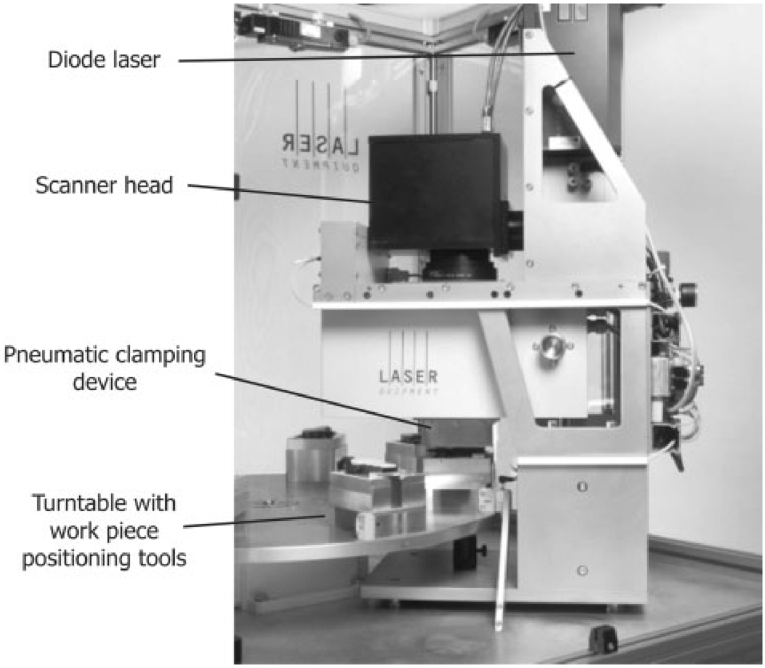
Diode laser
Scanner head
Pneumatic clamping device
Turntable with work piece positioning tools
LASER
LASER

Figure 2.38 Laser welding system for integration into a production chain [29].

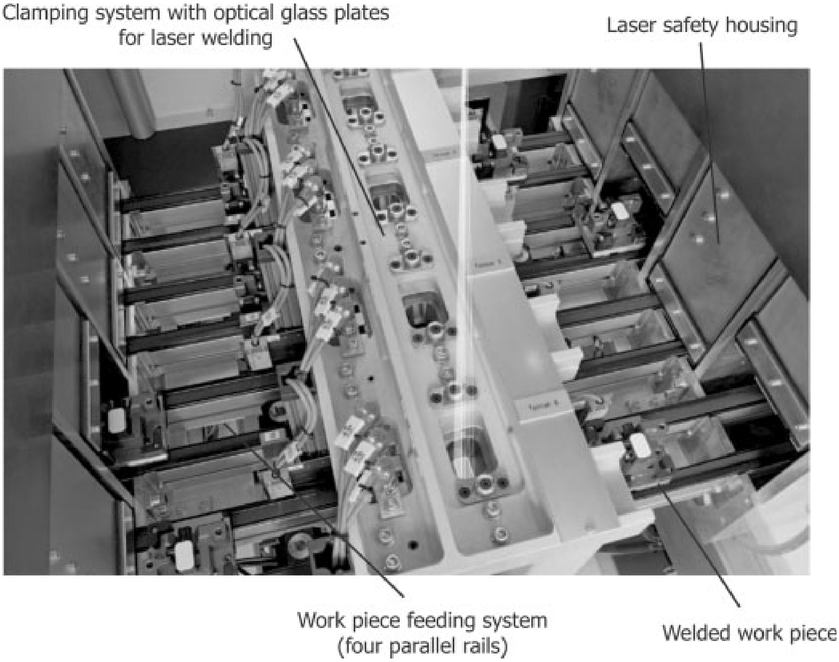
Clamping system with optical glass plates for laser welding
Laser safety housing
Work piece feeding system (four parallel rails)
Welded work piece

Figure 2.39 Integrated laser welding system with work piece feeding system [30].

diode-laser source, glass-fiber beam-delivery system and scanner head for laser-beam focusing and geometrical beam-path manipulation for integration into an industrial work-piece feeding chain.

A device controller, laser power supply, laser cooler and other periphery systems are located in a separate cabinet with interfaces for signal exchange with the supervising controller unit of the entire production system.

The supply of the work pieces to the laser welding station is done by an automated feeding system like a conveyer-belt system, as shown in Figure 2.39 from [30]. The work pieces are already positioned on trays and are supplied automatically into the welding station. Inside the welding station the work pieces are clamped and laser welded and then moved on for further treatment or packaging.

References

1 Poprawe, R. *et al.* (2003) Lasertechnik I + II, lecture script on DVD, LLT an der RWTH Aachen.

2 Weber, H. and Herziger, G. (1972) *Laser-Grundlagen und Anwendungen*, Physik Verlag, Weinheim.

3 Breck Hitz, C., Ewing, J.J., and Hecht, J. (2001) *Introduction to Laser Technology*, J. Wiley & Sons, New York.

4 Hecht, J. (2001) *Understanding Lasers*, J. Wiley & Sons.

5 Herziger, G. and Loosen, P. (1993) *Werkstoffbearbeitung MIT Laserstrahlung*, C. Hanser, München.

6 Bachmann, F., Loosen, P., and Poprawe, R. (2007) *High Power Diode Lasers*, Springer, New York.

7 O'Neill, W. *et al.* (2004) High power high brightness industrial fiber laser technology. Proceedings ICALEO Conference.

8 Steele, R.V. (2007) Laser market place 2007: Diode-laser market takes a breather, in *LaserFocusWorld*, vol. **43/2**, PennWell Press.

9 Diehl, R. (2000) *High-Power Diode Laser – Fundamentals, Technology, Application*, Springer, Berlin.

10 Horn, W. (2005) Ein vielversprechendes Werkzeug. *Laser Technik Journal*, 1/2005, Wiley VCH Verlag, Weinheim, pp. 41–43.

11 N.N. (2008) Optotools™ Diode Laser, Company product brochure.

12 Iffländer, R. (2001) *Solid-State Lasers for Material Processing*, Springer, New York.

13 Koechner, W. (2006) *Solid-State Laser Engineering*, Springer, New York.

14 Zellmer, H. (2006) Der Faserlaser – Strahlquelle für viele Anwendungen. *Laser Technik Journal*, 2/2006, Wiley-VCH Verlag GmbH & Co. KGaA, Weinheim, pp. 52–55.

15 Nilsson, J. *et al.* (2003) High Power Fiber Lasers: New Developments, Technical Papers from SPI-Lasers, Southampton UK.

16 Zellmer, H., Nolte, S., and Tünnermann, A. (2005) Faserlaser. *Physik Journal*, **4** (6), 29–34.

17 Tünnermann, A. (2006) Novel developments and potentials of fiber laser technology. Proceedings of 2. Internationaler Workshop "Faserlaser", Fraunhofer-IWS, Dresden.

18 Lutzke, D. (1986) *Lichtwellenleiter-Technik*, Pflaum Verlag, München.

19 Midwinter, J.E. (2001) *Optical Fibers for Transmission*, J. Wiley & Sons, New York.

20 N.N. (2008) Strahlführungssystem HPLD600H, User Manual, Frank Optic Products, Berlin, (n.a.).

21 N.N. (2009) Hurryscan, Product brochure, Scannlab, Puchheim.

22 N.N. (2008) Welding of Plastics, Company brochure, Laserline, Mühlheim-Kärlich (n.a.).

23 Wenzlau, C. (2008) Laserschweissen – neue Möglichkeiten in der Verbindungstechnik, in *Kunststoffe in der Medizintechnik*, VDI-Verlag, Düsseldorf.

24 Abed, S. *et al.* (2004) Development of simultaneous laser welding process applied to thermoplastic polymers. Proceedings of the 23rd International Congress on Applications of Lasers & Electro-Optics.

25 Kujanpää, V. *et al.* (2008) Flexible Laser Welding Of Plastics With Ultra High Speeds, Final project report, Lappeenranta University of Technology.

26 N.N. (2009) Polar Uses Cencorp's Laser Welding System in the Manufacturing of Top Heart Rate Monitoring Products, Press release, Cencorp.

27 N.N. (2004) Laserstrahlschweissen Von Kunststoffen, Company brochure, Leister, Sarnen.

28 N.N. (2007) Press Release Materials for K-Show, bielomatik, Neuffen.

29 Klein, J. and Kraus, A. (2004) *Ist Laserstrahlschweissen wirtschaftlich?* Kunststoffe, 7/2004, C. Hanser Verlag, München.

30 N.N. (2010) Machines for Laser Welding of Plastics, Company brochure, bielomatik, Neuffen.

3
Basics of Laser Plastic Welding

3.1
Heat Generation and Dissipation

The initial processes forming a laser weld on thermoplastic materials are absorbing the incident laser radiation, transferring the laser energy into heat and dissipating the generated heat to adjoining resin areas by heat flow caused by temperature conduction. Depending on the material structure radiation absorption can be hindered sometimes by scattering on crystalline phases or filler materials like talcum or glass fibers.

3.1.1
Absorption of Laser Radiation

For absorbing laser radiation and generating process heat two different basic interaction processes between laser radiation and macromolecules of the resin can be distinguished, depending on the laser wavelength. These two interaction processes are direct and indirect absorption of laser radiation. Both interaction processes will be discussed briefly in the following.

3.1.1.1 Direct Absorption

Noticeable direct absorption of laser radiation occurs for laser wavelengths in the NIR spectrum region 1200 nm (e.g., diode or fiber lasers) and for MIR-laser radiation like CO_2 lasers ($\lambda = 10.6\,\mu m$).

Interaction processes for direct absorption of NIR radiation between 1200 and 2500 nm are higher-order oscillations and combination oscillations (see Section 1.4.5) [1, 2]. In particular, C−H, O−H, S−H and N−H groups in the macromolecule chain can be activated. Base oscillation frequencies of these groups are located in the MIR spectral range. For wavelengths above 2500 nm electromagnetic radiation will be increasingly effectively absorbed by excitation of molecular chain oscillations.

In the spectral range of MIR radiation, for example, CO_2 lasers, interaction between electromagnetic radiation and solid polymeric material occurs by excitation of elongation or bending oscillations of individual segments of the macromolecular

Laser Welding of Plastics, First Edition. Rolf Klein.
© 2011 Wiley-VCH Verlag GmbH & Co. KGaA. Published 2011 by Wiley-VCH Verlag GmbH & Co. KGaA.

chains (see Section 1.4.6) [3]. Typical oscillations for interaction with CO_2-laser radiation are frame oscillations of C atoms within the molecular chain as well as group oscillations of side-chain molecules like methyl or methylene groups [4].

Higher-order oscillation excitation of macromolecular components in the NIR spectral region is considerably weaker than excitation of macromolecular base oscillations within the MIR spectral range, resulting in deeper penetration of NIR radiation (up to some mm) than MIR radiation (up to some 100 μm) into the plastic resin.

3.1.1.2 **Indirect Absorption**

Natural thermoplastic resins typically have only weak absorption in the spectral range between 800 nm and 1200 nm and are rather transparent for the laser radiation. To increase the absorption of the resin, special agents like absorbing additives or absorbing surface coatings have to be used, depending on the demands of the application.

Absorbing additives mixed into the resin before extrusion or molding parts can be divided into inorganic pigments and organic dyes (see Section 1.4.7) [5, 6]. Concentration of the absorbing additives has a direct influence on the penetration depth of the laser radiation into the resin. Higher concentrations result in lower penetration depth and vice versa. A special case of absorbing additives are carbon black pigments, which have a high absorption over the entire spectrum and the concentration influence is weaker than for other inorganic or organic additives (see Sections 1.4.7 and 4.3.2).

Inorganic pigments like carbon black, copper phosphates or indium tin oxide are dispersed in the polymeric matrix as discrete particles (Figure 3.1a) with typical particle sizes between 0.5 and 5 μm, depending on the type of pigment [7]. They absorb and transfer the laser energy into process heat. The individual pigments are in contact with the macromolecular structure of the resin and transfer the process heat by heat conduction to the macromolecular structure.

Organic dyes like azo, perionon or perylene dyes are dissolved as molecular groups in the polymeric matrix (Figure 3.1b). Typical sizes of organic dye agglomerates as

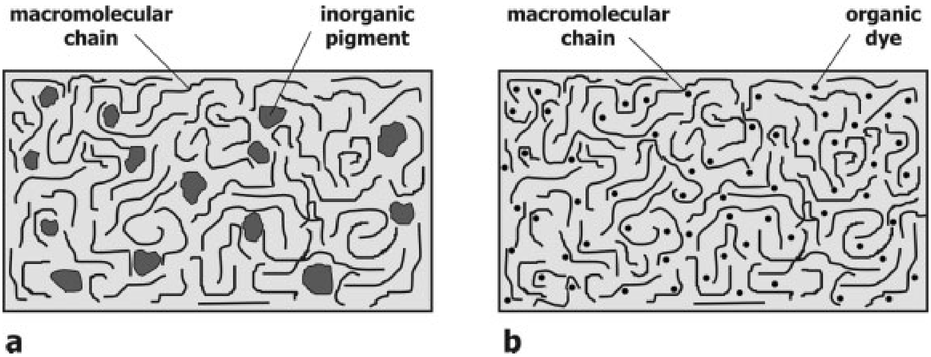

Figure 3.1 Dispersion of inorganic pigments (a) and solution of organic dyes (b) in the polymeric matrix.

powder additives are between 0.05 and 0.5 μm [8]. Ideally dissolved to particle sizes around 0.1 nm in the polymeric matrix, organic dye molecules are in close contact with the macromolecular chains and have a more homogeneous and fine distribution than inorganic pigments, resulting in high visual transparency. As for pigments, organic dyes absorb the laser radiation (see Section 1.4.7) and transfer the laser energy into process heat (see Section 4.3.3). Because of the homogeneous distribution and the direct contact to the macromolecular chains, the heat transfer is more effective than for inorganic pigments, resulting in lower required organic dye additive concentrations for laser absorption than for inorganic pigments. Typical concentrations of organic dyes are of the order of 0.01% compared to inorganic pigments with concentration in the order of 1%.

When using laser-absorbing additives in the resin is not possible for technical or economical reasons absorbing agents can be supplied to the surface of the plastic material as a thin layer by suitable technologies like liquid coating dispensing, laser-assisted powder application or thermal transfer printing [9, 10]. The absorbing layer can be built by organic dyes or inorganic pigments. It will absorb the laser radiation and transfer the radiation energy into process heat, which will be dissipated by heat conduction to the adjoining polymeric areas.

The time needed to absorb the laser radiation either by direct or indirect absorption and transfer into process heat is very short (of the order of 10^{-15} s for absorption and 10^{-9} to 10^{-12} s for energy dissipation by molecule oscillation [11]) compared with the dissipation of the process heat to adjoining resin areas to build a melt pool for the welding process. Deposition of the laser energy in the absorbing volume of the resin depends on radiation intensity, the absorption properties of the resin and duration of the laser to resin interaction. In principle, the absorbed laser energy has to heat up the interaction volume from the start temperature to a state above melting and below the decomposition range of the thermoplastic resin. Additional to the increase of the resin temperature a fraction of the laser energy is needed to induce the phase-transition process from the solid to the molten state.

3.1.1.3 **Hindered Absorption by Internal Scattering**

Absorption of laser radiation in thermoplastic resins can be hindered by scattering of the radiation at internal structures (see Section 1.4.3) especially in the laser-transparent component, for example, by crystalline phases or filler materials like talcum pigments or glass fibers (Figure 3.2).

The type of scattering depends on the size of the scattering structure. Crystalline phases like lamella packages with typical sizes of some 10–100 nm causes Rayleigh scattering with a scattering constant K^+ given by [12]:

$$K^+ = -\frac{N \cdot V^2}{\lambda^4} \tag{3.1}$$

N: number of scattering crystalline phases
V: volume of crystalline phases
λ: wavelength of radiation.

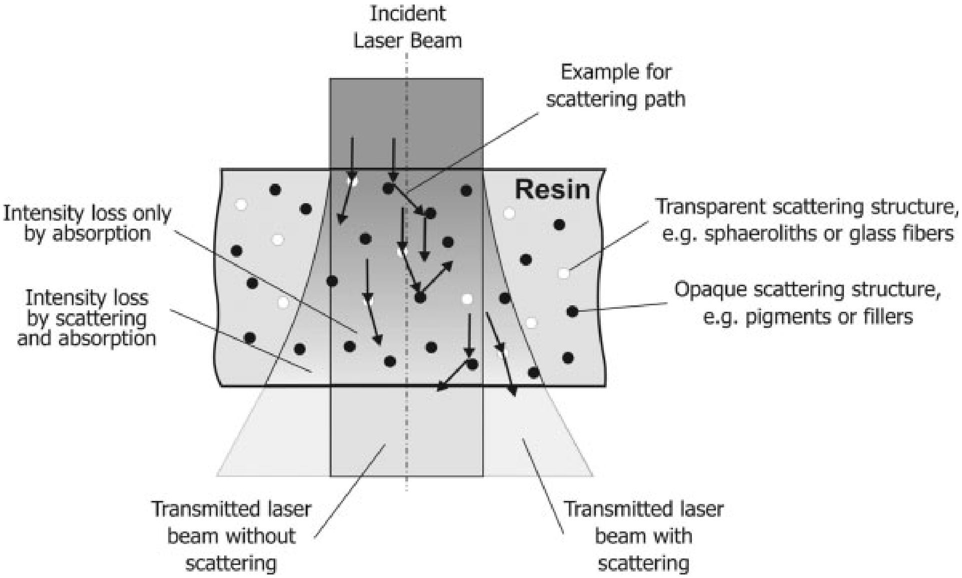

Figure 3.2 Scattering of laser radiation by inner structures resulting in increased transmitted laser beam diameter and decreased radiation intensity.

The scattering constant is proportional to the number N and the volume V of the crystalline lamellas as well as to the reciprocal fourth power of the radiation wavelength. For a given wavelength of the radiation the scattering will be in principal dependent on the concentration of crystalline lamellas in the thermoplastic resin. But in technical thermoplastic resins usually crystalline lamellas are combined into sphaerolithic structures with dimensions of some 10 to some 100 μm. These sphaerolithic structures will cause microscopic scattering with a scattering constant K^+ proportional to the number N and cross section ϱ of the scattering particles like for colorant and filler pigments as well as glass fibers [13]:

$$K^+ \propto N \cdot \varrho^2 \tag{3.2}$$

N: number of scattering particles
ϱ_i: scattering cross section of particle i.

The result of the internal scattering is an increase of the transmitted laser beam diameter as well as a decrease of the laser radiation intensity. Figure 3.3 shows as an example the increase of the laser beam diameter by scattering on sphaerolithic crystal structures in semicrystalline POM samples. Sample preparation was made for different thicknesses with varying molding parameters [14] resulting in different sphaerolith diameters of the molded resin. The beam diameter was measured behind the molded samples and is given in Figure 3.3 as the relative diameter with reference to the incident beam diameter. For sample thicknesses of 1 mm the scattering

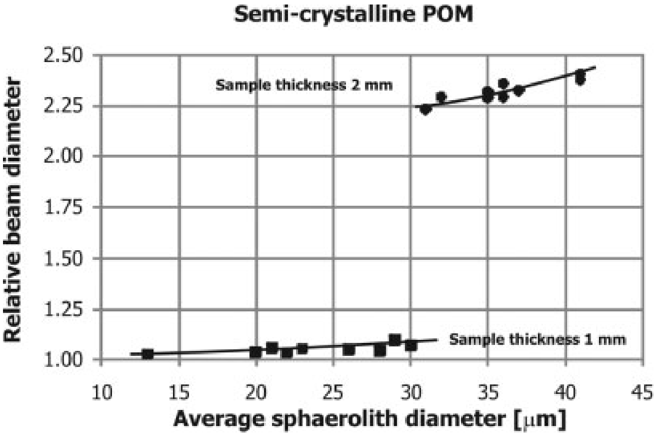

Figure 3.3 Increasing beam diameter caused by sphaerolithic crystalline structures in semicrystalline POM. Measured beam diameter is given as normalized to the incident beam diameter, computed using results from [14].

influence is not so evident as for 2 mm thickness, caused by the molding effects to the sphaerolithic structure sizes and the longer beam path in the thicker samples.

Similar to scattering by sphaerolithic crystal structures, scattering of laser radiation by colorant and filler pigments as well as glass fibers will depend on the concentration of the scattering elements proportional to the number N and cross section ϱ of the scattering particles.

As an example, Figure 3.4 shows the influence of varying glass-fiber concentration in PA6 to the increase of the laser-beam diameter after transmission of the resin samples with thicknesses of 2 mm [15].

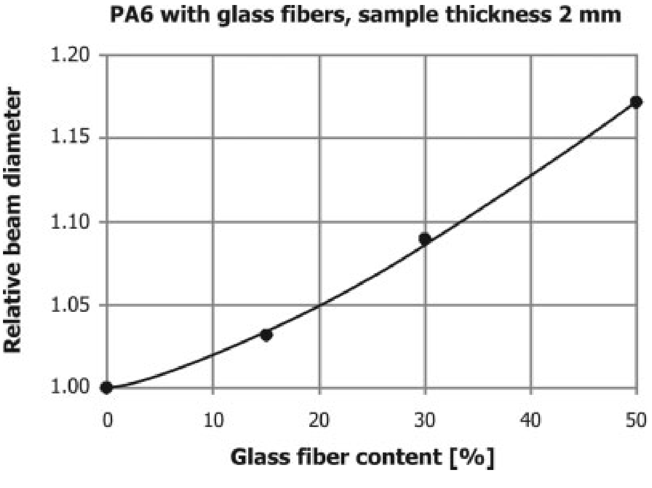

Figure 3.4 Increasing laser beam diameter on PA6 (2 mm) in relation to the glass-fiber content in the resin [15].

It has to be noted that increasing laser-beam diameter caused by macroscopic scattering processes on crystalline structures as well as pigments or glass fibers in the laser-transparent thermoplastic component will result in a decrease of the transmitted laser beam intensity. The decrease of intensity depends on the content of the scattering elements as well as on the thickness of the laser-transparent component.

The loss of laser-beam intensity can yield too low a laser energy for successful running of the laser-welding process. In some cases, the loss of laser energy can be balanced out by using higher laser power for the welding process. But higher laser power can also result in local absorbing on scattering structures with starting decomposition and burning processes.

For example, as a rule of thumb a glass-fiber content above 30% on laser-transparent components with thicknesses above 2 mm will prevent successful laser welding of the components [16].

The influence of scattering structures in the laser-absorbing component can usually be neglected if carbon black is used as the laser-absorbing additive. Carbon black with concentrations of 0.01% up to 0.6% has a high absorption with low penetration depth into the absorbing component.

Using organic dyes or inorganic pigments as laser-absorbing additive with higher optical penetration depth for the laser radiation in the absorbing component can interfere with the effect of the scattering structures like TiO_2 pigments for white coloration. In this case, the concentration of the absorbing additive has to be balanced out with the coloring pigment concentration for optimized absorption of the laser radiation.

3.1.2
Transfer of Laser Energy into Process Heat

The processes for transfer of absorbed laser energy into process heat can be distinguished in the limits of two basic processes, depending on the optical penetration depth and spot size of the radiation in relation to the penetration depth [17]: surface absorption with heat conduction and volume absorption with negligible heat conduction. The following discussion will be made for a solid material with thickness much larger than the optical penetration depth of the radiation (semi-infinite geometry).

In the case of low optical penetration depth and comparatively large spot size the laser energy will be absorbed on the surface of the resin (Figure 3.5a). Energy dissipation into deeper resin layers has to be done by heat conduction. Thereby, interaction times for laser processing are determined by thermal material properties.

In the case of high optical penetration depth and spot sizes of the order of the optical penetration depth absorption of the laser energy will be done in the volume of the resin (Figure 3.5b). Energy dissipation into deeper resin layers can be neglected with regard to adjusted interaction times.

For thermoplastic resins the optical penetration depth is correlated with the radiation wavelength and the macromolecular structure and composition of the resin. NIR radiation on natural resins has in principle a high optical penetration

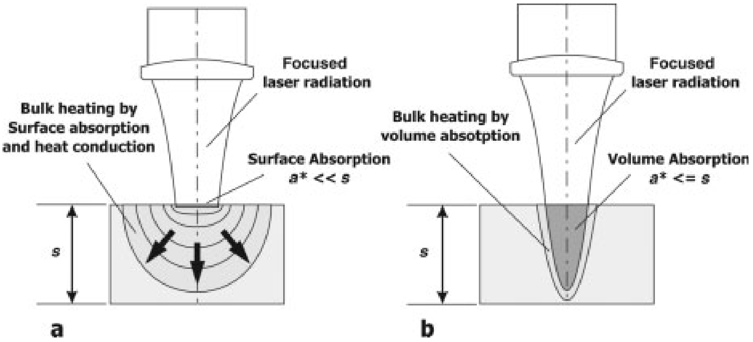

Figure 3.5 Surface (a) and volume absorption (b) of laser radiation on thermoplastic resins [17].

depth while MIR radiation has a low optical penetration depth. As discussed before using absorbing agents in combination with NIR radiation, absorption can be increased and thus the optical penetration depth is decreased.

Estimations of the temperature distribution in the material caused by radiation absorption can be described by several theoretical models. A simple model will be used in the following. More sophisticated models can be found in the literature [18–20].

As a basis for the model the general heat-conduction equation [21] valid for solid material will be used:

$$\frac{\partial}{\partial t}(\varrho c T) + v\nabla(\varrho c T) = \nabla(\lambda_{\mathrm{H}} \nabla T) + A(x, y, z, t) \tag{3.3}$$

ϱ: specific density of the resin
c: specific heat capacity
λ_{H}: specific heat conductivity
T: temperature
A: source term.

Equation 3.3 describes in principle the increase of temperature by a heat source A within a specific volume of the resin and the dissipation of the heat energy out of this volume. As an assumption, material parameters like specific density, specific heat capacity and conductivity will be taken as constants. Also, the stationary state ($v = 0$) will be taken as an attempt.

In reality, the values of these material parameters are dependent on the material temperature as described in Section 1.3. Especially for semicrystalline thermoplastic resins the specific heat capacity has a discontinuity in the temperature range of crystalline melting. More complex thermal models will take these facts into account. For the simple thermal model the values of the material parameters will be taken as average values within the limits of the observed temperature range.

The heat source in Equation 3.3 is the laser energy absorbed in the volume of the resin, energy losses by reflection on the surface of the resin and scattering inside will be neglected in this model. The absorption of the laser radiation inside the resin can be described by the Lambert law [22]:

$$I(z) = I_0 \mathrm{e}^{-\frac{z}{a}} \tag{3.4}$$

a: optical penetration depth
I_0: radiation intensity on the surface.

Using the Lambert law (3.4) as a one-dimensional approach in the z-direction into the material, the source term of Equation 3.3 will be given by:

$$A(z,t) = I_0(t)\mathrm{e}^{-\frac{z}{a}} \tag{3.5}$$

Inserting Equation 3.5 together with the expression for the temperature conductivity:

$$\kappa = \frac{\lambda_{\mathrm{H}}}{\varrho c} \tag{3.6}$$

into Equation 3.3 results in the one-dimensional heat-conduction Equation 3.7:

$$\frac{1}{\kappa}\frac{\vartheta T}{\vartheta t} - \nabla^2 T = \frac{1}{\lambda_{\mathrm{H}}} I_0(t)\mathrm{e}^{-\frac{z}{a}} \tag{3.7}$$

Regarding the limit conditions [23]

$$z = 0 : \left.\frac{\mathrm{d}T}{\mathrm{d}z}\right|_{z=0} = 0 \tag{3.8}$$

$$z = D \rightarrow \infty : \left.\frac{\mathrm{d}T}{\mathrm{d}z}\right|_{z=D} = 0 \tag{3.9}$$

an analytic solution of the heat conduction equation will be given by [23]:

$$\begin{aligned} T(z,t) = {} & \frac{a I_0}{2\lambda_{\mathrm{H}}}\left(\mathrm{e}^{\left(\frac{\kappa t}{a^2} - \frac{z}{a}\right)} \operatorname{erfc}\left(\frac{\sqrt{\kappa t}}{a} - \frac{z}{2\sqrt{\kappa t}}\right) + \mathrm{e}^{\left(\frac{\kappa t}{a^2} + \frac{z}{a}\right)} \operatorname{erfc}\left(\frac{\sqrt{kt}}{a} + \frac{z}{2\sqrt{\kappa t}}\right)\right) \\ & + \frac{2I_0}{\lambda_{\mathrm{H}}}\sqrt{\kappa t}\,\mathrm{ierfc}\left(\frac{z}{2\sqrt{\kappa t}}\right) + \frac{aI_0}{\lambda_{\mathrm{H}}}\mathrm{e}^{-\frac{z}{a}} \end{aligned} \tag{3.10}$$

I_0: radiation intensity
z: depth into material
t: time of interaction
a: optical penetration depth
λ_{H}: heat conductivity
κ: temperature conductivity.

The heat-conduction Equation 3.10 enables computer computation [23] of the material temperature as a function of the material depth "*z*" and the interaction time "*t*" in correlation with the incident radiation intensity "I_0," the optical penetration depth "*a*" and the thermal material properties heat conductivity "λ_H" and temperature conductivity "κ". For very low optical penetration depth the first and third term of Equation 3.10 tends to zero and the solution of the heat-conduction equation becomes the solution for a surface heat source (e.g., valid for CO_2-laser radiation or high carbon black concentration for NIR lasers).

By calculation of the 1-dimensional temperature distribution in the *z*-direction according to Equation 3.10 additional consumed process energy for initializing phase transitions like crystallite melting of semicrystalline resins are not taken into consideration. Also, optical and thermal material properties are taken as constant by increasing temperature as a simplification. More advanced temperature calculations using 3-dimensional heat-flow models, observing temperature-dependent material properties and phase-transition energies, can be found in the literature, for example, [24, 25].

Figures 3.6 and 3.7 give examples of calculated 1-dimensional temperature courses as a function of the material depth using Equation 3.10 for PA 6 with high and low optical penetration depths for the incident laser radiation. For both figures the spot size of the incident laser radiation on the target surface is 1 mm diameter and computation is made using different radiation power and interaction times of the incident laser radiation to the resin. The start of material degradation is taken as upper temperature limit for the calculation.

High optical penetration depth (Figure 3.6) is valid for PA 6 resin with low concentration of laser-absorbing additives like organic dyes or inorganic pigments adapted to the incident radiation wavelength or for natural PA 6 resin using a radiation wavelength adapted to the intrinsic absorption properties of the resin at this wavelength. The computed melting depth is of the order of 1.4 mm for all three

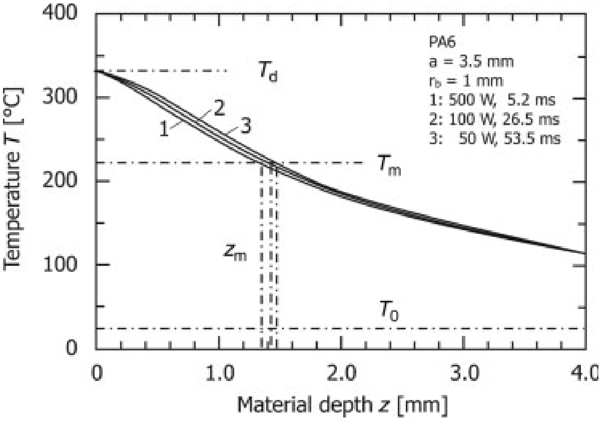

Figure 3.6 Temperature course according Equation 3.10 for high optical penetration depth "*a*" with spot size of 1 mm on the surface of the target and different radiation power and interaction time.

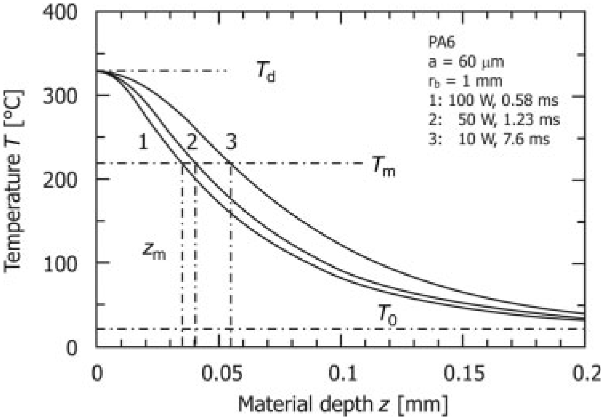

Figure 3.7 Temperature course according Equation 3.10 for low optical penetration depth "*a*" with spot size of 1 mm on the surface of the target and different radiation power and interaction time.

parameter settings of laser power and interaction time. Caused by the distinctive radiation absorption in the volume of the resin, heat conduction has no significant influence in this example. Backcalculated welding speeds would be, for example,, between approximately 20 mm/s for 50 W and 38 mm/s for 100 W of laser power.

Low optical penetration depth (Figure 3.7) is valid for PA 6 resin with high concentration of carbon black or very high concentration of laser-absorbing additives like organic dyes or inorganic pigments. Absorption of the laser radiation occurs predominately on the surface of the target with influence on the resulting melting depth by heat conduction into the resin. The melting depth varies for the used parameters of laser power and interaction time between 0.035 and 0.055 mm.

Compared to Figure 3.6 the corresponding backcalculated welding speeds would be between approximately 800 mm/s for 50 W and 1800 mm/s for 100 W of laser power.

The given examples for 1-dimensional calculation of the temperature course into the target *z*-direction using Equation 3.10 are valid as a rule of thumb for estimating temperature distributions in correlation with the processing parameters. More precise calculation for process simulation can be done using advanced calculation models, as briefly described in Section 3.1.4.

3.1.3
Dissipation of Process Heat

As discussed above, absorbing laser radiation by the thermoplastic resin will result in a temperature increase of the absorbing resin layer. The temperature difference between the heated resin layer and colder adjoining resin layers will cause a heat flow by temperature conduction.

A common process for laser welding thermoplastic components is "through transmission laser welding" (see Section 4.1.2). Hence, process a laser-transparent

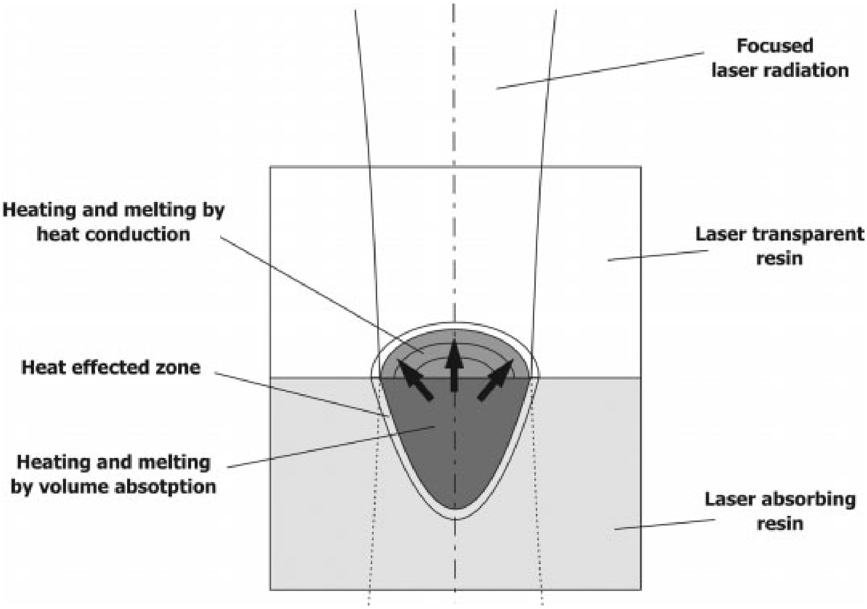

Figure 3.8 Heating the laser-transparent component interface by heat flow from the absorbing component.

and a laser-absorbing component will be joined together. Typically, both components are built by the same resin type, while the absorbing component incorporates additives like inorganic pigments (e.g., carbon black) or organic dyes to absorb the laser radiation and generate process heat, exceeding the melting temperature range of the used thermoplastic resin.

To create a joint between both components, the laser-transparent component also has to be heated up above the melting temperature (Figure 3.8). This will be done by heat flow from the absorbing to the transparent component. For optimized heat flow the interface surfaces of both components have to be in direct contact. Best heat-flow conditions will be achieved by ideally plane parallel surfaces.

Technical surfaces usually have a certain roughness that can hamper the heat flow during the beginning of the melting process (Figure 3.9). Melting of the transparent component surface will start at the contact spots between the transparent and the absorbing component. By the applied clamping pressure the molten resin spots will squeeze into the gaps between both interface surfaces [26] and will increase the heat flow from the absorbing resin to the transparent resin. Hence, both interfaces will be plasticized and will be welded together.

The rougher the surfaces are the more the heat flow will be hampered during the starting phase and longer interaction times of the laser radiation will be needed for evening out the roughness. For extreme situations with no direct contact of the interface surfaces a heat flow from the absorbing to the transparent interface will not occur and the welding joint will not be generated.

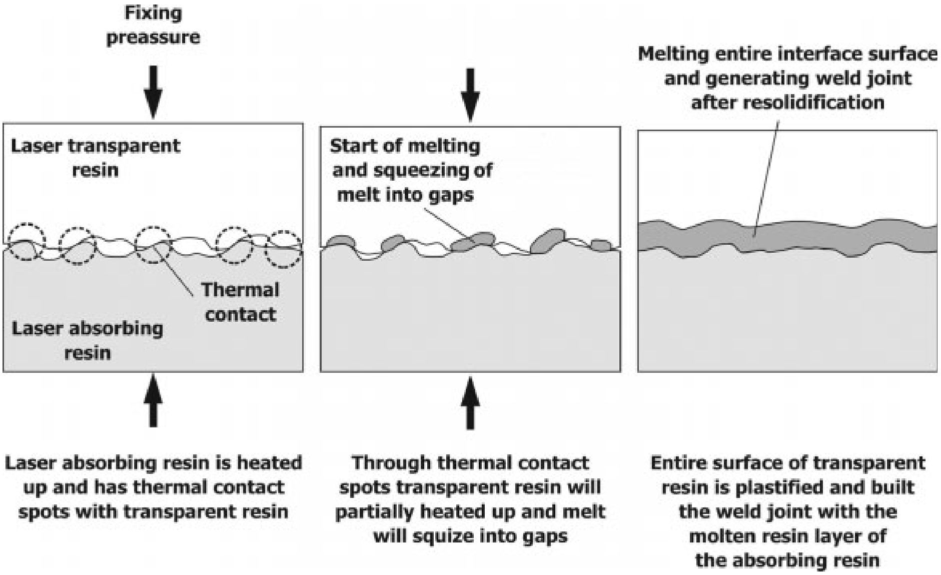
Fixing preassure
Laser transparent resin
Thermal contact
Laser absorbing resin
Start of melting and squeezing of melt into gaps
Melting entire interface surface and generating weld joint after resolidification
Laser absorbing resin is heated up and has thermal contact spots with transparent resin
Through thermal contact spots transparent resin will partially heated up and melt will squize into gaps
Entire surface of transparent resin is plastified and built the weld joint with the molten resin layer of the absorbing resin

Figure 3.9 Evening out of surface roughness during heat up.

Under the assumption of ideally plane component surfaces, the laser-absorbing layer and the laser-transparent layer will have immediate contact. Heating by absorption of laser radiation within the absorbing layer will be done in shorter times as heat flow into the transparent layer will occur. Hence, the heat flow into the transparent layer can be described analogously to using a contact heating tool for plastic welding. In this simplified case, the absorbing layer will act like a heating tool and heats up the laser-transparent layer by heat contact. Squeezing processes that occur during hot-plate welding will be neglected in the following consideration.

The contact surface of the absorbing layer is heated up above the melting temperature. At the start up of the heating process the surface of the transparent layer is at a temperature T_0 (Figure 3.10) and the temperature of the absorbing layer is at a certain value above the melting temperature T_m. With increasing interaction time heat flow into the transparent layer will generate increasing temperatures of the transparent layer. After a certain time t_m the transparent layer is molten up to the depth z_m.

Analogous to hot-plate welding the melting depth z_m can be estimated using Equation 3.11 [27]:

$$z_m = \frac{2}{1.06}\,(1-\theta_{fl})\,\sqrt{\kappa\, t} \tag{3.11}$$

κ: temperature conductivity
t: heat up time.

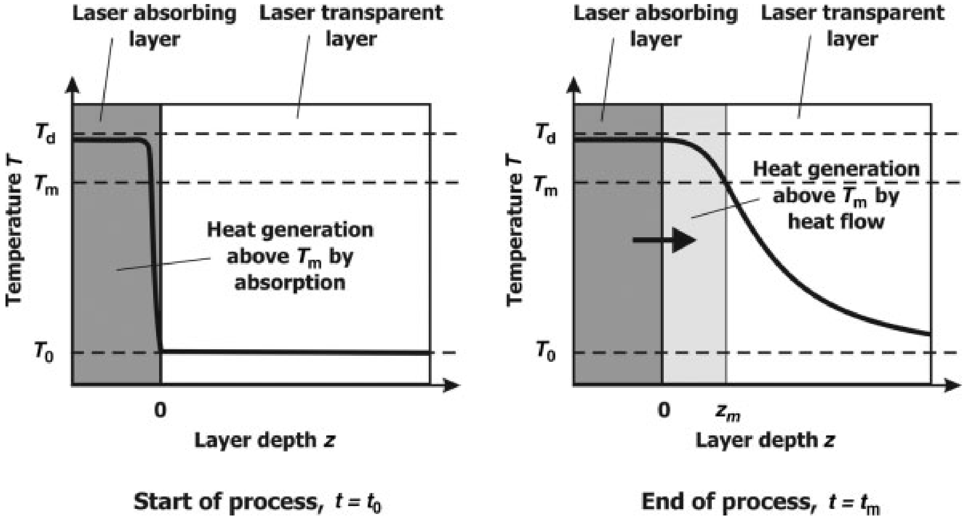

Figure 3.10 Heat dissipation from the absorbing into the transparent layer by heat conduction.

The term θ_{fl} is a correlation of temperature T_g at the heated interface of the absorbing resin, the resin melting temperature T_m and the starting temperature T_0 of the laser-transparent layer given by:

$$\theta_{fl} = \frac{T_m - T_0}{T_g - T_0} \tag{3.12}$$

T_m: melting temperature of resin
T_g: absorbing interface temperature
T_0: starting temperature (e.g., room temperature).

Calculation using Equation 3.11 will result in a rough estimation for the melting depth z_m of the laser-transparent resin layer as a function of the interaction time. Figure 3.11 shows as an example the calculation result of the time-dependent melting depth for laser transparent PA 6 using the surface temperature of the laser-absorbing layer from Figures 3.6 or 3.7.

For example, using process interaction times of 20 ms to 50 ms as shown in Figure 1.4.6 will result in a melting depth of the laser-transparent PA6 of the order of 18 to 28 μm compared to the calculated melting depth of the laser absorbing PA6 of the order of 1.4 mm.

3.1.4
Process Simulation by Complex Computation

The examples discussed in the previous considerations are only rough estimations for evaluating melting depths of the laser-transparent and -absorbing resin caused by

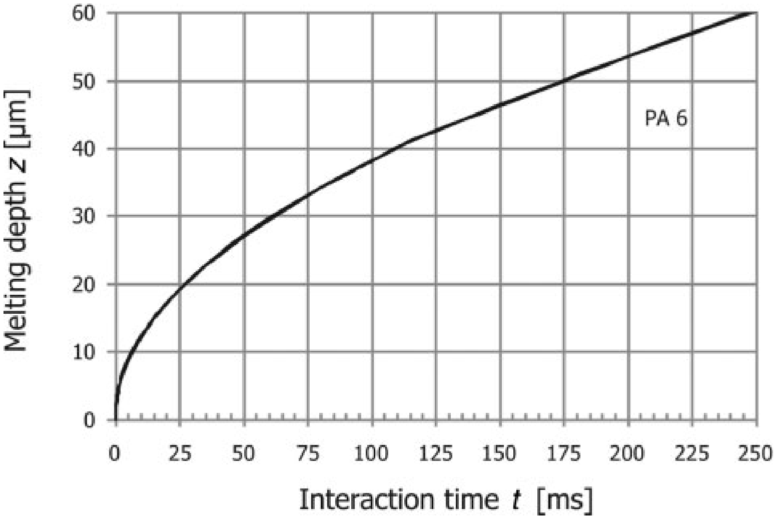

Figure 3.11 Increasing melting depth by interaction time in laser-transparent layer.

absorption and heating with laser radiation. Using one-dimensional heat flow and temperature-independent material properties result in a rough evaluation of the melting depths with limited accuracy.

For more exact calculation 3-dimensional heat-flow models considering temperature-dependent material properties and phase transitions are used for process simulation for example, by finite element method (FEM) computation. Examples of modeling of laser welding thermoplastics can be found in the literature [24, 25] and the results of such computations will be described briefly in the following.

Beside temperature-dependent thermal resin properties and temperature-dependent optical properties (transmission, reflection) also have to be noted. Especially for semicrystalline thermoplastics like PP or PA6 the optical properties can vary during the phase transition of melting the crystallites. Figure 3.12 shows, for example the

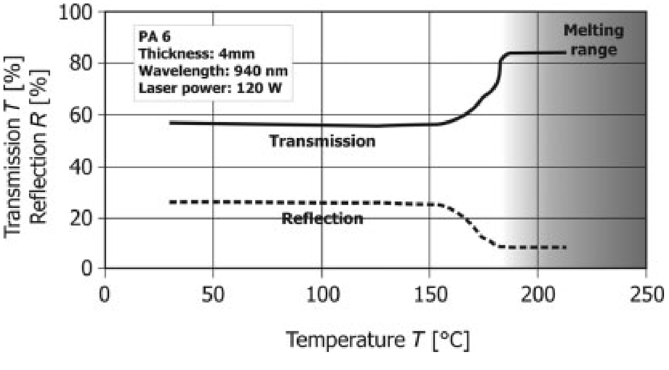

Figure 3.12 Temperature course of transmission and reflection of irradiation PA6 with a laser wavelength of 940 nm [24].

temperature dependence of transmission and reflection for PA6 at 940 nm laser wavelength [24].

Increasing the temperature of the PA6 resin up to approximately 150 °C has no significant effect to the optical properties of the resin. Reflection of the laser radiation is high because of internal reflection and backscattering of the radiation at the crystalline phases. Above 150 °C the crystalline phases start to melt and transmission increases and reflection decreases by rising temperature because internal reflection at the crystalline phases becomes a minor effect. In the molten state of the resin the crystalline phases have vanished and again the optical properties are constant with increasing temperature.

Changing of absorption properties by increasing temperature of the resin have to be assessed by FEM analysis. Figure 3.13 gives a principle example for the laser-intensity course in the laser-transparent and -absorbing component at the beginning (left) and during the welding process (right).

Heating up the absorbing and transparent resin by the laser radiation will result in changing the absorption properties of the resin for the laser radiation. Heating up will increase the radiation absorption and will speed up the temperature increase during irradiation by the laser radiation.

To compare the results of FEM computation with real welding results, extensive welding trials on PP using carbon black as the absorbing additive were made in [24]. The processing parameters welding speed and laser power are varied over a wide range to evaluate the process window for achieving successful laser welding. The results are summarized in Figure 3.14.

Process-parameter combinations marked in Figure 3.14 are used for process simulation by FEM analysis and the calculated temperature distributions were compared with results by laser welding as shown in Figure 3.15, demonstrated by microcut cross sections of the welded samples.

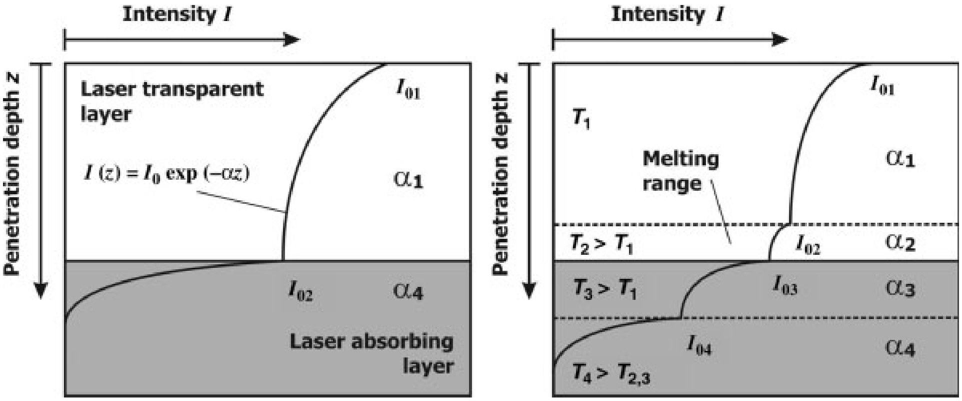

Figure 3.13 Schematic temperature-dependent radiation absorption using TTLW, left at process start and right during processing [24].

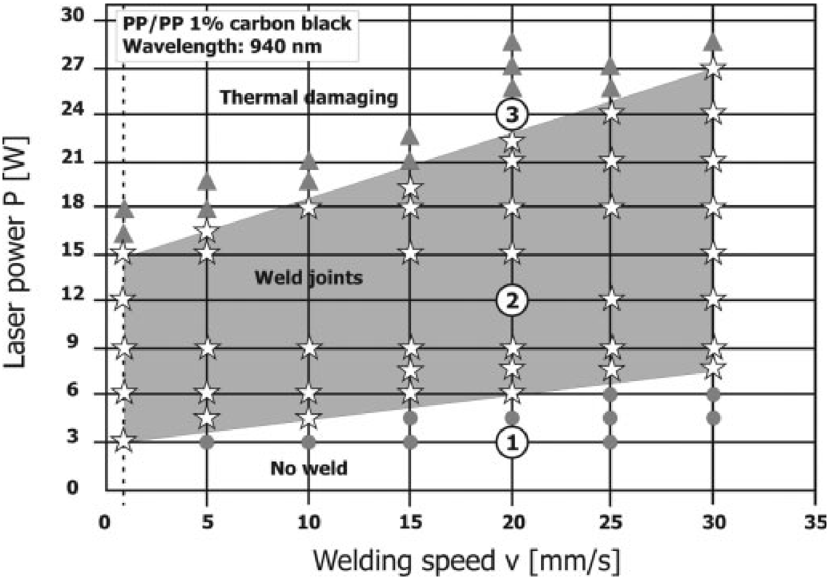

Figure 3.14 Evaluation of process window for TTLW on PP resin. Characteristic process parameter combinations inside and outside the process window are marked by numbers [24].

Comparison of the experimental and computation results shows good matching and demonstrates the ability of theoretical models for process evaluation.

Computer modeling can also be used for evaluation of the influence of joint gaps on the weld joint [25]. Figure 3.16 shows a computation result for laser heating of PP

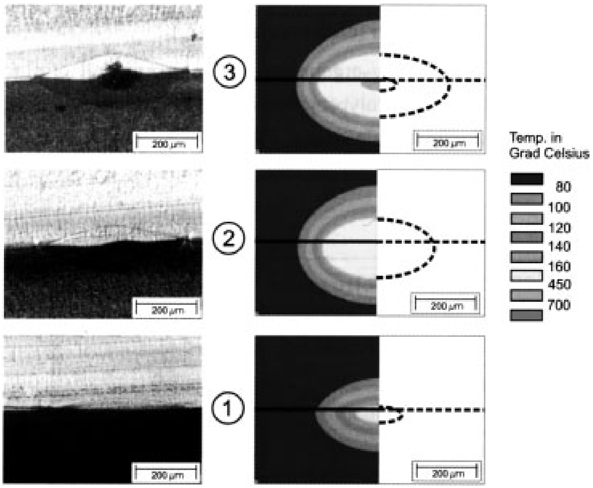

Figure 3.15 Comparison of calculated temperature distribution and real welding results using the parameter combinations marked in Figure 3.14. The dotted lines on the calculation results mark the isotherms of the melting temperature [24].

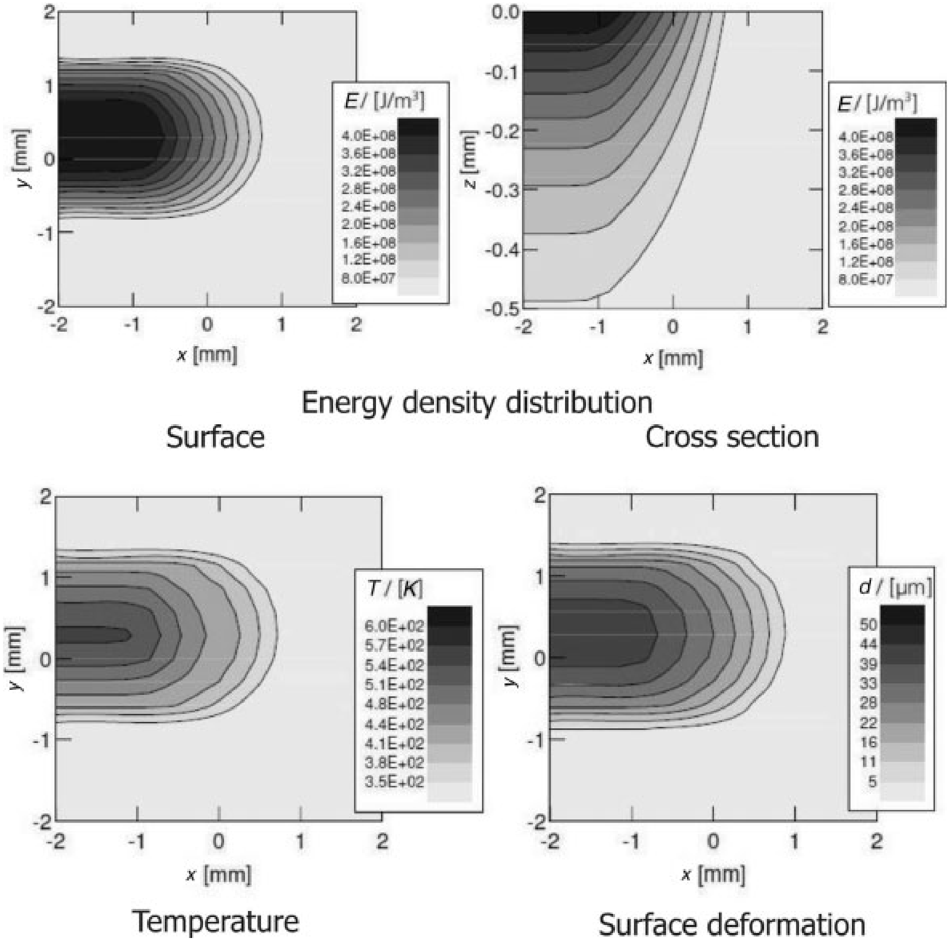

Figure 3.16 Computer modeling of thermal influence on resin expansion. Upper graphs show the thermal energy density distribution on the surface (left) and at a cross section (right) of the target. Lower graphs are the temperature distribution on the surface (left) and the thermally induced resin expansion (right) [25].

(0.5% carbon black as absorber). The upper plots give the computed thermal energy distribution at the surface (left) and a cross section of the target (right) while the lower plots show the temperature distribution (left) and the resulting thermally induced expansion of the PP resin (right). The computation results in a thermal expansion of approximately 45 μm in height.

Simulation of laser-welding process on joint geometries like an overlap with consideration of joint gaps in the computation model enables the evaluation of the gap influence on the weld joint. An example of simultaneous laser welding of an overlap joint on PP resin is given in Figure 3.17.

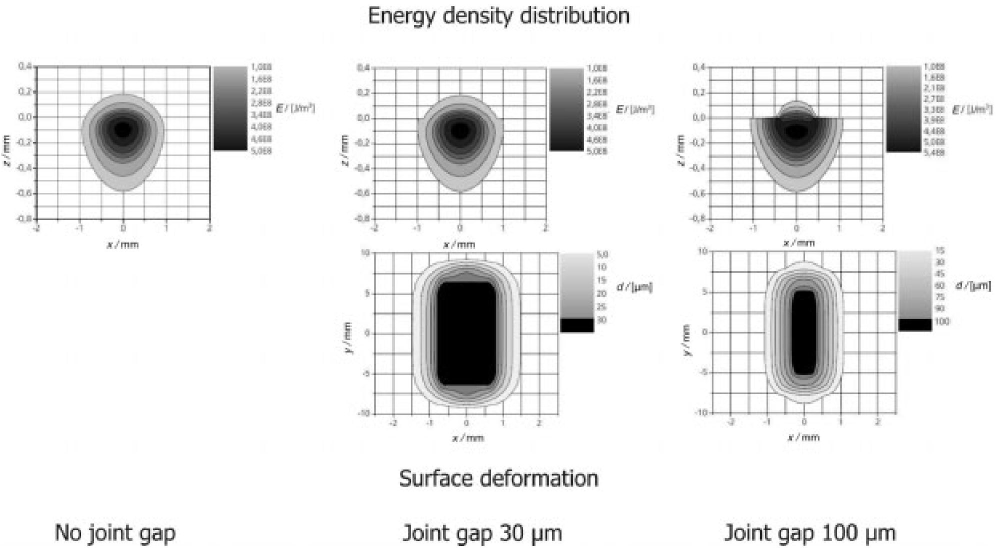

Figure 3.17 Simulation of gap bridging for simultaneous laser welding of a PP overlap joint. Left no gap, in the middle a gap of 30 µm and right a gap of 100 µm was considered during calculation [25].

No gap between laser-absorbing and -transparent layer results in optimized heating of the transparent layer (left). A gap of 30 µm between both layers can be bridged by the thermal expansion of the absorbing layer (middle) and the transparent layer will be heated up by heat conduction to generate a weld joint still of sufficient quality. Increasing gap height will result in decreasing ability to bridge the joint gap by heat expansion. The right side of Figure 3.17 shows the computation result for a gap height of 100 µm. The gap cannot be closed by the thermal resin expansion and heating the transparent layer is limited. The result will be no welding joint between the two layers.

3.2
Theory of Fusion Process

By heating with laser radiation in the absorbing component and heat flow into the transparent component, the contact interfaces of both thermoplastic components exceed the melting temperature and will change from a solid into the molten state. In this state the mobility of the polymer macromolecules will increase decisively. As an effect of the increasing temperature, the specific volume of the resin will also increase (see Section 1.3.2) and will generate an internal pressure between both molten interfaces. By applying an additional externally mechanical pressure to fix the components, macromolecules of each interfaces will penetrate into the other and will form the weld joint after resolidification.

The following discussions of fusion processes are at first sight valid for *amorphous thermoplastics*, processes for semicrystalline thermoplastics will be considered later.

3.2.1
Interdiffusion Process (Reptation Model)

The penetration process of the macromolecules can be described by the reptation model [28, 29]. This model is based on the mobility of a single macromolecular chain within the vicinity of other macromolecular chains. The surrounding macromolecular chains act as obstacles for the mobility like a cage for the free oscillation of the observed single macromolecular chain, as shown in Figure 3.18 for a chain segment AB.

The entire single macromolecular chain can be described as a sphere with statistical orientation of the individual chain segments. The distance between the chain ends is given by the expression "R," while the radius of gyration of the macromolecular chain is "R_g" (Figure 3.19, left).

For real macromolecular chains calculation of both quantities is not possible. Instead of the real structure a theoretical chain structure called Kuhn's sphere model will be used (Figure 3.19, right). The structure of this chain model is based on "N" chain segments with same segment length "l." Each chain segment represents a monomer unit of the macromolecular chain, showing statistical geometric orientation as a Gaussian distribution [27].

For Kuhn's sphere model the distance between the chain ends is defined by [27]:

$$R^2 = Nl^2 \tag{3.13}$$

The radius of gyration for this model is given by [27]:

$$R_g^2 = \frac{1}{6} Nl^2 \tag{3.14}$$

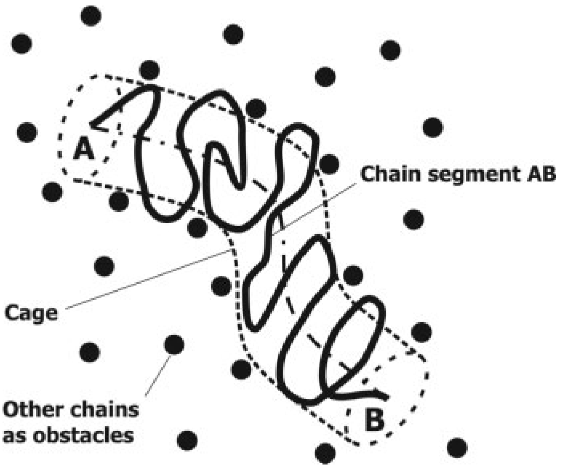

Figure 3.18 The chain segment AB is fixed in a cage by other chains as obstacles. Within the cage the chain segment is free to move between the fixed obstacles, but cannot cross any of them; from [29].

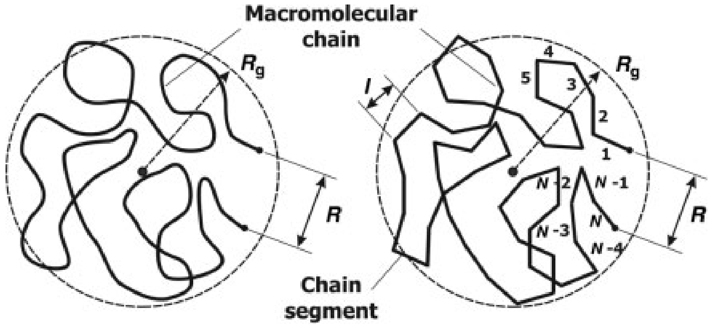

Statistical macromolecular chain sphere

Kuhn's chain sphere

Figure 3.19 Structure of statistical and Kuhn's sphere macromolecular chain model with definition of chain ends distance R and radius of gyration R_g [27].

Equation 3.14 shows that R_g is proportional to the square root of the molecular weight M of the macromolecular chain.

With Equations 3.13 and 3.14 the distance between the chains ends results in [27]:

$$R = \sqrt{6}\ R_g \tag{3.15}$$

Below the melting temperature of the resin, segments of the macromolecular chain can move position caused by Brown's micromobility, but cannot leave the cage. Exceeding the melting temperature, segments of the macromolecular chain, especially the end segments of the chain (called minor chains [30]), are able to start leaving the cage (Figure 3.20) induced by Brown's micromobility. After a certain time t_r, specified as reptation time, the macromolecular chain completely left the cage losing the origin position in the resin.

At the interface of one molten layer, macromolecular chain segments (minor chains) can step out of the surface of the layer (Figure 3.21) [31]. If the interface of the observed layer is in close contact with a second layer, which is also above the melting temperature, the chain segments will diffuse from the origin layer into the second layer.

With the reptation model the diffusion process into the second layer can be described by the distance "X" as the penetration depth of a minor chain into the second layer (see Figure 3.21). The penetration depth increases as a function of interaction time t [27]. Limited by the reptation time t_r, the penetration depth of minor chains will reach a maximum value given by:

$$X_\infty \approx 0.8\ R_g \tag{3.16}$$

For the time dependence of the penetration depth two cases can be distinguished [27]:

Case 1: $t < t_r$
Case 2: $t > t_r$.

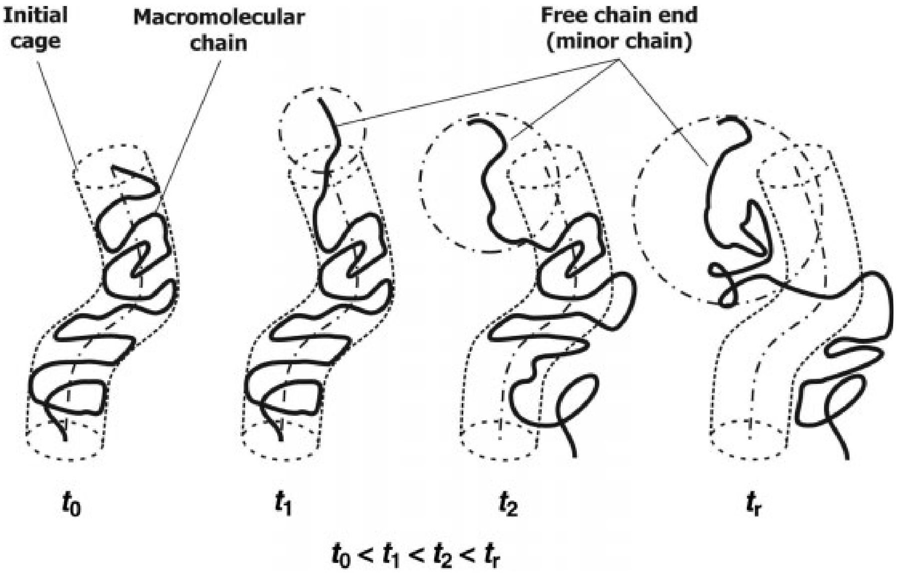

Figure 3.20 Reptation model for a macromolecular chain in the molten state [29].

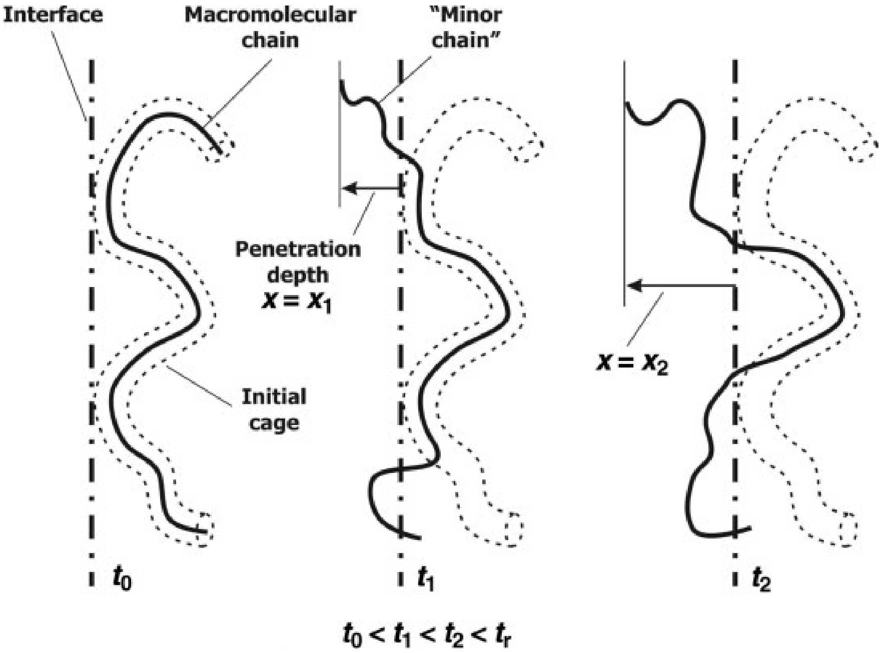

Figure 3.21 Disengagement of a chain from its initial tube near the interface [27].

For case 1 the penetration depth is given by

$$X(t) = X_\infty \sqrt[4]{\frac{t}{t_\mathrm{r}}} \tag{3.17}$$

and for case 2 by

$$X(t) = X_\infty \sqrt[2]{\frac{t}{t_\mathrm{r}}} \tag{3.18}$$

Using Einstein's law for unhampered diffusion in the first approach [27] will result in:

$$t = t_\mathrm{r}: \qquad X_\infty^2 \sim D_\infty t_\mathrm{r} \tag{3.19}$$

$$t < t_\mathrm{r}: \qquad X_{(\mathrm{t})}^2 \sim Dt \tag{3.20}$$

This results for the quotient of the diffusion coefficients in:

$$\frac{D}{D_\infty} = \left(\frac{X(t)}{X_\infty}\right)^2 \left(\frac{t_\mathrm{r}}{t}\right) \tag{3.21}$$

According to Equation 3.18 with

$$\frac{X(t)}{X_\infty} = \sqrt[4]{\left(\frac{t}{t_\mathrm{r}}\right)} \tag{3.22}$$

Equation 3.21 results in the quotient of the diffusion coefficients for case 1:

$$\frac{D}{D_\infty} = \sqrt{\frac{t_\mathrm{r}}{t}} \tag{3.23}$$

For case 2 with

$$\left(\frac{X(t)}{X_\infty}\right)^2 = \frac{t}{t_\mathrm{r}} \tag{3.24}$$

the quotient of the diffusion coefficients will become to:

$$\frac{D}{D_\infty} = 1 \tag{3.25}$$

Equations 3.23 and 3.25 show that for case 1 the diffusion coefficient D is a function of time, while for case 2 the diffusion coefficient is constant by time [27].

Case 2 is valid for the circumstance when two resin surfaces are in close contact without additional heating and a diffusion process will occur by chain segment exchange driven by a self-diffusion process, which will not be considered here.

For laser welding thermoplastics case 1 is of interest for further discussion. The diffusion coefficient D and the penetration depth X of minor chains will increase with time. Both quantities are also a function of the temperature. Rising temperature will increase the diffusion coefficient and the penetration depth.

The temperature dependency of the diffusion coefficient D can be described by using the Arrhenius function:

$$D(T) = D_{\infty}\, \mathrm{e}^{\left(\frac{-E_a}{RT}\right)} \tag{3.26}$$

where E_a is the activation energy and R is the Boltzmann constant (1.3807×10^{-23} J/K).

Also, the temperature dependency of the penetration depth X can be described using the Arrhenius function [15]:

$$X \propto \exp\left(\frac{-E_a}{2\,RT}\right)\sqrt{t} \tag{3.27}$$

Equations 3.26 and 3.27 shows that the diffusion coefficient and the penetration depth of minor chains will increase with increasing temperature of the resin layers.

In particular, the penetration depth as a function of interaction time and interface layer temperature has a significant influence on the mechanical strength of the weld joint. Figure 3.22 shows schematically the interdiffusion process of macromolecule chain segments between the two molten layers [32, 33].

In principle, it is the same effect if for constant layer temperature the interaction time increases or if for constant interaction time the layer temperature increases. For both cases the penetration depth will increase and the interdiffusion zone with mixing of macromolecules from both layers will become larger. Under real conditions both cases are correlated and during increasing interaction time the temperature of the layers will also increase, resulting in an increase of the interdiffusion process for the macromolecular chain segments [34].

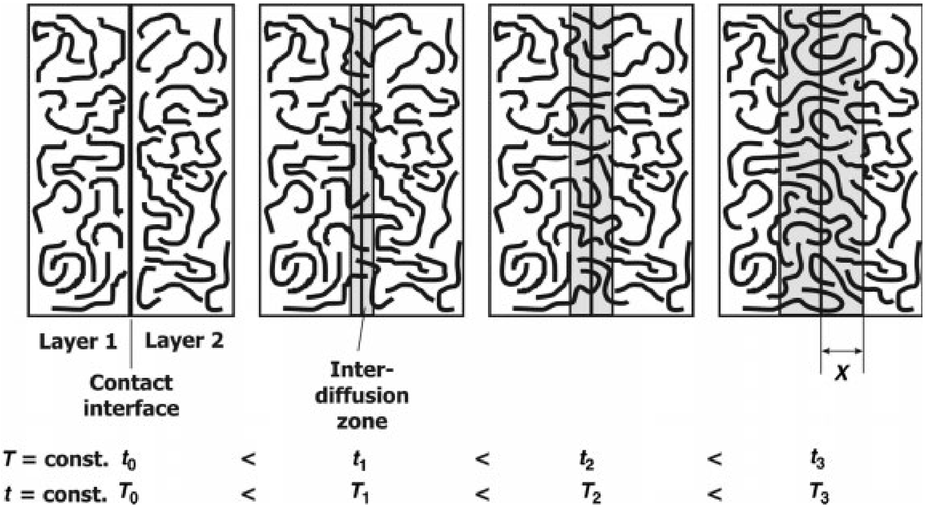

Figure 3.22 Interdiffusion of macromolecular chain segments between two molten layers. The interdiffusion zone will increase by interaction time and constant layer and vice versa.

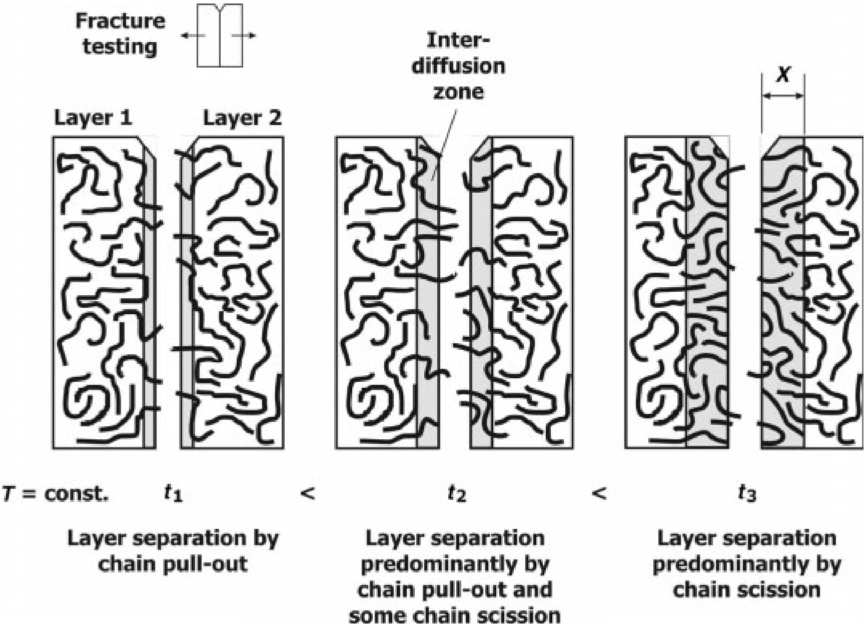
Fracture testing
Inter-diffusion zone
X
Layer 1
Layer 2
T = const.
t_1
<
t_2
<
t_3
Layer separation by chain pull-out
Layer separation predominantly by chain pull-out and some chain scission
Layer separation predominantly by chain scission

Figure 3.23 Fracture testing of welded layers. Laser welding was done at constant temperature and different interaction times [35].

The more the macromolecule chain segments can interdiffuse from the origin into the adjacent layer the more the joint strength will increase up to the maximum strength value of the parent material [35]. Figure 3.23 demonstrates schematically the mechanical separation of two laser-welded layers depending on the interaction time at constant temperature during the welding process.

For short interaction time t_1 some short-chain segments will diffuse through the interface into the other layer. The resulting weld strength is low. Separation of both layers will occur easily by pull out of the chain segments from the layer interfaces.

Increasing interaction time t_2 will result in diffusion of longer-chain segments through the interface into the other layer. The weld strength will increase, but will not reach the properties of the parent resin. Separation of both layers will occur by pull out of chain segments and additionally macromolecular chain scission.

For a long interaction time t_3 the macromolecular chains diffuse sufficiently long into the other layer so that after resolidification both layers looks like the structure of the parent material. Ideally, the weld strength will reach the strength of the parent material. Separation of both layers will occur predominantly by chain scission.

3.2.2
Interchange of Macromolecules by Squeeze Flow Process

Besides the interdiffusion process as discussed previously, welding of two thermoplastic layers will be supported by interchange of macromolecules between the layers generated by squeeze-flow processes [26, 36]. Figure 3.22 illustrates that during the

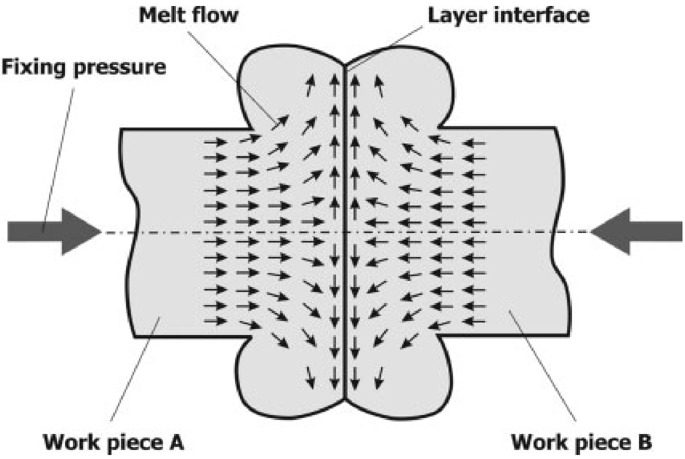

Figure 3.24 Melt flow by squeezing caused by external fixing pressure [36].

heating process the contact areas of both layers starts to melt. The melting process is accompanied by an increase of the volume and applying an external fixing pressure the molten areas begin to squeeze into the free spaces between both layers.

From hot-plate welding of thermoplastic resins it is well known that macromolecules with parallel orientation to the interface surface will be stretched in the molten state along the squeeze-flow direction.

For hot-plate welding both component interfaces to be welded are melted and then pressed together by applying a fixing pressure. The fixing pressure causes a melt flow vertical to the fixing direction, as shown in Figure 3.24.

Accompanying the melt flow stretching of macromolecules parallel to the flow direction occurs [27]. In particular, macromolecules at the interface are forced to be elongated (Figure 3.25). In the beginning of resolidification, the stretched macromolecules are subjected to a relaxation process and they try to get back to their original structure. The interface layers are still molten and segments of the macromolecules are able to interchange between both layers. This situation will become static by complete resolidification of the resin layers and will generate the joint between both layers.

This process is in principle also valid for laser welding plastics in addition to the interdiffusion process of macromolecule chain segments. Beside, this, the squeeze-flow process can also induce microswirling of the melt. The laser-absorbing layer and the transparent layer may have slightly different temperatures, which also causes different melt-flow properties. At the interface of both layers the molten resins start macroscopic mixing, generating microswirls after resolidification (Figure 3.26).

3.2.3
Mixing of Crystalline Phases

Up to now, all discussions were made previously for amorphous thermoplastic resins. In contrast to this on semicrystalline thermoplastics an additional process can be observed as mixing of crystalline phases between the molten layers.

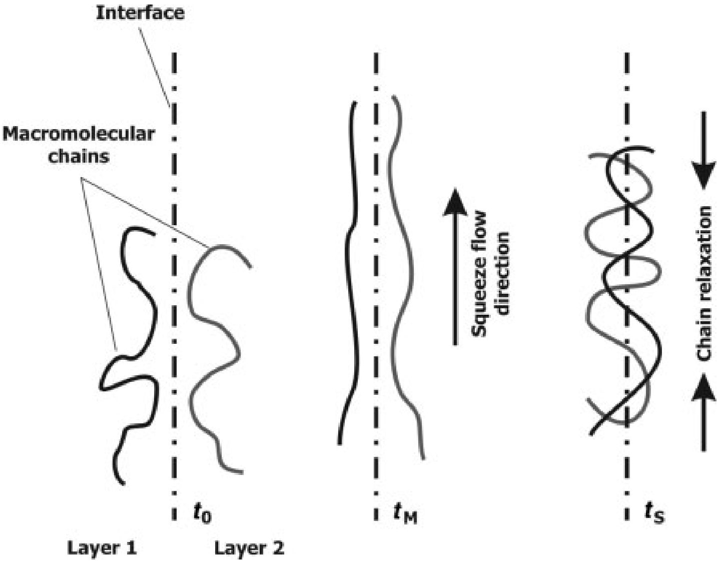

Figure 3.25 Macromolecule stretching caused by squeeze flow and interchange of molecule segments during resolidification [27].

Melting of semicrystalline thermoplastics occurs by exceeding the crystalline melting temperature. The near-order bonding forces generating the crystalline structure will be balanced out and the crystalline structure will be lost in the melt. In the molten state the behavior of semicrystalline thermoplastics is in principle comparable to amorphous thermoplastics and all processes discussed before are also valid for laser welding semicrystalline thermoplastic resins [15, 37, 38].

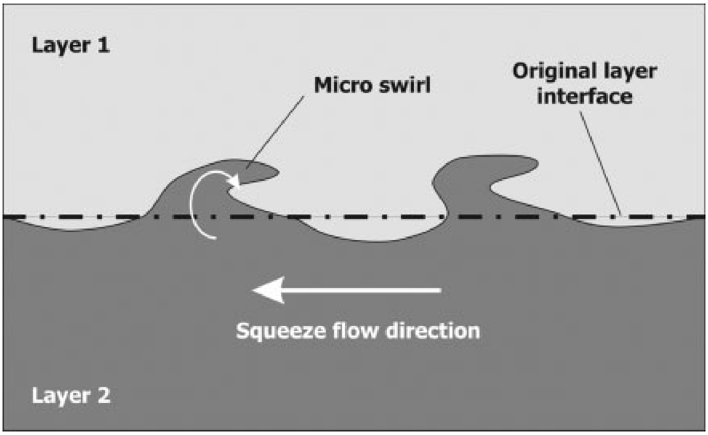

Figure 3.26 Microswirls caused by squeezing process.

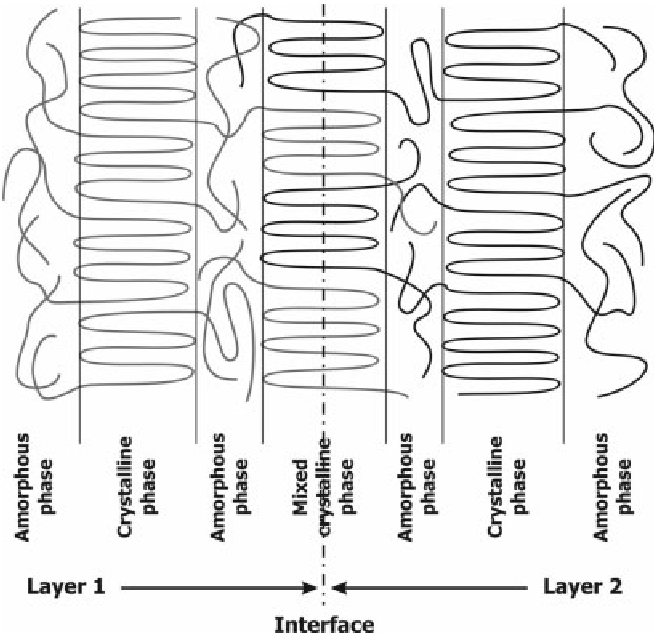

Figure 3.27 Mixed crystalline phases at the interface of two welded semicrystalline thermoplastics [15].

During resolidification of semicrystalline thermoplastic layers the recrystallization process will start and will build new crystalline phases inside the resin layers. The interface of both layers will resolidify right at the end of the process.

At the interface of both layers mixed crystalline phases will be generated having macromolecule partners from both layers, as shown schematically in Figure 3.27.

Generation and growth of mixed crystalline phases are influenced by the interaction time of the laser radiation. Short interaction times will also cause a quick cooling phase and generation of mixed crystalline phases can be hindered. Longer interaction times in connection with higher molten resin volumes will support the generation of more distinctive crystalline phases, resulting in stronger weld joints.

3.3
Material Compatibility

For welding two components together, the resin materials have to be compatible with each other. Conditions, given by the material properties, which have an influence on resin compatibility, are for example, [27]:

- chemical structure – polymeric molecules have to be miscible between each other;
- thermal properties – the melt temperature ranges should overlap, heat expansion coefficients should be of the same order;

- surface energetic properties – the polar surface energy should be of the same order;
- rheological properties – the melt-flow index should be of the same order.

Usually, welding two components of the same resin will meet the given conditions. More complex is the welding of dissimilar resin materials. As a first approach, to be weldable both resins have to have similar chemistry (i.e. they must be miscible) and overlapping melt temperature ranges (e.g., see Figure 1.19).

Also, the melt-flow index (MFI) of the resins can have some influence on thermoplastic resin welding. The MFI value describes the viscosity of the molten resin. If the MFI value of the resins to be welded differs too much, the miscibility of both molten layers can be hindered for successful welding.

A general rule of thumb is that two materials can be laser welded if another welding method like heat contact welding or ultrasonic welding is capable.

As an example for heat contact welding of dissimilar resin materials it was found [27] that the relation of polar surface energy and heat expansion coefficient of both resins have to meet certain limits for successful welding. Equations 3.28 and 3.29 give the limits of both quantities when the welding will become inefficient [39].

$$\frac{\alpha_1}{\alpha_2} > 1.2 \tag{3.28}$$

α_1, α_2: polar surface energy of resin 1 and 2

$$\frac{\gamma_1^p}{\gamma_2^p} > 2.0 \tag{3.29}$$

γ_1, γ_2: heat expansion coefficient of resin 1 and 2 at constant pressure

Table 3.1 lists for heat contact welding of dissimilar resin materials the achievable relative weld strength during welding trials in correlation with the relation of polar surface energy and heat expansion coefficient for the given resin combinations. A value “0” is equivalent to unsuccessful welding. For ultrasonic welding nearly identical conditions were found [40].

Laser welding of similar and dissimilar thermoplastics was evaluated by several companies. Figure 3.28 shows a summary of welding results achieved by BASF [41], Gentex Corp. [42] and Jenoptik [43].

The results for laser-beam welding of dissimilar thermoplastics shown in Figure 3.28 can be used only as rule of thumb because of the wide variety of thermoplastic resin types. Even for the same type of resin, resin structure can vary by chain-length distribution, melt-flow index or thermal and chemical properties. For industrial application of laser welding thermoplastics the weldability of dissimilar thermoplastic resins have to be evaluated case by case.

A special case of laser welding dissimilar resins is welding of thermoplastic elastomers to thermoplastic resins. The physical and chemical properties of TPEs vary over a wide range, depending on the material composition and structure of TPEs (see Section 1.2.4).

Table 3.1 Relative weld strength for heat contact welding of dissimilar resin materials, "0" stands for unsuccessful welding [27].

Resin combination	Polar surface energy coefficient α_1/α_2	Heat expansion coefficient γ_1/γ_2	Relative weld strength [%]
PMMA/PVC	1.04	1.07	99
PVC/ABS	1.08	1.57	57
PMMA/ABS	1.03	1.67	85
PMMA/PS	1.05	1.48	87
HDPE/PP	1.08	2.29	59
PVC/PS	1.20	1.39	0
ABS/PS	1.30	1.12	63
ABS/PP	1.59	2.03	0
PVC/PP	1.72	3.18	0
ABS/HDPE	1.88	1.12	0
PP/PS	2.07	2.29	0
PS/HDPE	2.44	1.00	0

TPE-V and TPE-O for example are TPE blends with a thermoplastic matrix like PP or PE and in the matrix well dispersed softer particles like EPDM (TPE-V) or two-component elastomer systems like EPR and EPDM (TPE-O).

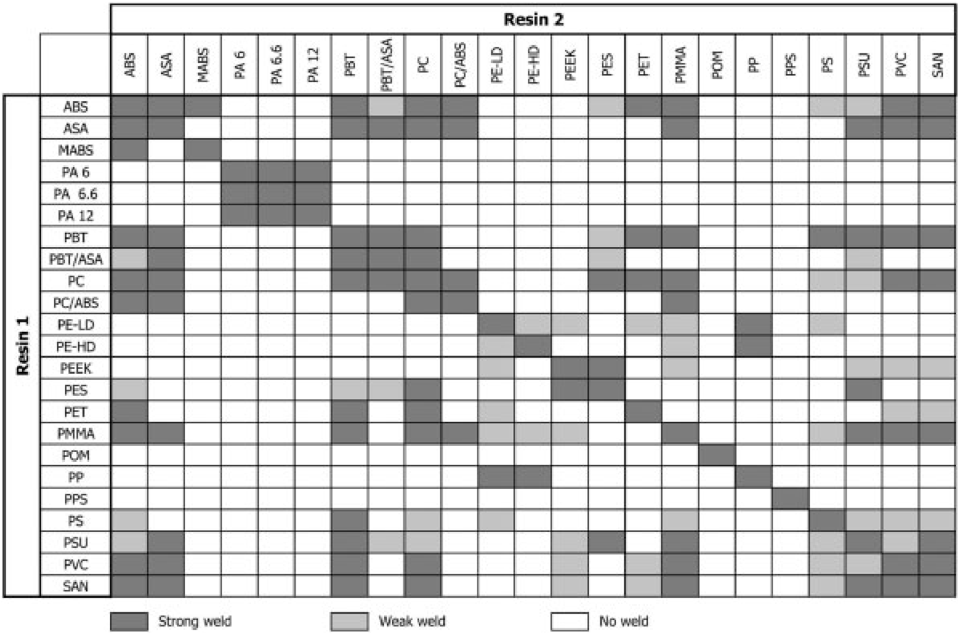

		Resin 2																						
		ABS	ASA	MABS	PA 6	PA 6.6	PA 12	PBT	PBT/ASA	PC	PC/ABS	PE-LD	PE-HD	PEEK	PES	PET	PMMA	POM	PP	PPS	PS	PSU	PVC	SAN
Resin 1	ABS	■	■	■	□	□	□	■	▒	■	■	□	□	□	▒	■	■	□	□	□	▒	▒	■	■
	ASA	■	■	□	□	□	□	■	■	■	■	□	□	□	□	□	■	□	□	□	□	■	■	■
	MABS	■	□	■	□	□	□	□	□	□	□	□	□	□	□	□	□	□	□	□	□	□	□	□
	PA 6	□	□	□	■	■	■	□	□	□	□	□	□	□	□	□	□	□	□	□	□	□	□	□
	PA 6.6	□	□	□	■	■	■	□	□	□	□	□	□	□	□	□	□	□	□	□	□	□	□	□
	PA 12	□	□	□	■	■	■	□	□	□	□	□	□	□	□	□	□	□	□	□	□	□	□	□
	PBT	■	■	□	□	□	□	■	■	■	□	□	□	□	▒	■	■	□	□	□	■	■	■	■
	PBT/ASA	▒	■	□	□	□	□	■	■	■	□	□	□	□	▒	□	□	□	□	□	□	▒	□	□
	PC	■	■	□	□	□	□	■	■	■	■	□	□	□	■	■	■	□	□	□	▒	▒	■	■
	PC/ABS	■	■	□	□	□	□	□	□	■	■	□	□	□	□	□	■	□	□	□	□	□	□	□
	PE-LD	□	□	□	□	□	□	□	□	□	□	■	▒	▒	□	▒	▒	□	■	□	▒	□	□	□
	PE-HD	□	□	□	□	□	□	□	□	□	□	▒	■	□	□	□	▒	□	■	□	□	□	□	□
	PEEK	□	□	□	□	□	□	□	□	□	□	▒	□	■	■	□	▒	□	□	□	□	▒	▒	▒
	PES	▒	□	□	□	□	□	▒	▒	■	□	□	□	■	■	□	□	□	□	□	□	■	□	□
	PET	■	□	□	□	□	□	■	□	■	□	▒	□	□	□	■	□	□	□	□	□	□	▒	▒
	PMMA	■	■	□	□	□	□	■	□	■	■	▒	▒	▒	□	□	■	□	□	□	▒	■	■	■
	POM	□	□	□	□	□	□	□	□	□	□	□	□	□	□	□	□	■	□	□	□	□	□	□
	PP	□	□	□	□	□	□	□	□	□	□	■	■	□	□	□	□	□	■	□	□	□	□	□
	PPS	□	□	□	□	□	□	□	□	□	□	□	□	□	□	□	□	□	□	■	□	□	□	□
	PS	▒	□	□	□	□	□	■	□	▒	□	▒	□	□	□	□	▒	□	□	□	■	▒	▒	▒
	PSU	▒	■	□	□	□	□	■	▒	▒	□	□	□	▒	■	□	■	□	□	□	▒	■	▒	■
	PVC	■	■	□	□	□	□	■	□	■	□	□	□	▒	□	▒	■	□	□	□	▒	▒	■	■
	SAN	■	■	□	□	□	□	■	□	■	□	□	□	▒	□	▒	■	□	□	□	▒	■	■	■

■ Strong weld ▒ Weak weld □ No weld

Figure 3.28 Result summary of laser-beam welding of similar and dissimilar thermoplastic resins from various R&D evaluations.

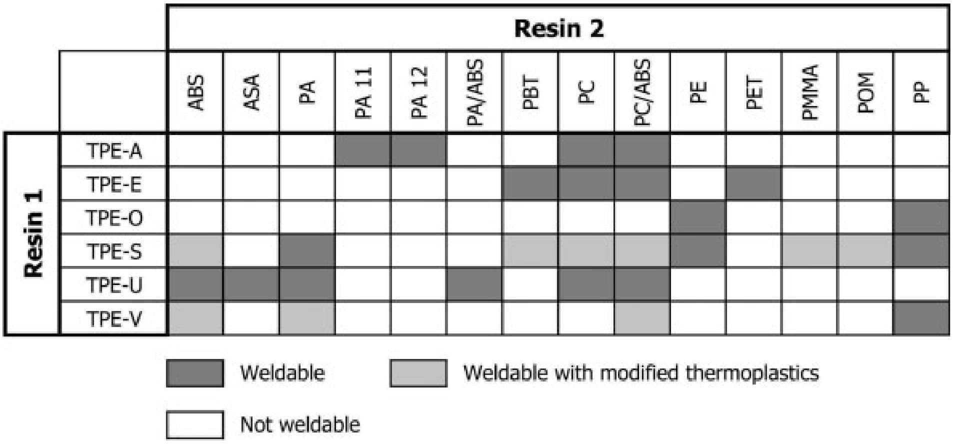

		Resin 2													
		ABS	ASA	PA	PA 11	PA 12	PA/ABS	PBT	PC	PC/ABS	PE	PET	PMMA	POM	PP
Resin 1	TPE-A				▓	▓			▓	▓					
	TPE-E							▓	▓	▓		▓			
	TPE-O										▓				▓
	TPE-S	░		▓				░	░	░	▓		░	░	▓
	TPE-U	▓	▓	▓			▓		▓	▓					
	TPE-V	░		░						░					▓

▓ Weldable ░ Weldable with modified thermoplastics

□ Not weldable

Figure 3.29 Welding of TPEs to thermoplastic resins.

In TPE block copolymers the thermoplastic and elastomer segments are linked within the macromolecules. Depending on the type of thermoplastic elements it can be distinguished for example, in TPE-A with polyamide elements, TPE-S with styrene elements or TPE-U with polyurethane elements.

Based on the type of thermoplastic component in the TPE, TPEs can be welded with various thermoplastic resins [44]. Figure 3.29 lists the types of TPEs and compatible partners for welding. Some of the partner polymers have to be modified to achieve optimized welding results.

References

1 Hesse, M., Meier, H., and Zeeh, B. (2005) *Sperktroskopische Methoden in der Organischen Chemie*, Georg Thieme Verlag, Stuttgart.
2 Marquardt, J. (2003) Nah-Infrarot-Spektroskopie für die schnelle Polymeranalytik und die zerstörungsfreie Evaluierung von Materialeigenschaften, Thesis, Albert-Ludwigs-Universität Freiburg i. Br.
3 Hummel, D. (1974) *Polymerspectroscopie*, Verlag Chemie, Weinheim.
4 Stuart, H.A. (1967) *Molekülstruktur*, Springer-Verlag, Berlin.
5 Glaser, S. and Ebenhög, M. (2008) Farbmittel und Additive zum Laserschweissen von Kunststoffe, in *Kunststoffe in ver Medizintechnik*, VDI-Verlag, Düsseldorf.
6 Masterbatch Association (2003) *Color and Additive Masterbatches in Practice*, VM Verlag, Köln-Eggenstein.
7 Kremer, J. and Hahn, W. (2001) *Einfärben von Kunststoffen*, Vogel Buchverlag, Würzburg.
8 Bastian, M. (2010) *Einfärben Von Kunststoffen*, C. Hanser Verlag, München.
9 Klein, R. (2007) Laserstrahlschweissen transparenter und farbiger Kunststoffe. *Laser Technik Journal*, 4/2007, Wiley-VCH Verlag, Weinheim, pp. 41–44.
10 Klein, R. and Wissemborski, R. (2010) Welding and marking of plastics with lasers. *Laser Technik Journal*, 5/2010, Wiley-VCH Verlag, Weinheim, pp. 19–22.
11 Engelke, F. (1985) *Aufbau der Moleküle*, B.G. Teubner Verlag, Stuttgart.

12 Brügel, W. (1961) *Physik und Technik der Ultrarotstrahlung*, C. R. Vincentz Verlag, Hannover.

13 Kreker, M. (1969) *The Scattering of Light*, Academic Press, New York.

14 Lützeler, R.R. (2006) Laser Transmission Welding of Semi-Crystalline Thermoplastics, Thesis, RWTH Aachen.

15 Hänsch, D. (2001) *Die Optischen Eigenschaften von Polymeren und ihre Bedeutung für das Durchstrahlschweissen mit Diodenlaser*, Shaker Verlag, Aachen.

16 Schulz, J. (2002) Werkstoff-, Prozess- und Bauteiluntersuchungen zum Laserdurchstrahlschweissen von Kunststoffen, Thesis, RWTH Aachen.

17 Klein, R. (1990) Bearbeitung von Polymerwerkstoffen mit Infraroter Laserstrahlung, Thesis, RWTH Aachen.

18 Potente, H. and Fiegler, G. (2004) Laser transmission welding of thermoplastics – modelling of flows and temperature profiles. Proceedings ANTEC 2004 conference.

19 Grewell, D. and Benatar, A. (2003) Modeling heat flow for a moving heat source to describe scan micro-laser welding. Proceedings ANTEC 2003 conference.

20 Kennish, Y.Ch. (2003) Development and Modelling of a New Laser Welding Process for Polymers, Thesis, University of Cambridge (UK).

21 Carslaw, H.S. and Jaeger, J.C. (1959) *Conduction of Heat in Solids*, 2nd edn, Clarendon Press, Oxford.

22 Hecht, E. and Zajac, A. (1974) *Optics*, Addison-Wesley Publishing, Massachusetts.

23 Aden, M. *et al.* (1988) Numerische und Analytische Lösungen Eindimensionaler Wärmeleitungsprobleme, internal report, Fraunhofer Institute for Lasertechnology, Aachen.

24 Frick, Th. (2007) *Untersuchung der Prozessbestimmenden Strahl-Stoff-Wechselwirkungen beim Laserstrahlschweissen von Kunststoffen*, Meisenbach Verlag, Bamberg.

25 Russek, U.A. (2006) *Prozesstechnische Aspekte des Laserdurchstrahlschweissens von Thermoplasten;*, Shaker Verlag, Aachen.

26 Grewell, D.A. (2005) Modeling of Molecular Healing for Micro-Laser Welding of Plastics With Diffractive Optical Elements as Spatial Modulators, Thesis, The Ohio State University.

27 Potente, H. (2004) BT Fügen von Kunststoffen, C. Hanser Verlag, München.

28 De Gennes, P.G. (1971) Reptation of a polymer chain in the presence of fixed obstacles. *J. Chem. Phys.*, **55** (2), 572.

29 Doi, M. and Edwards, S.F. (1986) *The Theory of Polymer Dynamics*, Clarendon Press, Oxford.

30 Wool, R.P., Yuan, B.L., and McGarel, O.J. (1989) Welding of Polymer Interfaces, *Polym. Eng. Sci.*, **29/1989/19**, 1341–1367.

31 Wool, R.P. (1995) *Polymer Interfaces; Structure and Strength*, C. Hanser Verlag, München.

32 Voyutskii, S.S. (1963) *Autohesion and Adhesion of High Polymers*, John Wiley and Sons.

33 Jabbari, E. and Peppas, N.A. (1994) Polymer-polymer interdiffusion and adhesion. *Macromol. Chem. Phys.*, **C34/2**, pp. 205–241.

34 Anderson, K.L., Wescott, J.T., Carver, T.J., and Windle, A.H. (2004) Mesoscale modelling of polymer welding. *Mater. Sci. Eng.*, **A365**, 14–24, Elsevier Publ.

35 Wise, R. (2008) *What Really Happens – Current Theories for Welding Plastics*, Internal report, TWI, Cambridge UK.

36 Bonten, C. (1998) Beitrag zur Erklärung des Wirkmechanismus in Schweissverbindungen aus Teilkristallinen Thermoplasten, Thesis, Universität GH Essen.

37 Scholten, F.L. and Oesterhold, D.J.A. (1996) Schweisseignung und Kerbunempfindlichkeit von Rohren aus vernetztem Poyethylen, Bericht GDT/MAT96319/Sch/052, Nl-Apeldorn – Gastec N.V.

38 Kryszewski, M. (1995) Über die Diffusion von Komponenten in den Grenzflächenschichten von Polymermischungen. *Plaste und Kautschuk*, **20** (10), p. 743.

39 Potente, H. and Gabler, K. (1980) Weldability of Dissimilar Thermoplastics -

Experiments in Heated Tool Welding, *J. Adhes.*, **11**, 145–163.

40 Sancactar, E. (1999) Polymer Adhesion by Ultrasonic Welding, *J. Adhes. Sci. Technol.*, **13/2**, 179–201.

41 Mattus, V. and Kuriykov, Y. (2007) Verfahrensoptimierte Werkstoffpaarungen zum Kunststoffschweissen mit Laserstrahlung – Polylas, Final Report Joint BMBF-Project 03N3116F, BASF.

42 N.N. (2008) Polymer Compatibility for Laser Welding, http://www.clearweld.com/education-center.aspx.

43 Krug, M. (2005) Workshop 3: Laser-Transmissionsschweissen von Kunststoffen. Proceedings of 3rd *Jenoptik Laser Forum* 2005.

44 Klein, R., McGrath, G., and Hopfner, M. (2006) Advanced laser welding of TPE using nir-absorbers. Proceedings of TPE-conference, Munich.

4
Process of Laser Plastic Welding

4.1
Basic Process Principles

Laser welding of thermoplastics is a thermal fusion process induced by absorption of laser light and generation of process heat as discussed in Chapter 4. By history, the process of laser welding plastics is separated into butt-joint welding and through-transmission laser welding (TTLW).

Today, TTLW is the common process for industrial application of laser welding plastic components [1, 2]. But with new laser sources, working with wavelengths above 1200 nm, butt-joint welding has also some potential for new applications [3]. Both types of processes will be discussed in the following.

4.1.1
Butt-Joint Welding

The principle of butt-joint welding is joining parallel surfaces of two component parts together as shown in Figure 4.1. The focused laser beam hits the surface of the two components parallel to the joint interface. Depending on the wavelength of the laser radiation and the optical material properties absorption can be separated into surface and volume absorption [4].

Surface absorption (Figure 4.1, left) in thermoplastic resins will exist for example, for use of CO_2-laser radiation or for NIR lasers in combination with high-absorbing additives in the resin, like high carbon black concentration. The laser energy will be transferred into process heat at the surface and will be dissipated into the resin by heat conduction to melt the resin for joining. Because of the low heat conductivity of thermoplastic resins, this process is in general only suitable for thin thermoplastic components like plastic films.

Volume absorption (Figure 4.1, right) occurs when the optical penetration depth of the laser radiation is in the range of the material thickness. Commonly, natural thermoplastic resins are more or less transparent for NIR-laser radiation. By the use

Laser Welding of Plastics, First Edition. Rolf Klein.
© 2011 Wiley-VCH Verlag GmbH & Co. KGaA. Published 2011 by Wiley-VCH Verlag GmbH & Co. KGaA.

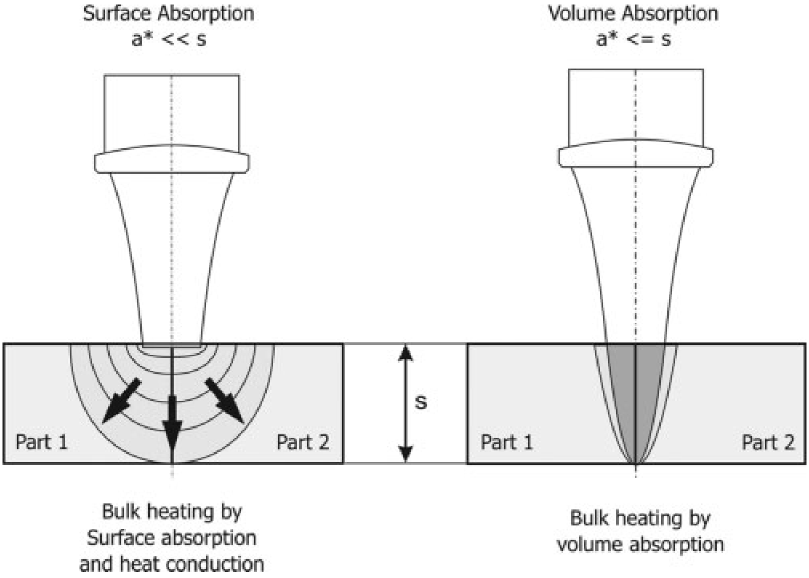

Figure 4.1 Principle of butt-joint welding with laser.

of absorbing additives in suitable concentrations or by special laser wavelengths above 1200 nm the penetration depth of the laser radiation can be well adjusted to the optical material properties and thickness of the work piece to generate the joint through the entire material thickness by simultaneously applying an appropriate clamping pressure.

Figure 4.2 shows examples of butt welding with surface and volume absorption. The left side of Figure 4.2 is a cross section of a HDPE sample welded with a CO_2 laser ($\lambda = 10.6$ μm) showing melting of the resin by surface absorption and heat conduc-

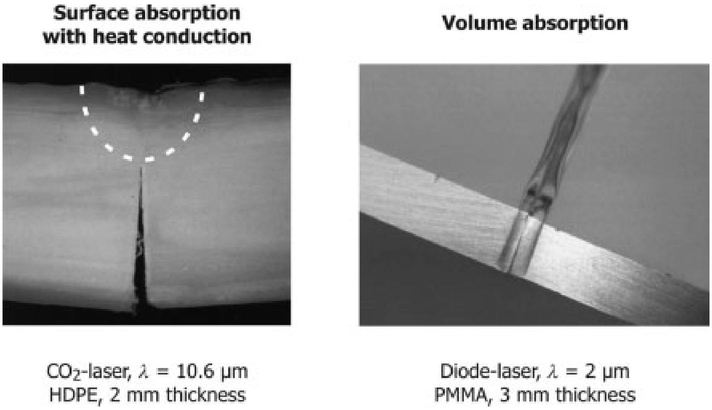

Figure 4.2 Examples for butt-joint welding with laser.

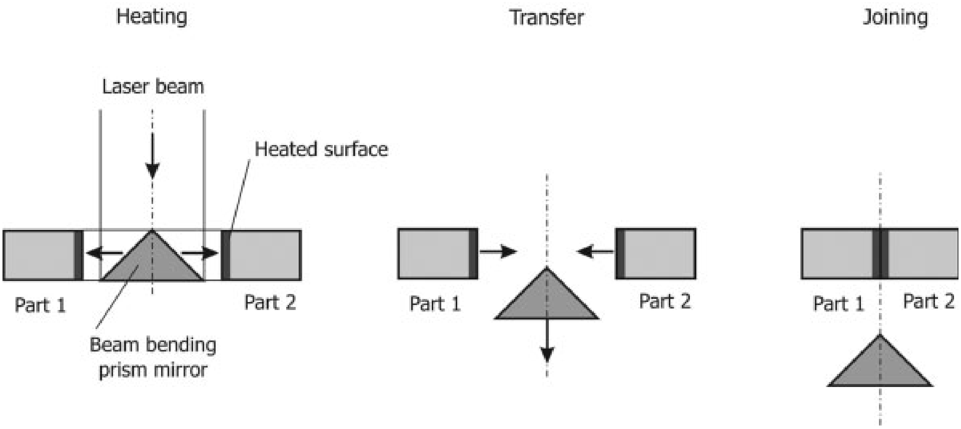

Figure 4.3 Laser butt welding in analogy to hot-plate welding.

tion. The right side gives an example for laser welding transparent PMMA (thickness 3 mm) using a diode laser of 2 μm wavelength [5].

An early approach for butt-joint welding of thermoplastic components was using CO_2-laser radiation by analogy with hot-plate welding (see Figure 4.3) [6]. The interface surfaces of both components are heated by the laser radiation using a beamsplitter like a prism mirror reflecting the irradiated laser radiation to the component surfaces. After melting the surfaces the beamsplitter is moved out and the molten surfaces were pressed together to generate the weld joint during resolidification.

This process never really got through to intense industrial application because of high investment costs for CO_2 lasers and beam-delivery devices compared to conventional welding processes at that time.

Today, butt-joint welding is a niche process not commonly used in industrial application of laser welding thermoplastic components. But imagine the adaption of laser-beam absorption by suitable additives in the resin with economic concentrations or using new laser sources with wavelengths adapted to the absorption properties of the thermoplastic resin, butt-joint welding could possibly become an interesting alternative for welding thermoplastic components.

To realize this by absorbing additives like organic dyes or inorganic pigments in the resin, the concentration of the absorbing additives has to be matched to the thickness of the components to be welded and to the laser wavelength used. On the other hand, new laser sources like diode lasers or fiber lasers with wavelengths above 1200 nm can be applied having well-adapted absorption properties for the thermoplastic resin used.

4.1.2
Through-Transmission Welding

Today, laser welding of thermoplastic components is well established in industrial application by using the process of through-transmission laser welding (TTLW).

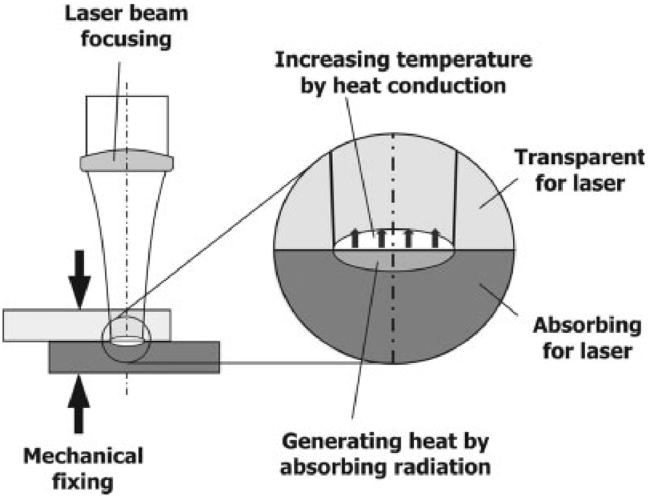
Laser beam focusing
Increasing temperature by heat conduction
Transparent for laser
Absorbing for laser
Mechanical fixing
Generating heat by absorbing radiation

Figure 4.4 Through-transmission laser-welding process.

The basic principle of this process is using a laser-transparent component and a laser-absorbing resin to form the joint (see Figure 4.4).

The laser beam hits the surface of the laser-transparent component and is transmitted through the component to the laser-absorbing part. The absorbing part converts the laser energy into process heat to melt the resin. Absorption of the laser radiation and conversion into heat will be done within a resin interface thickness correlated with the optical penetration depth of the laser radiation in the absorbing resin. By immediate contact of the absorbing part to the laser transparent, the contact interface of the transparent part will be heated and melted by heat conduction. Simultaneously applying a mechanical fixing pressure during melting and resolidification will generate a mechanically stable joint between both components.

Usually, thermoplastic resins are transparent to NIR-laser radiation. To adapt thermoplastics for laser absorption in the NIR spectral range of commonly used laser sources with wavelengths between 800 nm and 1000 nm like diode, Nd:YAG or fiber lasers, absorbing additives have to be mixed into the resin.

A typical additive used is carbon black, which has a high absorption over the entire wavelength spectrum. However, with carbon black, plastics are restricted to dark colors and transparent plastic components are not possible. To enable flexible color matching of the resin also with light colors or working with visually transparent resins special laser-absorbing additives like organic dyes or inorganic pigments have to be mixed into the absorbing resin (see Section 2.4.7).

A special type of TTLW is using laser-absorbing coatings [7, 8], enabling laser welding of visually transparent components (see Figure 4.5). The coating consists of a solvent like acetone or ethanol with dissolved organic dyes or well-dispersed inorganic pigments. The coating will be applied to one or both surfaces at the interface of the components to be welded. After evaporation of the solvent a thin layer of the absorbing agent will remain on the surface.

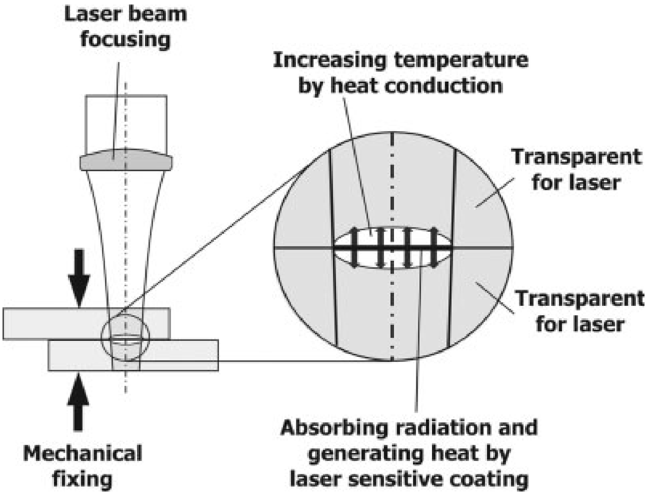
Laser beam focusing
Increasing temperature by heat conduction
Transparent for laser
Transparent for laser
Mechanical fixing
Absorbing radiation and generating heat by laser sensitive coating

Figure 4.5 Through-transmission laser welding using absorbing surface coatings.

After clamping of the components the welding will be done by absorption of the laser radiation by the coating layer. The coating layer will transform the laser energy into process heat and will pass on the process heat to the component interfaces by heat conduction to form the weld. A more detailed description of this process will be given in Section 5.3.1.

4.2
Process Types

As mentioned before, TTLW is the mostly applied process for industrial application of laser welding plastic components. This process is basically used in three modifications as contour welding, quasisimultaneous welding and simultaneous welding. Based on these basic modifications several subtypes as process combinations can be found under development and in industrial application.

The three basic process modifications as well as several process combinations will be discussed in the following.

4.2.1
Contour Welding

To generate a laser welded joint on a work piece by contour welding a single focused laser beam is moved along the joint path on the work piece (Figure 4.6). During processing the laser beam locally hits the joint interface, heats up the resin layers and generates the weld joint. During processing a constant clamping pressure is applied to the work piece to support the weld process.

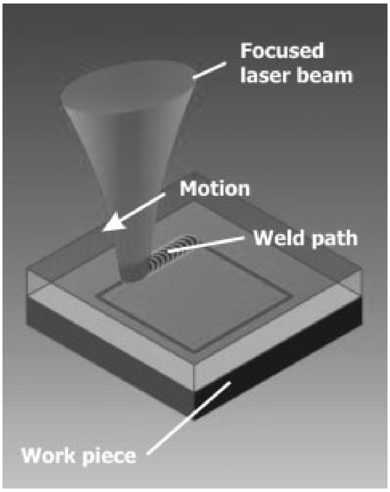

Figure 4.6 Principle of contour laser welding [9].

The main processing parameters for laser contour welding are:

- laser power;
- welding speed;
- laser beam focusing (focusing length, focus position);
- clamping pressure.

The ratio of laser power to welding speed results in the term of needed laser line energy (Equation 4.1), which is an often used number to describe a laser-welding process as a normalized quantity. In certain limits, laser welding results in the same line energy but different quantities of laser power and welding speed should result in comparable weld qualities.

$$E_s = \frac{P}{v} \tag{4.1}$$

E_s: line energy [W s/m]
P: laser power [W]
v: welding speed [m/s]

The laser welding quality, for example, achievable weld strength, is directly correlated with the applied laser line energy. Low laser line energy results in weld joints with low weld strength, even the optical quality of the joint can be good. On the other hand, high laser line energy also results in poor weld strength, in this case caused by joint failures like partly decomposition of the resin. Between both limits a process window exists with good correlation between applied laser line energy and achieved weld strength. The width of the process window is dependent on the thermal and mechanical properties of the resin and the laser process parameters like laser power and welding speed.

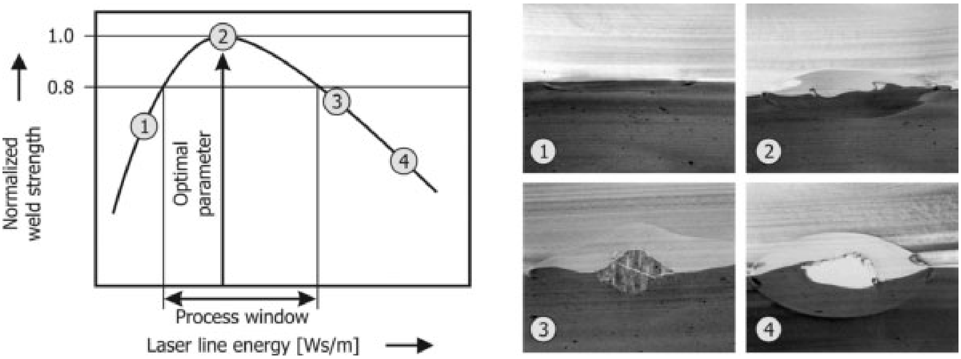

Figure 4.7 Correlation of achievable weld quality and applied line energy, sample 1 is of low weld strength, sample 2 of optimal quality and samples 3 and 4 overheated having low weld strengths [10].

In Figure 4.7 a schematic diagram of the weld strength correlation with the laser line energy is given with corresponding microcuts of welding results [10].

- Sample 1 welded with low line energy is only a sticking joint with low strength but good optical quality.
- Sample 2 is welded with optimal parameters and is of good quality and high strength.
- Sample 3 and 4 are welded with too high line energy, sample 3 is overheated with pores in the joint and sample 4 has thermal degradation in the joint with insufficient weld strength.

Laser beam focusing depends on the quality of the laser beam. Using the same focusing optics for different laser-beam qualities result in different focal spot sizes and depth of field (Rayleigh length) of the focused beam. The better the beam quality, the smaller is the spot size and the larger the depth of field. To acquire a laser spot size adapted to the needed weld width the focusing length of the optics has to be matched to the joint geometry.

An appropriate clamping pressure has to be applied to the work piece during laser welding to fix the work piece in a well-defined position and to build up the internal pressure to support the generation of a tight weld joint.

Relative movement between the laser beam and work piece can be done by using several different robotic methods like moving the work piece under the fixed laser beam, moving the laser beam along the fixed work piece or a combination of both. A common method for moving the focused laser beam along a fixed work piece is using a scanning optic device.

For contour laser welding the interfaces of the components to be joined have to have intimate contact. A lack of contact between the interfaces will interrupt the heat transfer from the laser-absorbing to the laser-transparent part and will result in low weld strength or failures in the weld joint. Also, the start/stop sequence of welding has to be adjusted properly, for example, by ramping the laser power to avoid a lack of laser power or overheating at the start/stop point of the weld path.

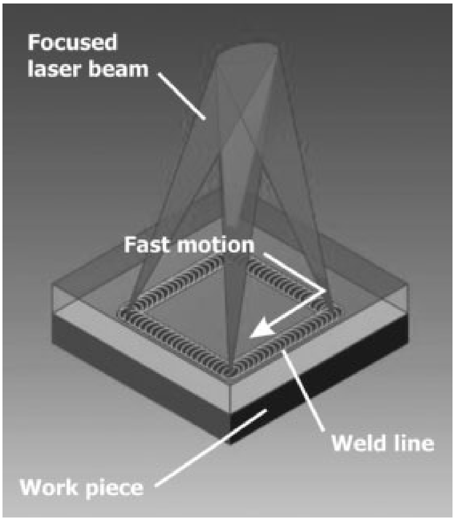

Figure 4.8 Principle of quasisimultaneous laser welding [9].

4.2.2
Quasisimultaneous Welding

Like contour laser welding, quasisimultaneous laser welding is based on a single focused laser beam. The difference from contour laser welding is that the laser beam is moved several times along the joint geometry at high speed (Figure 4.8).

Each time the laser beam hits the same point of the joint path, the temperature of the joint interface will increase. After certain repetitions the melt temperature of the resin will be reached. Figure 4.9 demonstrates schematically the temperature increase at a single point of the joint path by laser welding using one repetition (contour welding), 5 and 20 repetitions as conventional quasisimultaneous welding and 40 repetitions as high-speed quasisimultaneous welding with a temperature increase comparable to real simultaneous welding [11].

Processing speed and number of repetitions has to be matched to the thermal properties of the resin. By quasisimultaneous welding the entire joint path will be molten at the same time. This avoids problems with a start/stop sequence as for contour laser welding.

External clamping pressure can be used for generating a controlled squeeze flow to form the welding joint (Figure 4.10). In contrast to contour laser welding the squeeze flow enables a set path for the filling of gaps between the component interfaces to be welded, resulting in high-quality weld joints.

The main processing parameters for laser quasisimultaneous welding are:

- laser power;
- welding time, given by processing speed and number of repetitions;
- laser beam focusing (focusing length, focus position);
- clamping pressure.

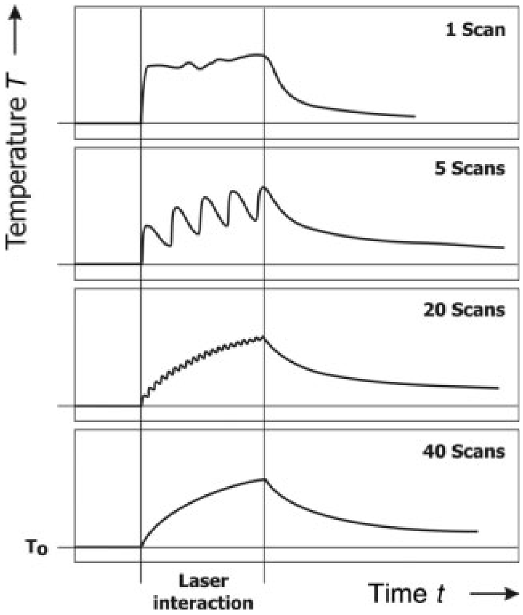

Figure 4.9 Heating process by quasisimultaneous laser welding [11].

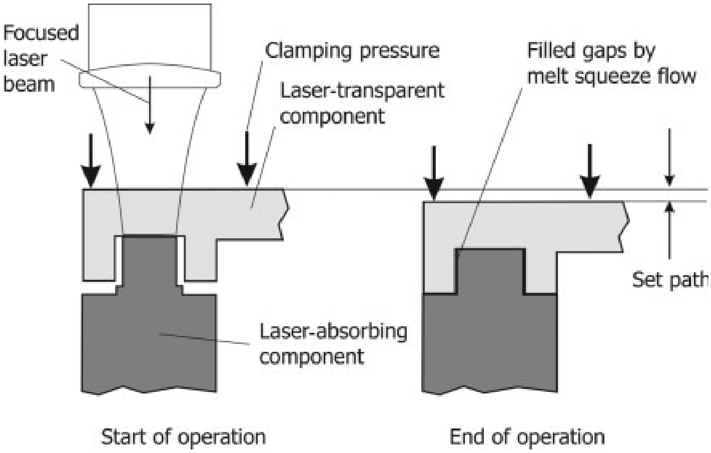
Focused laser beam
Clamping pressure
Laser-transparent component
Filled gaps by melt squeeze flow
Set path
Laser-absorbing component
Start of operation
End of operation

Figure 4.10 Squeeze flow of the melt during quasisimultaneously laser welding.

Analogous to contour welding, laser power, welding time and joint path length will give a quantity for the required laser line energy:

$$E_s = \frac{Pt}{l} \tag{4.2}$$

E_s: line energy [W s/m]
P: laser power [W]

t: interaction time [s]
v: meld length [m]

To enable high processing speeds commonly scanning optic devices are used (see Section 3.3.2), built by two galvanic-driven mirrors and a focusing lens system. Computer-controlled driving of the mirrors allows a flexible programming of the weld path. Using special scanner devices with adapted controller ultra high scanning speeds can be achieved with process features like simultaneous laser welding.

4.2.3
Simultaneous Welding

Real simultaneous laser welding uses a technique different from contour and quasisimultaneous laser welding. The entire joint path is irradiated by laser radiation at the same time and will generate the laser-welded joint without moving part or laser beam during processing. As for quasisimultaneous laser welding part tolerances and fit-up are not as critical as for contour laser welding because melt down with a set path is possible. In addition, there are no problems with start/stop sequences as possibly for contour laser welding.

The process of simultaneous laser welding can be realized by two different techniques using a couple of laser sources or one laser source with beam-shaping optics.

Simultaneous laser welding with a couple of laser sources is shown schematically in Figure 4.11. In this case four laser sources with rectangular beam shape are used to form the weld geometry.

In the case of laser welding more complex geometries it is possible to use flexible arrays of diode lasers, as shown in Figure 4.12 [12]. A number of diode-laser sources are mounted on a flexible backbone. The backbone keeps a relative constant

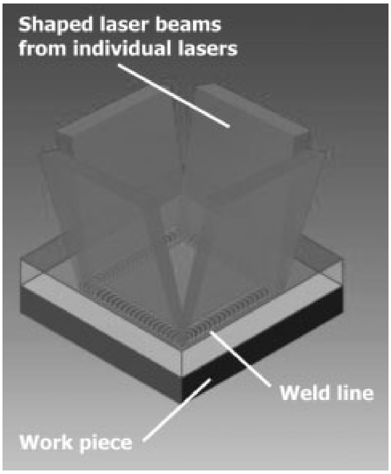

Figure 4.11 Principle of simultaneous laser welding with four direct emitting laser sources [9].

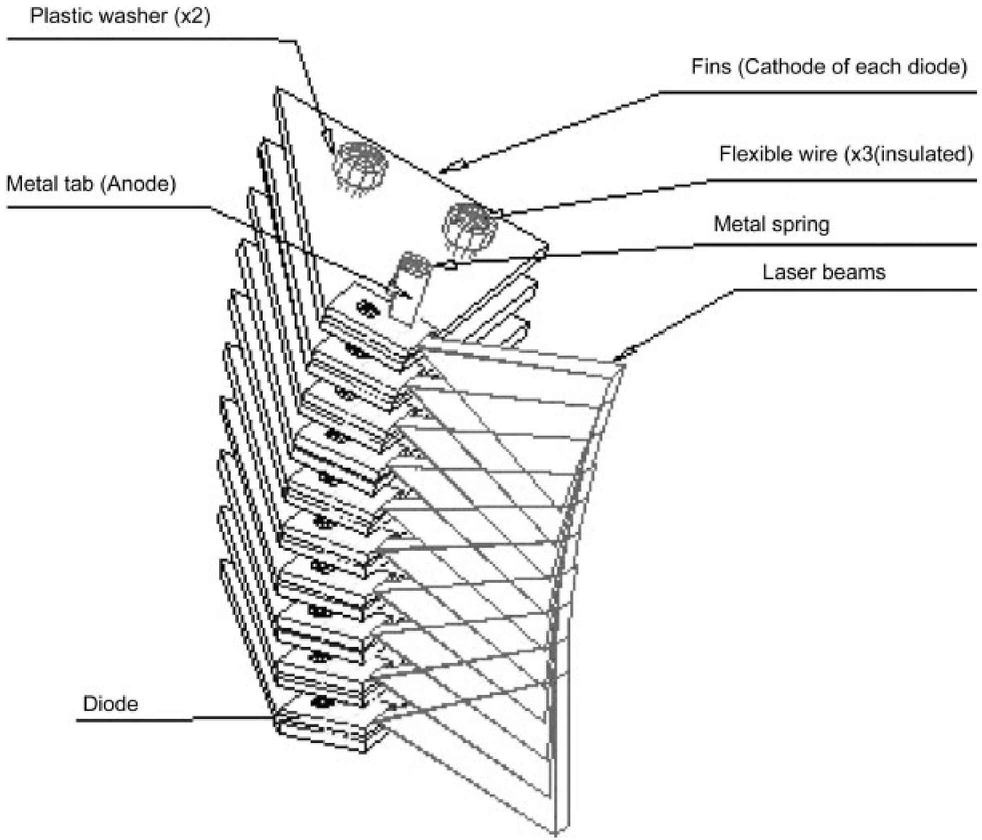

Figure 4.12 Schematically setup of a number of diode lasers to form a weld line [12].

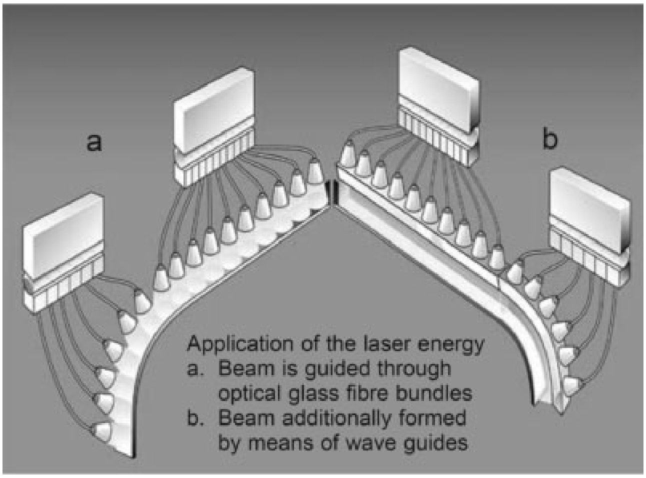
a
b
Application of the laser energy
a. Beam is guided through
optical glass fibre bundles
b. Beam additionally formed
by means of wave guides

Figure 4.13 Principle of simultaneous laser welding with fiber-coupled diode-laser sources [13].

distance between the individual diodes and allows electrical connections. The spatial geometry of this backbone is then matched to the spatial relationship of the weld geometry.

Alternatively, a number of fiber-coupled diode lasers can be used instead of direct emitting diode-laser sources. Examples of this technique are schematically given in Figure 4.13 [13]. Configuration "a" on the left side of Figure 4.13 uses laser bars with single emitters, each coupled to a glass-fiber guide. The glass fibers transmit the laser radiation to focusing elements at the end of the glass fibers. The sum of the focusing elements will form the welding line by overlapping of the single focal spots to process the work piece.

Critical issues of configuration "a" are the repeatable laser power and beam quality of each emitter as well as the positioning of the focusing elements to each other to form a homogeneous laser energy distribution for the welding process.

Configuration "b", right side of Figure 4.13, uses additional optical elements with functionality as a wave guide to homogenize the laser energy distribution. The laser radiation of each emitter will be transmitted by glass fibers to the focusing elements. The focusing elements couple the laser radiation into the wave guides and by multiple internal reflection the single laser beams are matched together to form a homogeneous laser energy distribution for processing the work piece. The disadvantage of this configuration is the laser power loss by reflection during incoupling of the laser radiation into the wave guides.

Simultaneous laser welding with one laser source in combination with specially designed beam-shaping optics is an alternative to using a couple of laser sources [14, 15]. Figure 4.14 shows as an example a circular beam-shaping optics for generating two concentric laser beam circles for laser welding. A single laser beam delivered by a glass fiber will be transformed to two beam circles by specially designed diffractive optical elements of the optic device.

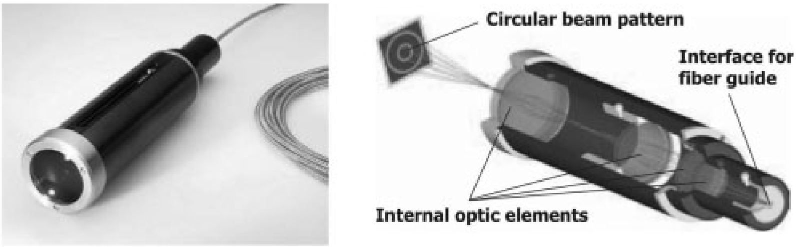

Circular beam shaping optics **Schematical optic setup**

Figure 4.14 Generating two circular beam shapes by beam-shaping optic device for simultaneously laser welding [14].

A special technique to generate a dedicated beam pattern for laser welding is described by Grewell [16]. This method uses holographic masks as diffractive elements to transform a uniform collimated laser beam to a desired beam pattern like a circle, as shown in Figure 4.15.

Aside from diffractive optical elements reflecting optical elements can also be used to transform a uniform collimated laser beam to geometries like circles for simultaneous laser welding. Figure 4.16 shows a laboratory setup of such a mirror optic device for laser welding at the circumference of a cylindrical component.

The laser beam, coming from a fiber guide, is collimated to a uniform circular beam shape and will be transformed into a ring and rectangle reflected by a cone mirror. The fist ring mirror reflects the ring-shaped beam parallel to the optical axis of the system, while the second ring mirror reflects the ring beam on to the part to be welded, which is centered on the optical axis of the system by a fixing tool.

The use of such a beam-shaping optic has the advantages that only a single laser source is needed and the part is stationary fixed without moving by a CNC rotational device. In combination with an automatic part-feeding system short cycle times are achievable without the need for start/stop cycle steps for a rotation movement of the parts.

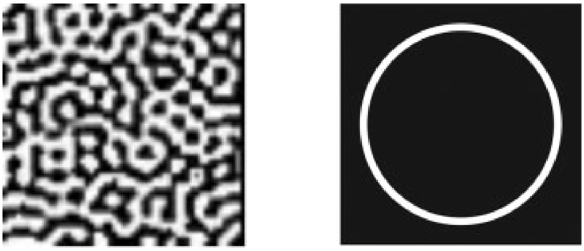

Holographic mask as diffractive element **Resulting circular beam pattern**

Figure 4.15 Holographic mask as a diffractive element to generate a circle for laser welding [16].

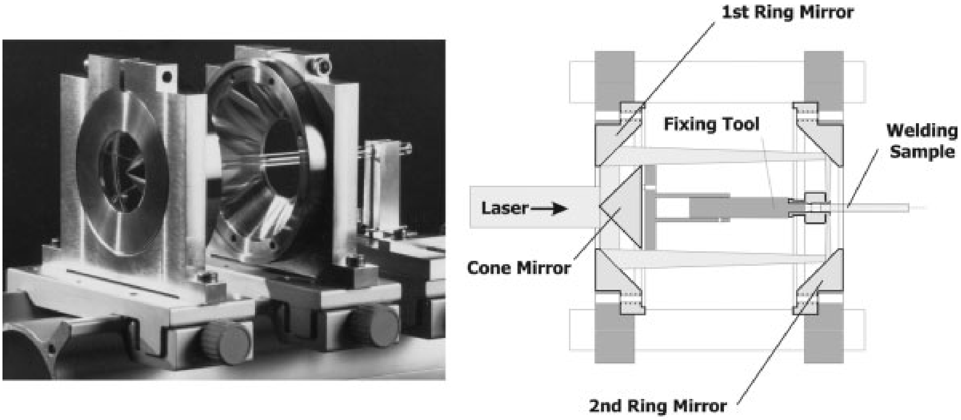

Laboratory setup

Schematical drawing

Figure 4.16 Mirror setup for simultaneous laser welding of cylindrical components.

In principle, the process of simultaneously laser welding is not as flexible as contour or quasisimultaneously laser welding for application with varying weld path geometries. The process is more suited to high mass production with work pieces of the same welding contour. But in current industrial applications for laser welding thermoplastic components simultaneous laser welding has a marginal presence compared to contour or quasisimultaneous laser welding because of flexibility and economic reasons.

4.2.4
Special Processes

4.2.4.1 Mask Laser Welding

Especially for laser welding of complex contours with small dimension mask laser welding is used. The desired joint contour will be generated by a metallic mask at which the contour is cut out for example, by laser or chemically etched. The mask is positioned above the work piece. To weld the work piece the mask is illuminated by line-shaped laser radiation that will be moved along the mask (Figure 4.17).

Generating the laser line can be done by several techniques, for example, using a diode laser with a rectangular beam shape and appropriate focusing optics to achieve the needed laser intensity for welding or using a fiber-coupled laser with specially designed optics to transform the circular laser beam to the laser line. In both cases the welding processes are a combination of simultaneous and contour laser welding because the laser line is moved one time across the mask and the work piece.

An alternative is using a single focused beam in combination with a scanner device. The scanner will produce the laser line by fast scanning in one axis and will move the laser line in the perpendicular direction at relatively slow speed. In this case mask welding is a combination of quasisimultaneous and contour laser welding.

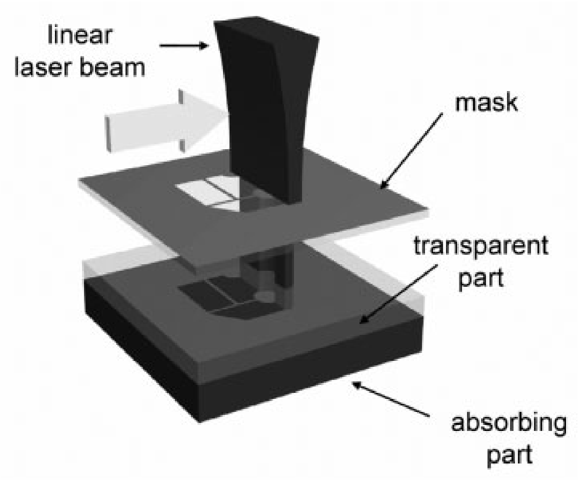

Figure 4.17 Principle of mask laser welding [17].

The advantage of this process is the possibility to match the line width to the mask contour to avoid overheating of the mask.

Flexibility of mask laser welding for different joint contours is given by easy exchange of the masks.

Using mask laser welding joint widths of the order of 100 μm with tolerances down to 5 μm [18] can be achieved. Because of the small melt volume gap bridging is restricted and the components to be welded need to have immediate interface contact.

4.2.4.2 **TWIST Laser Welding**

Focusing of high beam quality laser radiation, like from fiber lasers, will generate high intensities in the focal spot resulting in easy degradation of thermoplastic materials. To avoid degradation during laser welding thermoplastics the TWIST process can be used.

TWIST is an acronym for transmission welding by an incremental scanning technique [19]. The TWIST process is generated by a superposition of a fast rotating and slow linear motion of a focused high-quality laser beam (Figure 4.18 left). In addition to simple fast rotation of the focused laser beam other geometries like zigzag or Bernoulli's Lemniskate geometries can be used (Figure 4.18 middle and right). Hence, TWIST laser welding is a combination of contour and quasisimultaneous laser welding [20].

The fast motion of the focused laser beam with speed up to 4 m/s will be generated by high-speed scanner technique. Fast motion will homogenize and reduce the energy input to the plastic resin, e.g. by adjustment of the circle radius, circle overlapping and rotation frequency in combination with the linear motion weld width and depth can be adapted to the demands of the weld process for the work piece.

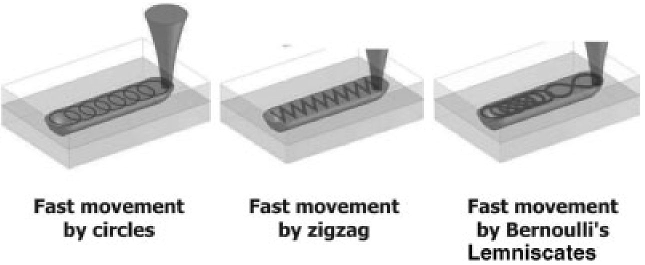

Fast movement by circles

Fast movement by zigzag

Fast movement by Bernoulli's Lemniscates

Figure 4.18 Principle of TWIST laser welding [20].

With TWIST laser welding small weld width down to 130 μm with reduced heat input can be realized, suitable for laser welding of geometries like microchannels in lab-on-a-chip devices with channel widths of 50 μm. By using fiber lasers with wavelengths above 1200 nm it is also possible to weld transparent thermoplastics without the need for additional absorbing additives as for conventional laser-welding processes (Figure 4.19) [21].

4.2.4.3 **Globo Laser Welding**

Globo laser welding is a contour laser-welding process with integrated work-piece clamping system by a glass ball [22]. Focusing optics for the laser radiation and glass ball are assembled together in a processing head. Focusing of the laser radiation to the work piece will be done through the glass ball, as shown schematically in Figure 4.20 [23].

The glass ball is mounted to the processing head by a pressurized-air bearing, enabling the glass ball for rotation during the processing head to be moved along the work piece. While moving the processing head along the joint contour, the processing

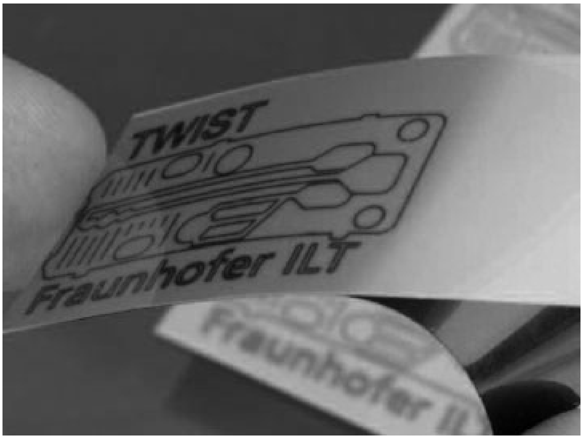

Figure 4.19 Laser welding of transparent plastic components using TWIST laser welding in combination with laser wavelengths adapted to the optical properties of the resin [21].

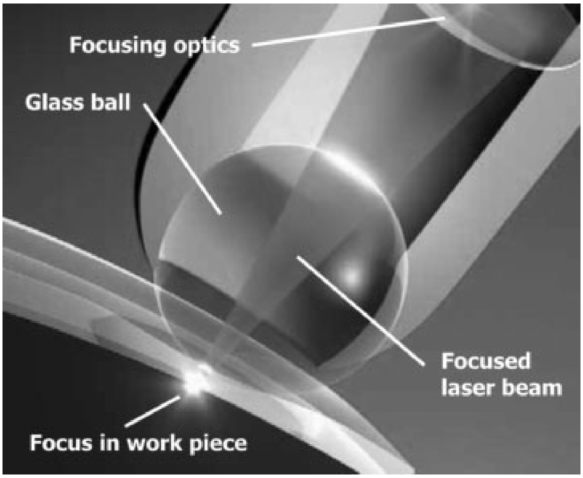

Figure 4.20 Principle of Globo laser welding [23].

head will be pneumatically pressed onto the work piece to generate the desired external welding pressure locally at the process area by the glass ball.

The focal position in the work piece and weld width can be adapted to the needs by adjustment of the focusing optics relative to the glass ball position.

By mounting the Globo head to a robotic system three-dimensional work piece contours can be welded as shown in Figure 4.21 with the example of laser welding

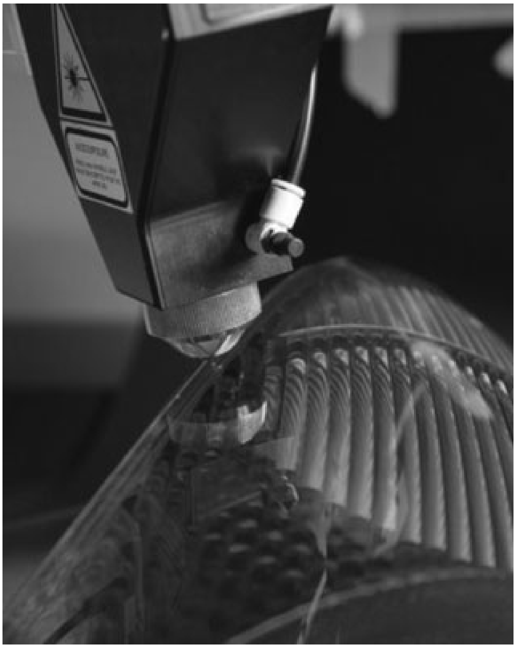

Figure 4.21 Globo laser welding of automotive lamp housings [23].

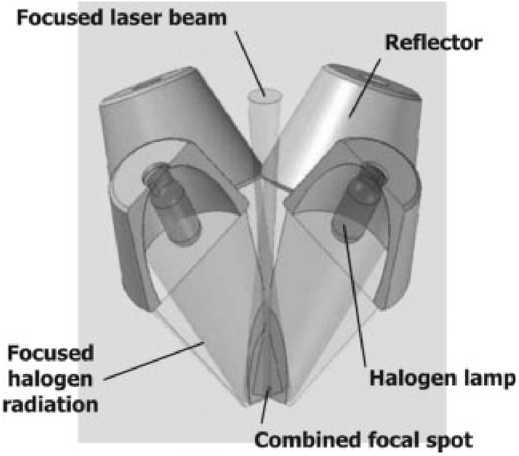

Figure 4.22 Principle of IR-hybrid laser welding [24].

automotive lamps. But also flexible work pieces like plastic fabrics can be welded using the Globo head [23].

4.2.4.4 **IR-Hybrid Laser Welding**

This laser-welding process combines conventional contour laser welding with simultaneous application of NIR radiation for additional heating of the work piece. The laser radiation is focused onto the work piece. Around the focus position NIR radiation from several halogen lamps is also focused onto the work piece, as shown schematically in Figure 4.22 [24].

The spectral wavelength distribution of NIR-radiation coming from halogen lamps starts at approximately 800 nm up to 1600 nm with noticeable radiation intensity (Figure 4.23) [25]. The radiation of the halogen lambs will be absorbed at the lower laser-absorbing component as well as partially within the laser-transparent component.

The focal spot of the NIR lamps is larger than the laser beam focus. Hence, the irradiation has three basic functions:

- preheating the work piece before laser welding;
- slowing down the cooling rate to avoid thermal stress by fast cool down;
- optimize the diffusion process of the molten interfaces during processing.

The result of simultaneous application of the NIR lamp and laser radiation is an increase of processing speed, enhanced joint gap bridging and higher strength of the laser-welded joints. Absorbing the NIR radiation in the laser-transparent component will gain a locally lower stiffness of the resin, enabling application of a direct clamping force by a clamping tool integrated into the hybrid processing head as shown in Figure 4.24. Such processing heads are for example, in industrial applications for laser welding automotive light housings [24].

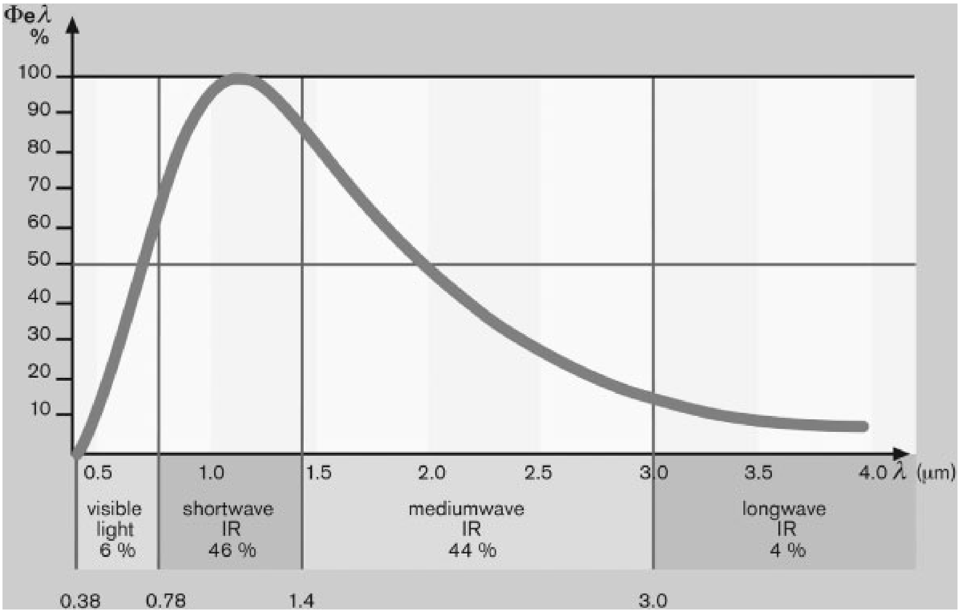

Figure 4.23 Spectral distribution of halogen lamps (2450 K color temperature) [25].

4.2.4.5 **Ultrasonic Hybrid Laser Welding**

Combination of ultrasonic and laser power as a processing method for joining thermoplastics aims to decrease mechanical stress to the components as well as increase the joint strength compared to conventional ultrasonic welding.

During application of ultrasonic power a laser beam will simultaneously heat up the joint interfaces. By softening the joint interfaces with the laser radiation

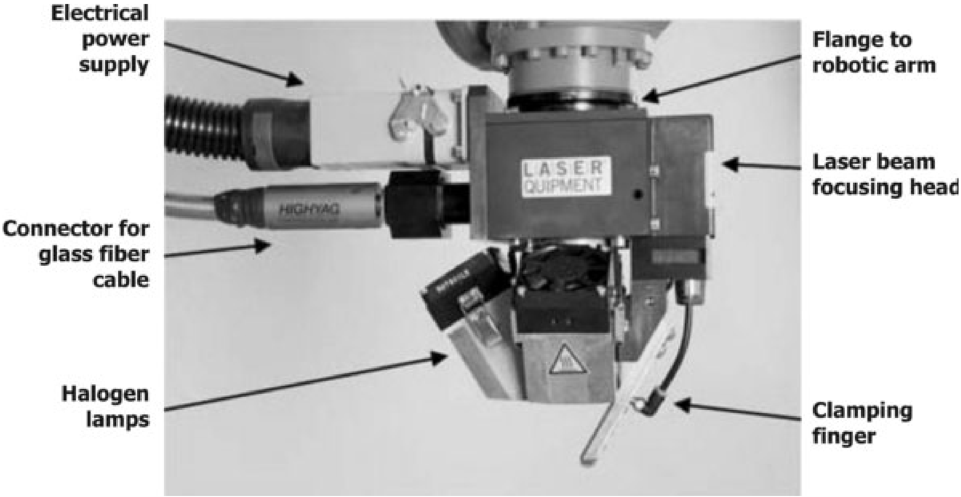

Figure 4.24 IR hybrid laser welding head [24].

the ultrasonic process needs lower amplitude and electrical power than conventional ultrasonic-wave application [26, 27]. The result is reduced mechanical vibration stress to the work piece and components in the work piece like electronics or micromechanics.

Ultrasonic hybrid laser welding can also be used for joining mechanically fragile materials like thermoplastic fabrics. Conventional ultrasonic welding of fabrics will disturb the filament structure of the fabrics in the joint area by the applied mechanical pressure. Softening and pressurizing the filaments results in a change of the filament geometry and in the worst case the filament will melt together causing undesired higher stiffness of the fabric at the weld joint.

Using ultrasonic hybrid laser welding can reduce the mechanical stress on the filaments of the fabric. A specially designed laser sewing system allows simultaneous welding of fabrics with a combination of ultrasonic and laser process, as shown in Figure 4.25 [28]. The ultrasonic power will be applied to the fabric by the roller feeding system for transport of the fabric, while the laser radiation will be irradiated onto the fabric as through transmission process just before the roller feeding by an integrated focusing optics.

4.2.4.6 **Laser-Assisted Tape Laying and Winding**

Tape laying or winding is used as a production method for composite parts with special mechanical features. Commonly, thermoset resins in a state of incomplete polymerization with longitudinal fiber reinforcement, built by carbon, aramid or glass fibers, as preimpregnated tapes or sheets (called prepreg) are laid down to form a component where the directions of the fibers are in the direction of the effective forces in the component [29]. After build up of the component, the resin has to be solidified by a thermal-treatment-induced polymerization using an autoclave.

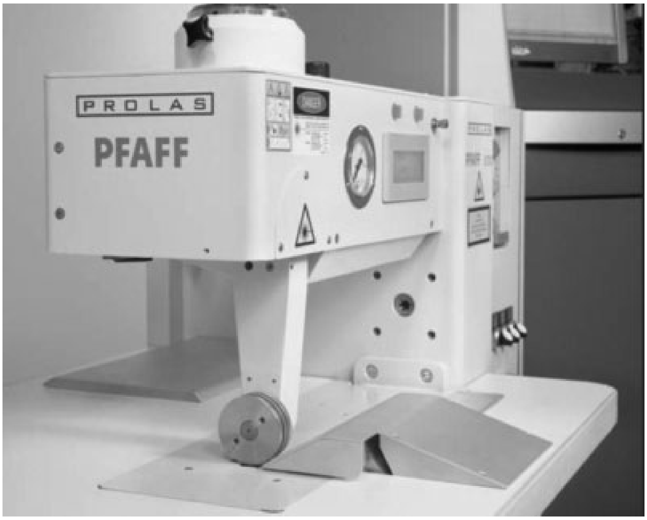

Figure 4.25 Laser sewing system for ultrasonic and laser welding thermoplastic fabrics [28].

This thermal treatment and the circumstance that the preimpregnated materials have a limited shelf life before processing makes the process complicated and time consuming. Nevertheless, thermoset filament winding technology can be considered well developed with many facilities producing parts commercially.

An alternative method is the use of thermoplastic resin for example, like PEEK, PPS or PSU as matrix to build the preimpregnated tapes or sheets. The matrix of such thermoplastic prepregs is already polymerized and shelf life is no problem. Thermoplastic composite materials furthermore offer the advantage of high impact toughness, higher manufacturing productivity, increased quality and improved material properties as well as recyclability. In addition to favorable mechanical properties, thermoplastics offer a wide range of manufacturing options.

During manufacturing of the component, the thermoplastic resin is melted locally by a heat source like IR radiation, hot air or metallic heat devices and consolidated by external pressure without the need for an additional autoclave process. Also, IR lasers like CO_2 laser [30, 31] or NIR lasers like Nd:YAG lasers [32] are capable of being used as a heat source to drive the process.

Figure 4.26 shows exemplarily the laser-assisted processes of tape laying and winding [32, 33]. The focused laser radiation is irradiated into the contact interface in-between the laid-down tape and the already consolidated tape body. Adapting to the process the laser radiation is shaped and focused to a rectangular line geometry with a beam width corresponding to the tape width. The laser radiation heats up the thermoplastic matrix of both layers and the molten matrix will form a weld joint by applying an external pressure force.

An example of laser-assisted tape winding is given in Figure 4.27 for laser welding of glass-fiber-reinforced PET using Nd:YAG-laser radiation to generate a spiral-bounded body.

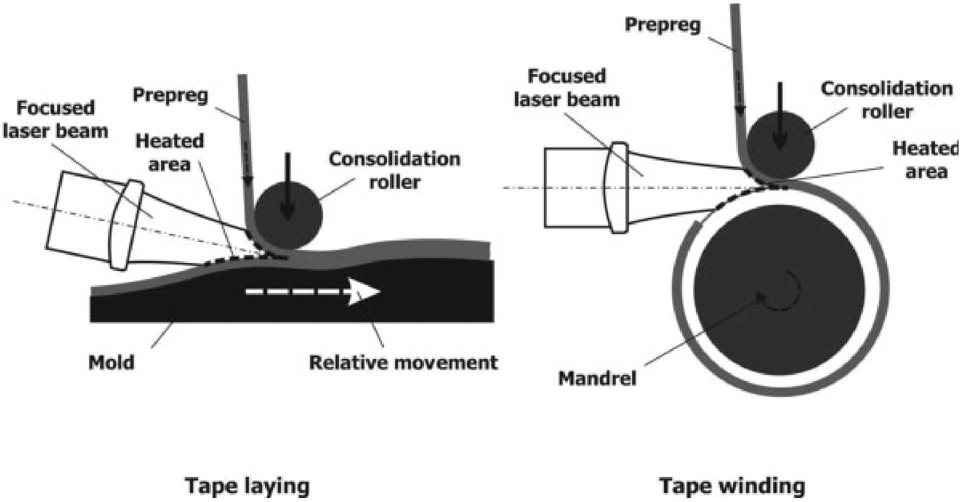

Figure 4.26 Principle of laser-assisted tape laying (left) and winding (right) [32, 33].

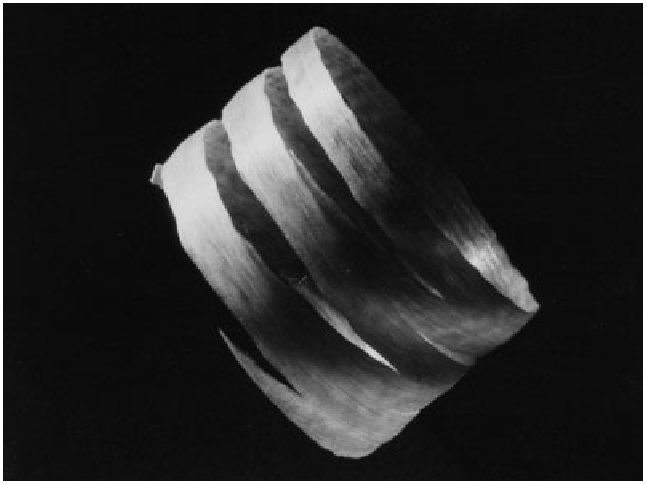

Figure 4.27 Spiral-bound tube of glass-fiber-reinforced PA6 generated by laser-assisted tape winding using Nd:YAG-laser radiation for consolidation [32].

Today, industrial production of tape winding or laying uses diode laser radiation as a heat source for production of components for example, for aircraft construction built by carbon-fiber-reinforced PEEK prepregs. Figure 4.28 shows as an example a robotic system for laser-assisted tape laying with a complex processing head including a diode-laser source and feeding system for thermoplastic prepreg tapes.

Such tape-laying systems are equipped with special focusing optics forming a beam shape adapted to the process geometry as well as a thermal process control device to control the weld quality of the processed component [34].

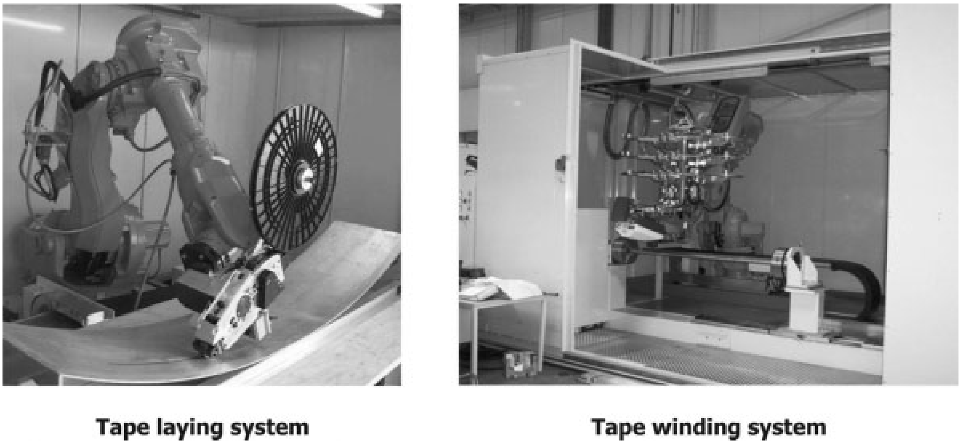

Tape laying system

Tape winding system

Figure 4.28 Robotic system for laser-assisted tape laying and winding using diode laser [33].

4.3
Adaption of Absorption

For laser welding plastics in industrial applications commonly NIR lasers in the wavelength range between 800 nm and 1100 nm like diode, fiber or Nd:YAG lasers are used. Natural or colored thermoplastic resins have insignificant or limited absorption in this wavelength range.

To adapt thermoplastic resins for laser welding, absorbing agents as special surface coatings or additives in the laser-absorbing component have to be used. Alternatively, lasers with wavelengths above 1200 nm with noticeable absorption without additional absorbers in the thermoplastic resin are an option for plastic welding.

Enabling laser welding of thermoplastic components by using absorbing surface coatings, additives in the resin and adapted laser wavelengths will be discussed in the following sections.

4.3.1
Use of Surface Coatings

Laser welding of thermoplastic components with conventional NIR lasers needs an adaption of the optical properties of the resin to absorb the laser radiation and generate the process heat. One possibility for adaption is the application of an absorbing surface coating as a layer at the joint interface of the components to be welded, as shown in Figure 4.29.

Application of such an absorbing layer to the joint interface can be done by several different techniques. A common process is the application of a liquid coating with a dissolved or dispersed absorbing agent in a solvent like acetone, ethanol or MEK [7, 8].

Using different liquid-coating technologies the laser absorber has to be deposed at the joint path of at least one of the parts to be welded. The coating process depends

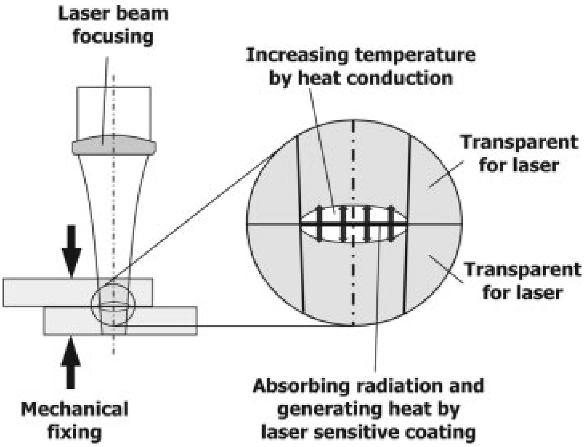
Laser beam focusing
Increasing temperature by heat conduction
Transparent for laser
Transparent for laser
Mechanical fixing
Absorbing radiation and generating heat by laser sensitive coating

Figure 4.29 Through-transmission laser welding using absorbing layer at the joint interface.

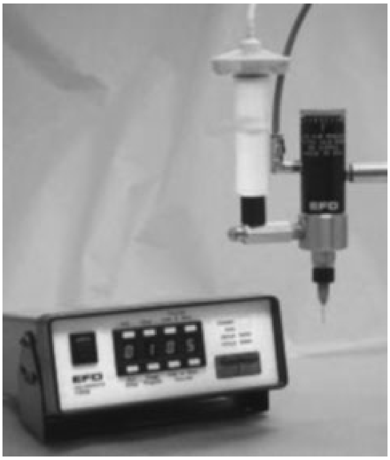

Figure 4.30 Needle-tip dispenser for coating application [35].

upon accurate and repeatable application of the NIR absorbing layer at the joint interface. If the application of the absorber is uneven, the weld can overheat in some areas while being not welded in other areas. Consistent application is critical in obtaining consistent weld quality and strength. Possible methods of application are liquid dispensing and spray coating, which will be described briefly in the following.

Liquid dispensing of solvents with organic dyes as laser absorber can be done for example, by using needle-tip dispenser (Figure 4.30) [35, 36]. Needle-tip dispensing is a well-known method of applying liquids to a wide variety of surfaces. The liquid is dispensed from a pneumatic valve; it is opened and closed by means of air pressure. A spring-loaded needle is held against a valve seat to prevent flow from the valve orifice when air pressure is off. When air pressure is turned on, the needle is lifted from the seat and liquid can then flow through the valve and out of the valve orifice.

The liquid that is being dispensed is stored in a small fluid reservoir that is connected to the valve. By applying low air pressure to the reservoir, the fluid will be forced through the valve when the needle is opened. Liquid solvent coatings are applied in small quantities (nanoliters or microliters) [36]. Therefore, control of the volume being dispensed is critical. The volume of material dispensed is controlled by the amount that the valve is opened, the pressure applied to the liquid reservoir and the length of time that the valve is opened. When the air is turned off, the needle closes and the flow of liquid is stopped.

A needle-tip adapter (needle tip) is attached to the outlet side of the valve orifice. The needle tip is used to guide the liquid from the valve to the surface that is being coated. Between the end of the needle tip and the surface of the work piece to be coated a constant gap is needed for proper coating of the surface. The constant gap height is important because the liquid being dispensed must form a continual film that is dragged around the surface being coated. The gap height is affected by the size of the drop being formed. Therefore, smaller bore needles will have to be closer to the

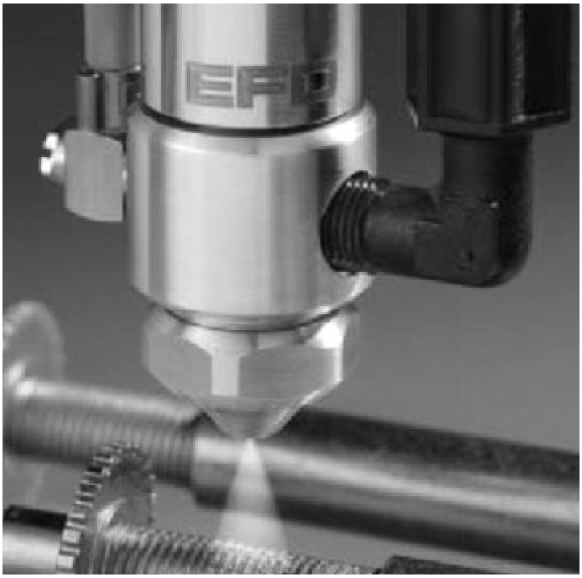

Figure 4.31 Pneumatic spray device for covering lager areas with laser absorbing coatings [37].

surface being coated. In addition, variations in surfaces must be accounted for in the dispensing programming.

The needle-tip dispenser can be attached to a numerically controlled (NC) moving system allowing the dispenser to accurately trace the outline of the part to be coated.

With needle-tip dispenser coating width from approximately 1 mm to 5 mm can be achieved [36]. For coating larger line widths up to 50 mm or entire surfaces low-volume–low-pressure (LVLP) pneumatic spray valves [37] are suitable for application (Figure 4.31).

Such LVLP valves are designed for use with low to medium viscosity fluids. They are suitable for application of solvent coatings containing dissolved organic dyes as well as for coatings with well-dispersed laser-absorbing pigments. Using coating dispersions a possible clogging by remaining pigments in the valve has to be considered, which is no problem using solvent coatings. Micro- to milliliter amounts of fluid can be dispensed in round or oval patterns.

Pneumatic valves (e.g., [38]) use an internal needle to restrict the flow of liquid through the valve. Air pressure is used to force the needle away from its seat when the valve is opened. The liquid is stored in a fluid reservoir that is connected to the inlet port of the valve. Low air pressure forces the fluid from the reservoir through the valve when the valve is opened. The amount of liquid that flows through the valve is controlled by the needle stroke (flow adjustment knob), the fluid reservoir pressure and the length of time that the valve is opened. When the air to the valve is turned off, a spring forces the needle back to its seat and stops the flow of liquid.

The major difference between a spray valve and a needle tip valve is the application of air to the nozzle. Low pressure air is fed to a mixing head (air cap) at the outlet of the

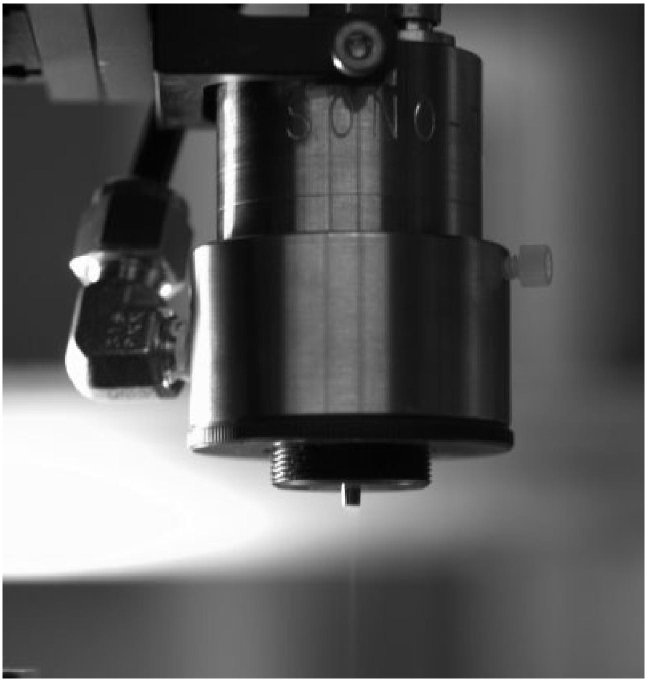

Figure 4.32 Ultrasonic spray device for homogeneous and precise application of laser-absorbing coating.

valve. This creates a pressure differential that causes the liquid to be atomized into a mist as it leaves the valve. The absorbing material will be applied as a very thin film. The total absorber content per unit area will therefore be less than that achieved with needle-tip dispensing. The width of the coating pattern depends on the air cap outlet diameter and the distance of the valve to the surface to be coated.

Ultrasonic nozzles (Figure 4.32) use the technique of ultrasonic atomization to create a fine mist at the outlet of the nozzle [39]. When a liquid is placed on a smooth surface and vibrational energy applied to the surface, the energy is transformed into standing waves within the liquid. When the energy is increased, the amplitude of the waves will increase until the height of the wave exceeds that required to maintain their stability. This results in a collapse of the waves and the ejection of tiny drops of liquid from the waves. Generated drop diameters from ultrasonic nozzles are much smaller than produced by pneumatic spray valves, resulting in a more homogeneous spray pattern on the surface to be coated.

The ultrasonic nozzle consists of an internal feed tube that allows liquid to pass through the nozzle. The coating liquid is again stored in a fluid reservoir. The reservoir can be a vessel with low pressure used to force the liquid to the nozzle or a metering device such as a syringe pump. A series of piezoelectric transducers are attached to the exterior of the tube and provide the energy necessary to atomize the liquid. An ultrasonic generator provides the input to the transducers [34].

At the nozzle orifice, low pressure air (0.07–0.20 bar) is used to direct the mist toward the surface that is to be coated.

An ultrasonic nozzle has no moving parts and won't clog using solvent coatings. Application of dispersion coatings is also possible but clogging can occur during processing and has to be avoided by using special techniques to prevent the dispersion for separation of the pigments from the solvent.

The ultrasonic nozzle produces a "soft spray" that reduces the chances of overspraying and thus reduces material usage. The spray patterns can also be shaped for precise coating applications. Different ultrasonic nozzle types are available to generate coating widths between 0.7 mm and 10 mm, adjustable also by the distance of the nozzle to the work piece and the air pressure of the air shroud [40].

What kind of coating-application system will be used is dependent on the size of the weld joint and the geometry of the components to be welded. Dispensing systems will create line widths of approximately 1 mm to 5 mm and spray systems will be used for 5 mm to 50 mm line widths. Needle-tip dispensing systems work with droplet contact to the surface and are practicable for flat contours. Spray-coating systems working contact free and are more suitable for three-dimensional component geometries.

As stated before laser-absorbing liquid coatings can be solvents containing organic dyes or dispersions of inorganic pigments. A special process using organic dyes as absorber is the Clearweld coating process developed by TWI Ltd., Cambridge (UK) [41, 42] and commercialized by Gentex Corp., Carbondale (US) [43].

The Clearweld coating contains a special organic dye dissolved in a solvent like Acetone, Ethanol or MEK. The organic dye has high absorption for NIR lasers between approximately 900 and 1100 nm and some low absorption in the visible optical spectrum [44]. Also, an organic dye with absorption at higher wavelengths is available, as shown in Figure 4.33.

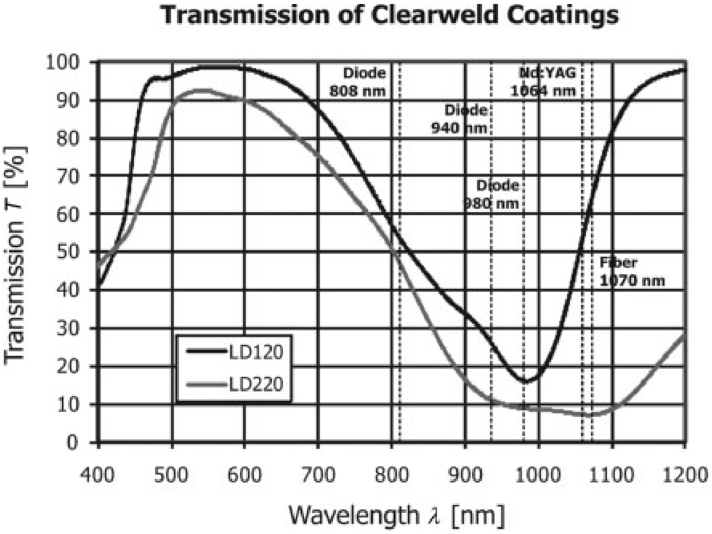

Figure 4.33 Transmission spectra of Clearweld coatings in the visible and NIR spectral ranges [45].

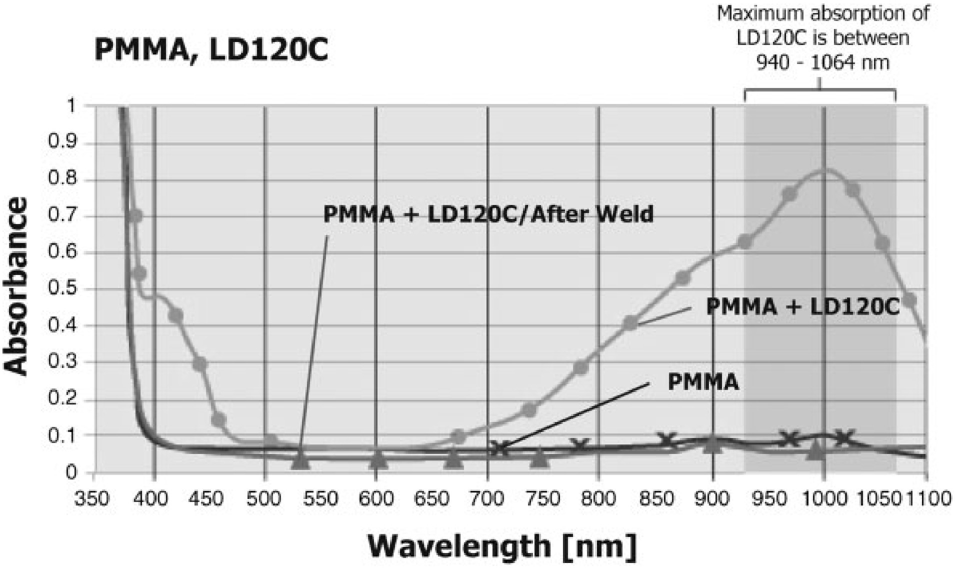

Figure 4.34 Spectral absorption of Clearweld coating before and after laser welding compared to the absorption behavior of the resin to be coated [46].

After applying the Clearweld coating to the surface of a work piece, the coating dries rapidly by evaporation of the solvent and leaves a very thin deposit on the joint interface surface. After drying, the absorber has a slightly transparent coloration in the visible range. This coloration will be lost during the laser-welding process [44]. Figure 4.34 shows as an example the spectral absorption of Clearweld Coating on a PMMA resin before and after the welding process compared to the absorption spectrum of the natural PMMA resin [46].

To create the weld the laser radiation is absorbed by the Clearweld dye and simultaneously converted into heat within the absorber layer. The material at the interface to the absorber layer is heated and melted by heat conduction and creates the weld seam after solidification.

During heating, the absorber gets an optical degradation and loses visible coloration as well as absorption properties for the laser radiation completely. A clear and transparent weld joint at transparent plastics is the result (Figure 4.35). The optical degradation during processing Clearweld coating can be used for contour and simultaneous laser welding but this is limited for quasisimultaneous laser welding.

Because the absorptive layer is very thin, the components to be welded need close contact at the joint interface. Joint gap bridging is restricted and clamping the components needs higher mechanical forces than laser welding using absorbing resins. But using well-adapted processing parameters weld joints of good visual appearance and high joint strength close to the mechanical strength of the parent resin can be achieved [47–49].

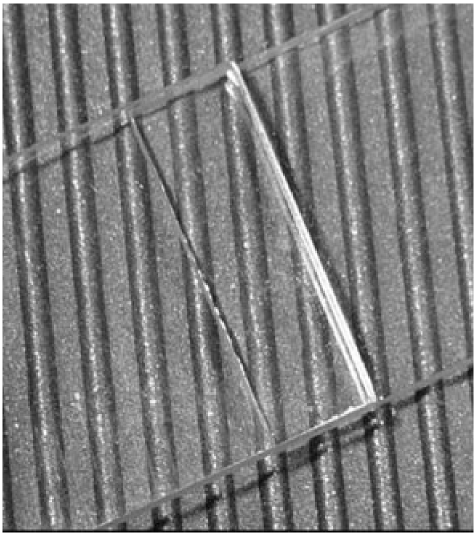

Figure 4.35 Contour laser-welded PMMA sample using Clearweld coating [45].

Alternatively to organic dyes special inorganic pigments can also be used as a laser-absorbing layer on the joint interface of work pieces to be laser welded [8, 50]. Such inorganic materials are for example, Fabulase pigments based on copper phosphates and dispersed in a solvent like acetone or isopropyl alcohol.

Like Clearweld coating the Fabulase dispersion can be applied to at least one surface at the joining area of the work pieces using suitable dispensing technologies like pneumatic or ultrasonic spray nozzles. After evaporation of the solvent a thin light white laser pigment layer remains on the surface of the work piece (Figure 4.36, left).

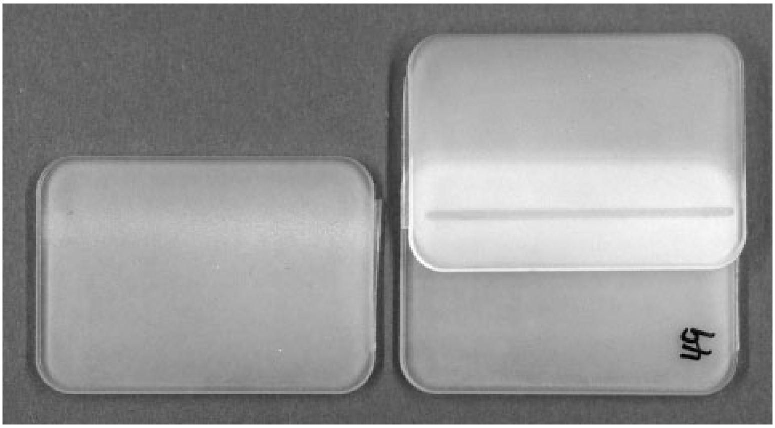

Figure 4.36 Laser-welded LDPE sample using Fabulase coating [44].

During laser welding, the laser radiation will be absorbed by the laser pigment coating and transformed into process heat. The resin layers that are in contact with the coating will be plasticized by the process heat and generates the weld joint under simultaneously applied clamping pressure. During the plasticization process the coating pigments will be dispersed into the melt, affecting a considerably reduced color influence by the pigments. Figure 4.36 shows on the right as an example a laser weld on LDPE using Fabulase pigment coating. Achievable weld strengths using laser pigment coating are of the order of comparable processes.

As an alternative to liquid-coating application at the joint interface the laser-absorbing dye or pigment can be incorporated into thin thermoplastic films [7, 51]. Manufacturing of such films with typical film thickness from 50 to 250 μm is possible by blow molding or extrusion using tailor-made laser-absorbing resins. The laser-absorbing film will be placed between the components for laser welding (Figure 4.37).

The absorbing film can be cut to the required geometry and applied as an additional layer between the joining partners or can be placed into the molding tool before molding the part.

Similar to laser welding with a laser-absorbing coating the laser radiation will be only absorbed in the area where the weld seam has to be generated. Compared to the use of coating a better gap tolerance is given and no solvent has to be used during the processing.

Comolding of plastic components is also a possibility to apply laser-absorbing resin as a separate layer [52]. The comolding can be done in a single step using specially designed multiresin-injecting molding tools or in a second step molding the absorptive layer to a ready-molded component. Figure 4.38 shows a laser welded sample as shown in [52] where the absorptive layer was molded to the base body of the part.

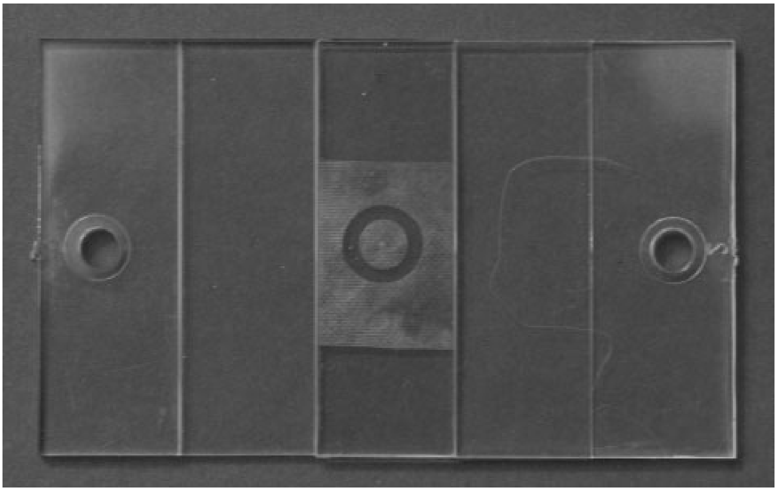

Figure 4.37 Laser-welding transparent PC with absorbing PC film layer.

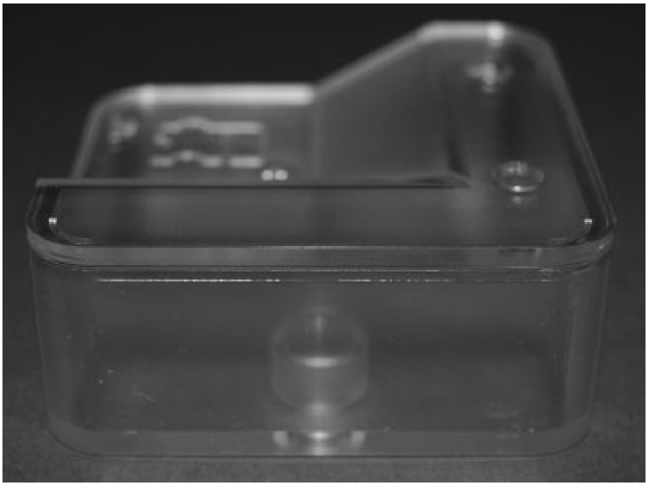

Figure 4.38 Laser welding with absorbing layer by comolding.

After the molding process the lid was positioned and fixed to the base body and laser welding was carried out. The absorbing layer of the body was plasticized by the laser radiation and generated the weld joint to the lid by heat transfer. Like using absorbing films, this welding method is more tolerant to gap bridging than a liquid-absorbing coating application.

Further possible techniques to apply a laser-absorbing layer are thermotransfer printing [53], laser-assisted direct powder application or robot-supported thread extrusion [8, 50].

Laser-assisted thermotransfer application is using a thermotransfer film with an absorber (organic dye or inorganic pigment) on one side. The absorber side of the film will be oriented to the surface of the part to be coated. Laser radiation or a thermal heat source is used to heat the thermotransfer film and to induce a transfer of the absorber from the film to the surface of the work piece. A thin layer of the absorber will remain on the joint interface of the component for laser welding. In principle, laser welding using thermotransfer film will be equivalent to liquid coating.

Using thermally stable laser-absorbing materials like Fabulase powder the material can be applied to the joint interface of one component by laser-assisted powder application. Laser-assisted powder application is using laser radiation to heat the powder before hitting the surface. The heated powder will locally melt the surface and will adhere tightly to the surface. After application of the absorber the components will be clamped together and laser welded.

By robot-supported thread extrusion a laser-absorbing layer will be extruded as a heated thread to the work-piece component. With this process a layer of laser-absorbing resin will be applied to the work piece at the joint area for laser welding similar to comolding.

The main advantage of laser-absorbing surface layers is that the absorber is only applied to the joint interface of plastic components to be laser welded. Using through-

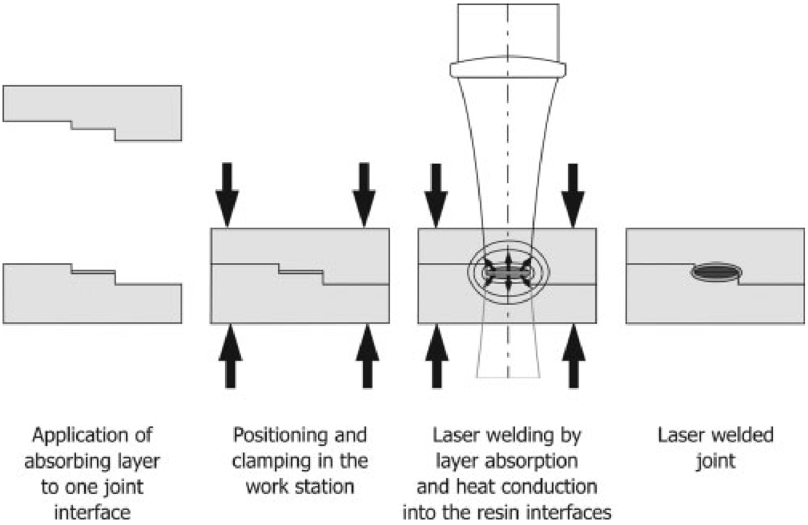
Application of absorbing layer to one joint interface
Positioning and clamping in the work station
Laser welding by layer absorption and heat conduction into the resin interfaces
Laser welded joint

Figure 4.39 Process of laser welding with absorbing surface layer.

transmission laser welding the upper and lower component can be of the same resin type and needs no special preparation for laser welding by absorbing additives in the lower component. The disadvantage of laser-absorbing surface coatings is the need for an additional processing step before laser welding (Figure 4.39) with investment costs into the application technology for the absorbing layer.

Advantages and disadvantages have to be balanced by economical process evaluation to find the right decision. Using laser-absorbing surface coatings can be the right choice when:

- process evaluation without the need of laser absorbing resins has to carried out;
- small or midsized production rates have to be laser welded;
- the volume of the lower component is very high compared to the joint interface;
- optically transparent colorless components have to be welded with the same optical appearance of the weld joint (especially using the Clearweld process).

4.3.2
Use of Absorbing Additives

Today, most common industrial laser-welding applications use absorbing additives in the lower component to be welded. Compared to applying an absorbing layer on the joint interface as discussed before, no additional processing step for component preparation is needed. The molded or extruded components will be directly positioned and clamped in the laser-welding system for processing (Figure 4.40).

Ready-prepared resins as compounds or masterbatches for dilution to the resin ready for processing at the factory will be delivered from the resin supplier (resin manufacturer, compounders or masterbatchers) for manufacturing the components.

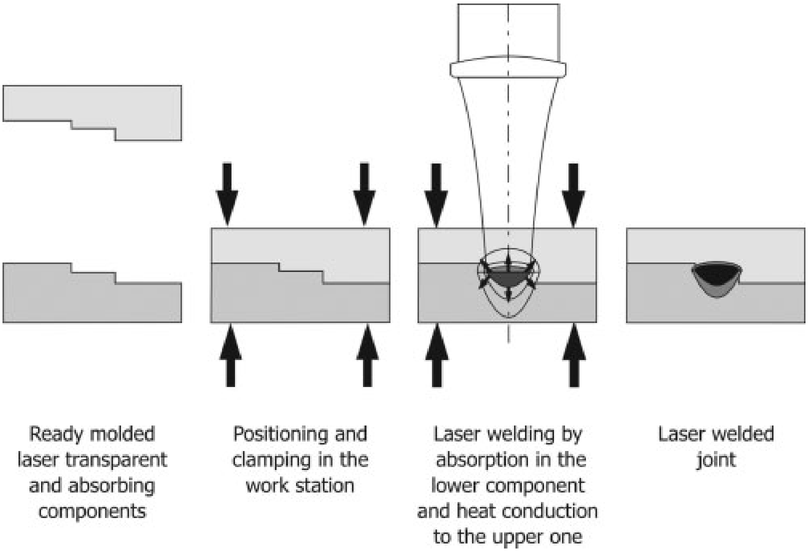
Ready molded laser transparent and absorbing components
Positioning and clamping in the work station
Laser welding by absorption in the lower component and heat conduction to the upper one
Laser welded joint

Figure 4.40 Process of laser welding with absorbing additive in the lower component.

The only issue is the fact that two different resins for the laser-transparent and -absorbing component have to be used and both resins should not mix during preparation and component molding or extrusion.

If coloration of the parts does not matter, carbon black as the absorbing additive in the resin is preferred because of high absorption properties in the NIR region, good processing stability for extrusion or molding of parts and low costs for the additive. The high absorption of carbon black causes a limited penetration depth into the absorbing resin of less than 500 μm depending on the concentration of carbon black pigments in the resin (see Section 2.4.7, Figure 1.52). Nevertheless, carbon black is used in a large number of industrial applications (see Chapter 6) with excellent welding performance and high achievable mechanical strength of the weld joint. Figure 4.41 shows as an example a laser-welded electronic car key with carbon black in the absorbing component [3].

When part coloration is an issue regarding design or functional aspects, especially for visual transparent parts, carbon black cannot be used as laser-absorbing additive. Alternatives to enable laser welding of flexible colored or visual transparent parts are laser-absorbing organic dyes (like Lumogen [54] or Clearweld dyes [55]) or inorganic pigments (like Fabulase pigments [50]) as additives in the resin in combination with conventional NIR lasers operating at wavelengths between 800 nm and 1100 nm (see Section 2.4.7). Nano-ITO pigments are also an option as absorbing additive for laser welding with wavelengths of 1064 nm or higher [56].

These specific laser absorbers have the feature of low absorption in the visible and high absorption for a dedicated wavelength range in the NIR. The specific absorption in the NIR spectral range of organic dyes or inorganic pigments is less than for carbon black. Hence, the optical penetration depth into the absorbing resin is higher than for

Figure 4.41 Laser welded electronic car key with carbon black in the absorbing component [3].

carbon black, depending on the concentration of the specific absorbing additive. Typical used concentrations for laser-absorbing organic dyes are in the range of 0.1 to 0.01% [57], while the concentration for laser-absorbing inorganic pigments is between 0.5 and 2% [50].

Figures 4.42 and 4.43 show as examples the penetration depth of an organic dye (Clearweld LWA 267) and an inorganic pigment (Fabulase 322) for diode laser radiation with wavelength of 940 nm in correlation with the additive weight percentage concentration in the resin.

By the choice of concentration of the absorbing additive in the resin the optical penetration depth for the laser radiation into the resin and thus the melting depth (volume of melt) can be adapted to the demands of the work piece. This enables better balancing of geometric work-piece tolerances and gap bridging during laser welding than using carbon black as absorber.

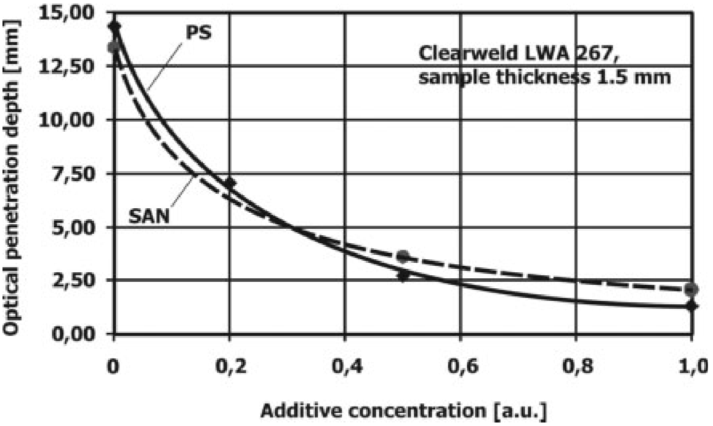

Figure 4.42 Optical penetration depth for 940 nm diode laser in PS and SAN using Clearweld LWA 267 dye as absorber.

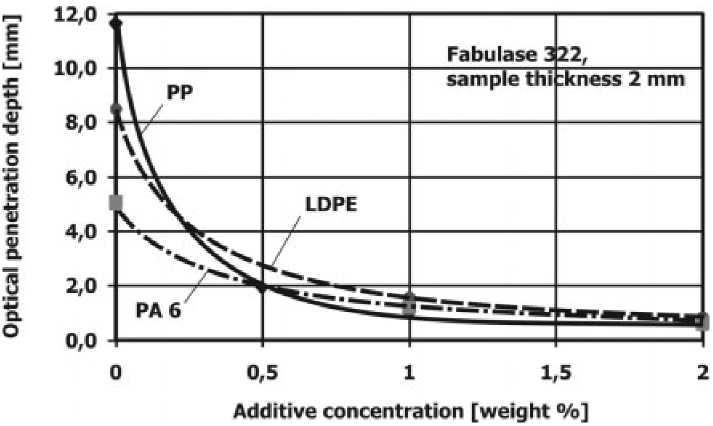

Figure 4.43 Optical penetration depth for 940 nm diode laser in PA 6, PP and LDPE using Fabulase 322 pigment as absorber.

Laser-absorbing organic dyes are dissolved in the thermoplastic resin matrix like conventional dyes used for coloring of thermoplastic resins. Mixing such laser-absorbing dyes to optical transparent resins like PC, PMMA or PETG will maintain the visual transparency with some slightly color input to the resin depending on the concentration of the absorbing dye.

By color correction during resin preparation for component molding or extrusion the same color for laser-transparent and laser-absorbing components can be achieved, as shown in Figure 4.44 for visible transparent PETG samples of different colors, used as laser-welded demo parts (luggage tags) on the K2007 trade fair. In the picture, the laser-absorbing components are marked by a tape.

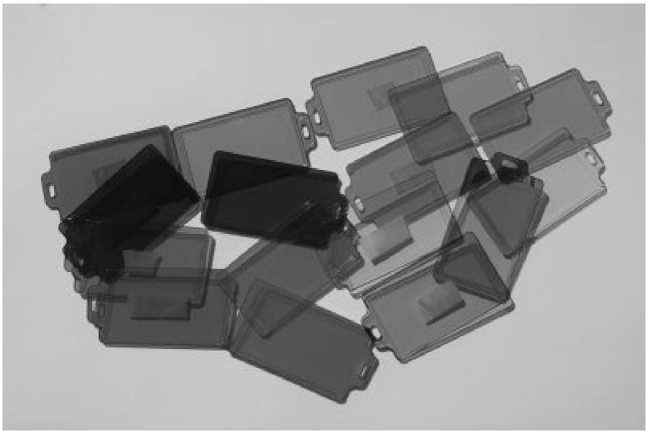

Figure 4.44 Color-corrected laser-transparent and -absorbing PETG components using organic dye in the absorbing component (marked with tapes).

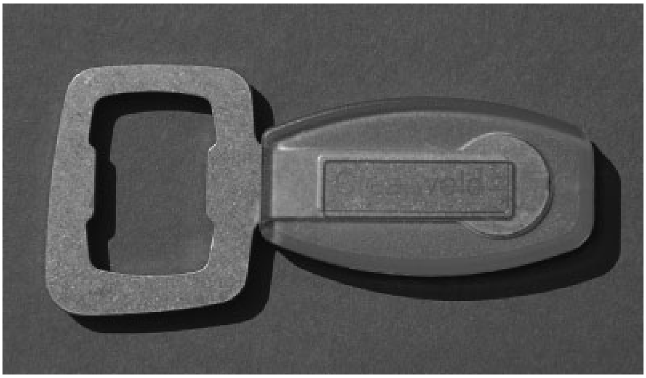

Figure 4.45 Color-corrected opaque samples using Clearweld LWA 267 in the absorbing component.

Color correction between laser-transparent and -absorbing parts on visible opaque colored thermoplastic resins can also be done easily using laser-absorbing dyes, as shown in Figure 4.45. The picture shows a laser-welded demo part with laser absorbing red ABS incorporating Clearweld dye LWA 267 and transparent PMMA.

Inorganic pigments are dispersed in the resin matrix adding a haze and some color input to transparent thermoplastics, depending on the concentration because of light scattering on the pigments in the thermoplastic matrix. Such laser absorbers are well suited for use in semicrystalline opaque thermoplastics like PE, PP or PA6. An example of the use of laser-absorbing Fabulase 322 additive in natural HDPE with concentrations of 0.5, 1 and 2% in the laser-absorbing part is given in Figure 4.46 on

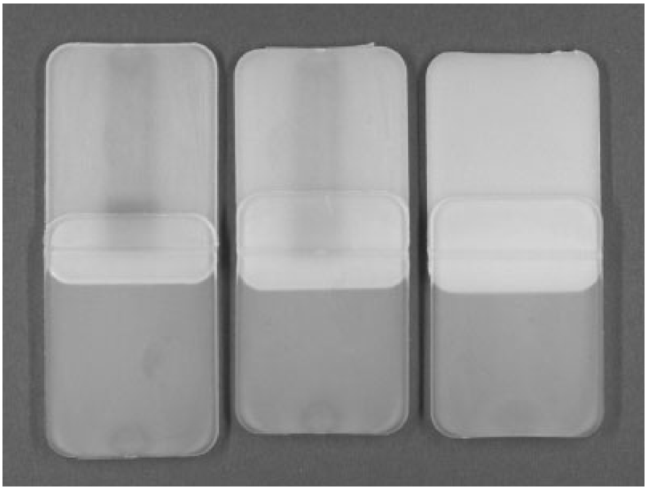

Figure 4.46 Laser-welded natural HDPE samples using Fabulase 322 pigments with concentration of 0.5, 1 and 2% in the absorbing part [50].

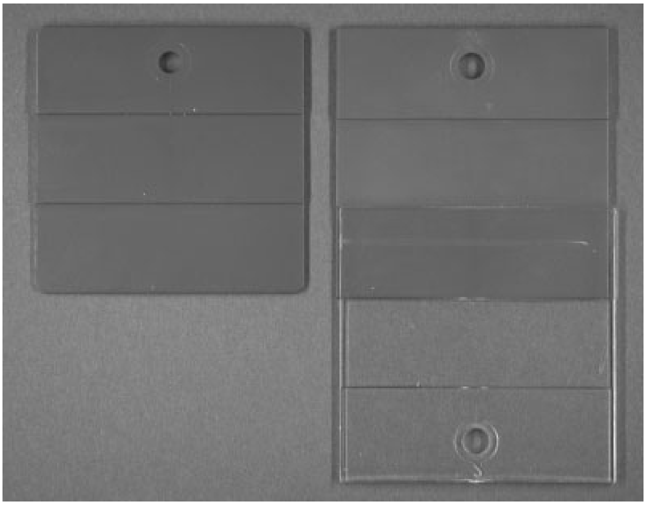

Figure 4.47 Color-corrected opaque red laser absorbing PC/ABS sample using inorganic pigment in the absorbing component [50].

laser-welded samples, demonstrating the color influence by the absorbing pigment depending on the absorber concentration.

The color-correctable color influence in the visible of the Fabulase laser pigments as an NIR-absorbing additive enables these absorbers to be used in applications with light work-piece coloration like yellow or red, and gives a high variability for color design. Figure 4.47 shows as example of a laser weld on red-colored ABS containing 1% of Fabulase 322 pigment in combination with natural transparent PMMA as the welding partner. Left beside the weld sample a red ABS sample without laser pigment is given for demonstration of the low color influence, which can be easily color corrected.

Fabulase laser pigments are also suitable for laser marking of plastics. For applications on components that have to be laser welded and also laser marked, the mixing of an additional absorbing additive for laser marking is not necessary in most cases. Figure 4.48 shows a red ABS/PC sample with laser pigment concentration of 1%, which has been laser marked with a fiber laser (1064 nm) prior to welding to a transparent PMMA using a diode laser (940 nm).

Most of the laser-absorbing agents are available as powder and can be mixed to resins like other color pigments or dyes during preparation of masterbatches or compounds. They are suited for use in a large number of thermoplastics and thermoplastic elastomers for molding or extrusion processes. Formulation of resin batches with these laser-absorbing agents will be done in accordance with compatibility of absorber agent and resin, demands for coloring and by the welding process.

But organic dyes and inorganic pigments as laser-absorbing additives are more sensitive to processing conditions by molding or extrusion and material compatibility

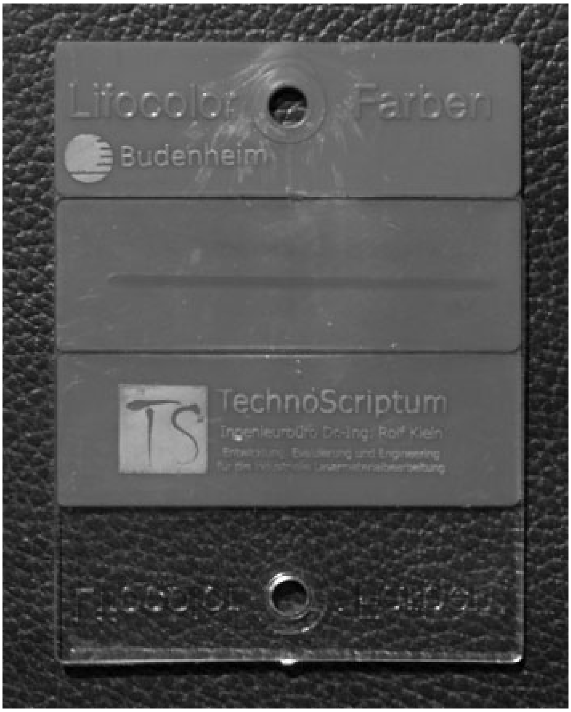

Figure 4.48 Laser marking and welding of PC/ABS with PMMA using Fabulase 322 pigments.

to the resin than carbon black. Most organic dyes as laser-absorbing additives are sensitive to high molding temperatures above approximately 300 °C and high shear stress during processing and cannot be used in high-temperature thermoplastics like PPS or PEEK.

By the high ability to take thermal stress, laser pigments can also be used for high-performance plastics (e.g., PPS or PEEK). Mixed in polyolefin resins like PP or PE as well as in thermoplastic elastomers laser pigments provide a drastically reduced tendency for migration compared to organic dyes as absorber. But use of inorganic pigments can be limited for application in thermoplastics like PMMA or PC because of possible material incompatibilities.

Which laser-absorbing additive, and in what concentration in the resin, will be best for a dedicated application has usually tested case by case.

4.3.3
Use of Special Lasers

In some cases, the use of absorbing coatings or additives is not desired because of design aspects or component-application reasons. An example of application reasons is the laser welding of medical device components. Although absorbing coatings or additives are tested for use with medical device components according to FDA regulations, component manufacturers tend towards avoiding additional agents for component manufacturing because of expensive testing and registration reasons. In such cases, the use of lasers like diode or fiber lasers with wavelengths above 1200 nm is a possible alternative for plastic welding.

To enable laser welding of thermoplastics without additional absorbing agents three basic conditions have to be fulfilled:

- The laser wavelength has to be matched to the intrinsic absorption properties of the thermoplastic resin.
- The laser intensity has to be sufficient high at the joint interface of the components to melt the resin.
- The laser intensity on the top surface of the work piece has to be sufficiently low to avoid damaging of the surface.

An example of successful application of such a laser-welding process is welding of a natural polyamide resin (e.g., PA 6-3-T) [58] using a fiber laser of 1550 nm wavelength.

For this wavelength, the PA resin has a transmission of approximately 60% for a sample thickness of 2 mm. This corresponds to an optical penetration depth of around 4 mm for the laser radiation into the resin, comparable with a laser-absorbing resin containing absorbing additives of low or medium concentration.

Through-transmission laser welding with conventional focusing optics would result in a noticeable melting of the upper component and a weak bonding of the two components at the joint interface. For successful laser welding the laser beam focusing has to be adapted to the process, as shown schematically in Figure 4.49. Using a focusing optics with large aperture and short focal length will result in focusing the laser radiation at the joint interface with high laser intensity at the joint interface for melting the resin and low intensity at the upper surface of the work piece to avoid thermal damaging of the surface.

A cross section of a laser-welded PA sample using 1550 nm fiber laser and the focusing principle described above is shown in Figure 4.50. The laser beam was focused to a spot diameter of approximately 300 μm and the weld was carried out with 30 W laser power and 200 mm/min feed rate.

The observation of the cross section by polarization microscopy shows a large heat-affected zone that is approximately twice as wide as the spot diameter of the laser beam.

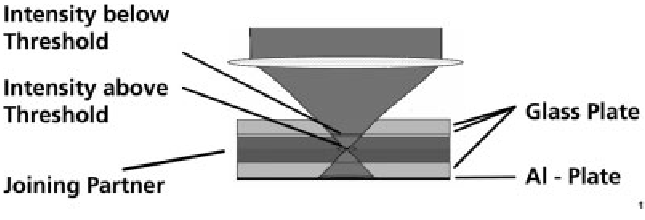

Figure 4.49 Schematic setup of a laser beam focusing optic for through-transmission laser welding of thermoplastic resins without additional absorber [58].

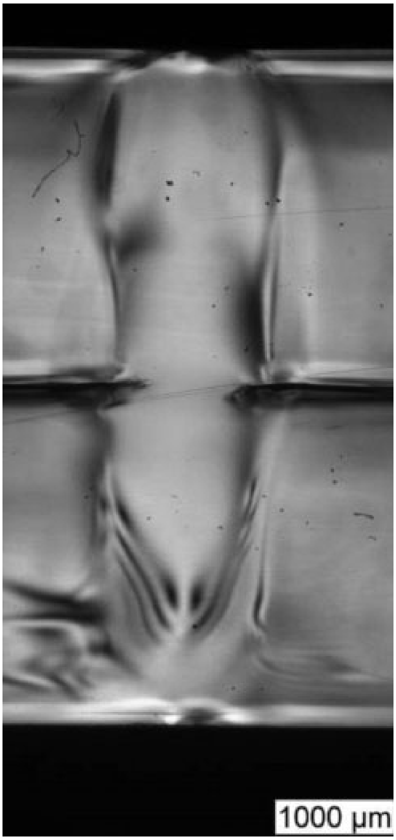

Figure 4.50 Cross section of welded PA 6 3 T using 1550 nm fiber laser, thickness of one layer is 2 mm [58].

An example of laser welding a transparent thermoplastic resin with the laser wavelength adapted to the absorption properties of the resin is given in Figure 4.51. The picture shows a microfluidic mixer device made of PA (Trogamid CX) laser welded with a 1550-nm fiber laser.

The main advantage of laser welding thermoplastic components with radiation wavelength matched to the absorption properties of the used resin is that no additional absorbing agent is needed as for conventional laser welding of thermoplastics. This can be an important issue for laser welding medical device components or other high-tech products.

But application of laser sources with suitable wavelengths for such processes can be restricted by available laser power and economical reasons caused by high investment cost for such laser sources. Additionally, the welding process needs specially designed focusing optics with large aperture and short focusing length. The short focusing length results in short working distance between the focusing optics and the work piece and highly accurate positioning of the focused laser spot to the

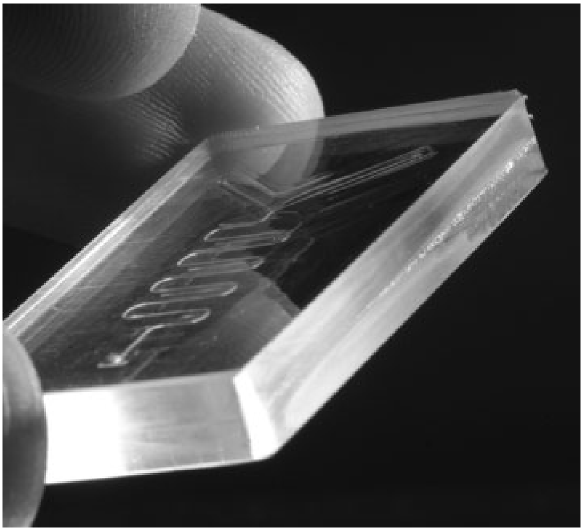

Figure 4.51 Laser welded microfluidic mixer device made of PA using focused laser radiation of a 1550 nm fiber laser [58].

joint interface by the handling system. Above and below the melting interaction zone the resin gets a noticeable heat input that can be of negative influence on the work piece. Also, it is possible that similar thermoplastic resins of different material suppliers can have a different interaction with the laser radiation at a certain wavelength.

Nevertheless, laser welding with matched wavelength to the absorption properties of thermoplastic resins is an appropriate alternative to laser welding of thermoplastics using laser-absorbing agents like additives or coatings and has to be assessed case by case.

4.4

Design of Joint Geometry

Besides common technical guidelines and rules that have to be taken generally into consideration for part design of thermoplastic components the design of the joint geometry for laser welding application needs special attention. Additionally to adaption of laser radiation absorption by the thermoplastic resin the design of the joint geometry is a major issue for successful laser welding of plastic components using through-transmission laser welding (TTLW) as the common process for industrial application. Application of different laser-welding process types like contour, quasisimultaneously and simultaneously laser welding or other processes like hybrid laser welding requires dedicated demands on the joint geometry [59].

Independent from the applied TTLW process demands to a well-adapted part design are [60]:

- General technical guidelines and rules for part construction have to be taken into consideration.
- Laser-transparent and -absorbing component have to be placed in the right order to enable TTLW.
- The joint interfaces of the components have to be fixed tight and parallel to each other by appropriate clamping devices.
- The components to be welded need to be centered properly.
- The focused laser radiation should hit the joint interface nearly vertical to the interface.
- The joint interface has to be accessible for the laser radiation.
- Surface roughness of the joint interface should be as low as possible.
- No molding flash formation should be at the joint interface.

In principle, different joint geometries for laser welding application are possible as discussed in the following. Attention has to be paid to geometry tolerances to avoid joint gaps as well as to possible obstacles hampering a successful laser welding. A recently developed process to reconcile joint gaps during laser welding will also be discussed in the following.

4.4.1
Joint Geometries

The basic demand for joint geometry design of plastic components well adapted to TTLW is that the joint interfaces need close contact between laser-absorbing and laser-transparent components to ensure an effective heat flow for melting the laser-transparent interface. Part design and manufacturing conditions during molding or extrusion of the work-piece components have to ensure that the close contact of the joint interfaces will be enabled.

Additional to this, the geometry of the work piece has to be designed in a way that clamping pressure can be applied to the work piece to generate a uniform welding pressure over the entire joint area.

Regarding these demands different fundamental joint geometries, as shown in Figure 4.52 can be used.

The design of the joint geometry depends on the applied laser-welding process. Contour laser welding works without squeeze flow of the generated melt while quasisimultaneously and simultaneously laser welding enables the use of melt squeeze flow to balance possible joint gaps within certain limits.

For contour laser welding the laser-absorbing and -transparent components need close contact supported by the applied clamping force (Figure 4.53). Heating and melting of the joint interfaces will be done locally while moving the focused laser beam along the joint contour. The clamping force has to reliably fix the component position and sufficient clamping pressure is needed to ensure the mixing of the molten interfaces, enabling a high joint strength after resolidification. At the joint interface no additional space is necessary to offset a melt flow.

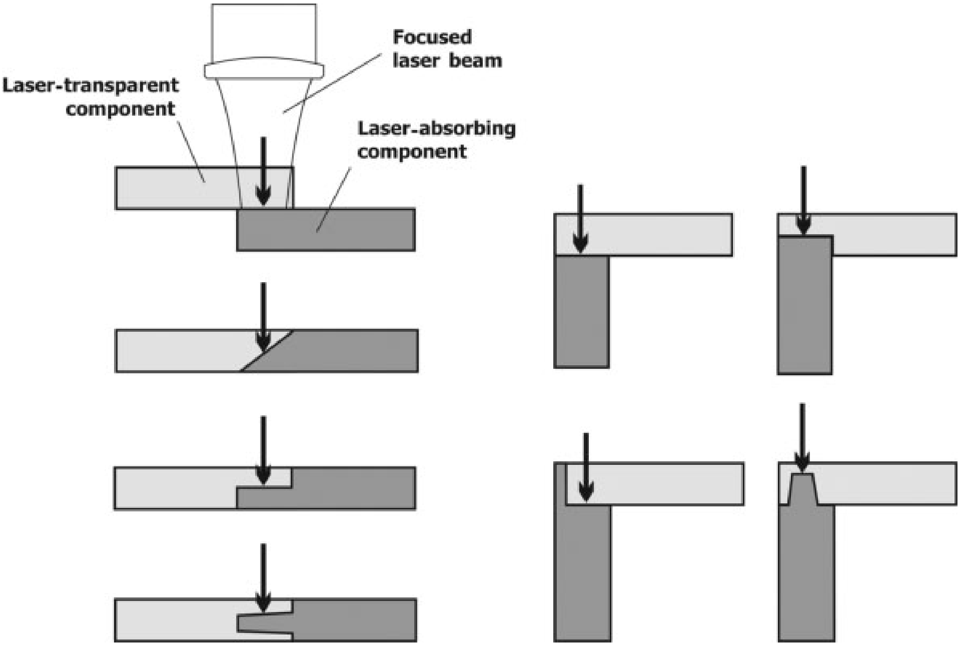

Figure 4.52 Principle joint designs for TTLW.

During quasisimultaneous or simultaneous laser welding the entire joint contour will be heated up and melted at the same time. This allows by a simultaneously applied clamping force the use of a set path between laser-transparent and -absorbing components to balance out possible joint gaps by melt squeeze flow. The design of the joint geometry has to be done in a way to capture the squeeze flow by additional space

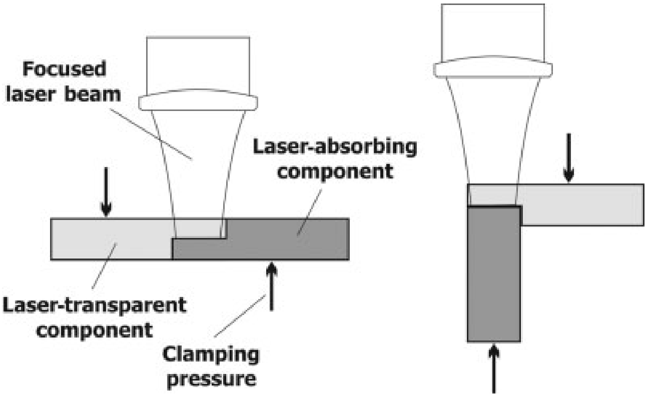

Figure 4.53 Examples of joint design using contour laser welding.

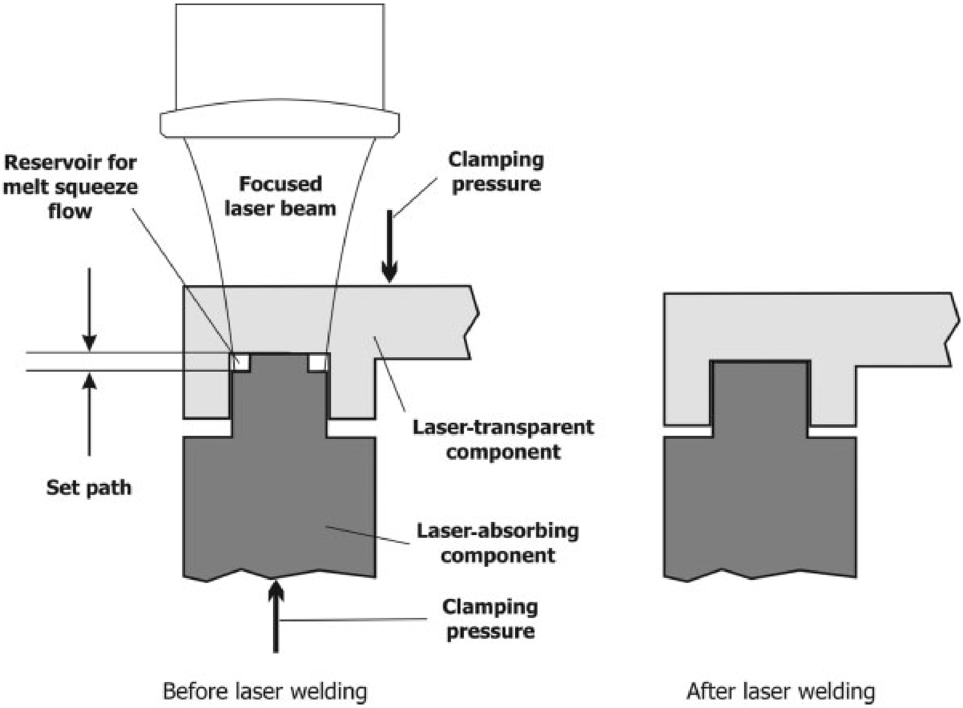

Figure 4.54 Example of joint design using laser welding with a set path.

around the joint interface (Figure 4.54) without influencing the visual appearance of the work piece. Also, the geometry of the work-piece joint including the set path has to be designed properly so that the laser-welding process will result in a reproducible shape of the entire work piece.

A special type of joint geometry is the tight press fit joint used for example for concentrically circular components (Figure 4.55) or lids pressed into a base body to be laser welded. The inner circular component or the joint interface of the lid will have some geometrical excess amount compared to the outer circular component or the base body. The excess amount will generate an internal clamping pressure after pressing both components to each other. No additional outer clamping force is needed and the internal pressure will enable the mixing of the molten interfaces during application of the laser radiation to melt the interfaces.

The demands of joint designs for special laser welding techniques like mask, TWIST, Globo or IR-hybrid laser welding are in principle equivalent to contour laser welding. Mask and TWIST laser welding need close contact of the joint interfaces without a set path and application of a uniform clamping pressure to the work piece [61, 62]. Globo welding applies a localized clamping pressure simultaneously to the welding process and enables gap bridging in some limits by the clamping force [22]. IR-hybrid laser welding generates an additional heating of the laser-transparent component resulting in local softening of the resin [24]. Simultaneous

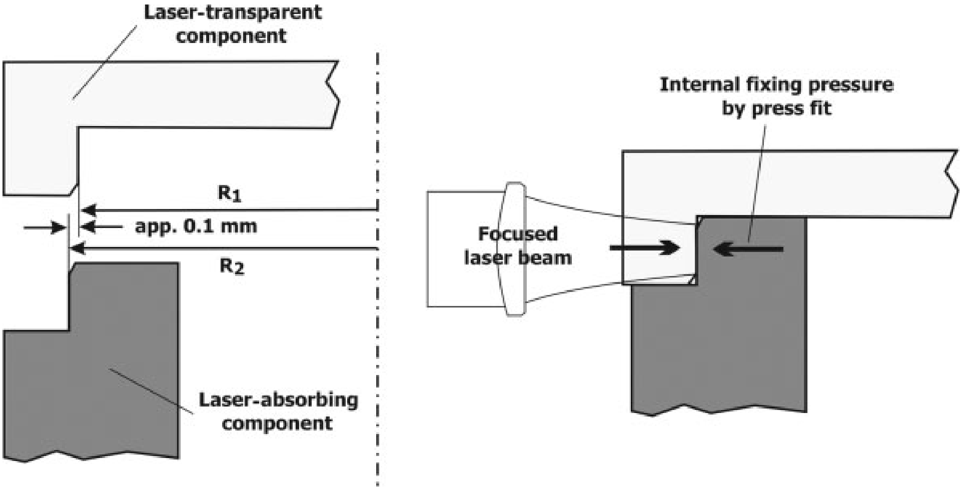
Laser-transparent component
R1
app. 0.1 mm
R2
Laser-absorbing component
Internal fixing pressure by press fit
Focused laser beam

Figure 4.55 Joint design using a press fit for laser welding [59].

application of a pressure force by a clamping finger will generate a close contact of the interfaces to generate the weld joint.

Special requirements for the joint design are given by the thermoplastic resin types used for the laser-transparent component. Semicrystalline thermoplastics, thermoplastic resins with glass-fiber reinforcements or containing pigments like titanium dioxide and other filler additives will scatter the incident laser radiation and will prevent successful laser welding above a limited thickness of the laser-transparent component (Figure 4.56). As an example, using 30% glass-fiber reinforcement in the laser-transparent component will limit the component thickness “s” to approximately 2 mm for laser welding [63].

Additional requirements for the joint-interface geometry are given by using laser-absorbing liquid coatings to at least one surface of the components to be laser welded. The joint design has to ensure that the laser-absorbing coating can be applied to the joint interface without overflow. Typical joint designs for coating application are given in Figure 4.57 using for example, grooves or ledges to limit the coating flow to the joint during drying by evaporation of the solvent.

In combination with visually transparent amorphous thermoplastic resins like PMMA or PC the layer thickness as laser-transparent component can be larger than for semicrystalline resins or thermoplastic resins with reinforcements or other light-scattering additives. In amorphous thermoplastics without additional additives the laser radiation will be transmitted through the laser-transparent component with negligible intensity loss by absorption or scattering. The only issue to be considered for dimensioning the laser-focusing length is the influence of the resin refractive index on the laser radiation focusing inside the laser-transparent resin.

A special case for laser welding of transparent amorphous thermoplastic resins like PMMA or PC is the use of laser-absorbing organic dyes like Clearweld® coating materials. Such absorbing layers enable simultaneous laser welding of several

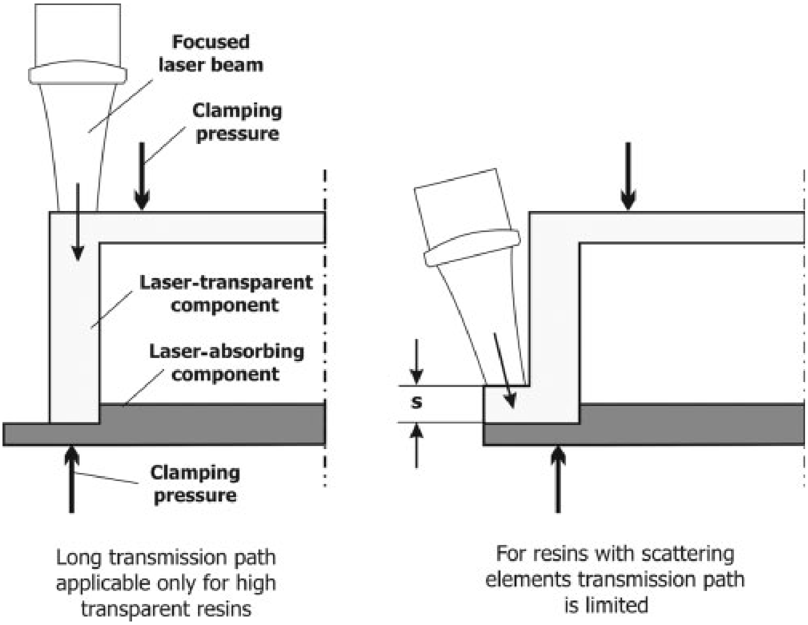
Focused laser beam
Clamping pressure
Laser-transparent component
Laser-absorbing component
Clamping pressure
s
Long transmission path applicable only for high transparent resins
For resins with scattering elements transmission path is limited

Figure 4.56 Applicable joint design for resins with semicrystalline structure or glass-fiber reinforcements or other radiation-scattering additives in laser-transparent components.

component layers, as shown exemplarily for laser welding of two lids to a cylinder (Figure 4.58) [45].

The laser-absorbing coating is applied to the edges of the cylinder. The lids are positioned onto the cylinder and laser welding is done in one circular path, irradiating the focused laser beam from the top through the lid to the edge of the cylinder.

During the laser-welding process, the absorbing coating on the first edge is heated and instantaneously loses the functionality to absorb the laser radiation. Simultaneously, the laser radiation is guided through the cylinder wall by internal reflection to the lower edge and is absorbed to generate the second weld joint. The laser-welding process results in fluid-tight joints of high strength.

4.4.2
Tolerances and Clamping

Geometrical joint tolerances are caused by the difference between theoretically designed and the achieved joint geometries of the manufacturing processes of the work pieces. Also, positioning and alignment of the components to each other can be flawed with tolerances.

Processing conditions during molding or extrusion of the component have a direct influence on the geometrical shape of the components and needs to be well adapted for reliable component manufacturing. Nevertheless, industrial component manufacturing results in component shapes having certain geometrical tolerances.

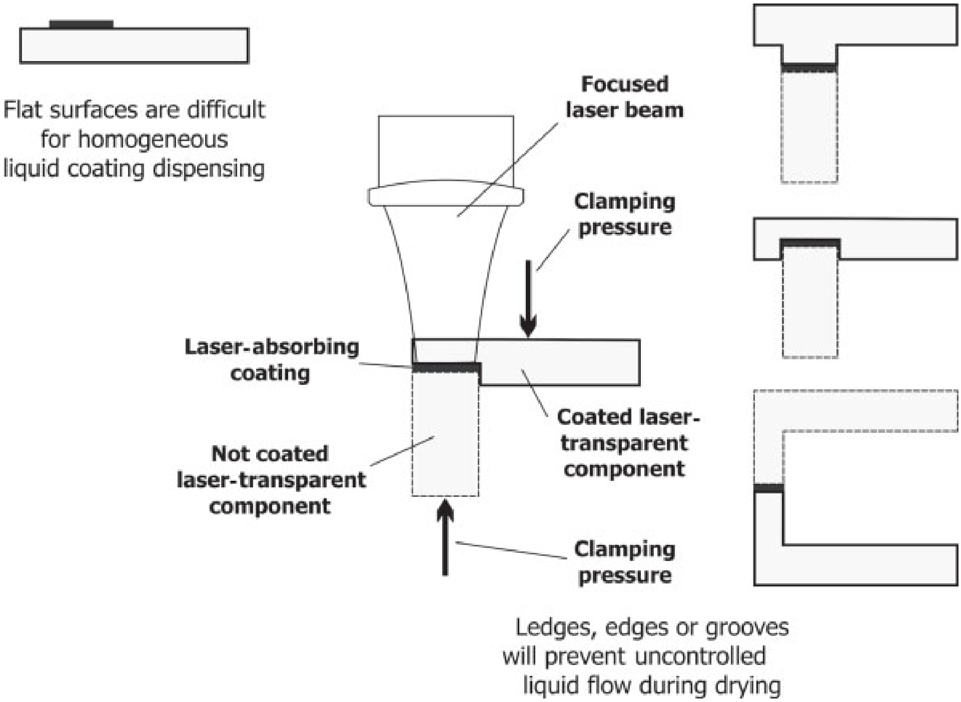
Flat surfaces are difficult for homogeneous liquid coating dispensing
Focused laser beam
Clamping pressure
Laser-absorbing coating
Coated laser-transparent component
Not coated laser-transparent component
Clamping pressure
Ledges, edges or grooves will prevent uncontrolled liquid flow during drying

Figure 4.57 Example for joint design using laser welding with liquid coating.

In particular, the cooling down phase after molding or extrusion needs special attention. The thermally induced material shrinkage during the cooling down has to be regarded during design of the component and changing the intended cooling rate will cause changes in the geometrical shape, resulting in increased joint-gap tolerances.

The balancing of tolerances by joint gaps during laser welding is dependent on the laser-welding process used. Permissible gap tolerances for successful contour laser welding are much smaller than for quasisimultaneous or simultaneous laser welding.

Using contour laser welding no balancing of joint tolerances applying a set path is possible. Possible joint gaps can only be bridged by the thermal expansion of the thermoplastic resin during the welding process. This results in increased demands to the limits of bridgeable joint-gap tolerances.

For a plane joint shape as shown in Figure 4.59 the geometrical tolerances of the joint interfaces may not exceed 0.08 mm [60].

Using curved joint shapes and for liquid- or gas-tight joints the joint interfaces need a tolerance of parallel shape not exceeding 0.15 mm [60]. At the joint interfaces no pull-out marks are permissible (Figure 4.60).

To reduce joint gaps and fix the components for leaser welding adequate clamping devices have to be used. The clamping force should be applied directly to the joint or

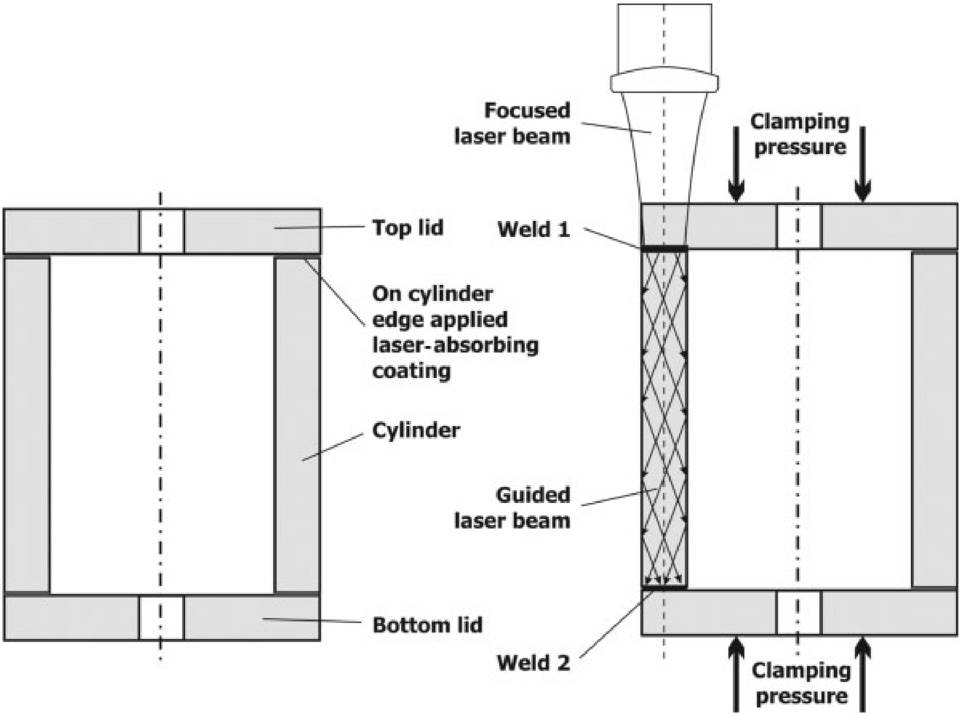

Figure 4.58 Simultaneous laser welding of two joints using laser-absorbing coating on amorphous thermoplastics.

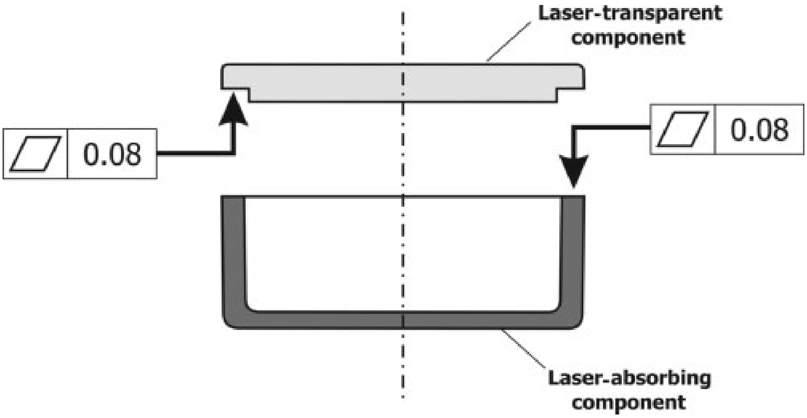

Figure 4.59 Geometrical joint tolerance limits for a plane joint shape using contour laser welding [60].

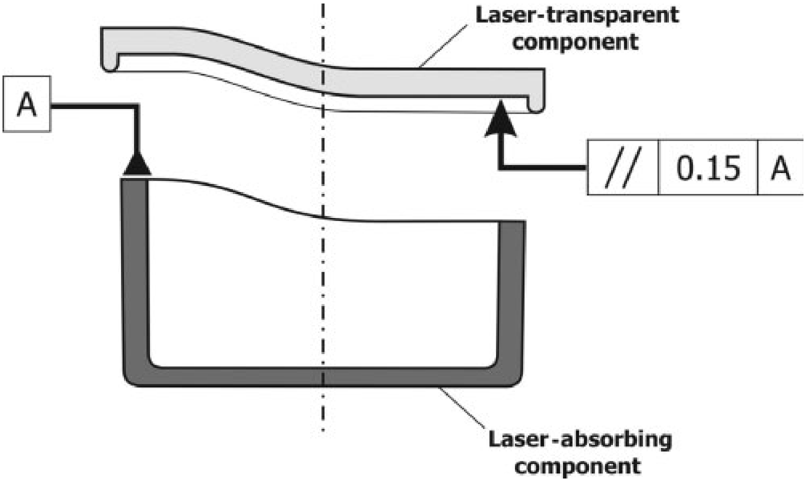

Figure 4.60 Parallelism limit of curved joint interfaces for contour laser welding.from [60].

as nearby as possible. A rule of thumb for applicable pressure forces are values between 1 N/mm^2 to 5 N/mm^2 regarding the weld joint area [60]. Application of clamping force can be done by clamping devices or alternatively by a press fit of the components.

Principle design of clamping tools can be done by using down-holder tools designed to the work piece contour (Figure 4.61, left) or glass plates (Figure 4.61, right). Down-holder tools can be designed as an entire frame clamping the work piece or segmented tools for applying fixing pressure to larger work pieces.

Both alternatives have their pros and cons for application. Obstacles for down-holder tools are the need of an additional edge at the components for sufficient incoupling of the pressure force. This will not be needed for using glass plates as the clamping tool. But glass plates can get dirty during the laser-welding process and can

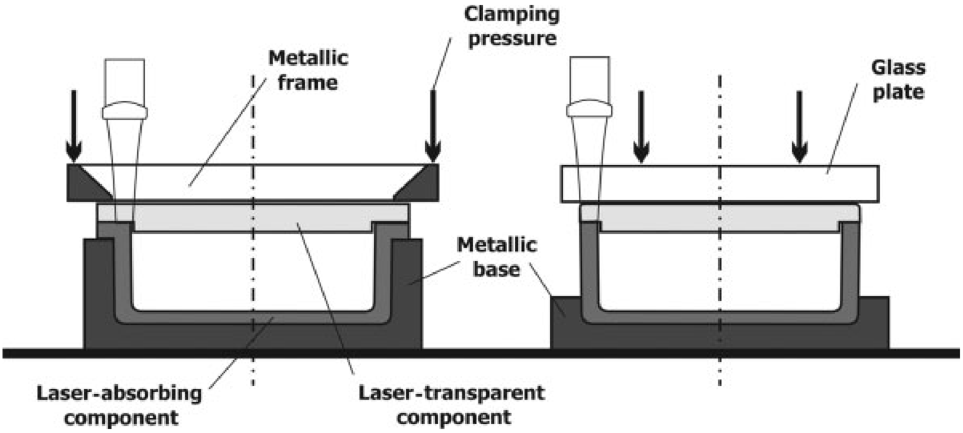

Figure 4.61 Alternatives for clamping tools [60].

hinder the transmission of the laser radiation or in the worst case can be damaged, which is not possible for using down-holder tools.

Using simultaneous or quasisimultaneous laser welding bridging of joint tolerances is enabled with increased limits than using contour welding by applying a set path during the laser-welding process. For application of the set path the components have to be clamped with adequate clamping devices. Appropriate clamping pressures are dependable of the type of thermoplastic resin used to manufacture the components and are usually in the range of 2 N/mm^2 to 5 N/mm^2 regarding the joint-interface area [60]. Residual gaps between the clamped components can be bridged and closed by the ongoing melting process.

The needed set path is dependent on the geometric tolerances of the components. Typical values of set paths are between 0.2 mm and 0.6 mm [60]. For achieving liquid or gas tight joints the set path has to be larger than the maximum gap between the components.

The set-path value has a direct influence to the production rate of the welding system. The better the geometrical tolerances are, the lower is the needed set path and the higher the production rate.

Alignment of the components to be welded can also be flawed with tolerances like the joint interfaces themselves. Proper alignment to fix the components in a well-defined position suitable for laser welding can be done by two basic principles: by geometrical design of the components or by a clamping tool.

Centering by the components is possible using adapted component contour shapes or by special centering flanges (Figure 4.62). Commonly, the components will be assembled to the work piece separately before positioning and clamping in the

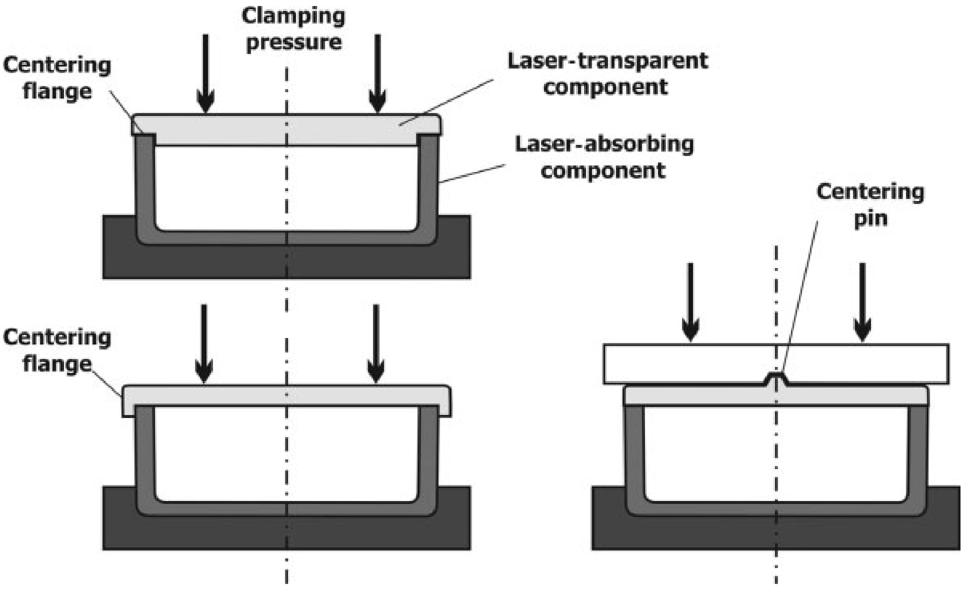

Figure 4.62 Component centering by part design [60].

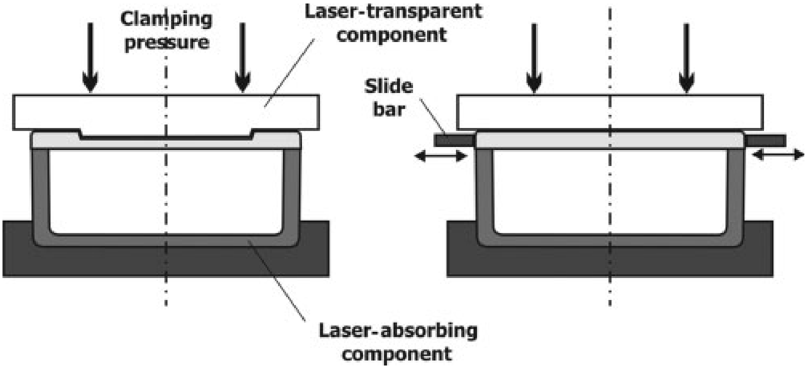

Figure 4.63 Component centering by clamping device with alignment tools [60].

laser welding system. The design of the clamping device can be done in a simple but reliable way for work-piece positioning without the need for expensive part-geometry-specific alignment precautions.

Working with centering by the components needs to consider the geometrical work-piece tolerances and the heat expansion during component manufacturing and laser welding itself. If the geometrical centering is not sufficiently well designed the centering will not be exact enough, again causing tolerances but also generating mechanical stress during laser welding is possible.

Work-piece centering by the clamping device has the advantage of alignment of the components to each other regarding tolerances by the fixing tools. Geometric shape design of the work-piece components is simpler than for centering by the component geometry. The ability for alignment has to be integrated into the clamping tools, which makes the tool design more complex with the needed alignment tools (Figure 4.63).

Commonly, the components will be supplied to the welding system separately, and reliably positioned into the clamping tools. The clamping device will drive the aligned components together and fix them with a pressure force for laser welding. It has to be noted that positioning of the components into the tooling should be done easily without sticking at the centering area.

4.4.3
Obstacles to Avoid

During the design phase for work piece and manufacturing tools for injection molding the work-piece components but also during manufacturing of the parts themselves different obstacles for successful laser welding of the work pieces have to be taken into account.

Proper work part and molding tool design should avoid placing separation gadgets for pull out of molded parts from the tooling at or nearby the joint interface. The separation gadgets could induce marks on the joint interface (Figure 4.64, left) acting like gaps for the laser-welding process reducing the achievable joint strength.

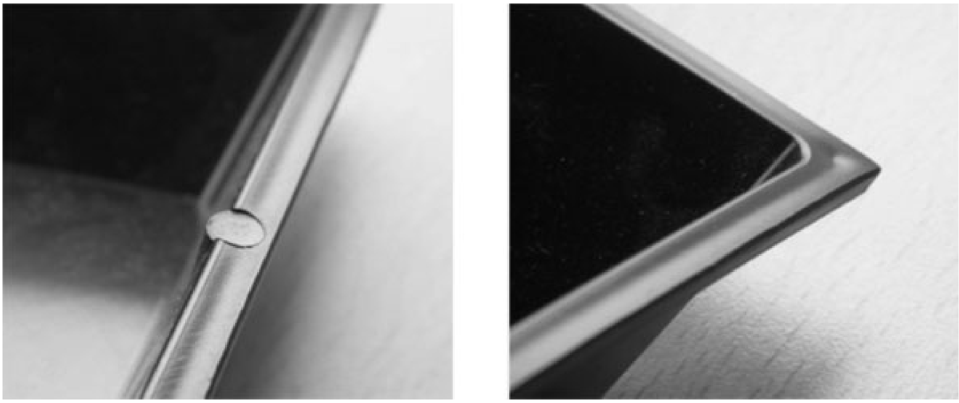

Figure 4.64 Obstacles for sufficient laser welding, left – pull out marks and right – material shrinkage on the joint interface [60].

The injection system of the molding tool needs to be placed in a way that after part pull out from the molding tool no injection residuals can remain on the joint interface. Such residuals can cause gap generation during combination of the components to be welded.

Especially for injection molding of laser-transparent components made by fiber-reinforced thermoplastic resins the injection system of the tool should not be placed nearby the joint interface. Depending on the mold design, positioning of the injection system and molding process parameters used the distribution of the fiber reinforcements can be irregular, causing transmission variations for the laser radiation along the joint interface.

Mismatched molding and cool-down conditions can cause uneven joint interfaces as shown exemplarily in Figure 4.64, right. The example shows an improper setting of the cooling cycle, resulting in shrinkage of the thermoplastic resin at the joint interface. Such shrinkage will cause joint gaps, preventing successful laser welding.

Another obstacle for laser welding plastic components can be surface coatings like paints, galvanic coatings or PVD coatings at the joint interface. If such coatings are not transparent to the laser radiation they can cause absorption or reflection of the laser radiation and will hamper the welding process. In the worst case the coating will be burned by the laser radiation, damaging the work piece and preventing successful joining of the components.

Very thin coating layers at the joint interface possibly could be broken by the melt motion during the welding process and could be incorporated into the melt resulting in generation of a weld joint. But such weld joints usually are of low strength and in principle it is recommended to avoid coating layers at the weld joint by appropriate measures.

In some cases, demolding support agents like silicone-based additives or lubricants are used for easy pull out of molded parts from the molding tool. If such materials remain on the joint interface successful laser welding can be hampered and only sticking joints with low strength will be generated.

The components need excessive cleaning before laser welding. Using silicone-based additives as a special case the cleaning has to be done immediately before laser welding. If the cleaning is done some time before laser welding the silicone-based additives can bleed out of the resin, again building a layer on the joint interface, hampering laser welding.

4.4.4
Gap Bridging

Joint gaps between the components to be laser welded will hinder the heat exchange between both components and will possibly prevent successful generation of the welding joint. Research studies dealing with laser welding of thermoplastics using carbon black as a laser-absorbing additive results in gap bridging of approximately 30–50 μm [10, 64].

An example of this is given in Figure 4.65, dealing with experimental investigations on contour laser welding of PP using different joint gap heights between 0 and 200 μm. Increasing gap heights result in decreasing shear strength of the welded samples. Gap heights of the order of 150 μm and more effects insufficient weld strength on PP and will hinder successful laser welding.

In principle, capabilities for gap bridging by thermal expansion of the resin during the laser-welding process are dependent on the temperature correlation of the resins specific volume. The higher the volume increase by rising temperature the better is the gap-bridging capability.

Larger gaps effectively prevent the interface layer contact and thus the heat exchange to the laser-transparent material. The result is the generation of joint interruptions in the weld seam (Figure 4.66, top).

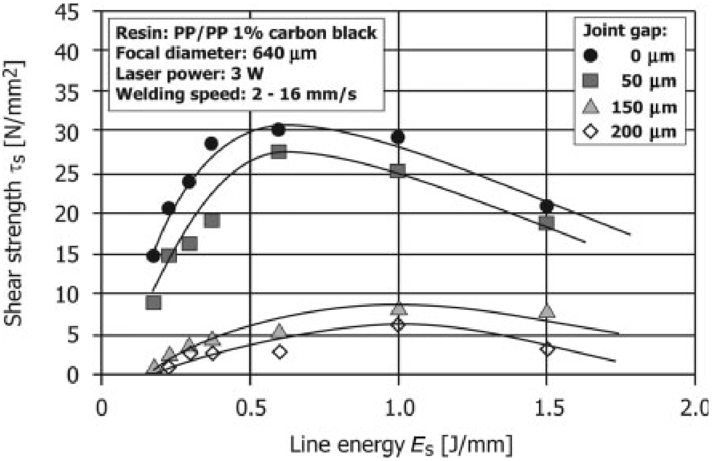

Figure 4.65 Influence of joint gaps to the weld quality for laser welding PP resin with carbon black (1%) [64].

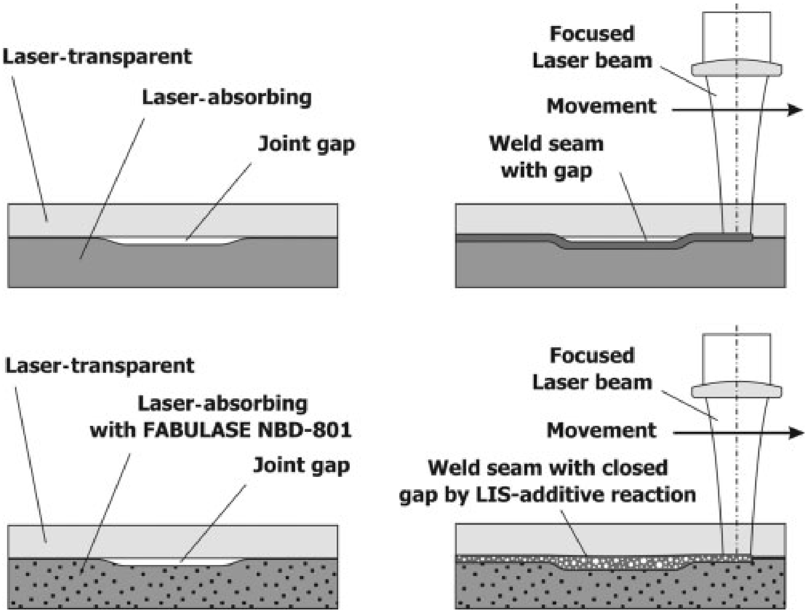

Figure 4.66 Joint gap causing a joint interruption (top) and avoiding this by using FABULASE NBD-801 in the laser-absorbing resin (bottom).

For enabling larger gap bridging, Chemische Fabrik Budenheim KG, Germany, has developed the innovative LIS process (laser-induced foaming process), using an additive composition (FABULASE NBD-801) for thermoplastic resins supporting a resin-volume increase of the laser-absorbing component during absorption of laser radiation (Figure 4.66, bottom).

This process is based on special heat-sensitive LIS agents that are mixed as additives into the resin before processing by molding or extrusion. During resin exposure to laser light, the laser-absorbing additive transforms the laser energy locally into process heat and heats up the resin. Simultaneously, a chemical reaction starts, resulting in local foaming of the resin in the area of laser interaction.

Thereby, the LIS process enables TTLW of plastic components having local joint gaps. At a joint gap the generated melt of the absorbing partner gets an additional volume expansion by a foaming process and can close gap dimensions to the laser-transparent component up to approximately 0.3 mm. By filling the gap the laser-transparent layer is melted and produces a close weld seam.

Figure 4.67 shows as an example the gap bridging for laser-beam welding of HDPE. As a process demonstration the gap was generated by a PET film of 350 μm thickness. The picture shows a micrograph of the cross section of the weld seam.

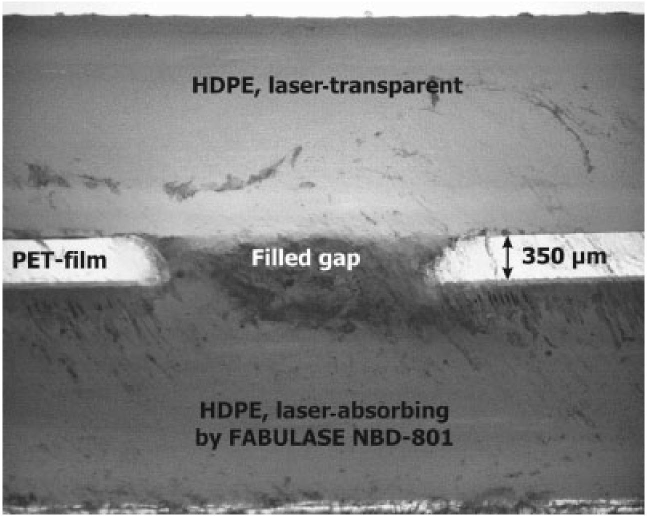

Figure 4.67 Gap bridging at laser-beam welding of HDPE by using FABULASE NBD-801, gap of 350 μm generated by PET film.

Caused by the local foam structure of the weld seam the strength of the weld can be possibly decreased somewhat. But the closed foam structure still enables a mechanically stable and tight weld of the components.

4.5
Methods of Quality Monitoring and Control

In most industrial applications of laser welding thermoplastic parts the laser-welding process is near to the end of the production chain. At this stage the product to be processed by laser radiation has gone through different previous process steps like component molding, assembling of internal mechanical or electronic components or other process steps. Hence, the work piece for laser welding has gained a monetary value and insufficient laser welding, especially for mass production, will become an economic issue.

During the entire laser application specific production chain part product quality monitoring and online control of the laser-welding process can be done to ensure high quality of the processed work pieces and avoid economic loss. Quality monitoring and control related to laser welding can be split into production stages before, during and after laser processing. Different monitoring and control techniques for these production stages are given in Figure 4.68.

Laser-welding-related monitoring and control techniques used before and during laser processing will be described in the following. Techniques for quality control after laser processing like mechanical testing of weld strength or optical analysis by

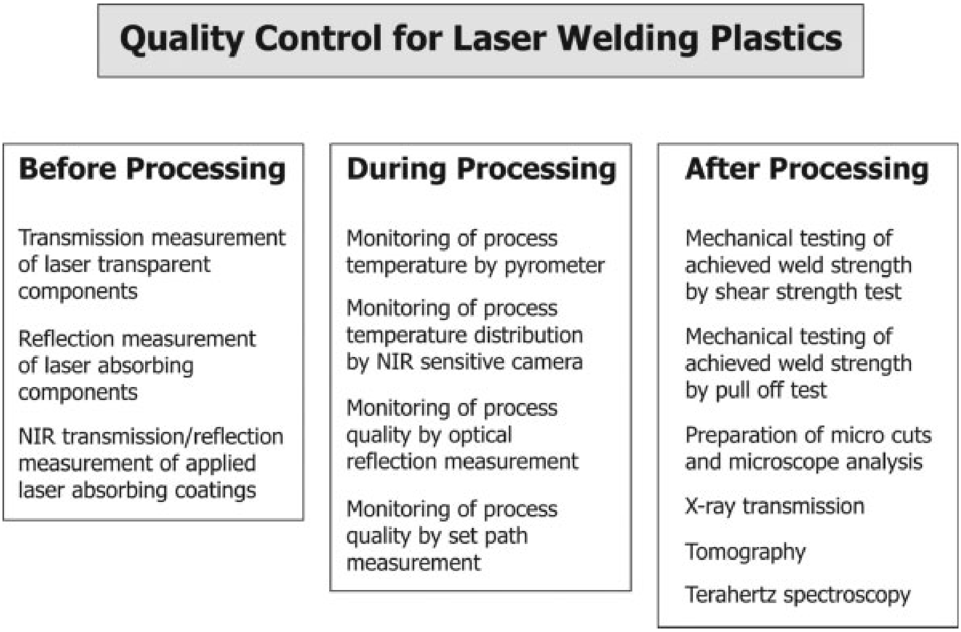
Quality Control for Laser Welding Plastics
Before Processing
Transmission measurement of laser transparent components
Reflection measurement of laser absorbing components
NIR transmission/reflection measurement of applied laser absorbing coatings
During Processing
Monitoring of process temperature by pyrometer
Monitoring of process temperature distribution by NIR sensitive camera
Monitoring of process quality by optical reflection measurement
Monitoring of process quality by set path measurement
After Processing
Mechanical testing of achieved weld strength by shear strength test
Mechanical testing of achieved weld strength by pull off test
Preparation of micro cuts and microscope analysis
X-ray transmission
Tomography
Terahertz spectroscopy

Figure 4.68 Quality monitoring and control techniques for laser welding thermoplastic components.

microscopy are also used for other conventional joining techniques and will not be considered in the following.

4.5.1
Quality Control before Processing

For successful laser welding of thermoplastic components, the optical properties of the used resins are an important quantity. Transmission of the laser-transparent component dedicated to the laser wavelength used as well as the absorption of the laser-absorbing component have to meet the processing demands for successful laser welding. Usually, the optical properties for laser-transparent and -absorbing resins are decided on preliminary application tests and the material supplier has to ensure the constant quality of the delivered resins.

Nevertheless, changing the material supplier or changing the resin composition by the supplier without notification the processing company can affect different optical properties of the resins regarding to the needs of the laser-welding process. Too low a transmission of the laser-transparent component caused by laser light scattering or absorbing additives will reduce the laser intensity at the joint interface and can hinder successful laser welding. On the other hand, too low or too high absorption of the laser light by the absorbing component at the joint interface will also produce insufficient laser welding results.

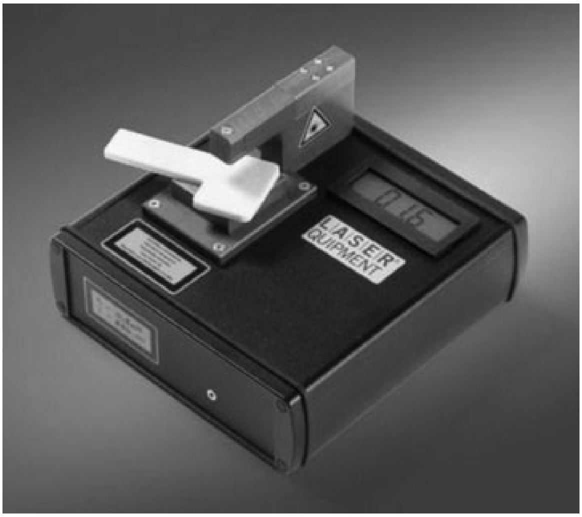

Figure 4.69 Control device for transmission measurement [66].

In the case of malfunctions during the welding process but also as permanent inline control to prevent interruptions of the production the optical properties of the components should be checked. This can be done by using different optical measurement devices.

For testing the transmission of the laser-transparent component in conjunction with the dedicated laser wavelength several measurement devices are available on the market [65, 66]. Figure 4.69 shows an example of such a transmission-measurement device.

The transmission measuring device shown in Figure 4.69 is equipped with a low-power laser diode having the same wavelength as used for laser welding of the components. In the case of interruptions of the laser-welding process the laser-transparent component can be checked for the transmission property to evaluate if the process malfunction is caused by insufficient transmission of the laser-transparent component.

Transmission-measuring devices can also be adapted as an inline control system for laser welding mass production [67] to ensure that only components with sufficient transparency will be supplied to the laser-welding process. The device will measure the transmission of the laser-transparent component and a supervising controller will compare the measured transmission value with a predefined value. If the measured transmission value does not match the predefined value in a given range the defective component will be separated from the production chain to avoid laser welding.

In some cases transmission testing using devices as shown in Figure 4.69 may not be sufficient for component quality monitoring before laser welding. Combined monitoring of transmission and coloration of the laser-transparent component as well as absorption and coloration of the absorbing component can be done by using spectral photometers like VIS-NIR spectrometers. Such devices can measure

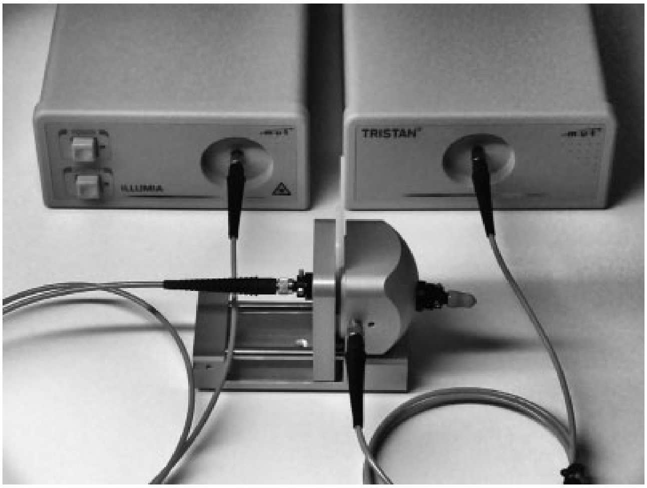

Figure 4.70 Low-cost fiber-coupled VIS-NIR spectrometer with sample holder and integrating sphere for transmission and reflection measurement.

transmission and reflection over the entire wavelength spectral range in the visible (VIS) and near-infrared (NIR) regions.

Beside, cost-intensive high-standard laboratory spectrometer equipment low-cost fiber coupled mobile spectrometers can be used for quick optical component analysis, as shown in Figure 4.70 [68]. The device consists of a light source (rear left) fiber coupled to the sample holder (in front) with an integrating sphere, the integrating sphere is again fiber coupled to the spectrometer device (rear right).

Figure 4.70 shows the system configuration for transmission measurement. The radiation from the light source will pass the component to be tested, will be collected by the integrating sphere and guided by the glass fiber to the spectrometer unit. For the reflection measurement configuration the glass fiber from the light source will be coupled into the integrating sphere by the connector at the right side of the sphere. For signal analysis the spectrometer is connected to a PC by an USB interface.

A special case for preprocessing quality control is the analysis of sufficient application of a laser-absorbing coating by NIR imaging. Depending on the optical properties of the component the measurement can be done by transmission through or reflection by the coated component using NIR radiation. Figure 4.71 gives an example of NIR-transmission imaging of a visually transparent component with (lower sample) and without (upper sample) applied laser-absorbing coating [69].

If the imaging recording is done by an electronic CCD camera, the images taken can be processed and analyzed by a PC as a control system to decide if the coating process was sufficient for laser welding or not. Insufficiently coated components will be separated from the production chain to avoid laser welding of defective components.

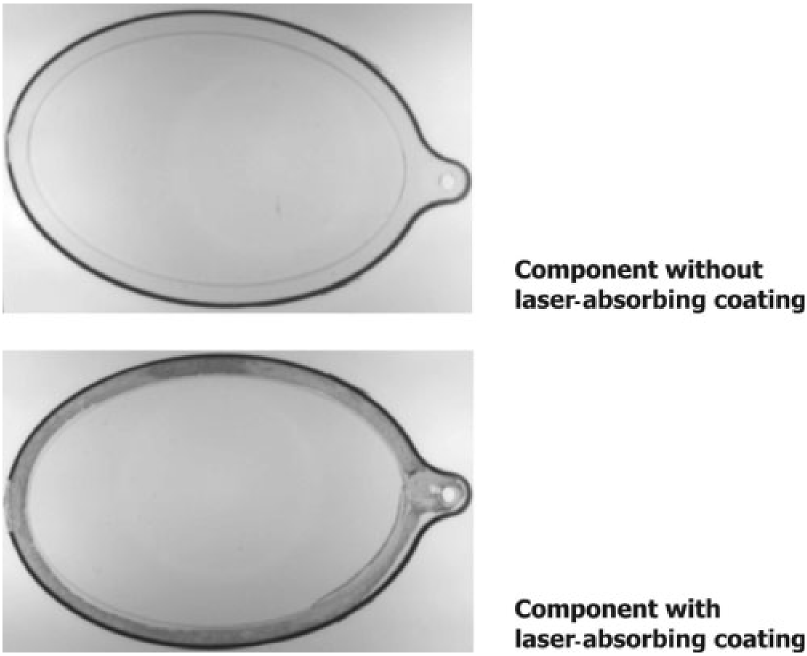
Component without laser-absorbing coating
Component with laser-absorbing coating

Figure 4.71 NIR imaging of uncoated sample and sample with laser-absorbing coating on the joint interface [69].

4.5.2
Quality Control During Processing

Laser welding of thermoplastic parts has the advantage of using different techniques to monitor the welding process for quality control of the processed work pieces. Techniques like thermal, optical or mechanical sensing during the laser-welding process are well developed for industrial application and enable quality control of the processed parts, to decide if the processed part is of sufficient quality or not.

Some of the applied monitoring techniques can also be used for closed-loop interaction to regulate the laser power during processing to achieve high-quality laser welding of the work piece. In the following, the different process-monitoring techniques used in industrial applications will be briefly described.

4.5.2.1 **Pyrometric Monitoring**

Laser welding of thermoplastic resins is based on absorption of the laser radiation and generation of heat at the joint interfaces of the components to be welded. The heating of the resin at the joint interfaces induce emission of thermal radiation with intensity and wavelength distribution correlated to the temperature of the resin (the resin is assumed to be a black-body emitter) according to Planck's radiation law (Figure 4.72) [70].

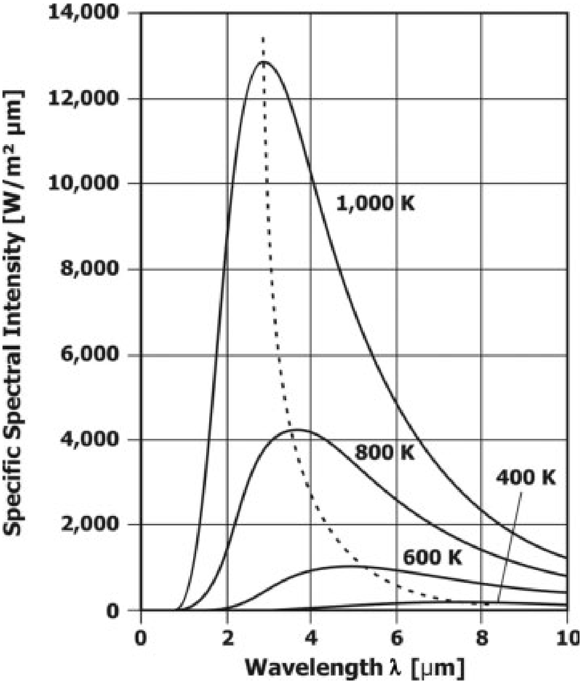

Figure 4.72 Planck's law for black body radiation for different temperatures of the emitting material.

In principle, Planck's law express that with increasing temperature of a solid body the wavelength with maximum intensity of the emitted spectrum will decrease to lower wavelengths and the entire spectrum will rise to higher intensity values. These changes of the spectral course can be measured for example, by spectrometers sensitive in the NIR and IR range. But low-cost spectrometers are typically not fast enough for online monitoring during laser welding or if they are capable they are of high investment costs.

Also, the intensity of the thermal radiation at temperatures of melting thermoplastics is very low and the intensity maximum is around 8–10 µm. To be suitable for temperature measurement of the laser welding interaction zone highly sensitive detector techniques working with wavelengths where the upper layer is transparent are necessary.

A common technique for online thermal sensing during laser welding thermoplastics is based on measuring the emitted spectral intensity in a dedicated small band wavelength range by using adequate sensor systems. Such a sensor system is for example a pyrometer (Figure 4.73) built by an optical detector sensitive to NIR radiation [71]. Typical detectors for this application are InGaAs detectors with sensitivity in the VIS and NIR region up to 2.5 µm [72].

An optical filter in front of the detector will reduce the wavelength range of the thermal radiation to, for example, 1.4–2.6 µm. The cutoff of shorter wavelengths will

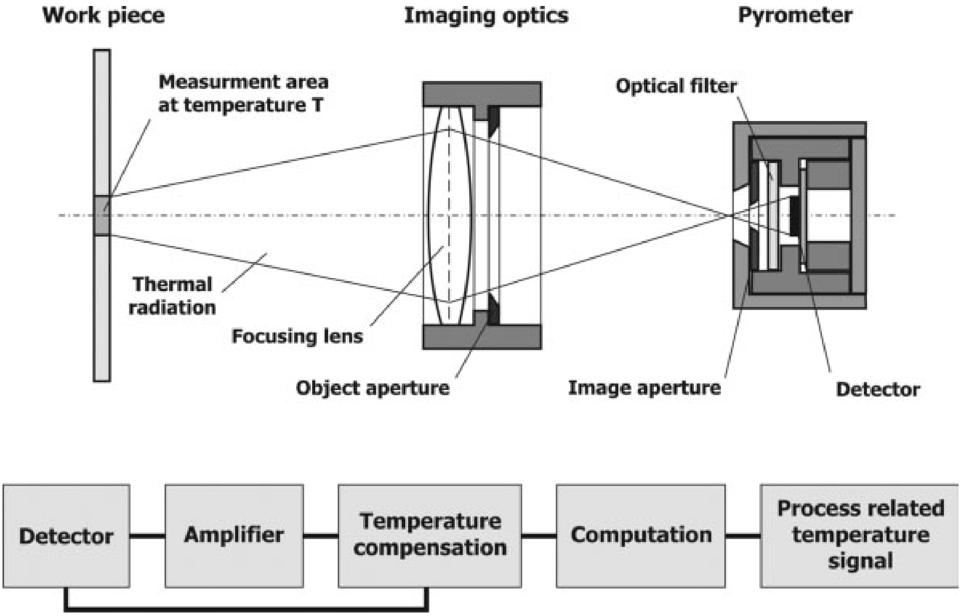

Figure 4.73 Principle setup of pyrometer sensor [71].

also prevent the detector from noticing from the component surfaces reflected laser radiation of the commonly used laser sources for plastic welding in the wavelength range from 800 to 1100 nm.

The optical detector transforms the measured intensity of the thermal radiation into an electrical signal that will be amplified and sent to an electronic controller device. Computation of the electrical signal by adequate software installed at the controller device will result in temperature information related to the laser-welding process.

Joining gaps, impurities of the material or carbonization of the resin by too high a laser intensity will cause changes of the thermal radiation and thus changes in the electrical signal sent by the pyrometer.

The recorded temperature course during the welding process can be electronically stored for inline-process monitoring to gain an assessment of the process quality to each laser-welded work piece or, when computation can be done quickly enough, for closed loop laser-welding process control to ensure high-quality processing.

Typically, the pyrometer is integrated into the focusing optics device, as shown schematically in Figure 4.74. The thermal radiation emitted by the laser interaction area passes the focusing lens and a semitransparent bending mirror and is focused onto the pyrometer detector.

For closed-loop control of the laser-welding process the measured temperature is compared with a preset temperature window by an electronic controller device. When the temperature window is left, the electronic controller will influencing process parameters, usually the laser power, to readjust the process temperature back to the process window.

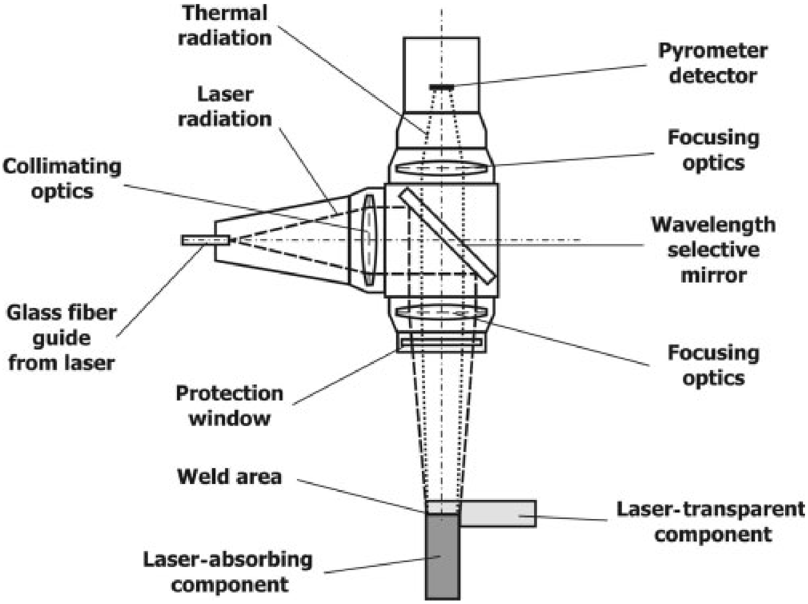

Figure 4.74 Laser-focusing head with integrated pyrometer.

Figure 4.75 gives an example of a closed-loop laser-welding process. The top photo and graphic shows the result of an uncontrolled laser welding. Using constant laser power results in overheating at the reverse points of the weld path because of speed ramping by the feeding system. With closed-loop control by temperature measurement and online regulation of the laser power a constant weld quality without overheating can be achieved.

An obstacle for temperature measurement at the joint interface by pyrometer is the transparency for the thermal radiation of the upper (laser-transparent) component resin. Small thicknesses, large grade of transmission in the detector range, negligible scattering influences as well as bridgeable gaps between the joining partners are the best conditions for application of pyrometers. Absorption and scattering of laser and heat radiation in the transparent joining partner diminish the pyrometer signal – increasingly with thickness of the transparent joining part. For glass-fiber-reinforced POM and PBT the use is limited to thicknesses of less than 2 mm [74].

When the resin has low transparency the pyrometer possibly will not detect the temperature signal of the interaction zone but a thermal history of the process at the surface of the laser-transparent part. In this case, the pyrometer measurement has only limited value for process control and the application has to be tested for reliability.

Pyrometers for temperature control are mainly used in conjunction with contour welding applications. They have only limited or no capability for use with quasisimultaneous and simultaneous laser welding. For such laser-welding processes thermography by an IR camera or digital imaging with NIR-sensitive cameras like

Without temperature control

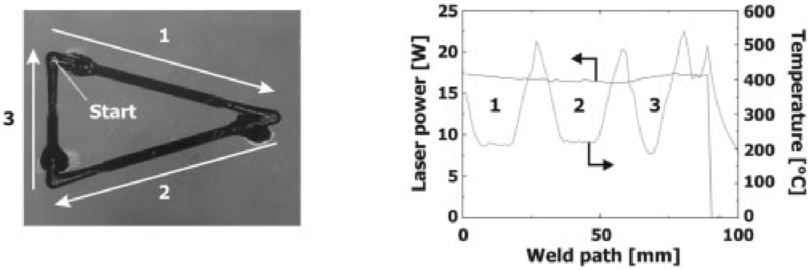

With temperature control

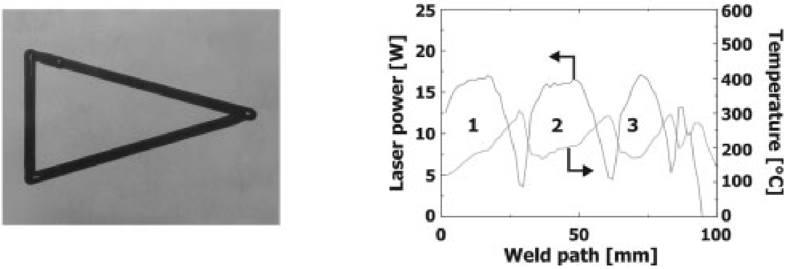

Figure 4.75 Laser welding of SAN without and with temperature control by pyrometer [73].

CCD or CMOS cameras are in principle alternatives for temperature control during laser welding. But both alternatives are limited in application.

4.5.2.2 **Thermography Monitoring**

Thermography cameras work in the spectral range of IR radiation, for example, having a spectral sensitivity range from 3.4 to 5 μm [75]. Radiation of this wavelength range will not be transmitted by typically used optical elements for NIR-laser beam guiding made from glass or fused silica glass elements for focusing lenses and beamsplitters. Hence, thermography cameras cannot be integrated into a laser focusing head like pyrometer detectors, but external positioning of a thermography camera can be an option as shown schematically in Figure 4.76.

The angle of observation with a thermography camera should be as close to the beam axis of the focusing head as mechanically possible to reduce image distortion for process sensing. IR-radiation emission hampering clamping components like PMMA or glass elements has to be avoided and the laser-transparent component of the work piece should be as thin as possible to enable thermal sensing of the joint interface of the work piece.

The controller of the thermography camera is linked to the laser welding system controller for start/stop of the sensing action simultaneously to start/stop the welding process. This enables thermal monitoring of the welding process for each work piece and storage of the thermal history allows assignment of the achieved weld quality to individual work pieces during serial production.

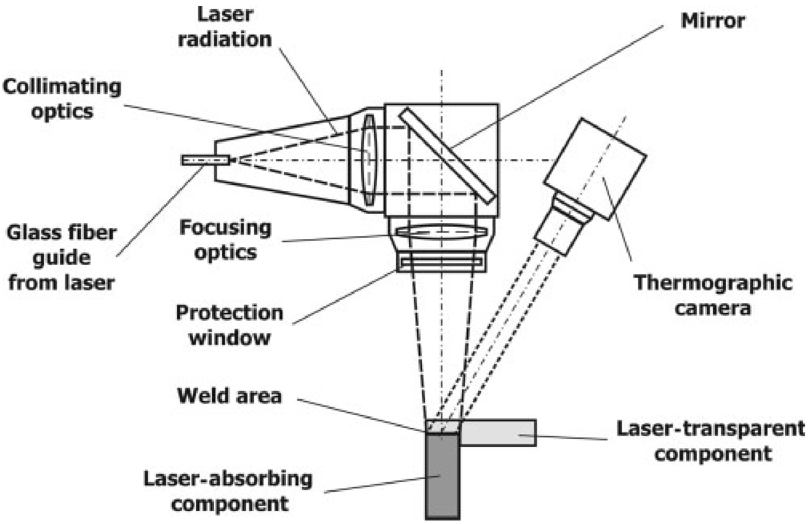

Figure 4.76 Laser-focusing head with external thermography camera.

The external positioning of the thermography camera to the laser focusing head enables thermal sensing independent of the welding process used. Thus, thermal process monitoring can be used for contour, quasisimultaneous and simultaneous laser welding thermoplastics.

Figure 4.76 gives an example of thermography camera sensing of contour laser welding PET films [76]. The thermographic images are taken with varying laser power and feed-rate parameters by constant focusing conditions and compared with the achieved peel strength of the welded film samples. The images left and right outside show more intensive thermal imprints than the center images corre-

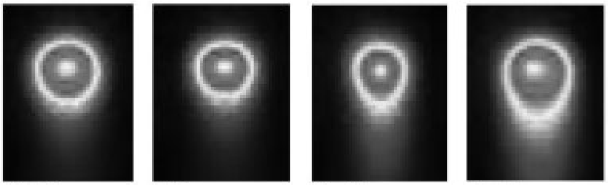

Number:	8_21	8_3	9_45	9_70
Power:	16,4 W	8,6 W	8,6 W	34,4 W
Feed rate:	33,3 mm/s	33,3 mm/s	100 mm/s	133,3 mm/s
Line Energy:	492 J/m	257,6 J/m	85,9 J/m	257,8 J/m
Peel Strength:	10,8 N	9,7 N	9,5 N	12,4 N
Thermo. Signal:	135,2 a.u.	126,1 a.u.	101,2 a.u.	136,6 a.u.

Figure 4.77 Thermography camera images of laser welding PET films using different welding parameters [76].

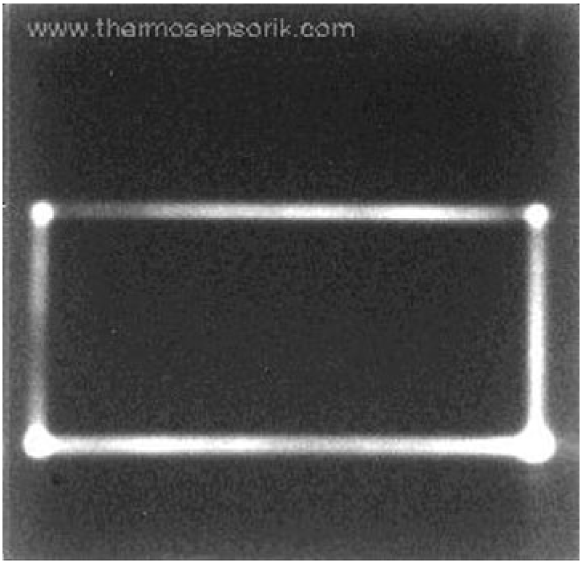

Figure 4.78 Thermography imaging of simultaneous laser-welding process [77].

sponding with higher peel strengths. Additionally, the two right images taken at higher feed rates demonstrate the speed-dependent cooling rates of the resin during processing.

An example of thermography-camera monitoring of a simultaneous laser-welding process is given in Figure 4.78. A rectangular work piece is irradiated simultaneously by six diode laser modules applying an entire laser power of 80 W during a time period of 0.6 s. The IR image of the weld seam geometry in Figure 4.78 was taken when the laser processing was stopped. Although a higher heat radiation emission is detected at the corners, the entire weld seam is tight and withstands a burst pressure of about 10 bar [77].

Commonly, high temperature at the corners as well as inhomogeneous intensity distribution corresponding to the emitted heat radiation along the straight segments may cause reduced weld quality by alternating areas of sticking, good weld joint and decomposition for the molten resin. Applying thermography camera monitoring enables adaption of the laser intensity distribution by power control and adjustment of the individual laser modules to generate uniform weld seams. By thermography camera monitoring of the welding process joint defects like gaps or overheating can be detected. Computation and analysis of the thermography camera signals by suitable image processing software can be used for assignment of the achieved weld quality to individual work pieces during serial production [77].

4.5.2.3 **Digital Imaging Monitoring**

For applying digital imaging techniques to monitor the laser-welding process of thermoplastics, CCD or CMOS cameras in combination with electronic image

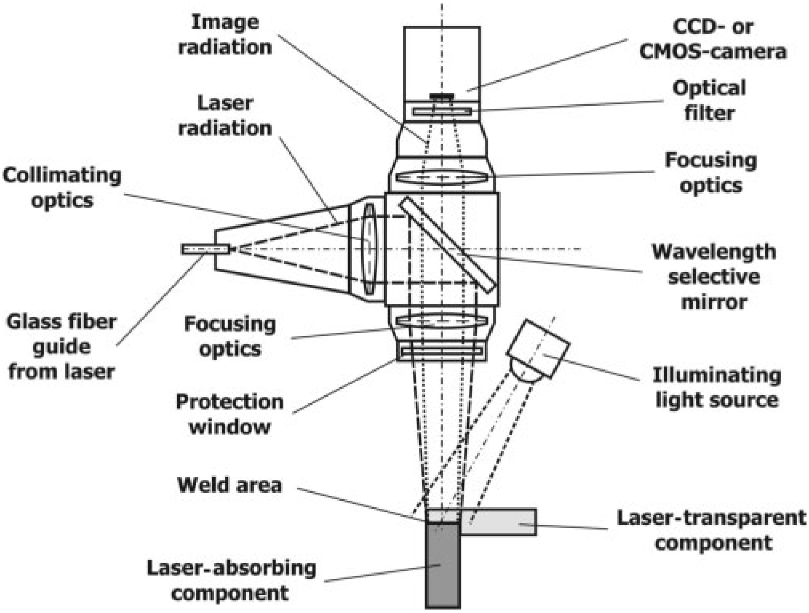

Figure 4.79 Laser focusing head with integrated digital imaging camera.

processing can be used. Adequate CCD- or CMOS-cameras are sensitive in the VIS and NIR spectral ranges, for example, from 400 nm up to 900 nm for a high-speed CMOS camera system [78]. Such camera systems can be integrated into a laser focusing head for inline temperature monitoring, as shown schematically in Figure 4.79.

Using external light sources to illuminate the laser interaction area will increase the camera sensitivity and supports the imaging process by the camera. Some camera systems can be sensitive up to wavelengths above 1000 nm. In this case, additional optical filters in the light path from the work piece to the camera have to be used to block the laser radiation, avoiding insufficient function of the camera.

Like using thermography cameras digital imaging cameras in combination with electronic image processing linked to the laser welding system controller can be taken for process monitoring of laser welding thermoplastics. Simultaneous start/stop action of the sensing camera and the laser-welding process enables monitoring of the welding process for each work piece and storage of the processed imaging course allows assignment of the achieved weld quality to individual work pieces during serial production.

Digital cameras integrated into the focusing optics enable quality monitoring during contour laser-welding process, as shown in Figure 4.80 for laser welding of PET films [76].

Quality monitoring of quasisimultaneous or simultaneous laser welding thermoplastics can also be done by digital imaging.

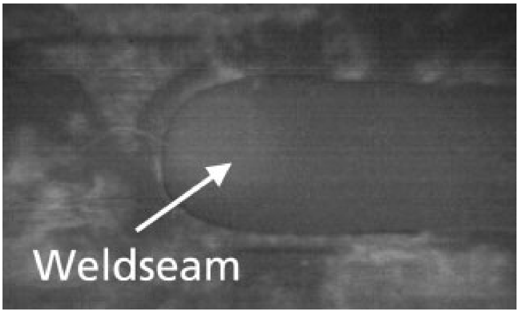

Figure 4.80 Digital imaging of contour laser welding PET films [76].

4.5.2.4 **Optical Reflection Monitoring**

Measurement of the optical reflection at the joint interface during the laser-welding process is an additional technique for weld-quality monitoring. The joint interface will be illuminated by an additional light source, for example, a visible laser pointer, and the backscattered reflected radiation will be measured by a photometric detector. Alternatively backscattered laser radiation can be used for online reflection monitoring.

During regular laser welding there is only one interface between the laser-transparent and the laser-absorbing component able to reflect a certain proportion of the incident laser radiation (Figure 4.81, left). In the case of joint gaps occurring, two interfaces will be available for radiation reflection, resulting in an increase of the

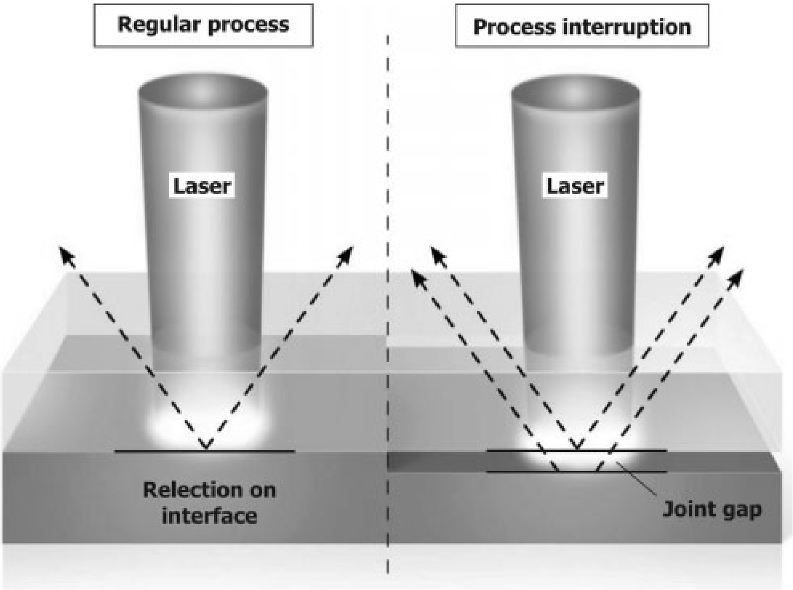

Figure 4.81 Reflection of laser radiation on the joint interface for regular and interrupted process [79].

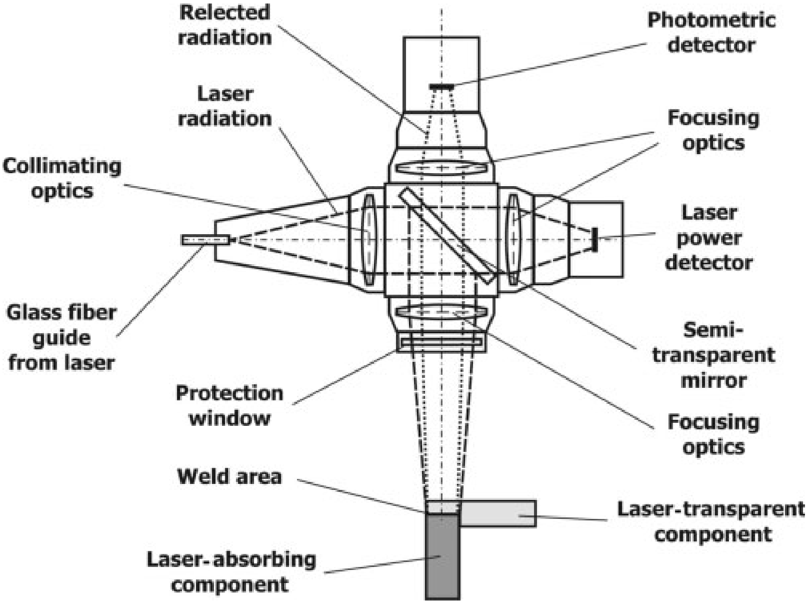

Figure 4.82 Laser-focusing head with integrated optical reflection measurement.

radiation intensity detectable by the photometric detector (Figure 4.81, right). Also, material impurities and carbonization of the resin will cause a change of the reflected radiation.

As for pyrometers, the photometric detector can be integrated into the focusing head, as shown schematically in Figure 4.82.

Alternatively, the reflection diagnostic can also be done as an offline detection process. In this case, the joint path of the work piece will be scanned by low-power laser radiation before and after the laser-welding process [80]. Comparison of both measurements enables the assessment of the weld-seam quality in terms of weld seam interruption, narrowed weld seam width as well as decomposition of the weld seam generated [74].

Like pyrometry, photometry is a monitoring technique suitable for contour laser-welding processes. Obstacles for photometry application are, for example, high crystallinity as well as high glass-fiber or other radiation-scattering additive contents of the laser-transparent component.

4.5.2.5 Mechanical Set-Path Monitoring

Quasisimultaneous or simultaneously laser welding of thermoplastics enables the use of a set path during the laser-welding process. As a quality criterion for the welding process the course of the set path during processing can be measured by monitoring the applied clamping force using piezo sensors or measuring the actual set-path course by mechanical motion sensors.

Figure 4.83 shows a measured set-path course as a function of the welding time during quasisimultaneous laser welding of PA6 with 0.1% carbon black in the laser-

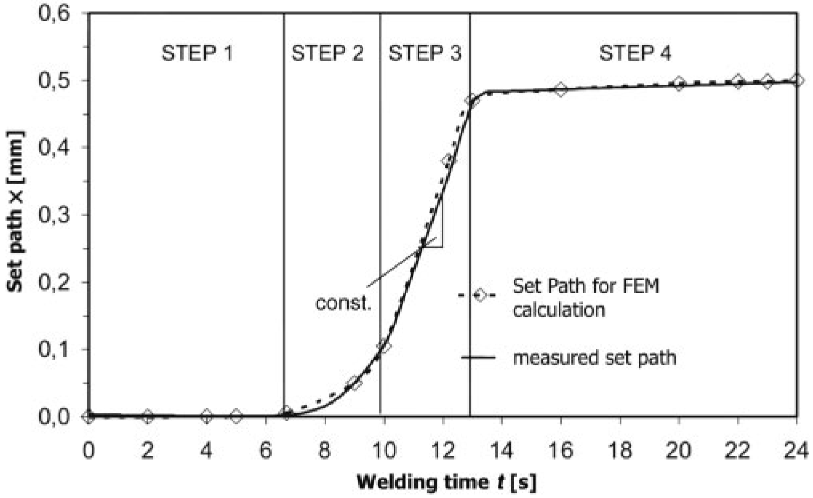

Figure 4.83 Measured set-path course in correlation with the welding time for quasisimultaneous laser welding of PA6 with 0.1% carbon black in the laser-absorbing component [81].

absorbing component, a scan speed of 8 m/s and a clamping pressure of 1 MPa [81]. The set-path course is distinguished into four process phases:

- Step 1: Start of laser irradiation and heating the resin without plastification.
- Step 2: Increasing temperature and start of plastification with nonlinear set-path course.
- Step 3: Increasing temperature with linear set-path course.
- Step 4: Stop of laser irradiation and cooling down of the resin.

During evaluation of suitable work piece processing parameters before start of mass production the set-path course corresponding to high-quality welding results will be stored as a data basis for comparison of measured set-path courses during production. Changes in the measured set-path course compared to the reference course will indicate insufficient weld-seam quality.

4.5.2.6 **Summary of Monitoring Techniques**

As briefly discussed previously, several different monitoring and control techniques can be applied for laser welding thermoplastic components to achieve information about the quality of the processed work piece. Reasons to use process and quality monitoring are, among others [82]:

- check infrared absorber is applied correctly to parts before welding;
- view of weld during process;
- indication that parts are in contact during process;
- indication that weld heating is being carried out and control of temperature;
- view of weld after completion;
- indication that parts are in contact after completion;

- indication that weld has been achieved after completion;
- indication that weld quality and strength are satisfactory.

Monitoring methods can give information for most of these points with varying degrees of confidence, however, it must be noted that a complete quality and weld strength assurance can only be achieved with destructive testing.

Several monitoring techniques like laser-power control, pyrometer, photometric detector or digital imaging can be integrated into the laser focusing head, as shown exemplarily for a contour laser welding head in Figure 4.84. Other techniques, like IR thermography can be added to the processing head or like set-path control can be integrated into the work-piece clamping device.

Some of the monitoring techniques are dedicated to contour laser welding while others are more suitable for quasisimultaneous or simultaneous laser welding. Table 4.1 gives an overview of the different monitoring techniques with main applications concerning the welding processes and the options of quality control for the processed work piece.

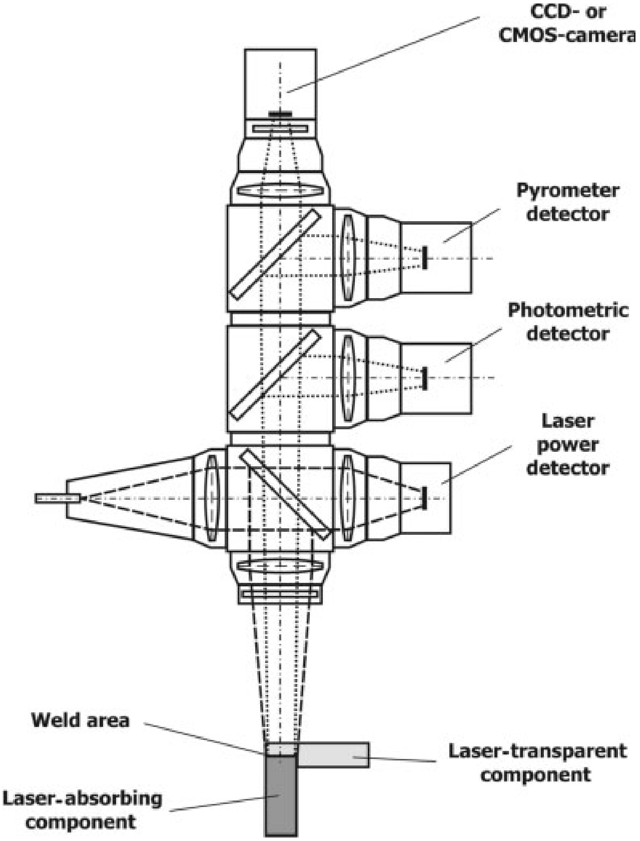

Figure 4.84 Options for process monitoring during laser welding thermoplastics.

Table 4.1 Quality-monitoring techniques and their main applications concerning basic plastic laser-welding processes as well as online process control used for industrial applications.

Sensor	Sensitive for	Type of measurement	Can be used with:			What can be detected	What can be controlled online during processing
			contour	quasisimult	simult		
Power meter	Laser power	Integral	■	■	■	Magnitude of laser power, time-dependent power fluctuations of laser	Laser power course during interaction
Pyrometer	Thermal radiation	Integral	■	□	□	Joint interruptions, thermal degradation	Laser power or welding speed course during interaction
Thermographic camera	Thermal radiation	Spatial	■	■	■	Homogeneity of laser intensity, joint interruptions, thermal degradation	
CCD or CMOS camera	Visible and NIR radiation	Spatial	■	■	■	Homogeneity of weld joint, joint interruptions, thermal degradation	
Photometric sensor		Reflected radiation	Spatial	■	■	■	Joint width, Joint interruptions, thermal degradation
Piezosensor	Set path	Linear way	□	■	■	Set path way	Time of laser power interaction during processing

References

1 Anscombe, N. (2004) Laser welding penetrates the plastic market. *Photon. Spectra*, **61**, 60–66.

2 Brunnecker, F. and Ebenhöh, C. (2006) Wettlauf mit Strahlen; *Kunststoffe, 10/2006*, C. Hanser Verlag, München, pp. 211–214.

3 Roesner, A., Boglea, A., and Olowinsky, A. (2008) Laserdurchstrahlschweissen von Thermoplasten. *Laser Technik Journal*, 4/2008, Wiley VCH Verlag, Weinheim, pp. 28–32.

4 Klein, R. (1990) Bearbeitung von Polymerwerkstoffen mit Infraroter Laserstrahlung, Thesis, RWTH Aachen.

5 Ebert, T. (1999) Den Durchblick behalten – Transparente Kunststoffe mit Laser Fügen, *Kunststoffe, 12/1999*, C. Hanser Verlag, München, pp. 58–60.

6 Korte, J. (1998) Laserschweissen von Thermoplasten, Thesis, Universität GH Paderborn.

7 Klein, R. (2007) Laserstrahlschweissen transparenter und farbiger Kunststoffe. *Laser Technik Journal*, 4/2007, Wiley-VCH Verlag, Weinheim, pp. 41–44.

8 Klein, R. and Wissemborski, R. (2010) Welding and marking of plastics with lasers. *Laser Technik Journal*, 5/2010, Wiley-VCH Verlag, Weinheim, pp. 19–22.

9 Roesner, A. (2010) Laserverfahren für Kunststoff-Metall-Verbindungen. Proceedings ALASKA-Seminar 2010, Aachen.

10 Russek, U.A. (2006) *Prozesstechnische Aspekte des Laserdurchstrahlschweissens von Thermoplasten*, Shaker Verlag, Aachen.

11 Jansson, A. and Kouvo, S. (2005) New innovations in quasi-simultaneous laser welding of polymers for mass-production application. Proceedings ALAC 2005 Conference.

12 Grewell, D. (2001) Laser Diode Array, US Patent 6,205,16.

13 N. N.; (2004) Iram-Technology – Laser Welding Systems, Branson technical info brochure.

14 Traub, M. and Hoffmann, H.-D. (2004) Prozessangepasste Optik zum Simultanschweissen von Kunststoffbauteilen, Annual Report 2003, Fraunhofer-Institute for Lasertechnology, p. 36.

15 Poggel, M., Gillner, A., and Russek, U. (2006) *Joining with Light; Kunststoffe, 3/2006*, C. Hanser Verlag, München.

16 Grewell, D.A. (2005) Modeling of Molecular Healing for Micro-Laser Welding of Plastics with Diffractive Optical Elements as Spatial Modulators, Thesis, The Ohio State University.

17 Haberstroh, E. and Hoffmann, W.M. (2007) Laser transmission welding of transparent plastic parts in micro technology. 4M2007 Conference Multi-Material Micro Manufacture, Borovets, Bulgaria.

18 Chen, J.W. and Hessler, T. (1999) Transmission laser welding of plastics for microsystem packaging. *Proc. Micro Eng.*, **99**, 81–88.

19 Olowinsky, A., Boglea, A., and Gedicke, J. (2008) Innovative laser welding processes – twist and shadow in microtechnology. *Laser Technik Journal*, 3/2008, Wiley-VCH Verlag GmbH & Co. KGaA, Weinheim, pp. 48–51.

20 Boglea, A. and Gillner, A. (2008) Twist – Neues Verfahren für das Mikro-Schweissen von Kunststoffen, Annual Report 2007, Fraunhofer-Institute for Lasertechnology, p. 88.

21 Boglea, A. and Gillner, A. (2009) Twist – Erweiterung der Prozessgrenzen beim Laserschweissen von Kunststoffen, Annual Report 2008, Fraunhofer-Institute for Lasertechnology, p. 93.

22 Chen, J.W. and Thielen, C. (2004) Globo-welding – ein innovatives Konzept für das 3D-Laserfügen von Thermoplasten im Durchstrahlverfahren. *Laser Technik Journal*, 2/2004, Wiley-VCH Verlag GmbH & Co. KGaA, Weinheim.

23 Hinz, O. (2008) *Laserstrahlschweissen von Kunststoffen; Maschinenbau 2/2008*, Publica-Press Heiden AG, Heiden, Schweiz, pp. 35–38.

24 Geiger, R., Brandmayer, O., and Frick, T. (2007) Hybrid welding of plastics - the combined utilization of laser radiation and heating radiation during the welding

process opens up totally new fields of application. *Joining Plastics*, **2** (07), 144–152. DVS Media, Düsseldorf.

25 N.N.; (2005) NIR Halogen Infrared Emitters for Heating and Drying Processes, Product information brochure, Heraeus Noblelight, Kleinostheim.

26 Chou, M.M., Tam, H., Yu, K.J.J., and Yu, K.T. (2000) Combined Ultrasonic and Laser Device and Method for Use, US Patent 6,039,565.

27 Keisuke, E. and Akihiko, T. (2007) Manufacturing Method of Optical Sheets for Display, Patent WO 2007/032451A.

28 Vatterodt, T. and Hänsch, D. (2006) *Nähen ohne Faden; Kunststoffe 10/2006,* C. Hanser Verlag, München, pp. 221–224.

29 Weck, M., Herberg, F., and Kerstiens, P. (1989) Entwicklung von Werkzeugmaschinenkomponenten aus Kohlefaserverstärktem Kunststoff. Proceedings of Symposium Faserverbundtechnologie für den Maschinenbau, Aachen, Germany, pp. 93–114.

30 Beyerler, E., Phillips, W., and Güceri, S.I. (1988) Experimental investigation of laser assisted thermoplastic tape consolidation. *J. Thermoplast. Compos.*, **1**, pp. 107–121.

31 Grove, S.M. (1988) Thermal modelling of tape laying with continuous carbon fibre-reinforced thermoplastics. *Composites*, **19** (5), pp. 367–375.

32 Klein, R. (1991) *Kunststoffe mit Laser verbinden; Technica 12/91,* Industrie Verlag AG, Zürich.

33 Kok, C. (2008) Laser welding of fiber reinforced thermoplastic plastics. Proceedings AKL'08, Aachen.

34 Kölzer, P. (2008) *Temperaturerfassungssystem und Prozessregelung des Laserunterstützten Wickelns und Tapelegens von endlos faserverstärkten Thermoplastischen Verbundwerkstoffen,* Shaker Verlag, Aachen.

35 N.N.; (2005) EFD automated dispensing systems for the clearweld process, Product information brochure, EFD Inc., Rhode Island, US.

36 Cawley, B. (2005) User's Guide For Clearweld/EFD Dispensing Kits, Product information brochure, Gentex Corp, Carbondale, US.

37 Klein, R. and McGrath, G. (2006) Creating transparent laser weldings on thermoplastic components. Proceedings Joining Plastics Conference 2006, London, UK.

38 N.N.; (2005) Consistent, Precise 781S Spray Valve Systems, Product information brochure, EFD Inc., Rhode Island, US.

39 Berger, H.L. (1998) *Ultrasonic Liquid Atomization – Theory and Application;,* Partridge Hill Publishers, Hyde Park, US.

40 N.N.; (2006) Ultrasonic Spray Nozzle Systems, Product information brochure, SonoTek, Milton, US.

41 Jones, I.A. and Wise, R.W. (1998) Welding Method; WO patent 00/20157.

42 Jones, I.A., Wise, R.W., and Hilton, P. (2001) The Clearweld Process for Laser Welding of Plastics and Fabrics, White paper, The Welding Institute (TWI). Cambridge, UK.

43 www.clearweld.com.

44 McGrath, G. (2003) *Laserschweißen Transparenter Bauteile, Kunststoffe 10/2003,* C. Hanser Verlag, München.

45 Klein, R. and McGrath, G. (2007) Process for laser welding transparent plastics. Proceedings LIM 2007 Conference, Munich, DE.

46 Klein, R. and McGrath, G. (2007) Laser welding transparent plastics. Proceedings LANE 2007 Conference, Erlangen, DE.

47 Woosman, N. and Sallavanti, R. (2003) Achievable weld strength for various thermoplastics using the clearweld process. Proceedings ANTEC'2003 Conference.

48 Anantharaman, S., Benatar, A., Woosman, N., and Hartley, S. (2003) Measurement of Residual Stresses in Clearwelds Using Photoelasticity. Proceedings ANTEC'2003 Conference.

49 Klein, R., Jansson, A., Kuovo, S., and Holt, T. (2006) The use of fiber lasers for welding polymers. ANTEC'2006 Conference.

50 Klein, R. and Wissemborski, R. (2011) *Marking and Welding in One Operation, Kunststoffe International 1/2011,* C. Hanser Verlag, München.

51 Haberstroh, E. and Hoffmann, W.M. (2011) *Schmelze aus der Zwischenschicht, Kunststoffe 6/2007*, C. Hanser Verlag, München, pp. 76–79.

52 Michaeli, W. and Hoffmann, W.M. (2008) Extending the joining spectrum of laser transmission welding NY multicomponent injection moulding. *Joining Plastics*, **2** (08), 134–149. DVS Media, Düsseldorf.

53 N.N.; (2005) LCT - Laser Color Transfer, Product information brochure, Merck KGaA, Darmstadt.

54 Boehm, A.J. and Glaser, A. (2004) The quaterrylimides - highly efficient NIR absorbers for plastics. Proceedings Antec.

55 Woosman, N.M. and Burrell, M. (2003) A study of the effect of weld parameters on strengths of clearwelded thermoplastics. Proceedings ICALEO.

56 Wolff, W. (2005) *Hochtransparente Kunststoffe dauerhaft Beschriften, Kunststoffe, 9/2005*, Carl Hanser Verlag, München.

57 N.N . Laser Transmission Welding at any Wavelength Product information brochure Lumogen, BASF SA (2007).

58 Roesner, A. (2007) Welding of transparent thermoplastics with fibre lasers. Proceedings LIM 2007 Conference, Munich, DE.

59 NN.; (2005) *Laserstrahlschweissen thermoplastischer Kunststoffe, Guideline DVS 2243*, DVS Media, Düsseldorf.

60 N.N.; Leitfaden zur fertigungstechnischen Gestaltung des Schweissbereiches beim Laserdurchstrahlschweissen von Thermoplasten, Supplementing document 2 for Guide line DVS 2243, DVS Media, Düsseldorf (to be published).

61 Poggel, M., Gillner, A., Otto, G., and Olowinsky, A. (2007) Welding of transparent thermoplastics with fibre lasers. Proceedings LIM 2007 Conference, Munich, DE.

62 Klein, H.M. (2001) Laser Beam Welding of Plastics in Micro Technology, Thesis, RWTH Aachen.

63 Schulz, J. (2002) Werkstoff-, Prozess- und Bauteiluntersuchungen zum Laserdurchstrahlschweissen von Kunststoffen, Thesis, RWTH Aachen.

64 Frick, Th. (2007) *Untersuchung der Prozessbestimmenden Strahl-Stoff-Wechselwirkungen beim Laserstrahlschweissen von Kunststoffen*, Meisenbach Verlag, Bamberg.

65 Vatterodt, T. and Hänsch, D. (2005) *Qualitätssicherung beim Laserschweissen, Laser 2-2005*, b-quadrat Verlag, Landsberg.

66 N.N.; (2006) LQ-TMG 2 Handheld Transmission Measurment for Plastics, Product information brochure, LPKF, Erlangen.

67 Polese, A. and Kirberg, K. (2005) Innovation in Laser Transmission Welding, DuPont Engineering Design Electroni Magazine 2005/2, pp. 14–15.

68 www.technoscriptum.de.

69 Klein, R. (2006) Laserschweissen Transparenter Kunststoffe mit dem Clearweldverfahren – Grundlagen und Anwendungen, Presentation 18. Oct. 2006 Fakuma Aussteller Forum.

70 Hecht, E. and Zajac, A. (1974) *Optics*, Addison-Wesley Publishing, Massachusetts.

71 Hollant, J., Hartmann, J., Gutschwager, B., and Struß, O. (2006) Strahlungsthermometrie – Temperaturen berührungslos Messen, atp-Sonderheft 6/2006.

72 N.N.; (2004) InGaAs-Detectors, Product information brochure, Teledyne Judson Technologies.

73 N.N.; (2001) Polyweld – Laser Diode Welding Of Polymers, Brite Euram Project, IMT/SMT programs, BE 97-4625, 1998–2001.

74 Russek, U.A. and Fox, T. (2007) Laser welding of polymers – process safety and industrial production. Proceedings Laser in Manufacturing (LIM) conference 2007, Munich.

75 N.N.; (2006) Variotherm Head, Product brochure, InfraTec GmbH, Jena.

76 Abels, P. *et al.* (2008) Various process monitoring approaches of transparent thermoplastics laser beam welding. Proceedings ICALEO 2008 Conference.

77 Russek, U.A. (2003) Innovative trends in laser beam welding of thermoplastics. Proceedings Laser in Manufacturing (LIM) Conference 2003, Munich, pp. 105–111.

78 N.N.; (2010) CMOS camera DS1 – D1312 Series, Product brochure, PhotonFocus AG, Lachen, Switzerland.

79 N.N.; (2010) *Licht als Qualitätsmanager*, Press Information LPKF, Erlangen.

80 Messler, A. (2004) Verfahren zum Herstellen und zur Kontrolle einer Schweissnaht mittels Laserstrahlung, Patent DE 102004036576B4.

81 Fiegler, G. (2007) *Ein Beitrag zum Prozessverständnis des Laser-Durchstrahlschweissens von Kunststoffen anhand der Verfahrensvarianten Quasi-Simultan- und Simultanschweissen*, Shaker Verlag, Aachen.

82 Jones, I. and Rudlin, J. (2006) Process monitoring methods in laser welding of plastics. Proceedings of Joining Plastics 2006 Conference, London.

5
Case Studies

Examples of process development of laser welding plastic parts will be given in the following, organized by the industrial branches automotive components, consumer goods, electronic devices, medical devices and others.

The majority of the examples given have been successfully transferred from the development state into industrial application with outstanding quality of the achieved weld joints and visual appearance of the processed parts showing the ability of laser welding plastics as an industrial joining method in competition with conventional joining technologies like adhesive bonding, ultrasonic welding, hot-plate welding or others.

Some of the given examples are results of feasibility studies not entering industrial production for some reason. But these examples still underpin the capacity and ability of laser plastic welding to achieve high-quality products and meet design and functional demands by this advanced joining technology.

The examples demonstrate the variety of part and joint sizes from the small scale, like microfluidic devices, up to the large scale like plastic chairs, as well as economical application of laser plastic welding for small and medium-sized production rates like oil reservoirs up to high mass production like air-bag sensors; laser welded several million parts per year.

Favorite laser-welding methods for industrial application are contour and quasi-simultaneously laser welding as shown by the case studies given. Simultaneous laser welding has only a marginal existence in industrial application and is not really present in the case studies given.

The case studies also demonstrate the fact that most of the applications use carbon black as an effective and economic additive for absorbing laser radiation. When black coloration of the laser-absorbing component is not desired and visual transparency or light coloration is required for design or functional reasons, organic dyes like Lumogen® or Clearweld® materials as additives or surface coatings are applied as laser-absorbing agents. Inorganic pigments like Fabulase are presently not in industrial application but in the state of entering production, offering economic benefits by lower costs than organic dyes in conjunction with good absorption properties for laser radiation and low influence to coloration of the parts.

Laser Welding of Plastics, First Edition. Rolf Klein.
© 2011 Wiley-VCH Verlag GmbH & Co. KGaA. Published 2011 by Wiley-VCH Verlag GmbH & Co. KGaA.

5.1
Automotive Components

Product: **Airbag Sensor**

Figure 5.1:

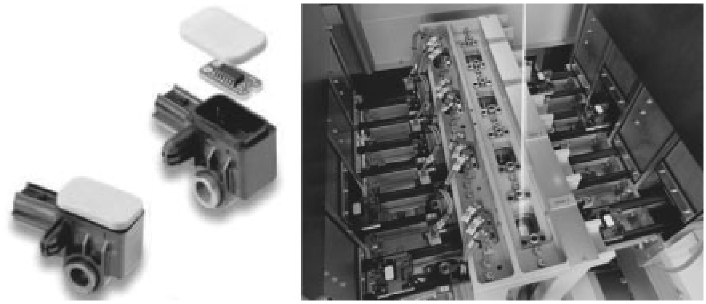

Material: Laser transparent: Cover white PBT GF 30,
Laser absorbing: Body black PBT GF 30 (carbon black as laser absorber)

Previous production method: New product, previous products joint by mechanical fasteners

Objectives: Gas- and liquid-tight weld seams, no temperature or vibration load of internal electronics, quality control of individual parts, enabling of part traceability, high mass production.

Solution: Quasisimultaneous laser welding, four parallel weld lines with one laser source and scanner, quality control by set path, quality assignment to each individual processed part.

Results: Welding of several million parts per year

Status: Industrial production

Source: System supplier: bielomatik, Neuffen, Germany
Product: Bosch, Spain

Product: **Display for Speedometer**

Figure 5.2:

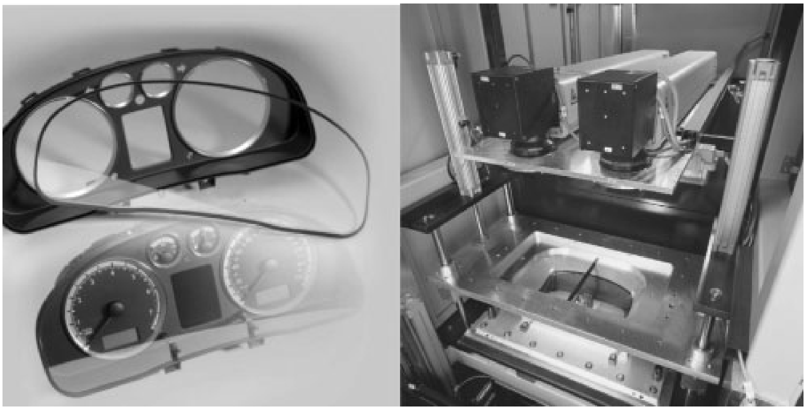

Material: Laser transparent: Lens transparent PMMA or PC,
Laser absorbing: Frame black ABS (carbon black as laser absorber)

Previous production method: Ultrasonic welding, vibration welding or mechanical fasteners

Objectives: No creaking noise, high optical appearance, quality control of individual parts, enabling of part traceability, mass production,

Solution: Quasisimultaneous laser welding, two laser source and scanners for part processing, quality control by set path detection, quality assignment to each individual processed part.

Results: High-quality weld joint, no creaking noise under use

Status: Industrial production

Source: System supplier: bielomatik, Neuffen, Germany
Product: Displays for Touran and Sharan; Continental, Germany

Product:	**Camshaft Sensor**
Figure 5.3:	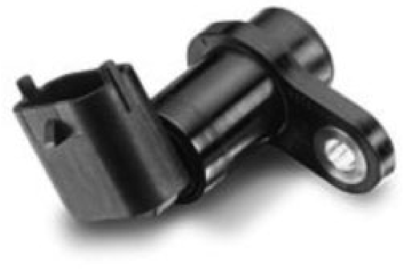
Material:	Laser transparent: Cover PA66 GF 30 laser-transparent black, Laser absorbing: Body black PA66 GF 30 (carbon black as laser absorber)
Previous production method:	Unknown
Objectives:	Strong, resistance against media (oil, gasoline, ethanol)
Solution:	Rotational laser welding (welding part rotates, fixed spot laser)
Results:	Strong resistant weld, short process time
Status:	Industrial production
Source:	System supplier: Leister Process Technologies, Switzerland Product: Delphi, Portugal

Product: **Fluid Reservoir for Hydraulic Pump**

Figure 5.4:

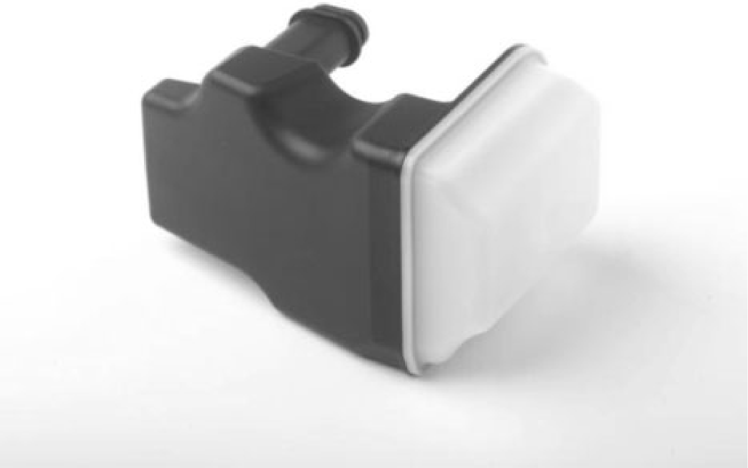

Material:	Laser transparent: Cover uncolored PA 66 (Grilon), Laser absorbing: Fluid reservoir black glass-sphere-filled PA66 (carbon black as laser absorber)
Previous production method:	Vibration welding and heating element welding
Objectives:	Withstand a pressure of 8 bar, absolutely watertight internally, lifetime of ten years under extreme specifications, no external leakage at any time
Solution:	Laser transmission welding (Quasisimultaneous welding)
Results:	Short cycle times, process-monitoring options, high strength of the weld seam, no additional materials required Laser transmission welding causes no vibrations and generates no particles
Status:	Industrial production
Source:	System supplier: LPKF, Erlangen, Germany Product: W. Lubas GesmbH, Austria

Product: **Fabrics for Air-Bag Systems**

Figure 5.5:

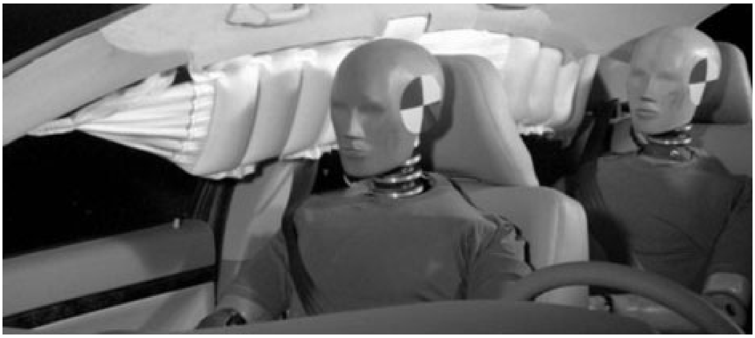

Image courtesy Autoliv

Material: Laser transparent: Textile layer uncolored PA fabric,
Laser absorbing: Textile layer uncolored PA fabric (laser absorbing by Clearweld coating application)

Previous production method: Sewing or ultrasonic welding

Objectives: Seals of high strength and reproducible quality are required, leaky seams are used for driver and passenger airbags that are designed to deflate rapidly after deployment, Curtain bags need to be sealed to stay inflated for 10s or more for vehicle-rollover protection

Solution: Laser transmission welding with Clearweld coating system

Results: Inflation performance matches stitched seams, laser welding offers a rapid and simplified production method compared to other techniques

Status: Feasibility study and process development

Source: System supplier: N.N.
Product: Autoliv, UK

5.2
Consumer Goods

Product:	**Plastic Chair "Mr. Impossible"**
Figure 5.6:	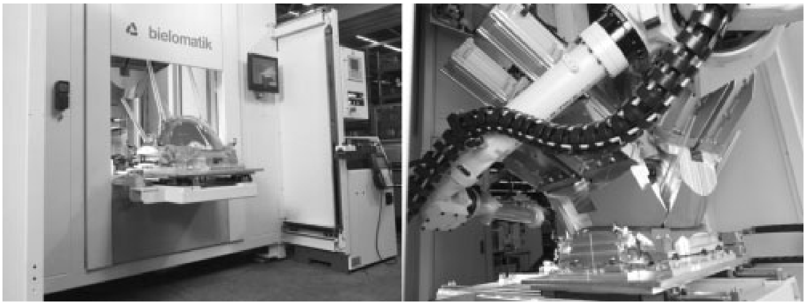
Material:	Laser transparent: Base frame uncolored PC Laser absorbing: Seat uncolored PC, transparent colored PC or opaque colored PC (laser absorbing of uncolored and transparent colored PC by Clearweld coating)
Previous production method:	Adhesive bonding
Objectives:	No curing time for adhesives, esthetical design of weld joint
Solution:	Contour laser welding with articulated arm robot, complex clamping tool enables large-scale 3D laser welding, quality control by optical imaging simultaneously behind laser processing
Results:	Excellent welding
Status:	Industrial production
Source:	System supplier: bielomatik, Neuffen, Germany Product: Kartell, Italy

Product: **Wrist Watch with Heart Rate Monitoring**

Figure 5.7:

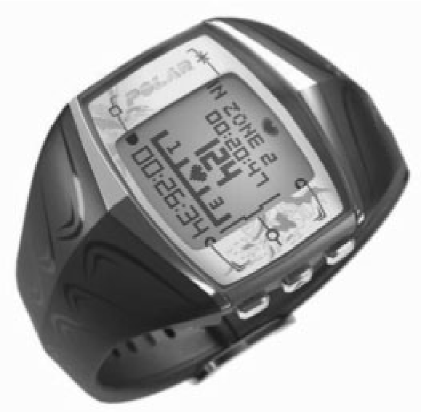

Material: Laser transparent: Lens-transparent uncolored PMMA
Laser absorbing: Body opaque colored ABS (laser absorbing by organic dye additive)

Previous production method: Ultrasonic welding

Objectives: Improvement of visual design, flexibility of component joining, water-tight weld seam

Solution: High-speed quasisimultaneous welding using Clearweld additive in ABS

Results: High-quality weld seam with outstanding visual appearance

Status: Industrial production

Source: System supplier: Cencorp Oy, Finland
Product: Polar Oy, Finland

Product: **Fluid Tank for a Self-Running Carpet Cleaner**

Figure 5.8:

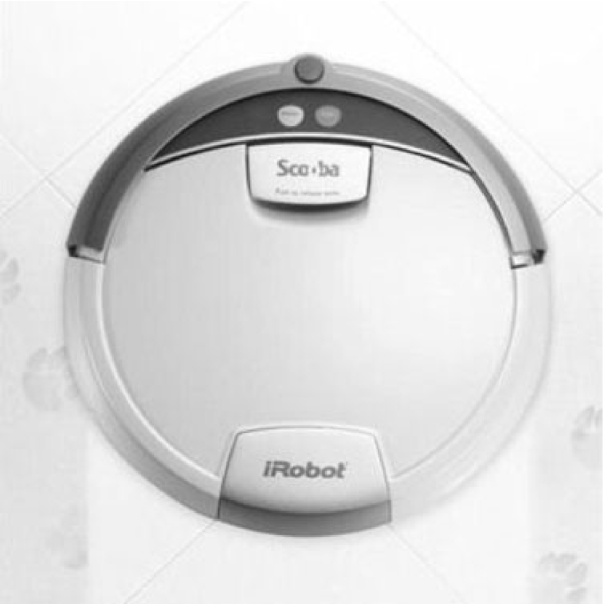

Material: Laser transparent: Injection molded component uncolored ABS
Laser absorbing: Injection-molded component light-colored ABS
(laser absorbing by organic dye additive)

Previous production method: New developed product

Objectives: Hermetic seals for covering fluids, free coloration of fluid tank top, no additional processing step

Solution: Laser welding of the main tank components using Clearweld additive in ABS

Results: Water-tight joints with reproducible high quality

Status: Feasibility study, ready for production

Source: System supplier: N.N.
Product: I-Robot, US

Product: **Garments Made of Plain Woven Fabrics**

Figure 5.9:

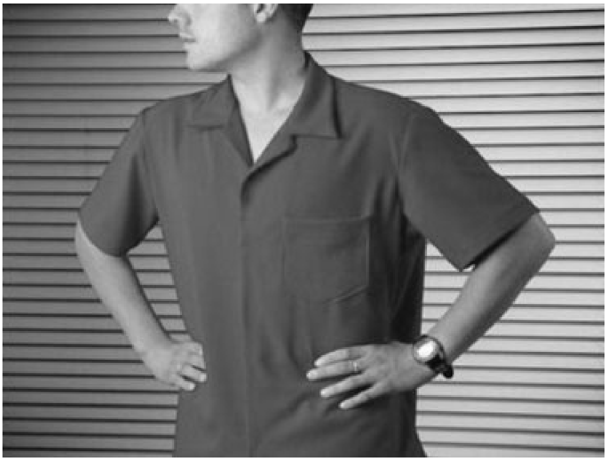

Image courtesy TWI Ltd.

Material: Laser transparent: colored polyester fabrics
Laser absorbing: colored polyester fabrics (laser absorbing by Clearweld coating)

Previous production method: Newly developed process instead of sewing

Objectives: Hermetic seals of high strength, optical appearance and economic benefits

Solution: Laser contour welding using Clearweld coating technology

Results: Successfully demonstration of laser welding entire shirts with high strength seals inside the fabric without disturbing the outer structure, pointing out that laser welding of fabrics can lead to greater automation, increased productivity and improved quality, offering manufacturers a competitive advantage and reducing the incentive to relocate production to regions with low labor costs. Producing finished goods close to where they are sold also reduces shipping costs and saves transportation time for real just-in-time delivery.

Status: Feasibility study within a joint research project

Source: System supplier: Laboratory welding system by TWI Ltd.
Product: TWI Ltd., UK

5.3
Electronic Devices

Product:	**Optical Sensor (Light Barrier)**
Figure 5.10:	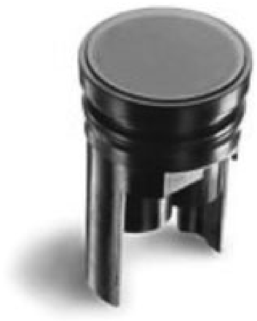
Material:	Laser transparent: Cover transparent-red PMMA, Laser absorbing: Body black PC (carbon black as laser absorber)
Previous production method:	Ultrasonic welding
Objectives:	Precise thin weld line, no particles
Solution:	Contour welding
Results:	Strong weld (>12 bar burst pressure), no particles, small welding area
Status:	Industrial production
Source:	System supplier: Leister Process Technologies, Switzerland Product: Pepperl + Fuchs, Singapore

Product: **Gas Measurement Device (~200 mm × 250 mm × 15 mm)**

Figure 5.11:

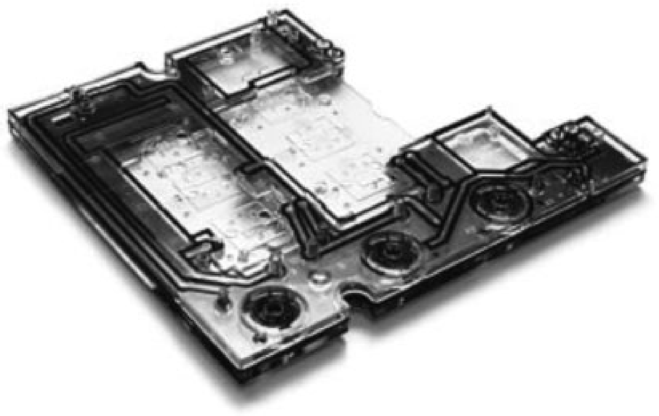

Material: Laser transparent: Cover clear ABS, Laser absorbing: Body black ABS (carbon black as laser absorber)

Previous production method: Previous product consists of many component parts that have been assembled with individual methods like screwing, plugging, gluing, and so on.

Objectives: Gas-tight joints of sandwich structure, reduction of assembly time

Solution: Contour welding of a total of 5 m weld line on both sides of the device

Results: Tight weld seams, reduced assembly time (from 1 d to 30 min)

Status: Industrial production

Source: System supplier: Leister Process Technologies, Switzerland
Product: Testo, Germany

Product: **Optical Sensor**

Figure 5.12:

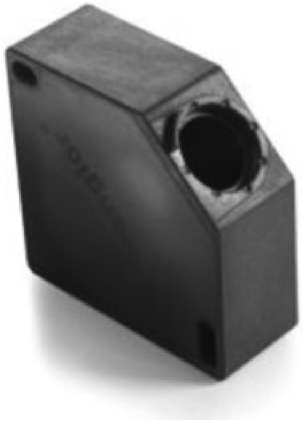

Material: Laser transparent: Cover blue PC, Laser absorbing: Body blue ABS (Lumogen additive as laser absorber)

Previous production method: Unknown

Objectives: Reliable welding process with good strength, weld line preferably invisible

Solution: Contour welding

Results: Tight, strong joint with good optical experience

Status: Industrial production

Source: System supplier: Leister Process Technologies, Switzerland
Product: Wenglor, Germany

Product: **Ink Cartridge for Large Size Printer**

Figure 5.13:

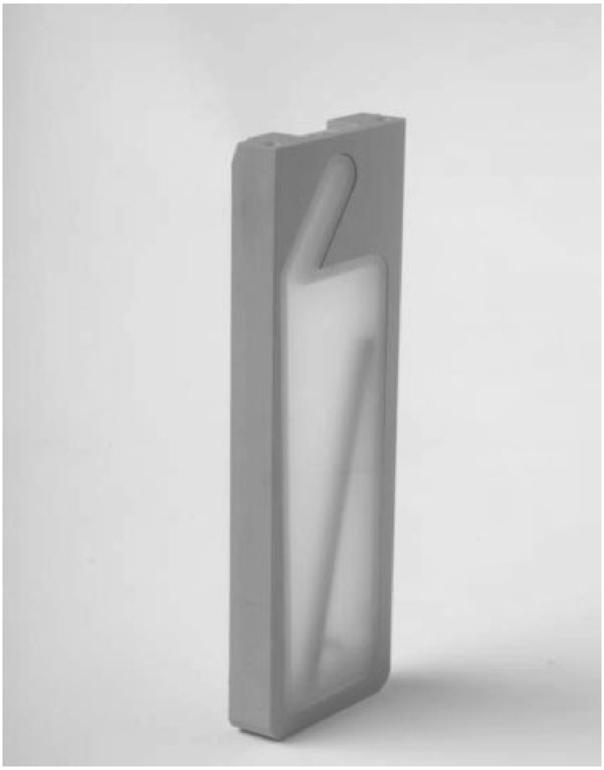

Material: Laser transparent: Cover PP natural, Laser absorbing: Body gray PP (absorber unknown)

Previous production method: Adhesive bonding

Objectives: Improve long-term stability of the joining area

Solution: Laser transmission welding (Contour welding)

Results: Long-term stable and airtight laser weld seam

Status: Industrial production

Source: System supplier: LPKF, Erlangen, Germany
Product: STAEDTLER Ink Jet

Product: **Printer Cartridge**

Figure 5.14:

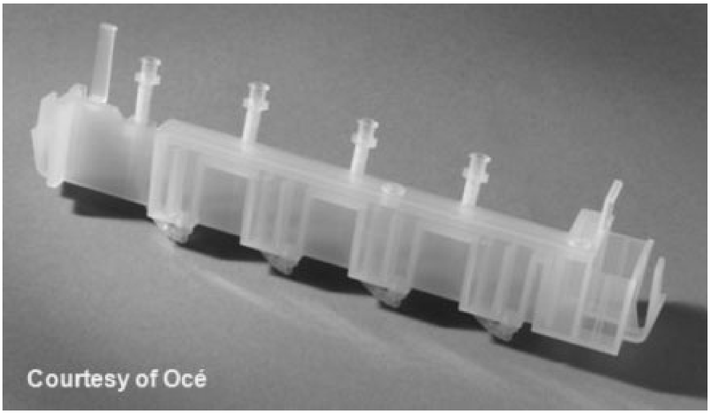

Courtesy of Océ

Material:	Laser transparent: Cover colorless PP, Laser absorbing: Body colorless PP (laser absorbing by Clearweld coating application)
Previous production method:	Ultrasonic welding
Objectives:	Reduction of friction between mating surfaces, avoid generating particulates during welding that could clog the cartridge, hermetic seals are required
Solution:	Contour laser welding with Clearweld coating system
Results:	Hermetic seals are created (cartridges are pressurized to 20 psi and submerged in water for 20 s), the highly localized heat zone of the process precludes deformation of material adjoining the weld area, thereby minimizing the scrap rate
Status:	Feasibility study
Source:	System supplier: N.N. Product: Oce, N.N.

5.4
Medical Devices

Product: **Microwell Plate (96 as well as 384 holes)**

Figure 5.15:

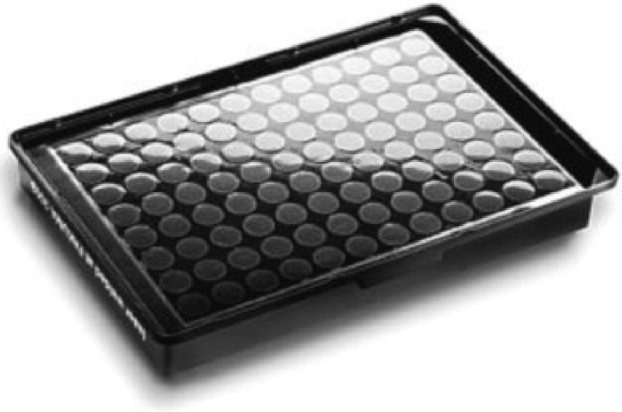

Material: Laser transparent: Cover uncolored PS film 190 µm, Laser absorbing: Body black PS (carbon black as laser absorber)

Previous production method: Adhesive bonding

Objectives: Faster, cleaner process

Solution: Mask welding with specially homogeneous line-shaped diode lasers

Results: Outstanding homogeneous and precise welds

Status: Industrial production

Source: System supplier: Leister Process Technologies, Switzerland
Product: N.N.

Product: **Microfluidic Device**

Figure 5.16:

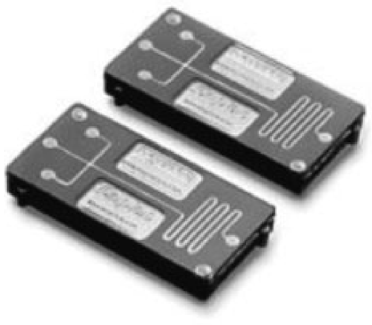

Material: Laser transparent: Cover uncolored PC, Laser absorbing: Body black PC (carbon black as laser absorber)

Previous production method: None (new product)

Objectives: Precise welding of microfluidic channels with minimal heat effected zone

Solution: Mask welding with specially homogeneous line-shaped diode lasers

Results: Precise and strong welds without negative effects on the channel profile

Status: N.N.

Source: System supplier: Leister Process Technologies, Switzerland
Product: N.N.

Product: **Infusion Pump**

Figure 5.17:

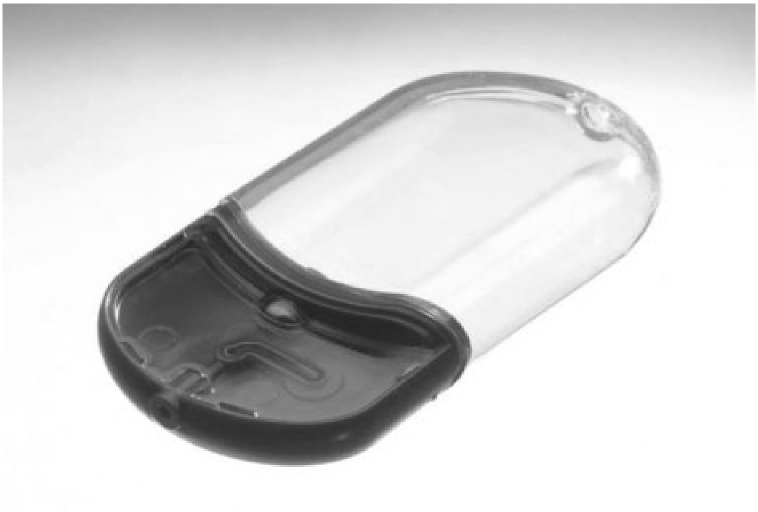

Material: Laser transparent: Cover component uncolored PC, Laser absorbing: Body component blue PC (with laser absorber)
For both components optimized resin type for medical technology.

Previous production method: None (new product)

Objectives: No particles, no contamination, High hygiene standards

Solution: Contour welding, process for two welding tasks, one on each side

Results: Clean process, tight welds, precise channel geometry

Status: Industrial production

Source: System supplier: Leister Process Technologies, Switzerland
Product: Rowemed, Germany

Product: **Cerumen Protectors**

Figure 5.18:

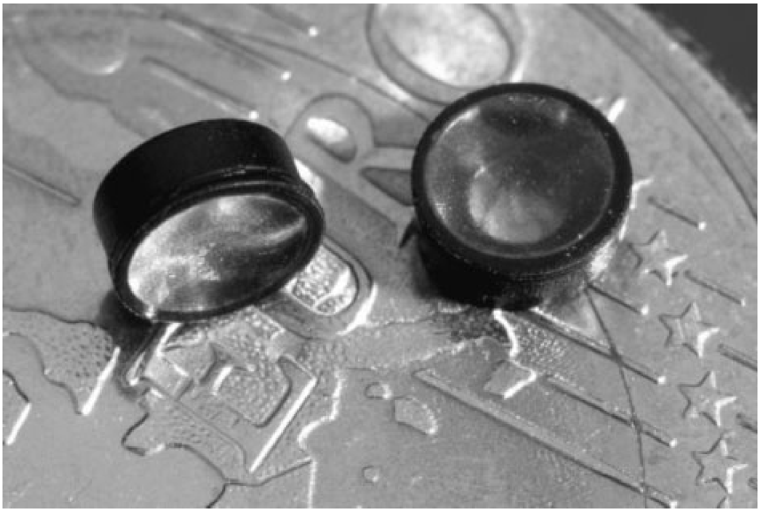

Material:	Laser transparent: Cover uncolored TPU-film 15 μm, Laser absorbing: Body black PA-rings (carbon black as laser absorber)
Previous production method:	Heat sealing, adhesive bonding
Objectives:	Minimum welding area, Precise positioning of weld, No welding bead, Excellent acoustic properties after welding
Solution:	Mask welding
Results:	Unique joining method that fulfils the requirements, 100 rings welded in one path, high throughput
Status:	Industrial production
Source:	System supplier: Leister Process Technologies, Switzerland Product: Phonak, Switzerland

Product:	**Microfluidic Disposable Cartridge for DNA and RNA Analysis**
Figure 5.19:	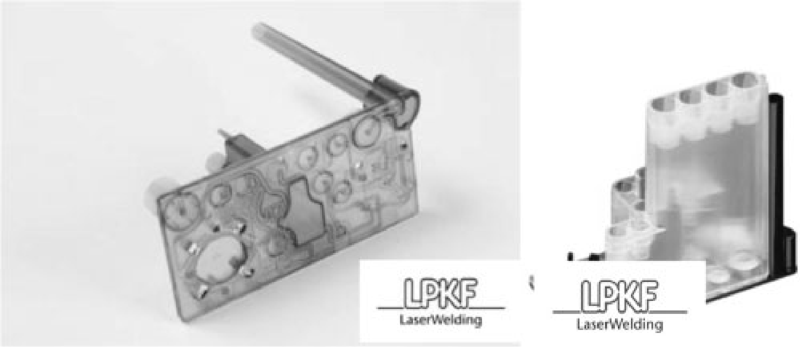
Material:	Laser transparent: Cover component by multicomponent injection molding made from transparent uncolored PC and TPE, Laser absorbing: Base body black or special colored PC (laser absorbing by carbon black or Lumogen additive)
Previous production method:	Adhesive bonding
Objectives:	Sealing the microchannels, almost two meters of joint lines have to be sealed absolutely tight, no negative impact on the cross section of the channels
Solution:	Contour laser welding
Results:	Short cycle times, process-monitoring options, reliability, high strength of the join line, no additives required. Easily set up in a clean room
Status:	Industrial production
Source:	System supplier: LPKF, Erlangen, Germany Product: Gerresheimer GmbH, Germany

Product: **Tubes with end Connectors for Medical Application**

Figure 5.20:

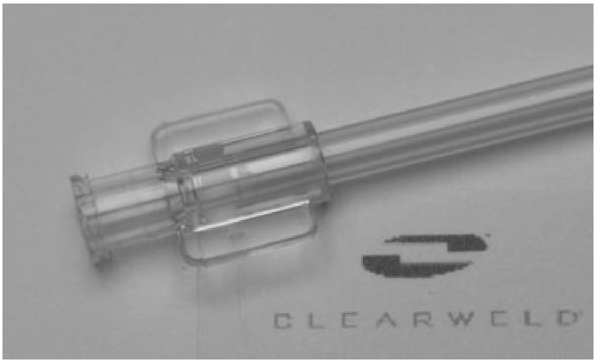

Material: Laser transparent: Luer connector uncolored PC
Laser absorbing: Coextruded tube inner sleeve PA, outer sleeve: TPU with organic dye as laser absorber

Previous production method: UV, Solvent or Loctite bonding of luers to tube ends, depending on materials used

Objectives: Reduction of assembling time, using one joining technology for different materials, optimizing joint geometry, hermetic seals required

Solution: Laser welding with Clearweld resin in outer sleeve of coextruded tube

Results: Fluid tight joint, joint strength equal to UV bonding but with reduced joint interface

Status: N.N.

Source: System supplier: Branson Ultrasonics, US
Product: Natvar Inc., US

5.5
Others

Product: **Fixing Tie**

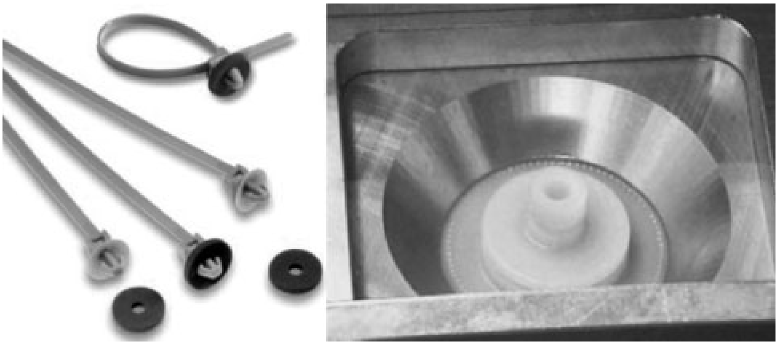

Figure 5.21:

Material:	Laser transparent: Fixing tie colored PA66, Laser absorbing: Black closed-cell foam ring (carbon black as laser absorber)
Previous production method:	New product
Objectives:	Short cycle time (0.8 s), generation of a reliable joint between a hard/soft material combination, quality control of individual parts, high mass production,
Solution:	Contour laser welding, quality control by digital imaging of individual parts, excluding failure parts from packaging
Results:	Industrial production, welding of several million parts per year
Source:	System supplier: bielomatik, Neuffen, Germany Product: HellermannTyton GmbH, Germany

Product: **Dryer Fabric for Paper Manufacturing Machinery (width 10 m, length 60 m, up to 12 m × 120 m)**

Figure 5.22:

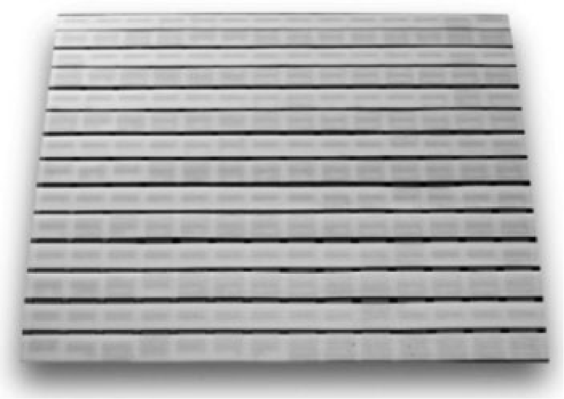

(cut-out)

Material: Laser transparent: uncolored Polyester,
Laser absorbing: black Polyester (carbon black as laser absorber)

Previous production method: Weaving of dryer fabric

Objectives: Manufacturing of welded web instead of weaving, increase of product life time

Solution: Globo welding (diode laser 940 nm, Globo-head)

Results: Excellent welding strength in fast continuous welding process, lifetime of product more than doubled

Status: N.N.

Source: System supplier: Leister Process Technologies, Switzerland Product: Heimbach, Germany

Product:	**Heavy-Duty Instruments for Ship Building**
Figure 5.23:	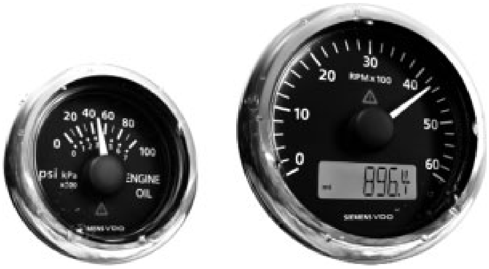 0 20 40 60 80 100 psi kPa ENGINE OIL 0 10 20 30 40 50 60 RPM x 100 896.4
Material:	Laser transparent: Lens uncolored PMMA, Laser absorbing: Body black PC (carbon black as laser absorber)
Previous production method:	Rubber sealing with snap on connector or flanging metal rings
Objectives:	Sealing against penetration of water, Strict IP 69 standard, Resistant against fuel and salt mist, Difficult material properties (high temperature TP, antifog coating . . .)
Solution:	Contour welding, process control with pyrometer
Results:	Laser welding fulfils all technical and economical needs
Status:	Industrial production
Source:	System supplier: Leister Process Technologies, Switzerland Product: Continental Automotive, Switzerland

Product: **Oil reservoir**

Figure 5.24:

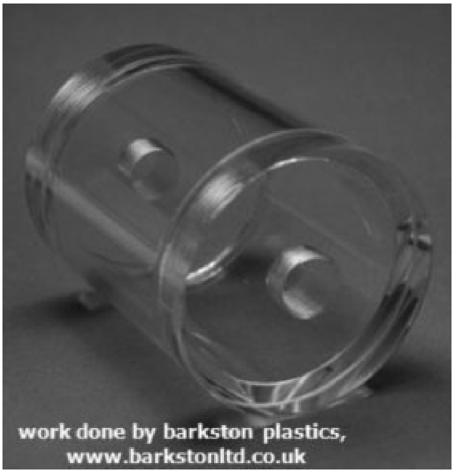

Material: Laser transparent: Two lids uncolored PMMA,
Laser absorbing: Tube uncolored PMMA (laser absorbing by Clearweld coating application)

Previous production method: Adhesive bonding or US welding of lids to tube

Objectives: Long-term stability of bond, no particles during US welding process, hermetic seals and fully transparent product required

Solution: Contour laser welding with Clearweld coating system of all components in one step by simultaneous welding of top and bottom lid to tube

Results: High weld strength to sustain oil pressure of 7.5 bar, transparent joints, economic small batch production (50 pieces per batch)

Status: Industrial production, small size serial production

Source: System supplier: N.N.
Product: Barkston Plastics, UK

Index

a
absorbing film 170, 171
absorption 42–46
– of carbon black 173
– constant 40, 43, 44
– of electromagnetic radiation 25, 52, 54, 57
– inhomogeneous line spreading of absorption spot 41
– Lambert absorption rule 43, 44
– of laser radiation 50, 109–114, 194, 199, 217
– of MIR-laser radiation 55–59
– of NIR-laser radiation 49, 50, 54, 63
– of PC 43
– plastics to NIR radiation, adaption of 2
– properties 49
– spectral absorption of Clearweld coating 168
– spectra of natural PMMA, PA6 and PP 55
– spectra of thermoplastic resins 54
– surface, in thermoplastic resins 141
additives 35, 36, 42
– absorbing, properties regarding laser welding applications 65
– adaptation of NIR-radiation absorption 59
– based on copper phosphates 63
– heat-sensitive LIS agents 194
– light-scattering 185
– like inorganic pigments 119
– nano-ITO 66, 173
– organic dyes 217
– silicone-based 192, 193
– use of absorbing additives 172–178
air-bag systems, fabrics for 222
aligned two-mirror beam-guiding system 95
amorphous thermoplastic resins
– material properties 10
– polycarbonate 10, 50
– polymethylmethacrylate 10
– polystyrene 5, 10
– polyvinylchloride 4, 6, 10
– temperature conductivity 33
amorphous thermoplastics 10, 12, 19, 21, 23, 27, 28, 32, 33, 46, 126, 134, 185, 188
Arrhenius function 131
asymmetric oscillation 54
automotive components 60, 217
– airbag sensor 218
azo dyes 66

b
beam diameter 113
beam-guiding systems 88
– glass-fiber systems 88–93
– mirror systems 93, 95
beam parameter product (BPP)
– focal length and Rayleigh length 77, 78
– of laser sources for plastic welding 76
beam propagation 74
– BPP as constant quantity for laser 76
– and focusing properties 73
– of TEM_{00} mode 75
– in transparent media 90
beam-shaping optics 100, 101
– device 153
beamsplitter 143
Bernoulli’s Lemniskate geometries 155
Boltzmann constant 131
BPP. *see* beam parameter product (BPP)
Brown’s micromobility 128
butadiene resin (BR) 13

Laser Welding of Plastics, First Edition. Rolf Klein.
© 2011 Wiley-VCH Verlag GmbH & Co. KGaA. Published 2011 by Wiley-VCH Verlag GmbH & Co. KGaA.

butt-joint welding 143
– in analogy to hot-plate welding 143
– with laser 142
– principle of 142
– of thermoplastic components 143

c
camshaft sensor 220
carbon black 173, 174
– pigments 59–61
case studies
– automotive components 217–222
– consumer goods 223–226
– electronic devices 227–231
– medical devices 232–237
– others 238–241
CCD camera, imaging recording 198
CD players 1
cerumen protectors 235
clamping device
– advantage of 191
– design of 191
clamping tools, alternatives for 189
Clearweld coating 167, 168
– contour laser-welded PMMA sample 169
– transmission spectra of 167
Clearweld process 172
CO_2-lasers 1, 35, 85, 86
– beam-bending mirror for 94
– principle setup of a waveguide 86
– slow-flow, principle setup 85
color-corrected laser-transparent 175
color-corrected opaque samples
– using Clearweld LWA 267, 176
communication technology 1
comolding
– laser welding with absorbing layer by 171
– of plastic components 170
component centering
– by clamping device 191
– using adapted component contour shapes 190
computer data storage 1
conformation angle 55
consumer goods 1, 2, 223
contour laser welding
– joint design using 183
– principle of 146
copolyamides 17
copolyester elastomers 17
copolymers 15, 16
crystallization temperature 11

d
decomposition temperature *Td* 13
diffusion coefficients 130, 131
diffusion process 128
digital imaging
– cameras 206
– of contour laser welding PET films 207
– techniques to monitor the laser-welding process 205
diode lasers 35, 74, 78–80
– with direct beam emission 80
– to form weld line 151
– high-power 1
– semiconductor materials and wavelengths of 79
– setup of 79
diode-pumped fiber laser, principle setup 84
dipole momentum 56
down-holder tools 189
dryer fabric, for paper manufacturing machinery 239

e
Einstein’s law 130
elasticity 7
elastomers 8, 13
– copolyester 17
– temperature behavior of mechanical properties 13
– thermoplastic 14, 15–18, 21, 177
–– polyolefin 16
–– polyurethane 17
electromagnetic radiation 59
– distribution in solid body, wave equation 36–42
– and material, interaction 35
– oscillation excitation by absorption of 58
electronic devices, optical sensor 227
electronic excitation, in polymers 41, 50
epoxy resin 13

f
Fabulase coating, laser-welded LDPE sample 169
Fabulase dispersion 169
Fabulase laser pigments 177
fiber-coupled diode laser 81
fiber lasers 83–85
– materials, wavelengths in NIR spectral range 84
finite element method (FEM) computation 122, 123
fixing tie 238

fluid tank, for self-running carpet cleaner 225
focusing elements 97
focusing properties, of laser beam 76, 77
focusing systems 95
– beam-shaping optics 100, 101
– dynamic focusing systems 99, 100
– static focusing systems 95–98
frame oscillations. *see* oscillations
Franck–Condon principle 50
frequency spectrum, for a linear molecule chain 25
fusion process theory 126–135
– crystalline phases mixing 133–135
– interdiffusion process (*see* reptation model)
– macromolecules interchange, by squeeze flow process 132, 133

g
gap bridging simulation 126
garments made of plain woven fabrics 226
gas measurement device 228
Gauß line spreading 40
Gaussian beam
– optics 91
– in TEM_{00} mode 76
Gaussian distribution 127
geometrical aberration 76
geometrical optics 89
geometrical translation symmetry 59
glass-fiber beam-delivery system 89
glass-fiber-reinforced PA6, spiral-bound tube of 162
glass-fiber reinforcements 185
glass-fiber system 88–93
– for high laser power 93
– with SMA connector for low laser power 92
glass temperature T_g 11
glass-transition temperature 23
Globo laser welding 156, 184
– of automotive lamp housings 157
– principle of 157

h
halogen lamps
– NIR radiation from 158
– spectral distribution of 159
heat capacity 24–27
heat conduction 20, 27–30
– influence of crystallization level 30
– in thermoplastics 27
– total heat conductivity 29
heat-conduction equation 115, 116
heat dissipation 121
heat transfer 31
heavy-duty instruments, for ship building 240
hydraulic pump, fluid reservoir for 221

i
indium tin oxide (ITO) 61, 64, 65
infusion pump 234
injection molding 191
ink cartridge, for large size printer 230
inorganic pigments 61–64, 66
– absorption of NIR radiation 61
integrated laser welding system 107
interaction processes 109
– between laser radiation and macromolecules 109
– within and between molecule chains 26
interdiffusion process 132
– of macromolecule chain segments 131
IR camera 202
IR-hybrid laser welding 184

j
joint geometry. *see also* laser plastic welding
– design of 181–186
– gap bridging 193–195
– obstacles to avoid 191–193
– tolerances/clamping 186–191

k
Kuhn's sphere model 127

l
Lambert law 116
larger gap bridging 194
laser absorbers 173, 176
laser-absorbing additives 111, 117, 177. *see also* additives
laser-absorbing coating 186
– liquid coatings 167
– surface coatings 172
– ultrasonic spray device for 166
laser-absorbing component 207
– black coloration of 217
– carbon black 209
laser-absorbing dyes, to optical transparent resins 175
laser-absorbing liquid, joint-interface geometry 185
laser-absorbing materials, Fabulase powder 171
laser-absorbing organic dyes 175

laser-absorbing resin
– comolding of plastic components 170
– FABULASE NBD-801 194, 195
laser-assisted tape winding 161
– principle of 161
– robotic system for 162
– using diode laser 162
laser-assisted thermotransfer application 171
laser beam 144
– focusing 147
– intensity distribution of 74
laser-beam diameter 114
laser-beam welding
– gap bridging 195
– HDPE, gap bridging for 194
laser contour welding, processing parameters 146
laser focusing head
– with integrated digital imaging camera 206
– with external thermography camera 204
– with integrated optical reflection measurement 208
– with integrated pyrometer 202
laser-induced foaming process 194
laser light scattering 196
laser line energy 146, 149
laser marking, of PC/ABS 178
laser plastic welding 217
– absorption, adaption of 163
–– absorbing additives, uses 172–178
–– special lasers, uses 178–181
–– surface coatings, uses 163–172
– butt-joint welding, principle of 141–143
– contour welding 145–148
– crystalline phases mixing 133–135
– fusion process theory 126–135
– Globo laser welding 156–158
– heat generation and dissipation 109–126
– industrial joining method 217
– interdiffusion process 131, 132
– IR-hybrid laser welding 158, 159
– joint geometry 181–193
– laser energy transfer into process heat 114–118
– laser radiation absorption 109–114
– laying/winding 160–162
– macromolecules interchange by squeeze flow process 132, 133
– mask laser welding 154, 155
– material compatibility 135–138
– process heat dissipation 118–121
– process simulation, by complex computation 121–126
– quality monitoring, and control methods 195–211
–– digital imaging monitoring 205–207
–– mechanical set-path monitoring 208, 209
–– monitoring techniques 209–211
–– optical reflection monitoring 207, 208
–– before processing 196–199
–– pyrometric monitoring 199–203
–– thermography monitoring 203–205
– quasisimultaneous laser welding 148–150
– simultaneous laser welding 150–154
– through-transmission laser welding (TTLW) 143–145
– TWIST laser welding 155, 156
– typical laser sources for 87
– ultrasonic hybrid laser welding 159, 160
laser quasisimultaneous welding
– processing parameters for 148
laser radiation 109–114, 156, 161
– absorption, properties for 218
– direct absorption 109, 110
– hindered absorption by internal scattering 111–114
– indirect absorption 110, 111
– NIR lamp and 158
– properties of 71–73, 76
– reflection of 207
laser sewing system 160
lasers, types of. *see* CO_2-lasers; diode lasers; fiber lasers; Nd:YAG-lasers
laser-transparent components 196
– interface 119
– radiation-scattering additives 186
– transmission of 196, 197
laser-transparent resin layer 121
– melting depth 122
laser wavelength 73
laser welding 150
– with absorbing additive 173
– with absorbing layer, by comolding 171
– with absorbing surface layer 172
– applications 181
– concentric laser beam circles 152
– electronic car 174
– gap bridging 174
– geometrical joint tolerance limits 188
– head, IR hybrid 159
– holographic mask as 153
– in industrial applications 2
– integrated temperature radiation measurement during 98
– IR-hybrid, principle of 158

– joint 145
– joint design 184, 185, 187
– joint gaps 193
– joints using laser-absorbing coating 188
– microfluidic mixer device 181
– monitoring and control techniques 195
– natural HDPE samples 176
– – using Fabulase 322 pigments 176
– obstacles for 192
– parallelism limit of 189
– of PC/ABS with PMMA 178
– PET films, digital imaging of 207
– plastic laser welding system, setup 102
– PP resin with carbon black 193
– quality 146
– of SAN without and with temperature control by pyrometer 203
– system, principle setup of 101
– of thermoplastics 141, 179, 199, 200
– – components 2, 143, 163, 180, 196, 209
– – fabrics 160
– – monitoring process 210
– – resins 163, 180, 185, 199
– ultrasonic hybrid 160
laser-welding methods, for industrial application 217
laser-welding process 158, 186, 190, 208. *see also* laser welding
– closed-loop control of 201
– coloration 168
– simulation 125
laser welding systems, principle setup of 101–107
– beam-shaping optics, for circular beam pattern 101
– CNC controller 104
– integration
– – into production chain 106
– – with work piece feeding system 107
– plastic laser welding system, typical setup 102
– pneumatic clamping device 103
– stand-alone laser welding system 105
– – for plastic chairs 106
– work-piece handling systems, basic configurations 102
laser-welding transparent PC, with absorbing PC film layer 170
Lazerflair® pigments 61, 62
lens material 95
– used for focusing 97
light amplification 1
liquid-coating application 170
liquid-coating technologies 163
Lorentz line spreading 41
Lorentz–Lorenz law 39
low-volume–low-pressure (LVLP) pneumatic spray valves 165

m
macromolecular chain
– coupling between atoms 3
– Kuhn's sphere model 128
– with no crosslinks 9
– orientation and length of 20
– oscillation (*see* vibronic excitation)
– reptation model 129
– segments, interdiffusion 131
macromolecules
– conformation types 5
– crosslinked 8
– helix type/statistical knotted 57
– interchange of 132, 133
– penetration process 127
– stretching 134
– van der Waals bonding 28
mask laser welding
– flexibility of 155
– principle of 155
medical devices 232
melt energy, for semicrystalline thermoplastics 22
melt-flow index (MFI) 136
– values 9
melting process 119
microfluidic device 233
microfluidic disposable cartridge
– for DNA and RNA analysis 236
MIR radiation 109
mirror systems, laser systems 93–95
molding process 171
molding tool, injection system 192
molecule groups, of polymer materials 38
monochromatic radiation 59
monomer units 3
multiresin-injecting molding tools 170

n
nano-ITO pigments 173
natural resins, NIR radiation 114
natural thermoplastic resins 110

Nd:YAG-lasers 1, 35, 74, 76, 80–83, 161, 163
- diode-pumped , principle setup 82
- lamp-pumped, principle setup 81
- laser-assisted tape winding 162
- radiations 53

near-order bonding forces, for crystalline structure 134
needle-tip dispenser, for coating application 164
needle-tip dispensing systems 167
NIR imaging, laser-absorbing coating on joint 199
NIR lamps 158
NIR-laser 35
- absorbing layer 164
- beam-bending mirror for 94
- radiation 144

NIR radiation
- in polymeric material 54
- spectral wavelength distribution of 158

NIR-radiation absorption by additives, adaptation of 59
- carbon black pigments 59–61
- inorganic pigments 61–64, 66
- organic dyes 66
- properties regarding laser welding application 65

NIR-sensitive cameras 202
NIR-transmission imaging 198

o

oil reservoir 241
optical constants 36–42
optical material properties absorption 141
optical penetration depth 174, 175
optical polarization 38
optical properties 35, 36
optical sensor 227, 229
organic dyes 66, 110
- absorption properties of thermoplastic resins 66
- dispersion 110

oscillation excitation, by absorption of electromagnetic radiation 58
oscillation frequency 57, 58
- methylene group 57

oscillations
- around their center positions 24
- C–H group 54, 55
- elastic 27, 29
- frame 56, 58, 110
- induced by acoustic/optical waves 26
- material by stimulating electron 35
- MIR spectrum inducing 35
- optical mode of grid, stimulation 25
- resonance 37
- rotation 24, 57
- side-chain molecules/end-chain molecule 56
- stimulation of dipole 42
- thermal effects 21
- types of atoms and atom groups 57
- vibration 35, 42

oscillation spectrum 25
- density distribution 26
- heat capacity at constant volume 26

p

PA6 fiber material
- absorption spectra 55
- influence of crystallite size 12
- influence of optical penetration depth 46
- monomers 4
- spiral-bound tube of glass-fiber-reinforced 162
- temperature course of transmission and 122
- transmission, in wavelength range from 53

PA6 resin 113, 117, 118
perionon dyes 66
perylene dyes 66
PET. *see* polyethylenterephtalate (PET)
phase transitions
- crystallite melting temperature (T_m) 20
- flow temperature (T_f) 20
- glass transition (T_g) 20
- thermal decomposition (T_d) 21, 22

phenolic resin 13
photometric detector 208
Planck's law 200
plasticization process 170
plastic laser-welding processes, quality-monitoring techniques 211
plastics
- basic structure of 3
- bonding partners and chain conformations 4
- classification 8
- composites consist of 9
- conformation types of macromolecules 5
- films 141
- molecular and macroscopic material properties 7

– monomers 4
– phase-transition temperatures 9
– physical and chemical structure of macromolecule 6
– processes for generation 4
– resin 155
– scattering of NIR- and IR-radiation in 46–49
– secondary valence forces 6, 7
– statistical distribution of macromolecule chain length 6
– types of 7, 8
plastic welding 1
– BPP of typical laser sources for 76
PMMA. *see* polymethylmethacrylate (PMMA)
pneumatic clamping device, principle setup 103
pneumatic spray device, with laser absorbing coatings 165
pneumatic valves 165
polarization microscopy, observation of cross section 179
polyaddition 3
polyamide (PA) 10
polycarbonates (PC) 10, 50
– reflection and transmission 43
polycondensation 3
polyester resin 13
polyethylenterephtalate (PET) 50, 161, 194, 195, 204, 206
polymer blends 14, 15
polymer composites 18
– classification 19
polymer compounds 14
polymeric matrix 110, 111
polymer macromolecules
– mobility 126
polymethylmethacrylate (PMMA)
– absorption spectra 55
– as amorphous thermoplastic resins 10
– contour laser-welded sample 169
– nano-ITO particles, transmission of 63
– phase-transition temperatures 21
– refractive index, temperature dependency of 40
– relative weld strength for 137
– temperature conductivity, average values of 34
polyphenylensulfide (PPS) 50
– material properties 11
– stimulated to oscillation by absorption of CO_2-laser radiation 58
polypropylene (PP) 10
– monomers 4
polystyrene molecules 5
polyurethane resin 13
printer cartridge 231
PVD coatings, at joint interface 192
pyrometers 202, 208
– detector 97

q
quasisimultaneous laser welding 150
– heating process 149
– laser beam 148
– melt squeeze flow 149
– principle of 148
– and simultaneous, quality monitoring 206

r
radius of gyration 127
red laser radiation 1
reflection 42–46
– materials used for 94
– radiation intensity weakening by 43
relaxation process 133
reptation model 127–132. *see also* interdiffusion process
resins. *see also* laser-absorbing resin; thermoplastic resins
– butadiene 13
– epoxy 13
– heat expansion coefficient 136
– laser-transparent 185
– melt-flow index (MFI) 136
– PA6, 123
– phenolic 13
– PMMA 168
– polyamide 179
– polyester 13
– polyolefin 66, 178
– temperature-dependent thermal 122
– thermoplastic 9, 10, 20, 133, 136, 176, 185, 192
ruby laser 1

s
scanner head 99
– basic setup 99
– in combination with a fiber-guide system 100

scattering
– caused by polymer matrix 48
– constant 111, 112
– of NIR- and IR-radiation in plastics 46–49
– structures in polymers and effect to radiation 49
semicrystalline thermoplastics 10–12, 33, 34
– behavior 134
– below the glass temperature 23
– heat capacity of 26
– heat conductivity in 30
– layers, resolidification 135
– melt energy for 22
– resins, temperature behavior 12
– temperature conductivity as function of 34
simultaneous laser welding
– beam-shaping optic device 153
– cylindrical components
–– mirror setup for 154
– principle of 150, 152
specific volume 22–24
– behavior of 23
speedometer 220
squeezing process 120
– microswirls caused by 134
static focusing device, principle setup 98
styrene block copolymers 17
styrene butadiene resin (SBR) 13

t
temperature conduction 30–32
temperature-dependent radiation absorption 123
temperature distributions
– rule of thumb 118
thermal fusion process 141
thermal models, complex 115
thermal oscillation of atoms 22
thermal process control device 162
thermal properties 19, 20
thermal resin expansion 126
thermal-treatment-induced polymerization 160
thermography camera 203, 206
– controller of 203
– images of laser welding PET films 204
– monitoring 205
thermography imaging, of simultaneous laser-welding process 205
thermoplastic copolymers, conditions of application 15
thermoplastic elastomer (TPE) blends 16
– copolymers 17
– structure 16
– types 16
– uncolored 18
thermoplastic elastomers (TPEs)
– physical and chemical properties 136
– types 138
– welding 138
thermoplastic resins 9, 10, 118
– absorption properties 181
– hot-plate welding 133
– laser radiation on 115
– melt-temperature ranges and 22
– optical penetration depth, for laser radiation 46
– phase-transition temperatures for 21
thermoplastics 7, 8. *see also* plastics
– average values of temperature conductivity 34
– macromolecular structure of 10
thermoplastic vulcanization elastomers 16
thermosets 8, 13
– temperature behavior 14
through-transmission laser welding (TTLW) 1, 141, 143, 144, 179, 181
– laser beam focusing optic, schematic setup of 179
– laser welding plastic components 145
– principle joint designs 183
– using absorbing layer 163
– using laser-absorbing coatings 144, 145
transmission 42–46, 53
– of Clearweld® A208 and A267 dye 64
– of FABULASE® 322, 63
– of Lazerflair® 825 in PP 62
– of Lumogen® dyes in PC 64
– measurement, control device for 197
– of nano-ITO particles in PMMA 63
– PA6 film 53
– welding 155
TTLW. *see* through-transmission laser welding (TTLW)

TWIST laser welding 155, 156
– principle of 156
– of transparent plastic components 156
two-mirror beam-guiding system 96

u
ultrasonic hybrid laser welding 160
ultrasonic nozzles 166, 167
– soft spray 167
ultrasonic power 160

v
valence angle forces 56
vibronic excitation 51, 52
VIS-NIR spectrometers 197

w
welding speed 104, 118, 123, 146
weld-quality monitoring 207
work-piece handling systems 102
wrist watch, with heart rate monitoring 224